

Cosmic necklaces in string theory and field theory

Lake, Matthew James

The copyright of this thesis rests with the author and no quotation from it or information derived from it may be published without the prior written consent of the author

For additional information about this publication click this link.

<https://qmro.qmul.ac.uk/jspui/handle/123456789/523>

Information about this research object was correct at the time of download; we occasionally make corrections to records, please therefore check the published record when citing. For more information contact scholarlycommunications@qmul.ac.uk

Cosmic Necklaces in String Theory and Field Theory

Matthew James Lake

Thesis submitted for the degree of
Doctor of Philosophy
of the University of London

Thesis supervisors
Prof. Bernard Carr*
Prof. Steven Thomas**

*Astronomy Unit, School of Mathematical Sciences

**Center for Research in String Theory, Department of Physics
Queen Mary, University of London
Mile End Road
London, E1 4NS
United Kingdom



September 2010

Let none turn over books, or roam the stars in quest of God, who sees him not in man.

Johann Kaspar Lavater, *Aphorisms on Man* (1788)

In memory of Professor Christopher Beiling.

For Selina.

Declaration

I declare that the material in this thesis is a representation of my own work, unless otherwise stated, and resulted from collaborations with Prof. Steven Thomas and Dr. John Ward. Much of the material in the thesis is based upon papers [1]-[3] and additional work carried out in collaboration with Prof. Tiberiu Harko, during the course of my PhD, is contained in [4].

Matthew Lake

Acknowledgements

First and foremost I would like to thank Prof. Steven Thomas, my supervisor in the Department of Physics, and also my collaborator and colleague for the past four years. For always having time for me, for all his support both professionally and personally, for teaching me a lot and for making it fun, I shall always be grateful. Needless to say, without him, this thesis would not have been possible.

Many thanks are also due to Prof. Bernard Carr, my supervisor in the School of Mathematical Sciences, who encouraged me to forge links with other departments and to pursue my interests in string theory and particle physics, as well as cosmology. Without his open-minded support for the projects I chose to pursue, this thesis would have been very different. His input helped direct the course of my work and mould its presentation, and there is much I learned from him which I am sure will prove invaluable throughout my scientific career. His guidance, support and encouragement were unwavering, and are greatly appreciated.

My sincerest gratitude to my fellow collaborators, Dr. John Ward and Prof. Tiberiu Harko, from whom I also learned a great deal. Many thanks also to Prof. Chris Beling who, together with Prof. Harko, welcomed me into their weekly philosophy meetings and into their friendship at the University of Hong Kong.

My work has been supported by the Science and Technology Funding Council (STFC) and by the Queen Mary EPSTAR consortium. I would especially like to thank Susan Blackwell at STFC and Jim Emerson, David Burgess, Carl Murray, Mark Jerrum, Bill Spence, Andreas Brandhuber, Steve Lloyd and Bill White at QMUL for their assistance. Special thanks are also due, for non-financial reasons, to Richard Nelson.

I would also like to thank Prof. Jim Lidsey and Dr. Sanjaye Ramgoolam for conducting my upgrade vivas and for the helpful and constructive advice they gave regarding my progress. To all the guys in the string theory group, Gadrielle, Rudolfo, David, Gianni, Dan, Andy, Moritz (for giving me coffee), Max and Dave T, thanks for making it such a fun place to work and for making me feel welcome. To the guys in the Astronomy Unit, Ian, K and Adam, thanks for all your support and encouragement. Sorry I couldn't be there

more often. Special thanks to Kate, for tea, cake and keeping me warm whenever she found me loitering in the Physics Department and to Vincenzo, for lending me his desk so that I didn't have to. Thanks also to the guys at Books for Amnesty, Piet, Sarah, Jane and Mary, for their flexibility in arranging and covering shifts, for their support and (above all) for their interest in this project.

Finally, thank you to all the friends who have helped me, in so many ways, throughout the past four years, especially the last two. In no particular order: Sara, Steve, Helen, Seb, Alex, Odette, Jason, Tamara, Abdol, Scutch, Ian, Fran, Jasmini, Mel, Kitty, Ben, Toria (and Aggs), John, Woza, Ajay, Rich, Irene, Dandan, Paneiz, Martin H-E, Nina, Ed, Tanya, Rosie, Tosin, Simon, Isabel, Mandy, Mathena and Amy.

Abstract

In this thesis we investigate astrophysical phenomena which arise in models with compact extra dimensions, focussing on the cosmological consequences of strings which wrap cycles in the internal space. Embedding our strings in the Klebanov-Strassler geometry we develop a concrete model of cosmic necklaces and investigate the formation of primordial black holes and dark matter relics from necklace collapse. Using data from the EGRET cosmic ray experiment, we place bounds on the parameters which define the warped deformed conifold, including the value of the warp factor and the radius of the compact space. Chapter 1 provides a brief overview, while background material is included in chapter 2, and these results are presented in chapter 3.

In chapter 4 we analyse the dynamics of wound strings with angular momentum in the compact dimensions and determine the equation of motion for a self-oscillating loop. Finally, in chapter 5 we suggest a field-theoretic dual for wound-string necklaces based on a modification of the standard Abelian-Higgs model. After introducing spatially-dependent couplings for the scalar and vector fields, we propose a static, non-cylindrically symmetric solution of the resulting field equations which describes a “pinched” string with neighbouring vortex and anti-vortex regions. The similarities between pinched strings and the four-dimensional appearance of wound-string states are then examined and a correspondence between field theory and string theory parameters is suggested.

We find that the topological winding number of the field theory vortex may be expressed in terms of parameters which define the winding of the dual string around the compact space. According to this relation, the topological charge is equal to unity when the string has zero windings, and the standard Nielsen-Olesen duality is recovered in this limit. One key result of this work is an estimate of the Higgs boson mass (at critical coupling) in terms of the parameters which define the Klebanov-Strassler geometry and which, in principle, may be constrained by cosmological observations.

Table of contents

DECLARATION	4
ACKNOWLEDGEMENTS	5
ABSTRACT	7
1 GENERAL INTRODUCTION	14
1.0.1 A note on additional work	17
2 BACKGROUND: PRIMORDIAL BLACK HOLES, COSMIC STRINGS, EXTRA DIMENSIONS AND COSMIC NECKLACES	19
2.1 Primordial black holes - history and overview	19
2.2 Cosmic strings - formation and evolution	23
2.2.1 Formation of topological defect strings	23
2.2.2 String evolution	31
2.2.3 String theory models: extra dimensions, cycloids and necklaces . . .	34
2.3 The Klebanov-Strassler geometry as an example of a flux-compactification and brane inflation	40
2.4 Topological defect strings vs “stringy strings”: (p, q) -strings in the KS throat	51
2.4.1 String species, internal structure and effective actions	51
2.4.2 The non-Abelian DBI action	54
2.4.3 Macroscopic and microscopic (p, q) -strings	57
3 PRIMORDIAL BLACK HOLES AND DARK MATTER FROM NECKLACE COLLAPSE	64
3.1 Introduction	64
3.2 Strings with non-trivial windings in the internal space	68
3.3 Stability analysis for string loops in the static ($l = 0$) case and necklace formation	72

3.4	Cosmological implications of necklace loops	78
3.4.1	Late time formation - the scaling regime	84
3.4.2	Early time formation	85
3.4.3	PBH formation	87
3.4.4	Quasi-stable necklaces	102
3.4.5	Comparison with the standard string-monopole network	104
3.5	Discussion	108
4	NON-TOPOLOGICAL CYCLOOPS	112
4.1	Introduction	112
4.2	Description of the tip geometry in Hopf coordinates	114
4.3	A dynamical model of winding formation	115
4.4	Comparison with the results of Blanco-Pillado and Iglesias	117
4.5	Loop dynamics after formation	123
4.6	Discussion	132
5	PINCHED STRINGS IN A MODIFIED ABELIAN-HIGGS MODEL	136
5.1	Introduction	136
5.2	Revisiting the Abelian-Higgs model	139
5.3	Calculation of the (constant) string tension for a cylindrically symmetric string $\mu_{ n }$	151
5.4	Introduction of the modified action and pinched string ansatz	156
5.5	Equations of motion for a pinched string	160
5.6	Solutions to the pinched string EOM	167
5.7	Calculation of the (periodic) string tension for non-cylindrically symmetric string $\mu_{ n }(z)$	171
5.8	Relation of the pinched string to wound F/D -strings	174
5.8.1	Argument for a time-dependent bead mass	184
5.9	Additional Notes	189
5.9.1	Effective actions	189
5.9.2	Model mixing	190
5.9.3	A note on the magnetic fields generated by pinched string beads	191
5.9.4	On the instability of non-integer windings	192
5.9.5	Alternative pinched/wound-string configurations	194
5.10	Conclusions and discussion of prospects for future work	195

6 FINAL CONCLUSIONS

198

APPENDICES

201

List of Figures

2.1	The Mexican hat potential for a broken $U(1)$ symmetry group showing a degenerate circle of minima. Taken from Vilenkin and Shellard [114].	25
2.2	Field configuration for a vortex string (b). A loop in physical space enclosing the vortex is mapped non-trivially into the degenerate circle of minima of the potential shown in (a). For a string with winding number $\pm n$, the circle of degenerate minima is traversed completely either clockwise (+) or anti-clockwise (-) (by convention) $ n $ times as the loop is traversed in physical space. Taken from Vilenkin and Shellard [114].	26
2.3	The string in three dimensions can be located by encircling it with a closed loop L . A non-zero winding number in the phase as the loop is traversed discloses the string within. Taken from Vilenkin and Shellard [114].	26
2.4	Winding formation in the random walk regime. The spatial structure of the strings in the extra dimensions, which is assumed to be Brownian, can give rise to non-trivial windings. Taken from Avgoustidis and Shellard [16].	35
2.5	Winding formation in the velocity-correlations regime. String velocities in the extra dimensions cannot be correlated over distances greater than the correlation length of the network at the time of loop formation $\xi(t_0)$. Thus the endpoints of a string segment of length $\xi(t_0)$ can be expected to have different velocities. This would tilt the string, as shown, to produce windings. Loops which then chop off from the network, even on scales $l(t_i) = \alpha t_i < \xi(t_i)$, will also contain non-trivial windings. Taken from Avgoustidis and Shellard [16].	36
2.6	This figure illustrates the difference between cycloids and necklace coils. A schematic representation of a periodic lifting potential V with degenerate minima (as a function of the spatial coordinates of the extra dimensions) is given below and its impact on winding formation is illustrated in the two pictures above. The right-hand-side shows a schematic representation of a necklace configuration for windings around an S^1 compact manifold. Taken from Matsuda [8].	38
2.7	This figure illustrates the geometry of the warped throat and is taken from lectures presented by F. Quevedo (The cosmology of string theory - inflation and beyond) at UniverseNet (2007). Here the coordinate r refers to the inter-brane distance, which is equal to the distance between the probe D_3 -brane and the tip of the throat.	47
2.8	This figure illustrates the difference between the geometry of the general conifold and the warped deformed conifold. Taken from Majumdar [191].	47

3.1	Plot of the static potential \mathcal{V} , setting the tension pre-factor term to unity and also $r^2 = 1$, $a_0^{-2}R^2 = 1$ and $n_\psi^2 = n_\theta^2 = n_\phi^2 = 1$	73
3.2	(a) shows strings winding smoothly across the effective potential \mathcal{V} on the (θ, ϕ) sub-manifold. (b) shows step-like configurations which minimise the total string energy within \mathcal{V}	77
3.3	Plots of the dynamic variables associated with winding formation as a function of the time of loop formation, t_i . The bead mass $M_b(t_i)$, number of beads $N_b(t_i) \sim 2n_w(t_i)$, fraction of the total string length contained in the windings $\omega_l(t_i)$, and the average inter-bead distance $d(t_i)$ are shown. In all plots model parameters have been set such that $a_0 = 0.1$, $\alpha' = 1$, $R = 5$, $\alpha = 0.8$ and $T_1\sqrt{1 + \frac{\Pi^2}{T_1^2\lambda^2}} = 1$	83
3.4	The total mass M_T contained within the beads of a necklace as a function of t_i . The model parameters have been fixed so that $a_0 = 0.1$, $\alpha' = 1$, $R = 5$, $\alpha = 0.8$ and $T_1\sqrt{1 + \frac{\Pi^2}{T_1^2\lambda^2}} = 1$	88
3.5	The total mass M_T contained within the beads of a necklace as a function of t_i , together with the early and late-time approximations given by (3.60)/(3.61), respectively. The same parameter choices were made as in figure 3.4. The blue (green) curves are the early (late) time approximations respectively. Note that the late time approximation seems to over-estimate the maximum mass.	89
3.6	Plot of the exact necklace mass M_T (red curve) and the approximate fit function $M_{T_{approx}}$ (green curve) as a function of t_i for $a_0 = 0.1, 0.05, 0.01, 0.001$ (top left to bottom right). In all the plots $\alpha' = 1$, $R = 5$, $\alpha = 0.8$ and $T_1\sqrt{1 + \frac{\Pi^2}{T_1^2\lambda^2}} = 1$	92
3.7	Zoom in of the four plots shown in figure 3.6, clearly exhibiting the early-time breakdown of the fit function $M_{T_{approx}}(t_i)$	92
3.8	Contour plot showing the allowed regions of $\{R, \kappa\}$ consistent with the bound $\Omega(t_0) < 10^{-9}$. Only a few contours are plotted. We have chosen $a_0 = 0.1$, $\alpha' = 1$, $\alpha = 0.8$ and $T_1 = 1$	101
3.9	Three-dimensional contour plots showing values of the flux parameter Π in the $(\text{Log}[a_0], R, \kappa)$ plane. Six surfaces are shown corresponding (from front to rear) to the values of $\Pi = 10^{12}, 10^{10}, 10^8, 10^6, 10^4, 10^2$. These plots take into account the observational bounds on $\{R, \kappa\}$ shown in figure 3.8. The remaining choice of parameters are as in figure 3.8.	102
4.1	This figure illustrates the behaviour of the solution (4.55) in the three qualitatively different regimes. For convenience, we have chosen $t_i = 1$, $\alpha = 0.5$ for all three curves and set $a_0^2 = 0.4, 0.5$ and 0.6	130
4.2	This figure illustrates the behaviour of $v(t) \sim \dot{s}(t)R$ in the three qualitatively different regimes. Again we have chosen $t_i = 1$, $\alpha = 0.5$ for all three curves and the values $a_0^2 = 0.4, 0.5$ and 0.6	130

4.3	This figure illustrates the behaviour of $r(t)$ for loops formed at three different epochs in the $a_0^2 < 1/2$ regime. For the sake of convenience we have fixed $a_0^2 = 0.4$ and $\alpha = 0.5$ for all three curves and set $t_i = 1$, $t_i = 1.2$, and $t_i = 1.5$.	131
4.4	This figure illustrates the behaviour of $v(t) \sim \dot{s}(t)R$ for loops formed at three different epochs in the $a_0^2 < 1/2$ regime. As in figure 4.3 we choose to set $a_0^2 = 0.4$ and $\alpha = 0.5$ for all three curves and consider $t_i = 1$, $t_i = 1.2$, and $t_i = 1.5$.	131
5.1	$H_{ n }(z)$ in the range $-3\Delta \leq z \leq 3\Delta$ with $\Delta = 1$ and $ n l_p = 0.1$.	159
5.2	Profile of the pinched string solution in the range $-3\Delta \leq z \leq 3\Delta$, with $\Delta = 1$, $ n l_p = 0.1$, $r_s = 0.5$ (blue curve) and $r_v = 0.75$ (red curve).	165
5.3	This figure illustrates the magnetic field around a pinched string with neighbouring $\pm n $ regions. Here we have assumed critical coupling and taken the limit $ n l_p \ll r_c$. The key point is that the magnetic flux is zero in the region of the pinch, so that flux lines cannot flow between neighbouring "beads".	192
5.4	Successive half-integer windings of a string in the ψ -direction of the three-sphere. Such a configuration is clearly unstable and its collapse results in the annihilation string section involved in the wrapping.	193

CHAPTER 1

GENERAL INTRODUCTION

In this thesis we investigate astrophysical phenomena which may arise in models with compact extra dimensions, focussing in particular on the cosmological consequences of string-like defects which wrap cycles in the internal space. For concreteness, we choose the Klebanov-Strassler (KS) model of the warped deformed conifold in which to embed our strings [5]. The KS background represents one of the best understood compactifications of type IIB string theory and is of particular cosmological interest because it provides a natural mechanism for brane inflation. In the most general models, inflation ends when the D_3 -brane of our universe collides with \overline{D}_3 -branes at the low energy or “Infra-red” (IR) tip of the throat. One consequence of this scenario is the copious production of defects at the end of the inflationary epoch, including large numbers of F - and D -string bound states which lie at the tip. We consider two separate winding formation mechanisms, the so-called random walk and velocity-correlations regimes, and argue that the first of these leads naturally to the creation of static cosmic string loops, while the second leads to the creation of loops with non-zero angular momentum in the compact directions.

As the manifold at the IR tip is simply connected, the question of stability arises. In the static case we demonstrate that the presence of a lifting potential in the compact space traps the windings, giving rise to loops with step-like winding configurations, referred to in the literature as cosmic necklaces. From a four-dimensional perspective the windings appear as a series of monopoles or “beads” connected by ordinary sections of string. Superficially these resemble the standard string-monopole networks found in field-theoretic models but their behaviour is, in many ways, fundamentally different. In stark contrast to previous predictions based on field theory defects, we find that the gravitational collapse of necklaces leads to the formation of primordial black holes (PBHs) during a “window” in the early universe, followed by the formation of Planck-scale relics in the scaling regime, which may act as dark matter (DM) candidates [6, 7]. The length of this window is extremely sensitive to the KS warp factor and may be small, or comparable to the cosmological time-scale, depending on its value.

The root cause of this difference appears to be the existence of a time-dependent bead mass in the necklace model as opposed to the constant bead mass of true monopoles connected by strings. This arises from the time-dependence of the lifting potential and is a somewhat unexpected result. Previous investigations of string necklaces assumed the ex-

istence of a constant potential and hence a constant bead mass, though these were based solely on generic arguments [6]-[9]. Our model is the first explicit realisation of necklace formation in string theory and shows that these assumptions must be modified, at least for the class of backgrounds we consider.

This raises two interesting possibilities: Either the formation of necklace-like objects is possible *only* in string theory, or there exists a previously unknown solution in a dual four-dimensional gauge theory which is equivalent to the objects we have described.¹ Using data from the EGRET cosmic ray experiment [12]-[14], which provides a bound for the PBH density of the universe, we are also able to constrain the underlying string-theoretic parameters which define the KS geometry at the tip of the throat, namely the warp factor a_0 and the radius of the S^3 which regularises the conifold, R .

In the non-static case we see that the windings are dynamically stabilised due to the presence of the angular momentum term which interacts with the string tension to influence the dynamics of the loop. We see that it is possible for the loop to oscillate between alternate phases of contraction and expansion or to remain stable at a constant radius, depending on the value of a_0 . For $a_0^2 < 1/2$ the loop undergoes an initial phase of expansion before recollapsing but for $a_0^2 > 1/2$ the loop initially contracts. The critical case corresponds to $a_0^2 = 1/2$. The period of oscillation is also determined by the ratio of the initial loop radius to the square of the warping.

Although we do not present a detailed analysis of the cosmological effects of these objects, we note that, in principle, such oscillations should give rise to distinct gravitational wave (GW) signatures, the future detection of which could provide indirect evidence for the existence of extra dimensions.

In the final part of this thesis we investigate the relationship between wound strings in type IIB string theory and topological defect strings. We propose a modification of the standard Abelian-Higgs model which introduces spatial dependence into the scalar and vector field couplings, such that $\sqrt{\lambda} \rightarrow \sqrt{\lambda}^{eff}(z)$ and $e \rightarrow e^{eff}(z)$ in the Lorentz frame of the string. This leads naturally to an ansatz for a static, non-cylindrically symmetric solution of the resulting field equations, since these couplings imply the existence of spatial-dependence in the corresponding boson masses and their associated Compton wavelengths (which set

¹A third possibility arises, whereby topological defect strings in gauge theory models with extra dimensions wrap windings in the compact space, rather than F/D -string bound states. However, the existence of extra dimensions is optional in field theories, whereas string theory requires a ten or eleven-dimensional space-time manifold to ensure mathematical consistency [10, 11]. Therefore, although the existence of necklace-like objects does not *necessarily* provide evidence for string theory, any observations which favour a compact-dimensional model may be interpreted as lending support to the string paradigm. We will return to the interesting question of wound gauge field strings in greater detail in our discussion of “model mixing” at the end of chapter 5.

the length scales for the string core radii).

The field configuration describes a “pinch” which interpolates between degenerate vacuum states along the string, labelled by equal but opposite winding numbers $\pm|n|$. This corresponds to a vortex which shrinks until it reaches the Planck scale l_p and re-emerges as an anti-vortex, resulting in the formation of a bead pair, with one bead either side of the intersection. The solution is then topologically stable. The key assumption is that quantities such as phase and winding number, along with those which depend on them such as the magnetic flux of the gauge field, become undefined at the Planck scale so that one region may be joined to the next via a Planck-sized segment of “neutral” string. Although this necessarily involves several further, and admittedly speculative, assumptions about the Planck-scale physics of vortices, our conclusions are important because the effective models may be matched smoothly onto existing well known solutions valid at larger scales.

The underlying physics of this solution is, in principle, scale-independent. In both the standard and modified Abelian-Higgs models the phase θ acts as an order parameter, changes in which (we suggest) are defined over a minimum characteristic scale $\sim l_p$. Any field theory, or effective field theory model (such as a condensed matter system), which allows symmetry-breaking phase transitions to occur and which admits stable vortex solutions *must* be endowed with some form of order parameter, which may be defined over a characteristic scale much larger than l_p . The size of the “neutral string” segment between neighbouring vortex/anti-vortex regions would then be determined by the characteristic scale of the order parameter in question, though we note that some analogue of the spatially-dependent field couplings would also be required, in order to generate a non-cylindrical vortex solution.

This work is motivated by the results presented in chapters 3 and 4. As mentioned previously, there is no known field theory analogue of necklaces formed from extra-dimensional windings. In particular, there is no known way to produce string-monopole networks with time-varying bead masses. The question of whether a dual field theory model exists is important because, if necklace-type objects *are* string-specific, their predicted effects on observable cosmological parameters could be used to obtain experimental evidence in favour of string theory.

However, we propose the pinched string solution as a dual necklace model and argue that a time-dependent bead mass may be obtained. Similarities between the pinched string and the effective four-dimensional appearance of wound strings are discussed and a correspondence between Higgs model and string theory parameters is suggested. In particular, we equate the radius of the defect string (at critical coupling), $r_s \approx (\sqrt{\lambda}\eta)^{-1} = r_v \approx (\sqrt{2}e\eta)^{-1} = r_c$, with the radius of the compact space, R . This allows us to interpret the effective couplings $\sqrt{\lambda}^{eff}(z)$ and $e^{eff}(z)$ in terms of the effective radius of the windings $R^{eff}(z)$. In

the KS model, R is proportional to the square root of the string coupling $\sqrt{g_s}$, so that the wound-string embedding generates an “effective” coupling $g_s^{eff}(z)$, which may also be expressed in terms of field-theoretic parameters. Hence the (somewhat bizarre) phenomenological device introduced to obtain the pinched string solution admits a relatively natural interpretation in terms of the dual string picture.

In addition to equating r_c and R , we draw correspondences between string theory parameters and the symmetry-breaking energy scale η and topological winding number $|n|$. These suggest that the pinched string solution represents a generalisation of the Nielsen-Olesen vortex since we recover the standard $n = \pm 1$ duality for a string in flat space, proposed in [15], in the limit that the string becomes unwound. An unexpected implication of this work is that it casts doubt on the proposal that wound-string relics may be viable DM candidates, as suggested in some of the literature (see [6]-[9] and [16]), since the dual defect string necessarily includes a gauge field vortex, which implies that it may emit and absorb the associated bosons. In the Abelian-Higgs model, these bosons resemble photons (i.e., they are spin-1) with non-zero mass. The study of wound-string interactions and their associated duals, with particular focus on electromagnetic (EM), or similar gauge field emission, may therefore be a useful avenue for future research.

Finally, perhaps the most interesting result is an estimate of the mass of the toy Abelian-Higgs model bosons (at critical coupling) in terms of the KS model parameters. In principle, these may be constrained using a number of cosmological observations, including CMB anisotropy and power-spectrum data, constraints from baryogenesis and large-scale structure (LSS) formation and the extragalactic gamma-ray flux, as in chapter 3. This analysis also suggests that it may be possible to construct dualities between defects formed in more complex (and more realistic) non-Abelian gauge theories and string species formed in other string compactification schemes. We may imagine equating field theory and string theory parameters in these models and constraining the former via cosmological bounds on the latter. Ideally, one could even hope to infer bounds on the standard model Higgs mass from cosmological data, using models containing strings.

Although an analysis of all these possibilities is clearly beyond the scope of this thesis, the work presented here provides a useful contribution to the increasing body of literature which aims to probe the structure of extra dimensions (if they exist) and the phenomenology of the early universe using cosmic strings.

1.0.1 A note on additional work

As part of my PhD, I have also investigated astrophysical phenomena in models with large extra dimensions, focussing on gravitational collapse in the Randall-Sundrum brane-world.

While this work was carried out by myself and Prof. Harko at the University of Hong Kong, it was in part supported by my STFC studentship and undertaken while I was a registered PhD student at Queen Mary, University of London.

My original plan was for this work to be included in this thesis and for it to form a counterpart to the analysis of phenomenology in models with compact internal manifolds. However, due to space limitations, it was necessary to omit these results, so a brief summary is given below.

Following the Shiromizu-Maeda-Sasaki formulation [17, 18] of the Randall-Sundrum type II braneworld [19, 20], we solved the field equations for the spherically symmetric collapse of a null fluid described by the barotropic and polytropic equations of state [21], as well as for a Hagedorn fluid [22, 23] and for strange quark matter described by the so-called “bag” model (where the bag constant is estimated using first order QCD calculations) [24]. The general class of spacetimes which correspond to this process was found to be characterised by two arbitrary functions of the advanced Eddington time coordinate, which determine both the initial (generally inhomogeneous) distribution of matter and the time-dependent dynamics of the collapse. Using natural ansatz choices for these functions, the causal structure of the resulting singularities was determined for each fluid.

In each case, the number and positions of the horizons were found to depend on the parameters which determine the equation of state, suggesting that brane-world models may give rise to black holes with “null fluid hair” [25]-[27], that is, to singularities with causal structures which retain information about the process of collapse leading to their formation. These results suggest that the No Hair Theorems [28, 29] formulated in four-dimensional general relativity may not extend to higher-dimensional brane-worlds (see [30, 31] for related articles). The possibility of naked singularity formation at future null infinity was also investigated and its implications for the Cosmic Censureship Conjecture [32]-[37] were briefly discussed. Finally, the implications of this work for the so-called Information Loss Paradox [38]-[42], in which the condition for unitary evolution of a quantum mechanical system is apparently broken, were also considered. A full account of this work is given in [4].

CHAPTER 2

BACKGROUND: PRIMORDIAL BLACK HOLES, COSMIC STRINGS, EXTRA DIMENSIONS AND COSMIC NECKLACES

2.1 Primordial black holes - history and overview

The term primordial black hole (PBH) was first introduced to describe black holes which may have formed from the gravitational collapse of overdense regions in the early universe [43]-[45]. The extremely high cosmological density during the first few moments of the big bang meant that even small-scale fluctuations could create regions in which gravitational attraction was able to overcome the supporting radiation pressure. In pre-inflationary models the existence of large primordial inhomogeneities was simply assumed, though bounds resulting from the cosmological consequences of PBHs could then be used to constrain the perturbation spectrum [46]-[48].

In a simplistic analysis it is necessary to assume that the overdensities are spherically symmetric regions larger than the Jeans length λ_J (the wavelength below which stable oscillations rather than gravitational collapse will occur), but smaller than the horizon size [49], as perturbations on scales larger than the horizon would collapse to form separate, closed universes [45]. Here the Jeans length is simply $\sqrt{\gamma}$ times the horizon distance,

$$\lambda_J(t) = c_s(t) \left(\frac{\pi}{G\rho(t)} \right)^{\frac{1}{2}} \sim \sqrt{\gamma} ct \quad (2.1)$$

where c_s denotes the speed of sound, G is the (four-dimensional) Newton constant and γ is the constant of proportionality in the equation of state, $p = \gamma\rho$ ($0 < \gamma < 1$).

Combining these two considerations has two important consequences: first, that PBHs formed from the collapse of inhomogeneities should have a mass of the order of the horizon mass

$$M_H(t) \sim \frac{c^3 t}{G}; \quad (2.2)$$

and second, that the fractional overdensity at the horizon epoch δ must satisfy $\delta > \gamma$. Assuming the primordial density fluctuations to be Gaussian, the fraction of regions of

mass M_H which undergo gravitational collapse is given by

$$\beta(M_H) \sim \epsilon(M_H) \exp\left(-\frac{\gamma^2}{2\epsilon^2(M_H)}\right) \quad (2.3)$$

where $\epsilon(M_H)$ is the root-mean-square of the fluctuation amplitude at the time corresponding to the horizon mass M_H . Assuming also that the power spectrum of the fluctuations is Harrison-Zeldovich (scale-invariant), we see that PBHs formed in this manner will have an extremely extended mass spectrum. Those formed at the Planck time ($t_p \sim 10^{-34}$ s) have a mass of the order of the Planck mass ($m_p \sim 10^4 g$), whereas those formed at, for example, $t \sim 1$ s have masses of order $10^5 M_\odot$, comparable to the mass of the supermassive black holes thought to reside in the centres of galaxies [50].

Using (2.3) and the expression for the horizon mass (2.2), it is possible work out the number density of PBHs as a function of time and hence the mass-spectrum, which is given by equation (2.4).

$$\frac{dn_{PBH}}{dM} = (\alpha - 2) \left(\frac{M}{M_*}\right)^{-\alpha} M_*^{-2} \Omega_{PBH}(M) \rho_c(M) \quad (2.4)$$

Here $M_* \sim 10^{15} g$ is the current mass-spectrum cut-off due to Hawking evaporation [51]-[55], Ω_{PBH} is the total PBH density in units of the critical density ρ_c and

$$\alpha = \frac{1 + 3\gamma}{1 + \gamma} + 1. \quad (2.5)$$

This implies that the density of PBHs with masses greater than M scales as $M^{-\frac{1}{2}}$, so that, although the masses of individual PBHs may vary over an incredibly large range, most of the total mass formed from collapsing scale-invariant perturbations would be contained in the smallest ones.

This is significant as we would expect the Hawking radiation from low-mass PBHs to contribute to both the extragalactic gamma-ray background flux and the galactic gamma-ray flux, if some are clumped in galaxy halos. It is highly likely that the PBHs exhibit some degree of clumping as those with masses $M \geq 10^{15} g$ are dynamically cold at the present epoch and even those of mass $M \sim 10^{15} g$ will have been cold throughout the process of galaxy formation. PBHs are therefore viable cold dark matter (CDM) candidates and no constraints exist excluding them in either the sublunar mass range ($10^{20} g < M < 10^{26} g$) [56]-[58] or intermediate mass range ($10^2 M_\odot < 10^4 M_\odot$) [59, 60]. However, the tightest constraints on the cosmological density of PBHs across all mass ranges (excluding a small range $\sim 10^{13} - 10^{14} g$ in which the damping of CMB anisotropies dominates) come from the extragalactic photon background and from the effects of their evaporations on big bang nucleosynthesis (BBN) [63].

Hawking's radiation formula [51] shows that black holes radiate with a temperature

$$T_{BH} = \frac{\hbar c^3}{8\pi G M k_B} \sim 10^7 \left(\frac{M}{M_\odot} \right)^{-1} K, \quad (2.6)$$

and hence that they evaporate completely on a timescale

$$\tau(M) \sim \frac{\hbar c^4}{G^2 M^3} \sim 10^{64} \left(\frac{M}{M_\odot} \right)^3 \text{ yr}, \quad (2.7)$$

Applying this to the mass spectrum above, we see that the smaller black holes contribute the most energy to gamma-ray flux, so that the integrated emission may be approximated by its lower bound at $M_* \sim 10^{15}g$. PBHs with masses of this order are expected to produce gamma-rays with peak energy of order $100MeV$ at the current epoch [61] and comparing the expected emission with the observed flux in this range implies

$$\Omega_{PBH}(t_0) < 10^{-8} \quad (2.8)$$

which is equivalent to $n_{PBH}(t_0) < 10^4 \text{ pc}^{-3}$. Although many other models of PBH formation have now been studied (see [63, 64] and references therein), in most the masses are concentrated in a narrow range centred on the value given in equation (2.2), so that the bound (2.8) remains valid.

In particular, since the inception of the inflationary paradigm [65, 66] the quantum fluctuations predicted by various inflationary scenarios have been studied as a means of producing a primordial perturbation spectrum. In some of these scenarios the fluctuation amplitude decreases as the characteristic scale of the fluctuation increases, so that PBHs form shortly after reheating (see [67]-[68], plus additional references within the more recent articles [69, 70]). In others the power spectrum contains a peak (resulting in a peak in the function dn_{PBH}/M) or exhibits a running spectral index (see [57]-[59], plus references within [71]).

Whatever the underlying spectrum of density perturbations, the cosmological effects of PBHs may be grouped into three categories, determined by their mass: As already mentioned, PBHs with masses $M > 10^{15}g$ would survive today to contribute to the mass-density within the galactic halo. Large PBHs might also influence the development of LSS [72]-[74], seed supermassive black holes [75]-[76] and generate observable GW signatures [77]-[79]. PBHs with mass $M \sim 10^{15}g$ would contribute to both the galactic and extragalactic gamma-ray flux, but may also generate gamma-ray and radio bursts [80]-[82] and the annihilation line radiation emitted from the centre of the galaxy [83, 84]. Lastly, PBHs with masses $M < 10^{15}g$ will have completely evaporated by the present epoch, but may have

influenced processes in the early universe, such as entropy generation [85], baryogenesis [86]-[89], neutrino generation [84, 90] and reionisation [91, 92]. It has also been proposed that PBHs may swallow magnetic monopoles (providing a possible non-inflationary solution to the monopole problem) and puncture domain walls [93]-[95]. If black hole evaporation leads to the production of Planck-mass relics, as suggested by some authors (see [57, 68] and [96]-[99]), these may also contribute to the present CDM density. However, even if PBHs did not cause any of these effects, or even if they never existed, it is still useful to study them as each process outlined above is associated with an upper limit on the fraction of the universe's mass-density which goes into PBH production, and a corresponding limit on primordial inhomogeneities.

Several other mechanisms have also been proposed as a means of creating PBHs. Among these are:

- The collapse of over-densities during a temporary softening of the equation of state. In this scenario the pressure support is spontaneously removed when the mass-energy of the universe is channeled into the production of particles which are sufficiently massive to behave non-relativistically at their epoch of formation [100]-[102]. This may happen during a phase transition (for example, at the onset of the QCD era [103]-[104]) or during slow reheating after inflation [68]. In either case, it may be shown that the probability of PBH formation depends only upon the fraction of regions which are sufficiently spherical to undergo collapse [49, 100] and that, for any underlying perturbation spectrum, PBH masses are concentrated in a narrow range, associated with the phase transition epoch.
- The gravitational collapse of domain walls [105]. These walls must be both sufficiently large and closed, though suitable candidates could be formed during a second order phase transition in the vacuum state of a scalar field associated with inflation [106, 107]. The resulting PBHs would have a characteristic mass-scale corresponding to that of a thermal phase transition under equilibrium conditions, though non-equilibrium scenarios have also been invoked [108] and these imply an extended mass distribution (with a fractal structure of smaller PBHs clustered around larger ones) [109].
- The collision of bubbles of broken symmetry in the early universe [110, 111]. However, this requires the bubble formation rate to be finely tuned so that it is approximately equal to the Hubble rate. If it is much less, bubbles are very rare and never collide, whereas, if it is much greater, the entire universe undergoes a phase transition and bubbles do not form at all. PBHs formed via this mechanism would also have a characteristic mass of the order of the horizon mass at the symmetry-breaking epoch. Those formed at the GUT epoch, at electroweak unification and at the QCD (quark-hadron) phase transition would therefore have masses of order $10^3 g$, $10^{28} g$ and $M_\odot \sim$

$2 \times 10^{33}g$, respectively. The production of PBHs from bubble collisions at the end of inflation has also been studied in [112, 113].

- The collapse of cosmic string loops. In this scenario cosmic strings are formed during phase transitions in the early universe (see section 2.2.1 for a more detailed discussion of this topic). String loops then “chop-off” from the resulting network and shrink through the emission of gravitational radiation. Assuming that the network reaches a scaling regime [114], the radius of a typical loop will be larger than the Schwarzschild radius associated with its mass by a factor of $(G\mu)^{-1}$, where μ is the string tension (mass per unit length). However, in a small percentage of cases it is possible for the loop to enter a configuration in which its entire mass lies within the gravitational radius, causing it to collapse into a black hole. This process was first studied by Hawking [115], but this initial analysis has now been extended by a number of authors [116]-[122]. Generally, the probability of collapse depends on both μ and the string correlation scale ξ . For a scaling network it may be shown that PBHs form with equal probability at every epoch, resulting in an extended mass spectrum $M_{PBH}(t_i) \sim \mu t_i$, where t_i is the time of loop formation.

Although it is not yet clear which, if any, of these processes took place, the study of PBHs (or at least “mini” black holes, even if their origin was not strictly primordial) in each of the contexts above has nevertheless enabled cosmologists to gain valuable insights. In many cases these insights take the form of constraints, for example, on inflationary parameters, primordial fluctuations or the cosmic string number and mass-density. The latter mechanism, the formation of PBHs from the collapse of cosmic string loops, is of particular relevance to this thesis and is discussed more fully in the next section.

2.2 Cosmic strings - formation and evolution

2.2.1 Formation of topological defect strings

Cosmic strings are a type of topological defect [114],[123]-[125] which may have formed during symmetry-breaking phase transitions in the very early universe [127]-[131]. Although there is no conclusive evidence for their existence, theories of Grand Unification (see [132]-[134]) strongly favour the formation of zero and one-dimensional defects (i.e. strings and monopoles). In addition, it has recently been proposed that anomalous gamma-ray bursts at high redshifts may be interpreted as observational evidence for superconducting strings [135].¹

¹Most cosmological gamma-ray bursts (GRBs) may be separated into two distinct classes characterised by either long durations and soft emission spectra, or short durations and hard emission spectra, where an observer frame time of $t \sim 2s$ is usually taken as the separation line (see [136] for a review). Bursts in the first class, which generally originate in irregular galaxies undergoing intense star formation, are thought

In quantum field theories (QFTs), particles are created and annihilated by the action of field operators on the vacuum state of the theory. These operators correspond to gauge field variables in the Lagrangian of the theory and become operators when the theory is quantised. The group of gauge transformations which leave the Lagrangian invariant is called the gauge group G and determines the particle spectrum described by the theory. For example, standard electromagnetism is a $U(1)$ gauge field theory and the standard model is an $SU(3) \times SU(2) \times U(1)$ gauge theory.

However, finite-temperature corrections in QFTs lead to temperature-dependent effective potentials in the Lagrangian. This means that the field configuration can change as the potential changes shape according to temperature. At high temperatures the potential terms in realistic gauge field theories typically have one energetically favourable minimum, the position of which determines the vacuum expectation values (VEVs) of the field operators. At lower temperatures a new global minimum or a number of energetically favourable local minima may occur. These may be finite or infinite in number and may be degenerate. The temperature at which the new global minimum or new local minima become energetically favourable is called the critical temperature T_c and marks the point of a phase transition.

Symmetry-breaking occurs when the field configuration drops into one of these new minima, which typically reduces the gauge group of the Lagrangian to a subgroup $H \subset G$ (although it is possible to restore symmetry at low temperatures in some models [143]). The original symmetry is said to be spontaneously broken and the vacuum state now varies, either continuously or discontinuously, as a function of the spacetime coordinates. For example, in one of the simplest spontaneous symmetry-breaking models, the Abelian-Higgs model, the Lagrangian for a complex scalar field ϕ at the top of a “Mexican hat” potential obeys $U(1)$ symmetry and has VEV $\langle \phi \rangle = 0$. This symmetry is broken when ϕ falls to bottom of the potential and the scalar acquires a non-zero VEV such that $\phi = \eta e^{i\theta}$, where the

to be produced by type Ib/c supernovae (i.e., by the collapse of very massive stars). Bursts belonging to the second class typically occur in nearby (early) galaxies with little star formation, and are thought to be associated with mergers of compact binaries. However, recent observations of GRBs with highly energetic emission spectra, typical for long duration bursts, but short emission periods (namely GRB 080913 at $z=6.7$ [137] and GRB 090423 and $z=8.2$ [138]) do not fall into either of these progenitor models. In addition, the star formation rate (SFR) predicted on the assumption that *all* hard-spectrum GRBs are produced by collapsars is too high to be in good agreement with data obtained from high redshift galaxy surveys [139]. This implies the presence of other astrophysical objects in the early universe capable of producing highly energetic bursts, of which superconducting strings [140] may be the most plausible candidates. Such strings, oscillating in the presence of cosmological magnetic fields, act as superconducting wires and the induced current leads to the emission of highly beamed gamma-ray bursts from the cusp regions (see [141] for a recent article). In the model proposed by Cheng, Yu and Harko, strong magnetic fields are assumed to emanate from charged domain walls. They show that, using this assumption in conjunction with known constraints on cosmic string parameters, both the anomalous GRB results quoted above *and* the SFR inferred from recent galaxy survey data (see also [142]) may be accounted for. This work holds out the possibility that future high redshift GRB observations, corresponding to times before the epoch of star formation, may be able to demonstrate conclusively the existence, or non-existence, of superconducting strings.

real constant η is the radius of the S^1 which defines the minimum and $e^{i\theta}$ is the phase factor. Physically, η has units of mass and represents the symmetry-breaking energy scale.² In this case the phase acts as an order parameter and the S^1 is known as the vacuum manifold - the space of degenerate vacuum states which the field may adopt after the phase transition. This is illustrated for the Mexican hat potential $V(|\phi|) = \frac{\lambda}{2}(|\phi|^2 - \eta^2)^2$ (where λ is the dimensionless scalar field coupling) in figure 2.1.

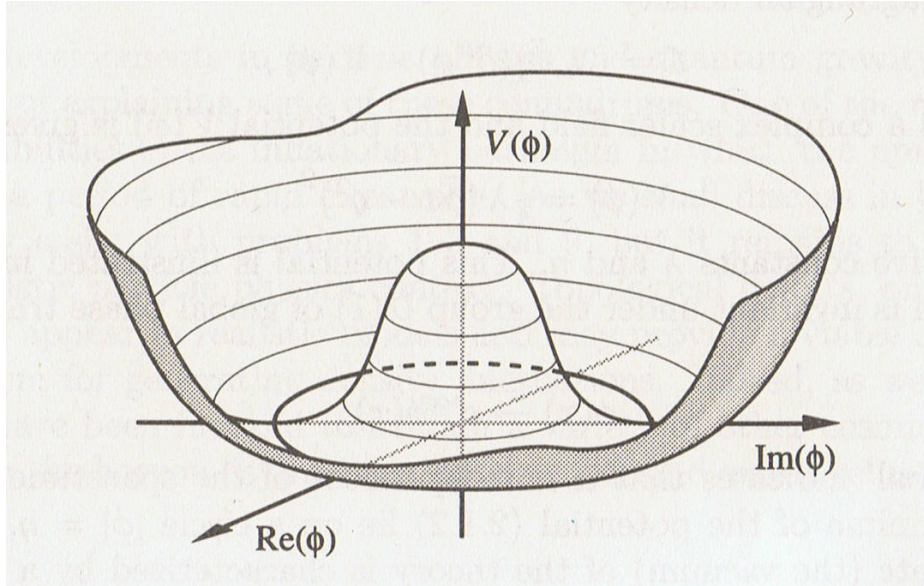


Figure 2.1: The Mexican hat potential for a broken $U(1)$ symmetry group showing a degenerate circle of minima. Taken from Vilenkin and Shellard [114].

In general the details of the symmetry-breaking process determine the vacuum manifold M in that $M = G/H$. The topology of the vacuum manifold is key to the formation of topological defects. For example, in the case of the Abelian-Higgs model, it is possible to imagine a configuration where, as one circles a particular point in the plane, the phase θ varies continuously between $0 \leq \theta < 2\pi n$ ($n \in \mathbb{Z}$). Such a configuration is known as a vortex and a continuum of vortex “slices” threading a section of three-dimensional space forms a cosmic string, whose mass per unit length (or tension) μ is related to the symmetry-breaking energy scale η , and the topological winding number n such that $\mu \propto \eta^2 n^2$. This is illustrated for an $n = 1$ vortex string by figures 2.2 and 2.3.

The string is topologically stable as there exists no diffeomorphism (that is, no continuous deformation) which will map the configuration of vacuum states into a uniform or random

²Note that when $\langle \phi \rangle = 0$ the phase of the complex field is undefined and so can be set equal to zero (i.e. $\theta = 0$) without loss of generality. In this model, at high temperatures such that $E > \eta$, the field has enough energy to “sit” at the top the potential (i.e. at the maximum where $\langle \phi \rangle = 0$), whereas at lower temperatures ϕ rolls down the potential slope to the circle of degenerate minima.

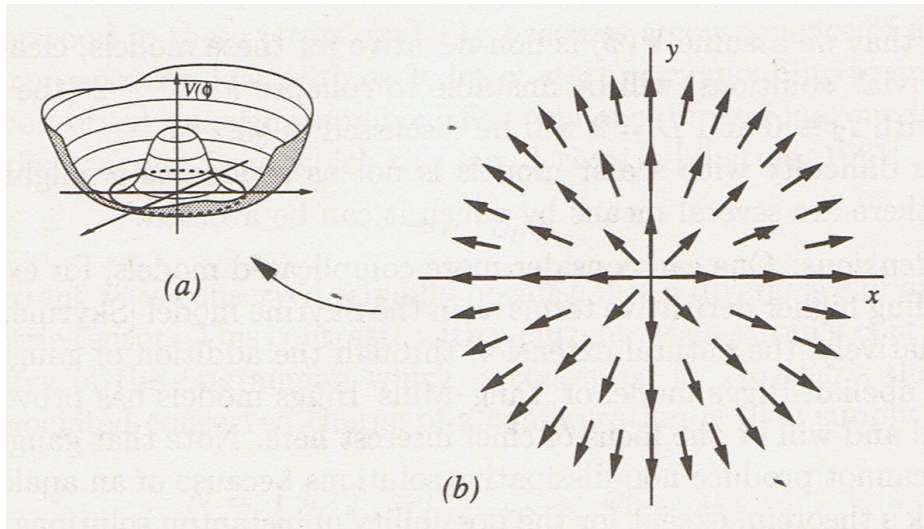


Figure 2.2: Field configuration for a vortex string (b). A loop in physical space enclosing the vortex is mapped non-trivially into the degenerate circle of minima of the potential shown in (a). For a string with winding number $\pm n$, the circle of degenerate minima is traversed completely either clockwise (+) or anti-clockwise (-) (by convention) $|n|$ times as the loop is traversed in physical space. Taken from Vilenkin and Shellard [114].

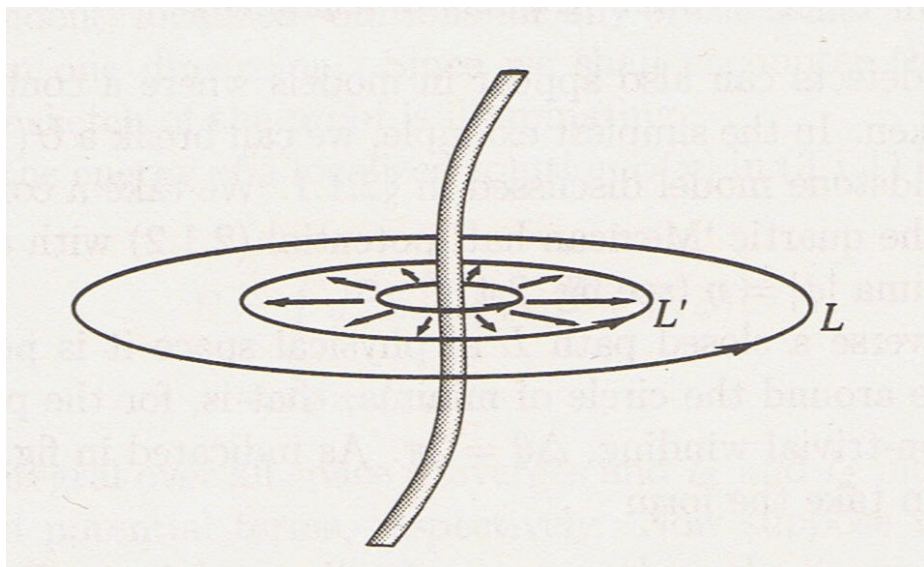


Figure 2.3: The string in three dimensions can be located by encircling it with a closed loop L . A non-zero winding number in the phase as the loop is traversed discloses the string within. Taken from Vilenkin and Shellard [114].

distribution. The VEV at the centre of the vortex is still $\langle\phi\rangle = 0$ (its pre-symmetry-breaking value) and the field at this point in space still lies at the top of the potential $V(|\phi|)$ ³ but the VEV of the scalar field tends asymptotically to the *post*-symmetry-breaking value η , so that

$$\phi_n(r, \theta) = \eta f(r) e^{in\theta} \quad (2.9)$$

where $f(r)$ is a dimensionless function with real values such that

$$\begin{aligned} f(r) &\rightarrow 0, & r &\rightarrow 0 \\ f(r) &\rightarrow 1, & r &\rightarrow \infty. \end{aligned} \quad (2.10)$$

One way to ensure that f is dimensionless is to rescale the r -coordinate so that it too is dimensionless, though we will leave our discussion of the appropriate scale to use until the end of this section.

If only the kinetic and potential terms for a complex scalar field are present in the Lagrangian of the theory, a global $U(1)$ symmetry exists and the resulting string, described above, is known as a global string. One, potentially unattractive, feature of global strings is that their tension is logarithmically divergent at large and small r [114, 124]. Physically, this problem is resolved by introducing an upper cut-off Δ corresponding to the distance between neighbouring strings and a lower cut-off δ corresponding to the width of the string core, so

$$\mu \sim 2\pi\eta^2 n^2 \ln\left(\frac{\Delta}{\delta}\right). \quad (2.11)$$

On dimensional grounds, one expects $\delta \sim (\sqrt{\lambda}\eta)^{-1}$. However, one way to obviate the need for taking the upper cut-off Δ to be the inter-string distance (which is potentially *very* large on cosmological scales) is to introduce a gauge field contribution. In this case the symmetry-breaking process is similar, but the broken symmetry is now a local $U(1)$ symmetry and the resulting string is known as a local, or gauge string. Taken schematically, the figures above may then represent not only the configuration of the scalar field (where the arrows in the vortex represent the phase of the complex scalar ϕ) but also the vortex structure of the gauge field, whose only non-zero component is the angular component A_θ . In order to cancel the logarithmic contributions to the energy density from the scalar field at large distances, the value of the gauge field must also be proportional to the winding number n ,

³In fact, along the centre of the string the symmetry is essentially *unbroken* and in this respect a cosmic string may be thought of as a line-like section of “ancient space” in which the the high temperature gauge symmetries of the field Lagrangian and the corresponding energy-density are preserved.

with opposite sign [114, 124]. We may then label the resulting field by ⁴

$$A_{n\theta}(r) = -\frac{n}{er}\alpha(r) \quad (2.12)$$

where e is the (dimensionless) gauge coupling and $\alpha(r)$ is also a dimensionless function such that

$$\begin{aligned} \alpha(r) &\rightarrow 0, & r &\rightarrow 0 \\ \alpha(r) &\rightarrow 1, & r &\rightarrow \infty \end{aligned} \quad (2.13)$$

if we work with a rescaled r -coordinate. Note that the factor of e in the denominator is necessary so that the magnetic flux Φ_n is quantised in units of the basic quantum $\frac{2\pi}{e}$ [15],

$$\Phi_n = \oint_B A_{n\theta} r d\theta = \frac{2\pi n}{e} \quad (2.14)$$

where the subscript B in the integral indicates the boundary at $r \rightarrow \infty$. Hence the gauge field also adopts a vortex configuration, with equal but opposite vorticity to the scalar field, and the resulting tension for the gauge string is

$$\mu = 2\pi\eta^2 n^2 \ln\left(\frac{r_v}{r_s}\right) \quad (2.15)$$

where r_v and r_s are the widths of the vector and scalar cores, respectively. Physically we require $r_v \geq r_s$, but both these values may be estimated directly by considering a more detailed analysis of the behaviour of the fields. ⁵

The Lagrangian density for full the Abelian-Higgs model, with $A_\mu \neq 0$, is simply the sum of the kinetic energy and gradient energy terms for both the scalar and vector fields (including interaction terms) and the potential. Using the (+ - - -) metric convention, this may be written succinctly in terms of the covariant derivative D_μ as

$$\mathcal{L} = \overline{D}_\mu \bar{\phi} D^\mu \phi - \frac{1}{4} F^{\mu\nu} F_{\mu\nu} - \frac{\lambda}{2} (|\phi|^2 - \eta^2)^2 \quad (2.16)$$

⁴Here we quote the standard results given in the literature (see [15, 114, 124, 125]). In chapter 5 we review the validity of the ansatz choice for A_θ , given in these sources, within the context of a fully covariant approach to the Abelian-Higgs vortex. As we shall see, the expression (2.12) is *not* consistent with the usual definition of the covariant derivative. We propose a fully covariant derivation of the equations of motion, though our results do not differ substantially with those presented in this chapter, and which may be found in the usual references.

⁵A subtlety arises here as may be shown that, in the so-called Bogomol'nyi limit (i.e. critical coupling $r_s = r_v \equiv \sqrt{\lambda}/\sqrt{2}e = 1$), the tension of a *stable* gauge string is $\mu = 2\pi\eta^2|n|$. However, we postpone discussion of this point until chapter 5, when the tension of the Abelian-Higgs string will be dealt with in detail.

where

$$D_\mu = \partial_\mu + ieA_\mu \quad (2.17)$$

and $F_{\mu\nu}$ is the usual EM field tensor,

$$F_{\mu\nu} = \partial_\mu A_\nu - \partial_\nu A_\mu. \quad (2.18)$$

This is manifestly invariant under the group of $U(1)$ gauge (i.e. local) transformations,

$$\begin{aligned} \phi(x) &\rightarrow e^{i\Lambda(x)}\phi(x) \\ A_\mu(x) &\rightarrow A_\mu(x) + e^{-1}\partial_\mu\Lambda(x) \end{aligned} \quad (2.19)$$

where $x = x^0, x^1, x^2 \dots$ are the spacetime coordinates and $\Lambda(x) \in \mathbb{R}$, even though the underlying vacuum state after sponaneous symmetry-breaking is not.

The gauge bosons corresponding to the quantized fluctuations of both the scalar and vector fields in the radial direction of the configuration space (in the post-symmetry-breaking field configurations) now acquire masses, which we label m_s and m_v , respectively. Rewriting the complex scalar ϕ in terms of two real scalars ϕ_1 and ϕ_2 with zero VEVs

$$\phi = \eta + \frac{1}{\sqrt{2}}(\phi_1 + i\phi_2), \quad (2.20)$$

allows us to rewrite the Lagrangian as

$$\mathcal{L} = \frac{1}{2}(\partial_\mu\phi_1)^2 - \frac{1}{2}m_s^2\phi_1^2 - \frac{1}{4}F^{\mu\nu}F_{\mu\nu} + \frac{1}{2}m_v^2A_\mu A^\mu + \mathcal{L}_{int} \quad (2.21)$$

where

$$\begin{aligned} m_s &= \sqrt{\lambda}\eta \\ m_v &= \sqrt{2}e\eta \end{aligned} \quad (2.22)$$

and \mathcal{L}_{int} contains all cubic and higher order terms. Thus the spontaneous symmetry-breaking does not result in the production of a massless (Goldstone) boson, as may have been expected to result from angular fluctuations, but the corresponding degree of freedom is absorbed into the vector field which now has three independent polarisations instead of the usual two. We also expect the Compton wavelengths corresponding to these mass scales to serve as good order of magnitude estimates of the radii of the scalar and vector vortex cores, r_s and r_v , introduced above:

$$\begin{aligned} r_s &\approx (m_s)^{-1} = (\sqrt{\lambda}\eta)^{-1} \\ r_v &\approx (m_v)^{-1} = (\sqrt{2}e\eta)^{-1} \end{aligned} \quad (2.23)$$

where $r_v > r_s \equiv \sqrt{\lambda}/\sqrt{2}e > 1$ corresponds to a type II superconducting regime. The creation of massive vector bosons is a generic feature of all Higgs field mediated symmetry-breaking processes, although the example discussed here is the simplest, and for non-Abelian models the number of massive bosons produced is equal to the number of unbroken symmetry generators [114]. Returning to the question of rescaling the r -coordinate, we see that r_s and r_v - which are well defined to within an order of magnitude - are natural scales to use in redefining the scalar and vector field ansatzes, which now become

$$\begin{aligned}\phi_n(R_s, \theta) &= \eta f(R_s) e^{in\theta} \\ A_{n\theta}(R_v) &= -\frac{n}{er} \alpha(R_v)\end{aligned}\tag{2.24}$$

where

$$R_s = \frac{r}{r_s}, \quad R_v = \frac{r}{r_v}.\tag{2.25}$$

Technically, the form (2.24) is found to be most convenient when determining (and solving) the equations of motion for the vortex configuration. Although exact solutions are not known, approximate asymptotic and small r solutions for the scalar field of the global string and for both the scalar and vector fields in the case of local strings may be obtained. These solutions are used to calculate the string tension by substituting into the standard formula

$$\mu_n = \int r d\theta dr \left[|\nabla\phi|^2 + \frac{1}{2}(\vec{E}^2 + \vec{B}^2) + V(|\phi|) \right].\tag{2.26}$$

which gives the results (2.11) and (2.15) quoted above.⁶ The Euler-Lagrange equations for the Abelian-Higgs model, and their solutions, will be studied extensively in chapter 5.

However, cosmic strings are not the only kind of topological defects able to form during cosmological phase transitions. If the vacuum manifold is disconnected, it is possible to form domain walls - two-dimensional kink-like soliton solutions which interpolate between disconnected minima in the vacuum manifold and mark the transition between regions of physical space in different degenerate vacuum states. It is also possible to form zero-dimensional defects such as magnetic monopoles (which form generically in any phase transition which leaves a $U(1)$ subgroup belonging to H) and three-dimensional configurations known as textures.⁷

As stated above, the type of defects which form in a given phase transition depends on the topology of the vacuum manifold. In particular, this is determined by the structure of

⁶The three terms in (2.26) represent the contributions to the total energy density of the vortex caused by the scalar field gradient, the magnetic flux and the potential, respectively.

⁷In theories containing extra dimensions the possibility of forming higher-dimensional textures also arises.

its homotopy groups. The m^{th} homotopy group $\pi_m(M = G/H)$ classifies distinct mappings from the m -dimensional sphere S^m into M . If M contains disconnected components, different types of domain walls (classified by the freely homotopic conjugacy classes of $\pi_0(M)$) may be formed. If M is *not* simply connected, i.e. if it contains unshrinkable loops, different types of strings (classified by the conjugacy classes of $\pi_1(M)$) may form. If M is simply connected, different types of monopoles (classified by the conjugacy classes of $\pi_2(M)$) may occur. Higher dimensional textures are classified by the conjugacy classes of the third homotopy group $\pi_3(M)$. Clearly, each string species in the Abelian-Higgs model is classified simply by specifying the winding number n , so that $\pi_1(M = S^1) = \mathbb{Z}$ and each conjugacy class contains a single element of $\pi_1(M = S^1)$. However, for vacuum manifolds with non-Abelian first homotopy groups, strings must be classified by the loop automorphism classes of $\pi_1(M)$ (see [114, 123]).

2.2.2 String evolution

After the initial phase transition it is believed that the cosmic strings should form a network, with individual strings threading their way continuously through a volume of free space of order ξ^3 , where ξ is the correlation length of the symmetry-breaking field [114, 123]. This determines the characteristic scale of the string network, or equivalently the typical length of a segment of “long” string. The energy density of the string network at any point in time, denoted $\rho_\infty(t)$, is then given by

$$\rho_\infty(t) = \frac{\mu}{\xi^2(t)} \quad (2.27)$$

where we note that the correlation length itself is time-dependent. However, when sections of the string network collide, there is a non-zero probability that the resulting string loop will “chop-off” from the network. For intersecting strings, specified by the elements $a, b \in \pi_1(M)$ belonging to distinct conjugacy classes, it may be shown that there exists a correspondence between a curve L enclosing the intersection and the class associated with the element $aba^{-1}b^{-1}$ [114]. For Abelian groups $\pi_1(M)$, $aba^{-1}b^{-1} = I$ (where I is the identity element) and the strings may simply pass through one another, as no topological obstruction exists to prevent this. Alternatively, it is possible for the product element $(ab)^{-1}$ to define a vertex from which both a and b emanate. Finally, if $a = b$, complete reconnection may occur where a and b “exchange partners” This is referred to as intercommutation and is the process which results in loop formation when single strings intercommute with themselves.

While all three of these outcomes are topologically acceptable, which process in fact occurs is determined by the string dynamics [114]. For strings classified by non-Abelian groups $\pi_1(M)$, $aba^{-1}b^{-1} = g$, where in general $g \neq I$. In this case, the intersection of

two such strings results in the formation of a third string, specified by the conjugacy class associated with the element g , which stretches between a and b . However, as we will deal mainly with Abelian strings in the course of this thesis, we now return to a discussion of the consequences of string intercommutation.

Following the chopping off of a loop from the network, resulting from a single string intercommuting with itself, the loop is free to “wobble” in free space, causing it to emit gravitational radiation and shrink according to

$$l(t, t_i) = l(t_i) - \Gamma\mu G(t - t_i) \quad (2.28)$$

where $l(t_i)$ is the loop length at the time of formation, Γ is a constant which determines the rate of radiative loss (determined by numerical simulation) and μ is the string tension. The precise network dynamics are extremely complicated but an important simplifying assumption can often be made which is in good agreement with more advanced simulations. In the one-scale model [144]-[146] it is assumed that the typical size of a loop l which chops-off from the network at t_i is some significant fraction α of the horizon size.

This scaling behaviour occurs as a result of the interaction of different processes affecting the evolution of the network: expansion due to the Hubble flow and entropic considerations favouring the complete fragmentation of the network into separate loops (see [147]-[150]). The two processes effectively compete to respectively increase/decrease the characteristic scale of the network, resulting in steady-state scale-invariant evolution. The expression for $l(t_i)$ is therefore

$$l(t_i) = \alpha t_i \quad (2.29)$$

where $0 < \alpha < 1$ and numerical simulations (for a single string species in a Friedman-Robertson-Walker (FRW) background) suggest a value for α of around 5×10^{-3} [114]. Note that here we are also using natural units so that $c = 1$. Using these assumptions, it is possible to compute the number density of loops of a given length l at time t in both the radiation and matter-dominated eras,

$$\begin{aligned} n_r(l, t) &\sim \frac{\nu_r}{t^{\frac{3}{2}}(l + \Gamma G\mu t)^{\frac{3}{2}}} \\ n_m(l, t) &\sim \frac{\nu_m}{t^2(l + \Gamma G\mu t)^2} \end{aligned} \quad (2.30)$$

where ν_r and ν_m are the number of long strings per Hubble volume in each era, respectively. These parameters are determined by the correlation length and, in the radiation era, the characteristic size of the loops which chop off from the string network. At very early times the string experiences a damping force due to the high background radiation density which

also damps the evolution of the correlation length of the network according to

$$\xi(t) \sim (t_d t)^{\frac{1}{2}} \quad (2.31)$$

where t_d is the characteristic time-scale for the damping, which is generally temperature-dependent. At later times the correlation length is expected to scale with the horizon size, so that

$$\xi_i(t) = \gamma_i t, \quad i \in \{r, m\} \quad (2.32)$$

where $0 < \gamma_i < 1$. Here the γ s are simply numerical constants and are not related to the equation of state, as in section 1.1. It may be shown that they are related to the root-mean-square velocity of the string (in each epoch) $\langle v_i^2 \rangle$ and to the measures of loop formation efficiency c_i via [114, 125]

$$\begin{aligned} c_r &= (1 - \langle v_r^2 \rangle) \gamma_r \\ c_m &= \frac{2}{3} (1 - 2 \langle v_m^2 \rangle) \gamma_m. \end{aligned} \quad (2.33)$$

The parameters ν_r and ν_m are then given by

$$\begin{aligned} \nu_r &= g c_r \sqrt{\alpha} \gamma_r^{-3} = g \sqrt{\alpha} (1 - \langle v_r^2 \rangle) \gamma_r^{-2} \\ \nu_m &= g c_m \gamma_m^{-3} = \frac{2}{3} g (1 - \langle v_m^2 \rangle) \gamma_m^{-2}, \end{aligned} \quad (2.34)$$

where g is a Lorentz factor, so that $\nu \sim \xi^{-3}$ in each case, as expected. From a simplistic analysis it is then possible to estimate the number of string loops which will, by chance, wiggle themselves into a configuration which is sufficiently spherical and sufficiently compact that the entire mass of the string lies within its own Schwarzschild radius. The fraction is given approximately by

$$f \sim (G\mu)^{2p-4} \quad (2.35)$$

where p is the number of approximately straight segments of the loop [115]. Although this analysis has been refined by numerical simulations [116, 117], it is clear that the fraction of loops undergoing collapse to form PBHs must be extremely small and is usually taken to be of order $f \sim 10^{-20}$. However, using equations (2.30) and (2.35), it is possible to estimate the mass-spectrum and density of PBHs formed in this way. Current constraints on their total density from the observed gamma-ray background at 100 MeV (taken from the EGRET experiment [12]-[14]) are comparable to the gamma-ray constraints on PBHs formed from cosmological density perturbations, namely $\Omega_{PBH}(t_0) < 10^{-9}$ [118]. Clearly, the exact constraints on $\Omega_{PBH}(t_0)$ implied by the data depend on the underlying mass spectrum and therefore on the mechanism(s) responsible for PBH formation. However, it seems reasonable to assume that $\Omega_{PBH}(t_0) < 10^{-9} - 10^{-8}$ gives a ‘‘ball park’’ upper bound for the PBH contribution to the current mass density of the universe.

2.2.3 String theory models: extra dimensions, cycloops and necklaces

Since the second superstring revolution ⁸ in the late 1990s cosmologists have become increasingly interested in the phenomenological implications of string theory. Indeed, as “stringy” effects such as the production of new types of particles and physics beyond the standard model are only likely to occur at very high energies, the early universe may prove to be a valuable testing ground for the theory. Much energy has therefore been devoted not only to explaining current phenomenological paradigms, such as inflation, in terms of string theory but also to the the study of potentially unique string phenomenology in cosmology.

An example of the latter approach is a series of papers by Avgoustidis and Shellard [16, 154], in which they consider cosmic strings wrapping non-trivial cycles in compact extra dimensions. Superstring theory requires the existence of nine spatial dimensions and one time dimension for mathematical consistency [10, 11]. As only three spatial dimensions are observed in our universe, one explanation for the apparent absence of the other six is that they are compactified on an internal manifold too small to be observed at ordinary length/energy scales, or those available in current particle accelerators. ⁹ For mathematical consistency it is also necessary that the internal manifold belong to a class known as Calabi-Yau (CY) manifolds, that is, Ricci-flat Kahler manifolds [157]-[160].

In [16] the authors considered an internal manifold which is not simply connected. In their scenario the end points of the string are free to move in the extra dimensions as long as it is connected to the cosmic string network, creating windings. However, when a string intercommutes with the network and chops off to form a loop, these windings become topologically trapped, forming an object they called a “cycloop”. The cycloop then shrinks as it loses mass-energy through the emission of GWs, eventually forming what appears to be a massive point-like particle from a four-dimensional perspective, that is, a type of monopole which only interacts with the rest of the universe gravitationally and acts as a DM candidate.

In particular, Avgoustidis and Shellard proposed two cosmologically viable winding formation mechanisms, the random walk and velocity-correlations regimes. In the first of these the “end point” of the string - the point which later intersects with the network and chops off to form a loop - undergoes continuous random motion in the compact space, prior to loop formation. In the second, the movement of the string in the extra dimensions is

⁸The term “second superstring revolution” refers to the discovery of D_p -branes [151]. Polchinski [152, 153] later showed that the p -dimensional hypersurfaces on which open strings could end were solitonic, thereby opening up the possibility that our universe exists as a three-dimensional hypersurface (D_3 -brane) in a higher-dimensional “bulk” space.

⁹However, there is some hope that extra-dimensional effects will be observable at future colliders. If at least some of the directions in the internal manifold are of order $0.1mm$, then the fundamental Planck mass is reduced to the TeV scale, which will be within the reach of the Large Hadron Collider (LHC) [49, 156]

coherent (i.e. correlated) over some time t_{cor} , but changes direction randomly after at the end of each coherent phase. If the velocity of the string end-point in the extra dimensions v_E is constant, this will result in correlated windings occurring over some length scale $\xi_{cor} \sim v_E t_{cor}$.¹⁰ In the random walk regime, therefore, the number of windings $n_w(t_i)$ contained in a string loop of initial length $l(t_i) = \alpha t_i$ is given approximately by

$$n_w(t_i) \approx \frac{\sqrt{\alpha \omega_l \epsilon_l t_i}}{R} \quad (2.36)$$

where ω_l is the total fraction of the string length present in the windings, $\epsilon_l < \xi_{cor}$ is the step length and R is the radius of the extra dimensions. In the velocity correlations regime the equivalent expression is [16]

$$n_w(t_i) \approx \frac{\omega_l \alpha}{R} t_i. \quad (2.37)$$

The two scenarios are illustrated schematically in figures 2.4 and 2.5.

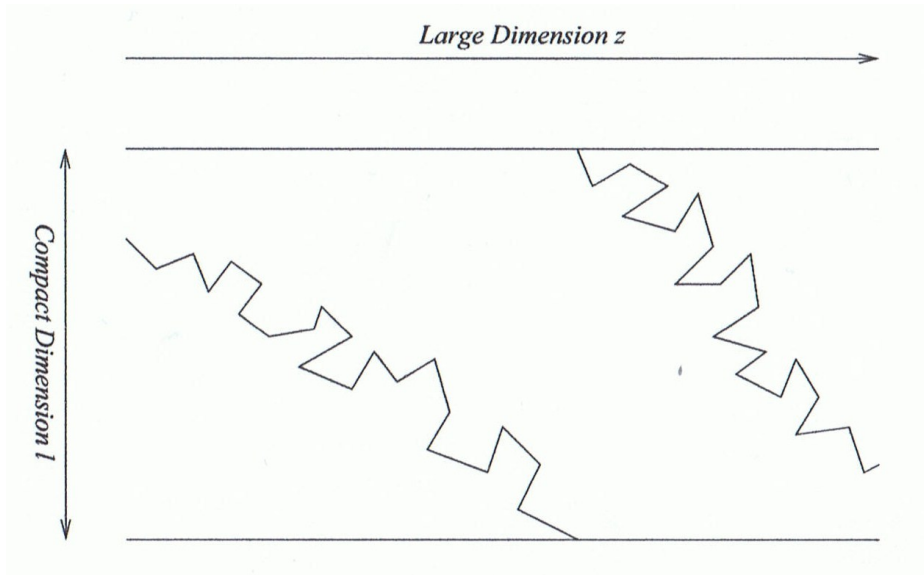


Figure 2.4: Winding formation in the random walk regime. The spatial structure of the strings in the extra dimensions, which is assumed to be Brownian, can give rise to non-trivial windings. Taken from Avgoustidis and Shellard [16].

Finally, we note that the presence of velocity-correlations is likely to lead to the presence of a non-zero angular momentum the compact space. This leaves open the possibility

¹⁰In chapters 3 and 5 we investigate the possibility of identifying the correlation length ξ_{cor} for F/D -strings with extra-dimensional windings with the ordinary definition of the correlation length ξ which, as stated above, is the characteristic scale of the string network (or equivalently the typical length scale of a long string segment). In chapter 5 we will also investigate the possibility of identifying this with the length scale over which successive vortex slices of a topological defect string with winding number n are correlated.

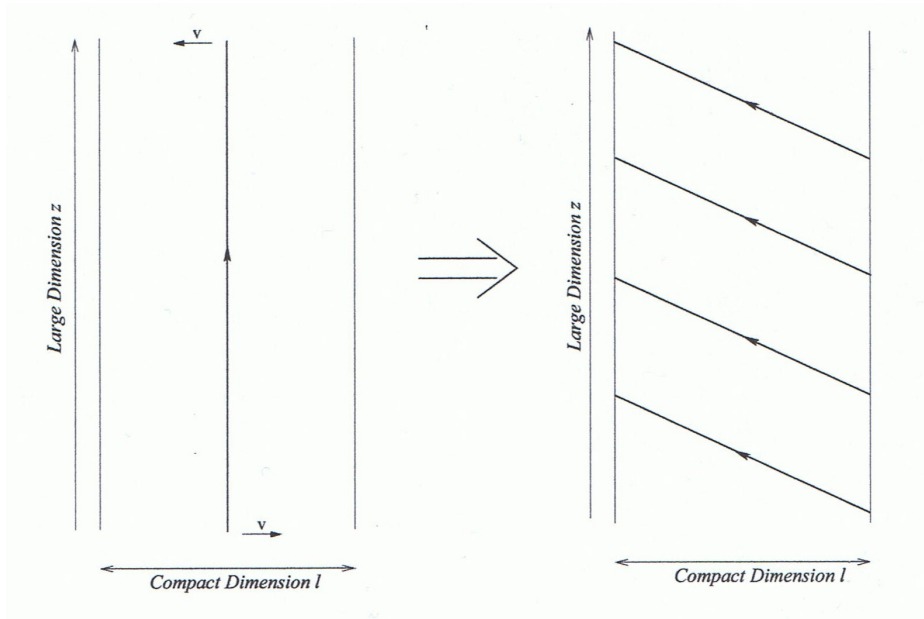


Figure 2.5: Winding formation in the velocity-correlations regime. String velocities in the extra dimensions cannot be correlated over distances greater than the correlation length of the network at the time of loop formation $\xi(t_0)$. Thus the endpoints of a string segment of length $\xi(t_0)$ can be expected to have different velocities. This would tilt the string, as shown, to produce windings. Loops which then chop off from the network, even on scales $l(t_i) = \alpha t_i < \xi(t_i)$, will also contain non-trivial windings. Taken from Avgoustidis and Shellard [16].

of dynamical stabilisation for the windings, even for spaces with simply connected internal manifolds - such as the KS geometry [5] - leading to the existence of “non-topological cycloops”. This possibility is explored in chapter 4 but we point out here that, even in the case of *static* strings wrapping a simply connected space, there exists an alternative stabilisation process which results in the production of at least quasi-stable windings, which persist over some period Δt .

As an alternative to cycloops Matsuda argued that in realistic string theory scenarios the end points of the string would not be free to move in the extra dimensions due to the presence of a “lifting potential” [6]-[9]. In reality the lifting potential is a geometric effect which results from the way the string wraps the internal space during the winding formation process. Physically, the distribution of the string tension (viewed as a *vector* quantity, i.e. as orientated along the direction of the string) is determined by the initial form of the windings. This determines the subsequent evolution and what stable (or quasi-stable) state is formed. The string acts as though it were in the presence of a potential energy density which is a function of the spatial coordinates of the compact dimensions - that is, as though it were in the presence of a potential which “lifts” the extra dimensions. Mathematically this is expressed via the Hamiltonian, which depends on both the metric $g_{\mu\nu}$ and the ansatz for the string configuration (see chapter 3).

In particular, Matsuda proposed that, if the potential contains a number of degenerate minima, then kink-type solutions would exist, in which the string interpolates between potential wells in the compact directions. From a four-dimensional perspective these kinks appear as beads on the string. The mass of the beads is then determined by the height of the potential hill which the end of string “overcame” in the internal directions in order to reach the new minimum. Figure 2.6 illustrates this scenario and is taken from [8]. The bottom picture shows a generic example of a lifting potential along one of the compact directions, while the difference between cycloops and necklace-windings is indicated in the two pictures above. A necklace configuration is illustrated schematically in the case of an S^1 internal manifold in the picture on the right.

This raises another interesting possibility. If the string configuration in the compact dimensions is now fixed by the potential, the string need not wrap non-trivial cycles in the internal manifold to ensure stability.¹¹ Indeed, as stated above, it is not even necessary that the internal manifold be simply connected. This means that the mass-energy contained in the extra dimensions - that is in the beads - is not topologically trapped.

In this scenario necklace loops chop off from the network and shrink through the emis-

¹¹However, there remains a subtlety here regarding whether integer windings are necessary in order to ensure the presence of a lifting potential initially. This matter is discussed in greater detail in chapter 3.

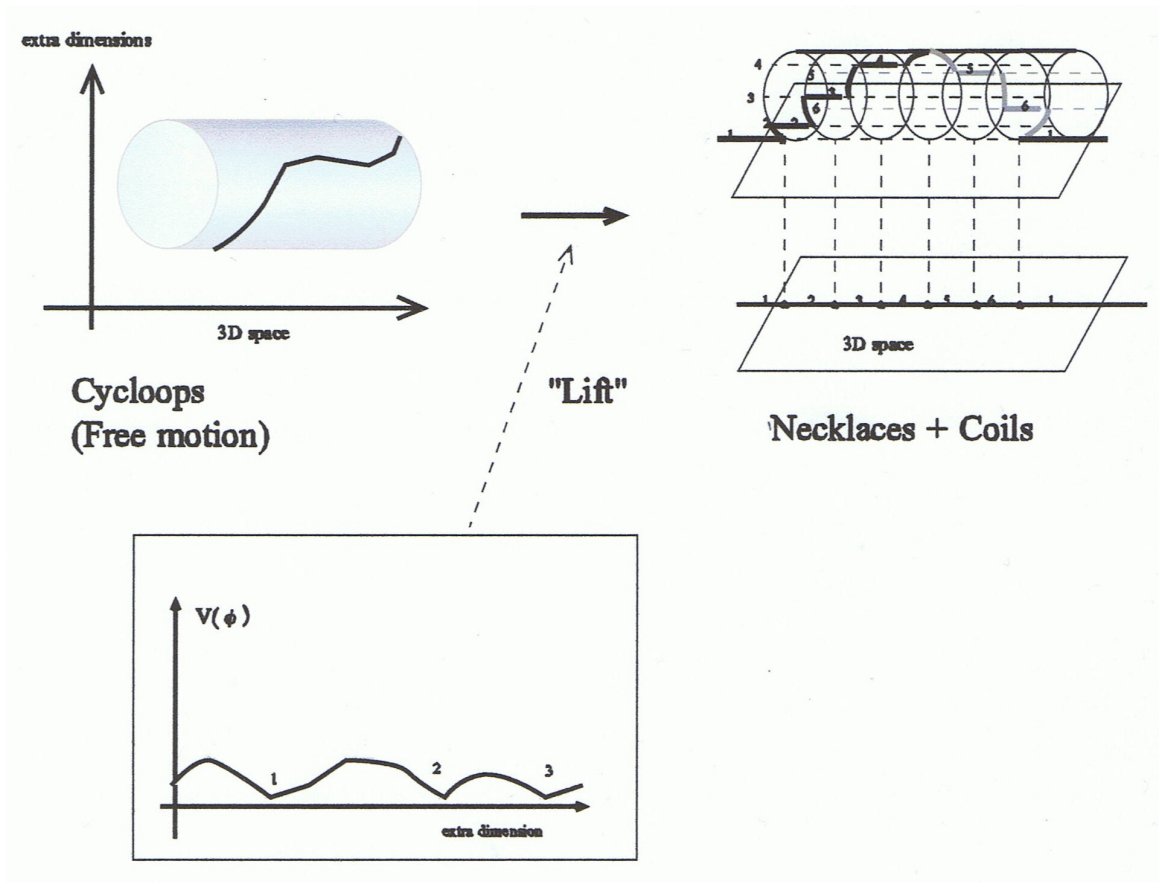


Figure 2.6: This figure illustrates the difference between cycloids and necklace coils. A schematic representation of a periodic lifting potential V with degenerate minima (as a function of the spatial coordinates of the extra dimensions) is given below and its impact on winding formation is illustrated in the two pictures above. The right-hand-side shows a schematic representation of a necklace configuration for windings around an S^1 compact manifold. Taken from Matsuda [8].

sion of gravitational radiation in the usual way. In principle, this may reduce the inter-bead distance but not the bead mass, which remains “trapped” in the extra dimensions by the presence of the lifting potential.¹² If sufficient mass remains in the form of beads for the Schwarzschild radius to be larger than the final loop radius (which is limited by the fundamental string width), then the necklace collapses to form a black hole. The key difference between this scenario and the one proposed by Avgoustidis and Shellard is that, as the bead mass is not topologically trapped, collapsing necklaces form black holes which decay via Hawking evaporation, rather than DM monopoles which cannot decay, even if their mass is sufficiently concentrated to fall within the Schwarzschild radius.

In fact, it is also possible for the necklace to wrap non-trivial cycles if the compact manifold, or part of the compact manifold, is not simply connected. In this case, after collapse, some of the bead mass will be emitted as Hawking radiation and we may conjecture that the remaining topologically trapped mass of the string (from windings in the non-simply-connected part of the internal space) will produce a DM relic which survives the black hole’s evaporation. In addition, if the compact dimensions are of the order of the Planck-scale, then the resulting relics will be of the order of the Planck-mass [8, 9]. In any case, a schematic analysis indicates that the mass of black holes formed from the collapse of cosmic necklaces is small. Hence they are referred to as PBHs, even though they are not necessarily primordial in the strict sense of the word.

This process should be contrasted with the standard scenario, where the fraction of cosmic string loops which collapse to form PBHs is extremely small ($f \sim 10^{-20}$). In this case, it is at least conceivable that nearly all the string loops which contain beads will eventually collapse to form PBHs ($f \sim 1$).¹³ As mentioned above, this also allows the interesting possibility of placing tight constraints on the necklace density (and density of PBHs formed from necklace collapse, Ω_{PBH}) from the observed gamma-ray flux, and hence potentially on certain free parameters in string theory models of flux-compactification.

In fact, the origin of the lifting potential is also related to the problem of flux-compactifications in string theory [161]-[164]. Ten-dimensional general relativity predicts that, if the four

¹²There remains a subtlety here regarding whether or not it is meaningful to talk about one section of the string “shrinking” while another remains fixed. By definition F/D -strings have no substructure and the same is true for topological defect strings along the direction of their length. The reparamaterisation invariance of the Nambu-Goto action - which is the mathematical expression of this assumption - then suggests that the string must either contract or expand along its entire length. This possibility is also discussed at greater length at the end of chapter 3. However, in the main part of our analysis we follow Matsuda [8] in his initial assumption that the bead mass remains fixed after loop formation.

¹³Those necklaces which do not contain sufficient mass in their beads to undergo gravitational collapse, even once their four-dimensional radius has shrunk to the scale of the fundamental string width, form relics which may also act as DM candidates (see chapter 3). However, this assumption may also be questioned (see chapter 5).

spacetime dimensions we observe today are expanding, then the additional six spatial dimensions should also expand. The ten-dimensional spacetime manifold must either contract or expand (or be stabilised by a fine-tuned cosmological constant) *as a whole*. However, as mentioned above, in string theory there exist non-perturbative objects called D_p -branes. These are $(p + 1)$ -dimensional surfaces in spacetime on which the end points of the string are free to move in the p spatial directions; they are the string theory analogues of solitons in field theory. Such branes can both “wrap” dimensions in the internal manifold and be the source of fluxes which create an effective potential for the the internal directions. This potential stabilises the CY moduli at certain values corresponding to the potential minima, fixing its size and topology. As the size and topology of the compact space (together with the string embedding, which we expect to be influenced by the winding formation mechanism, see chapters 3 and 4) determines the form of the lifting potential, the phenomenology associated with wound strings is clearly influenced by the parameters controlling the compactification. An example of a flux-compactification scheme of particular relevance to cosmology is the class of spacetime backgrounds described by the warped deformed conifold, first defined by Klebanov and Strassler [5]. The stabilisation of the moduli for this model and a brief overview of the method of brane inflation is given in the next section.

2.3 The Klebanov-Strassler geometry as an example of a flux-compactification and brane inflation

In the scenario of the warped deformed conifold our universe exists as a D_3 -brane at the bottom of an orbifold “throat” attached to the ten-dimensional bulk of a CY manifold. In this model the presence of fractional D_3 and anti- D_3 -branes (\overline{D}_3 -branes) distorts the CY space, generically giving rise to a singularity which lies at the tip of a higher-dimensional cone. For this reason conifold singularities are the most common type of singularity arising from compactifications in string theory - making them important objects to study in their own right - but they are of special interest to cosmologists since they also provide a natural mechanism for brane inflation [165, 166]. However, in order for physically viable theories to be constructed some method of regularising the singularity must first be found. One such method is described in the following section.

Generically the conifold is topologically equivalent to a non-compact singular manifold fibred over a $T^{1,1}$ base space [167] and may be conveniently described as a complex algebraic curve satisfying

$$f(z_1, z_2, z_3, z_4) = \sum_{i=1}^4 z_i^2 = 0 \tag{2.38}$$

2.3. THE KLEBANOV-STRASSLER GEOMETRY AS AN EXAMPLE OF A FLUX-COMPACTIFICATION AND BRANE INFLATION

where $z_i = x_i + iy_i$. It is clear that (2.38) defines a cone as, if z_i lies on the surface $f(z_i)$, then so does λz_i , $\lambda \in \mathbb{C}$. Intersecting the surface $f(z_i)$ with a seven-sphere of radius ρ , we see that the intersection is then defined by the equations

$$\begin{aligned} x_i x^i &= y_i y^i = \frac{1}{2} \rho^2 \\ x_i y^i &= 0, \end{aligned} \tag{2.39}$$

which describe the surface of a two-sphere fibred over a three-sphere. In this case, the structure group G is simply the trivial group consisting of the identity element, $G = \{I\}$, so that the resulting bundle is the Cartesian product, $S^2 \times S^3$. The singularity then occurs when *both* the S^2 and the S^3 to shrink to zero size, so that it may be regularised by allowing either or both spheres to remain finite.

The Einstein metric for the general conifold may also be written explicitly [167] as

$$ds_6^2 = d\rho^2 + \frac{\rho^2}{9} \left(d\Psi + \sum_{i=1}^2 \cos\theta_i d\phi_i \right)^2 + \frac{\rho^2}{6} \sum_{i=1}^2 (d\theta_i^2 + \sin^2\theta_i d\phi_i^2). \tag{2.40}$$

where $\Psi \in [0, 4\pi)$, $\theta_i \in [0, \pi)$ and $\phi_i \in [0, 2\pi)$. Here the base space is represented as a coset space $T^{1,1} = (SU(2) \times SU(2))/U(1)$ (with symmetry group $SU(2) \times SU(2) \times U(1)$) and is equivalent to two S^2 s linked by a $U(1)$ fibre. The $S^2 \times S^3$ topology remains. If we then allow the S^2 to shrink to zero radius, the resulting manifold is known as the resolved conifold, whereas if we allow the S^3 to shrink to zero radius we obtain the deformed conifold.

Mathematically the conifold geometry forms a perfectly consistent class of string backgrounds, but physically interesting scenarios arise when we take into account the action of gauge field fluxes from the Ramond-Ramond (R - R) and Neveu-Schwarz-Neveu-Schwarz (NS - NS) sectors.¹⁴ Physically this is necessary in order to create an effective potential

¹⁴Worldsheet fermions in superstring theories $\Psi^I(\tau, \sigma)$ must be either periodic or anti-periodic with respect to the spatial worldsheet coordinate σ . The condition for periodicity is also called Ramond boundary condition $\Psi^I(\tau, \pi) = +\Psi^I(\tau, -\pi)$, whereas that for anti-periodicity, $\Psi^I(\tau, \pi) = -\Psi^I(\tau, -\pi)$, is referred to as the Neveu-Schwarz boundary condition. These conditions define a number of inequivalent ground states, denoted $|NS\rangle$ and $|R^A\rangle$. Ramond fermions are more complicated than Neveu-Schwarz fermions because the eight classical zero modes (labelled d_0^I , $I \in \{1, 2, \dots, 8\}$) correspond to four creation and four annihilation operators when the theory is quantised. Requiring the existence of a *unique* vacuum $|0\rangle$ therefore gives rise to $2^4 = 16$ degenerate Ramond ground states $|R^A\rangle$, $A \in \{1, 2, \dots, 16\}$, which may be split into eight ground states with an even number of fermionic operators, $|R_1^a\rangle$, $a \in \{1, 2, \dots, 8\}$, and eight ground states with an odd number of fermionic operators, $|R_2^a\rangle$, $a \in \{1, 2, \dots, 8\}$. The state space basis of the open superstring theory is then obtained by taking all $|NS\rangle$ and $|R_2^a\rangle$ vectors with an odd number of fermions together with all $|R_1^a\rangle$ states with an even number of fermions and this is known as performing a Gliozzi-Scherk-Olive (GSO) projection [168](also see Zwiebach [155]). For the closed string theory we must also add left and right moving operators so that the four inequivalent sectors of the string are $|NS\rangle_L \otimes |NS\rangle_R \otimes |p_0, \vec{p}_T\rangle$, $|NS\rangle_L \otimes |R_j^b\rangle_R \otimes |p_0, \vec{p}_T\rangle$, $|R_i^a\rangle_L \otimes |NS\rangle_R \otimes |p_0, \vec{p}_T\rangle$ and $|R_i^a\rangle_L \otimes |R_j^b\rangle_R \otimes |p_0, \vec{p}_T\rangle$ where $i, j \in \{1, 2\}$ and $|p_0, \vec{p}_T\rangle$ represents the energy-momentum state. The first of these sectors, the NS - NS , gives rise to three massless bosonic fields: one spin-2 field $g_{\mu\nu}$, whose states are interpreted as gravitons, a

2.3. THE KLEBANOV-STRASSLER GEOMETRY AS AN EXAMPLE OF A
FLUX-COMPACTIFICATION AND BRANE INFLATION

for the CY moduli (in this case, the radii of the S^2 and S^3 manifolds), stabilising them at values corresponding to the potential minima (see [164]). In these models the D_3 -branes and fractional D_3 -branes at the tip of the throat are the sources of fluxes which wrap cycles in the compact directions. The resulting back-reaction on the large dimensions then gives rise to a “warped throat” geometry. Adding M fractional \overline{D}_3 -branes (i.e. \overline{D}_5 -branes wrapped over the S^2 of $T^{1,1}$) gives rise to M units of R - R 3-form flux (F_3) through the S^3 sub-cycle and adding N ordinary \overline{D}_3 -branes gives rise to N units of NS - NS 5-form flux (F_5) through the whole $T^{1,1}$, so that

$$\frac{1}{(2\pi)^2\alpha'} \int_{S^3} F_3 = M, \quad \frac{1}{(2\pi)^2\alpha'} \int_{T^{1,1}} F_5 = N \quad (2.41)$$

where $M, N \in \mathbb{Z}$ and each flux satisfies the Dirac quantisation condition [160]. Here α' is the slope parameter, which is related to the fundamental string length l_s via

$$l_s = \sqrt{\alpha'} \quad (2.42)$$

in natural units ($c = \hbar = 1$). The presence of the NS - NS 5-form flux is also related to the existence of additional non-trivial R - R 2-form and 4-form fluxes, which we label B_2 and C_4 , so that F_5 may be written as [5]

$$F_5 = dC_4 + B_2 \wedge F_3. \quad (2.43)$$

and the R - R 2-form flux is related to an NS - NS 3-form flux via

$$H_3 = dB_2. \quad (2.44)$$

In particular, the warped deformed conifold arises from the back-reaction of the R - R 3-form flux F_3 , threaded through the S^3 , and the NS - NS 3-form flux, H_3 , through the dual cycle $B \sim \rho \times S^2$ which creates the warped throat [5, 169]. We may expect the presence of these fluxes to deform the surface $f(z_i)$ defined in (2.38) so that

$$f(z_1, z_2, z_3, z_4) \rightarrow \tilde{f}(z_1, z_2, z_3, z_4) = \sum_{i=1}^4 z_i^2 = \epsilon^2, \quad (2.45)$$

spin-1 Kalb-Ramond field $B_{\mu\nu}$ (see later), and a spin-0 covariant scalar, known as the dilaton Φ . The last of these sectors, the R - R may then give rise to two separate closed string (type II) theories, known as type IIA and type IIB. In the type IIB theory the left and right R ground states are chosen to be the same, $i = j$, whereas in the type IIA they are different, $i \neq j$. The massless bosonic fields of the type IIB theory then include a scalar A , an additional Kalb-Ramond field $A_{\mu\nu}$ and a totally anti-symmetric gauge field $A_{\mu\nu\alpha\beta}$, whereas the type IIA theory contains a Maxwell field A_μ and another anti-symmetric gauge field $A_{\mu\nu\alpha}$.

2.3. THE KLEBANOV-STRASSLER GEOMETRY AS AN EXAMPLE OF A
FLUX-COMPACTIFICATION AND BRANE INFLATION

where ϵ is a small real paramter. Rewriting the metric (2.40) using a basis of 1-forms [170],

$$\begin{aligned} g_1 &= \frac{e^1 - e^2}{\sqrt{2}}, & g_2 &= \frac{e^2 - e^4}{\sqrt{2}} \\ g_3 &= \frac{e^1 + e^3}{\sqrt{2}}, & g_4 &= \frac{e^2 + e^4}{\sqrt{2}} \\ g_5 &= e^5 \end{aligned} \tag{2.46}$$

where

$$\begin{aligned} e^1 &= -\sin\theta_1 d\phi_1 \\ e^2 &= d\theta_1 \\ e^3 &= \cos\psi \sin\theta_2 d\phi_2 - \sin\psi d\theta_2 \\ e^4 &= \sin\psi \sin\theta_2 d\phi_2 + \cos\psi d\theta_2 \\ e^5 &= d\psi + \cos\theta_1 d\phi_1 + \cos\theta_2 d\phi_2, \end{aligned} \tag{2.47}$$

and accounting for the effect of the fluxes on the large dimensions, the full ten-dimensional metric of the warped throat geometry may be written as

$$\begin{aligned} ds_{10}^2 &= h^{-\frac{1}{2}}(\tau) dx_\mu dx^\mu \\ &+ \frac{1}{2} \epsilon^{\frac{4}{3}} h^{\frac{1}{2}}(\tau) K(\tau) \left[\frac{1}{3K^3(\tau)} (d\tau^2 + g_5^2) + \cosh^2\left(\frac{\tau}{2}\right) (g_3^2 + g_4^2) + \sinh^2\left(\frac{\tau}{2}\right) (g_1^2 + g_2^2) \right] \end{aligned} \tag{2.48}$$

where $\mu \in \{0, 1, 2, 3\}$ and $h(\tau)$, $K(\tau)$ are defined via

$$\begin{aligned} h(\tau) &= \alpha \frac{2^{2/3}}{4} \int_\tau^\infty \frac{x \coth(x) - 1}{\sinh^2(x)} (\sinh(2x) - 2x)^{1/3} dx \\ K(\tau) &= \frac{(\sinh(2\tau) - 2\tau)^{1/3}}{2^{1/3} \sinh(\tau)}. \end{aligned} \tag{2.49}$$

Here g_s is the string coupling, which is related to the size of the dilaton Φ by

$$e^\Phi = g_s \tag{2.50}$$

and α is a normalisation constant proportional to $(g_s M)^2$ [5]. It is important to note that the dilaton, and hence the string coupling, is constant in this background, though in chapter 5 we will see how an effective string coupling, which varies as a function of the spacetime coordinates, may be obtained for wound strings.

In (2.48) τ parameterises the radius of the S^2 , so that in the small limit τ limit the metric

reduces to

$$ds^2 = a_0^2 dx_\mu dx^\mu + b_0 g_s M \alpha' \left[\frac{1}{2} d\tau^2 + d\Omega_3^2 + \frac{1}{4} \tau^2 (g_1^2 + g_3^2) \right], \quad (2.51)$$

where b_0 is a numerical constant of order one, $d\Omega_3^2$ is the metric for the unit three-sphere and

$$a_0^2 = \text{Lim}_{\tau \rightarrow 0} h^{-\frac{1}{2}}(\tau) \quad (2.52)$$

is a real constant such that $0 < a_0^2 < 1$.¹⁵ The parameter a_0 is called the warp factor. For $\tau \rightarrow 0$ the first and last terms inside the square brackets (2.51) vanish which allows us to interpret $b_0 g_s M \alpha'$ as the square of the radius of the remaining S^3 , which we will label R , so that

$$R^2 = b_0 g_s M \alpha'. \quad (2.53)$$

The squares of the warp factor and the radius of the compact space, a_0^2 and R^2 , are related via the deformation parameter ϵ (which remains a free parameter in the theory) via

$$a_0^2 \sim \frac{\tilde{\epsilon}^{4/3}}{R^2}. \quad (2.54)$$

Here ϵ is rescaled to $\tilde{\epsilon}$ so that $\tilde{\epsilon}^{4/3} \propto \alpha'$ and we are assuming the supergravity (SUGRA) limit

$$g_s M \gg 1. \quad (2.55)$$

Physically viable theories can then be constructed since for practical purposes the bottom of the throat has been “smoothed-off” with an S^3 to remove the conifold singularity. The remaining CY modulus (i.e. the radius of the three-sphere R) depends on the value of the integral 3-form flux which wraps the space itself, as expected from a flux-compactification.

Finally, we note that there also exists an R - R 2-form flux C_2 which is proportional to M (and inversely proportional to g_s) and which, in addition to its relation to the CY moduli, also directly influences the dynamics of branes in the throat via its contribution to the Chern-Simons (CS) term of the action (see section 2.4.3).

By explicitly assuming the background gauge choice

$$\begin{aligned} \theta &= \theta_1 = -\theta_2 \\ \phi &= \phi_1 = -\phi_2 \end{aligned} \quad (2.56)$$

¹⁵Here we choose a different notation to that used in the original paper by Klebanov and Strassler [5] who showed that in the small τ limit, $h(\tau) \sim a_0 + a_1 \tau^2$ where a_0, a_1 are positive real constants. In [5] a_0 necessarily satisfies $a_0 > 1$. The a_0 defined in (2.52) is therefore equivalent to the quantity $h^{-1/2}(\tau \rightarrow 0) \sim a_0^{-1/2}$ defined in that paper and the two “ a_0 s” must not be confused.

2.3. THE KLEBANOV-STRASSLER GEOMETRY AS AN EXAMPLE OF A FLUX-COMPACTIFICATION AND BRANE INFLATION

(see [245]), we may write the 2-form flux in terms of the volume form, ω_2 , along the two-cycle parameterised by the variables θ and ϕ , and a simple function of ψ , so that

$$C_2 = \frac{1}{g_s} M \alpha' F(\psi) \omega_2 \quad (2.57)$$

where $F(\psi) \sim \psi - \sin(\psi) \cos(\psi)$. As mentioned previously, there also exists a corresponding R - R 2-form B_2 which wraps the S^2 . However, *at* the tip the conifold is regularised as $S^2 \rightarrow 0$ and $B_2 \rightarrow 0$. In terms of the parameter τ which controls the blow-up of the two-sphere, the 2-form may be written explicitly as [5, 276]

$$B_2 = g_s M \alpha' \left(\frac{\tau \coth(\tau) - 1}{4 \sinh(\tau)} \right) d\tau \wedge (\cosh(\tau) - 1) g_1 \wedge g_2 + (\cosh(\tau) + 1) g_3 \wedge g_4 \quad (2.58)$$

which clearly vanishes as $\tau \rightarrow 0$. The R - R scalar charge C_0 is trivial and may be set equal to zero, via an appropriate gauge transformation, throughout the KS background. For the sake of completeness we include the effective metric at the tip, in *canonical coordinates*:¹⁶

$$ds^2 = a_0^2 \eta_{\mu\nu} dx^\mu dx^\nu + R^2 (d\psi^2 + \sin^2 \psi (d\theta^2 + \sin^2 \theta d\phi^2)) \quad (2.59)$$

where $\psi \in [0, 4\pi)$ is the azimuthal angle and $\theta \in [0, \pi)$, $\phi \in [0, 2\pi)$ are the polar angles (note that the ψ -coordinate here is *not* the same as the Ψ -coordinate labelling the $U(1)$ fibre in equation (2.40)).

There then exist two mechanisms for brane inflation - otherwise known as DBI inflation after the Dirac-Born-Infeld action which describes the dynamics of D -branes¹⁷ [157]-[159]. In the most generic scenario, known as ultra-violet (UV) inflation [171, 172], the D_3 -brane of our universe ‘‘begins’’ somewhere in the bulk space of the CY manifold but is attracted down the throat by the presence of \overline{D}_3 -branes at the IR tip, and the moduli corresponding to the inter-brane distances along the various spatial coordinates of the throat act as the inflaton fields.¹⁸ Inflation then ends when we reach the bottom of the conifold.

¹⁶In chapter 5 we will find it convenient to parameterise the compact space in terms of Eulerian variables, using the so-called Hopf fibration of the three-sphere. This description turns out to be convenient when considering the dynamics of geodesic windings (which form a specific type of *geodesic* cycloop), whereas the parameterisation in canonical coordinates is more suited to the analysis on non-geodesic (i.e. necklace) configurations.

¹⁷We will return to the DBI action later in this chapter when we come to discuss its relation to the Nambu-Goto action in the case of D -strings (D_1 -branes).

¹⁸In the simplest possible scenario the brane moves down the centre of the cone, so that only one coordinate distance matters - the distance between the brane and the tip. This is a model of single field inflation where the energy driving the inflationary expansion of the brane is provided by the potential energy between it and the \overline{D}_3 -branes. Multi-field inflationary models can be constructed by having the brane follow a more complicated trajectory, introducing other coordinate distances which act as multiple fields [173]-[176]. One way to do this is to add angular momentum to the brane which then ‘‘cycles’’ around the throat [177]. Additional phenomenological models can be obtained by introducing other branes/anti-branes into the throat (i.e. not just at the tip), in addition to the brane of our universe, giving rise to the so called

At the base of the conifold then, the flux parameter M denotes the quantised 3-form flux in the extra dimensions (in units of the slope parameter α') and is given by the integral of this flux (from the type IIB SUGRA solution) over the S^3 . It is also equal to the number of fractional \overline{D}_3 -branes at the bottom of the conifold and so is generally positive, as expected for the SUGRA limit $M \gg g_s^{-1}$ with $g_s > 0$. In addition, throat geometries naturally reduce the amount of supersymmetry (SUSY) that the solution preserves and it may be shown that for the warped deformed conifold only $\mathcal{N} = 1$ SUSY remains [5].

In the second scenario, known as IR inflation [182, 183], the D_3 probe brane starts at the tip of the throat and is attracted “upward” toward the bulk space by the presence of branes/fluxes in other CY warped throats. However, this model requires some fine-tuning in order for inflation to end with a stable D_3 -brane (representing our universe) lying at the tip. One way of doing this is to insert some number \overline{N} of \overline{D}_3 -branes into the background “above” some number M of D_3 -branes, i.e. with the \overline{D}_3 -branes lying closer to the bulk space. The anti-branes (rather than the branes, as in the UV model) are then attracted down the throat and annihilate with the branes. For a warped deformed conifold with M units of D_3 -brane flux threading the S^3 , there are exactly $N = M - \overline{N}$ D_3 -branes remaining after the annihilation process.¹⁹

The simplest IR models assume $N = 1$ (i.e. the result is fine tuned), though generically N remains a free parameter. For $N > 1$ we would expect the remaining branes to be distributed randomly in the region of the tip and it has been shown that, if the inter-brane distance is greater than the string scale ($d_D \gg l_s$), their evolution is capable of creating a form of assisted inflation [184]-[189]. For large N the dynamics of branes near the tip are similar to those of the $N = 1$ models but for small N the brane actions are highly non-linear and specific solutions for $N = 2$ and $N = 3$ are given in [190].

The warped throat geometry is illustrated in figure 2.7, while figure 2.8 gives a schematic representation of the difference between the general conifold and the warped deformed conifold, taken from Majumdar [191].

Although the KS geometry allows us to construct a realistic and relatively natural inflationary mechanism, the question remains as to whether DBI inflation may be distinguished from other inflationary paradigms provided by string theory and field-theoretic models (see [192]). In order to answer this question, we must search for “stringy signatures” from the

DBI N -flation paradigm [178, 179], which is related to other N -field inflationary models in string theory [180, 181]

¹⁹Note that this N is not the same as that in (2.41), which refers to the number of units of 5-form flux used in the construction of the throat itself.

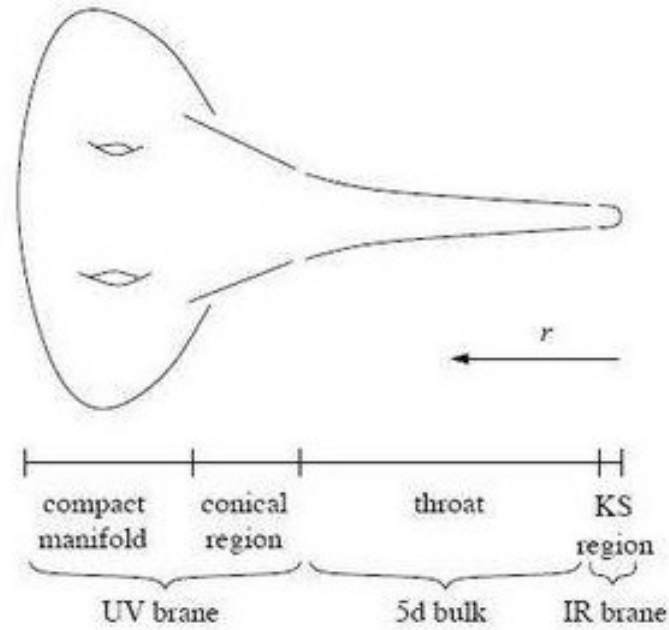


Figure 2.7: This figure illustrates the geometry of the warped throat and is taken from lectures presented by F. Quevedo (The cosmology of string theory - inflation and beyond) at UniverseNet (2007). Here the coordinate r refers to the inter-brane distance, which is equal to the distance between the probe D_3 -brane and the tip of the throat.

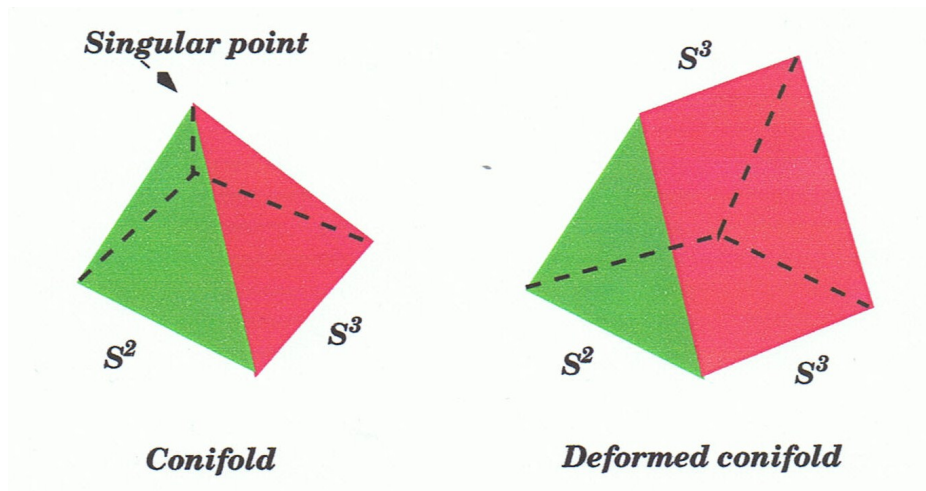


Figure 2.8: This figure illustrates the difference between the geometry of the general conifold and the warped deformed conifold. Taken from Majumdar [191].

inflationary epoch and investigate the cosmological consequences of any specific predictions of the DBI model. One such prediction is the production of string-like defects at the end of inflation, when the D_3 -brane of our universe collides and annihilates with a \overline{D}_3 -brane. K-theory tells us that the remnant branes have co-dimension two (see [10]) and these objects may be interpreted as D -strings which are charged under a linear combination of the original $U(1) \times U(1)$ gauge symmetry. It has also been shown that annihilation leads to the production of confining flux tubes, which may be interpreted as F -strings via gauge/gravity duality [193] (see also [194] and [195] for reviews of the AdS/CFT conjecture). The existence of single F/D -strings on the standard model brane then allows for the formation of bound states known as (p, q) -strings, where the letters p and q refer to the number of F - and D -strings, respectively. The dynamics of these objects is reviewed in the next section, with special emphasis on determining the spectrum of effective tensions in the warped throat geometry.

It has been shown that string networks with effective tensions comparable to the fundamental string tension (i.e. $\mathcal{T} \sim \alpha'^{-1}$) are automatically ruled out if we assume the fundamental string mass ($m_s \sim \sqrt{\alpha'^{-1}}$) to be of the order of the Planck mass m_p [196]. In fact, observational bounds place strict constraints on the spectrum of primordial density fluctuations in the early universe, and hence on the parameters which control them, in either stringy or field-theoretic models (see [197]-[209]). In particular the tensions of *any* string species must obey the bound

$$G\mu \leq \mathcal{O}(10^{-6}) \tag{2.60}$$

and their present day number density is required to be $\sim \mathcal{O}(1)$ per horizon volume [114]. More specifically, various bounds of this order have been obtained by considering cosmic strings as both sources of CMB anisotropy and as potential seeds for LSS. The unusual gravitational properties of strings create “stringy signatures”²⁰ in the CMB which may be distinguished from the effects of other massive objects. The passing of a string between a radiation source (such as the surface of last scattering) and an observer causes a discontinuous shift in the observed wavelength/temperature of the radiation, and this effect is unique to string gravity. This is more pronounced in certain regions due to the presence of small-scale structure along the string as the temperature shift is proportional to the string velocity, and local velocities, especially in the region of a cusp, may greatly exceed the drift velocity. Using the COBE data [210], Bennett *et al* [211] obtained the bound $G\mu \leq 2 \times 10^{-6}$, while a bound of $G\mu \leq 10^{-6} (\zeta\alpha^2)^{-1/3}$ was obtained by Turok and Brandenburger [212] based on considering strings as seeds for LSS formation using the “old string evolution scenario” [114]. Here the string motion is assumed to be Brownian on scales $L > \xi = \gamma t$, so that $\rho_\infty = \zeta\mu/t^2$ where $\zeta \sim \gamma^{-2}$, and $\zeta \sim \alpha \sim 1$. Although normalisation of $G\mu$ on the scale of

²⁰Note that here this phrase refers simply to the presence of strings of any kind and *not* to the presence of F/D - or (p, q) -strings, as opposed to topological defect strings.

2.3. THE KLEBANOV-STRASSLER GEOMETRY AS AN EXAMPLE OF A FLUX-COMPACTIFICATION AND BRANE INFLATION

rich clusters eventually ruled out this scenario for strings as seeds for LSS [114], the bound itself remains valid. Generically, we expect $G\mu \sim \eta^2/m_p^2$, so that, for GUT-scale strings, $G\mu \sim 10^{-6}$ [125], though recent pulsar data suggests $G\mu \leq 10^{-7}$ [213].²¹ Similar bounds have also been obtained from more recent CMB power-spectrum observations [199, 200].

Current observations may even favour a Λ CDM model [215]-[223] in which string-like defects may play a significant, but by no means dominant role in the creation of primordial CMB fluctuations [126]-[131]. Using field theory simulations of Abelian-Higgs strings (at critical coupling) and normalising the resulting perturbation spectrum to the WMAP 3-year data at multipole ten ($l = 10$),²² Bevis *et al* obtained an upper bound of $G\mu \sim 2 \times 10^{-6}$ [126]. Adding a stringy component to the primordial spectrum (resulting from inflation) with power-law tilt n_s , a subsequent multi-parameter fit [127] found a 2σ detection of strings giving a fractional contribution to the temperature power-spectrum (at $l = 10$) of $f_{10} \sim 0.11$. In fact, a Harrison-Zeldovich model ($n_s = 1$) including strings was found to be marginally favoured over the standard (zero-strings) model with variable tilt. Incorporating additional non-CMB data from the Hubble Key Project (HKP) [224] and big bang nucleosynthesis (BBN) [225] showed these models to be equally favourable and, in addition, allowed generic constraints of $f_{10} < 0.11$ and $G\mu < 0.7 \times 10^{-6}$ to be obtained for $n_s \neq 1$.²³ Subsequent improved calculations confirmed these results and demonstrated that an Abelian-Higgs string contribution to the power-spectrum, making up $f_{10} \sim 0.10$ at $l = 10$, would be larger than the primary Silk-damped adiabatic contribution on small scales ($l > 3500$) [128]. This opens up the possibility that observations from the Planck satellite [226] and other sub-orbital CMB projects may be able to detect them and, although the relevant calculations have not yet been performed, the same is clearly true for more exotic strings.

Similar hopes are raised by an analysis of the expected polarization power-spectra produced by adiabatic and stringy components (with special reference to the so-called B -modes) in which the string contribution is expected to dominate [130]. It has recently been argued that, even if defects contribute less than one percent to the total CMB temperature power-spectrum, their signatures in the local B -mode polarisation correlation function ought to dominate on small angular scales [131]. The same authors claim that B -mode observations from Planck will be able to constrain the tension of any string species to the level

²¹Gravitational radiation produced by string loops would add to the stochastic background [214], which introduces noise into the arrival times of millisecond pulsars. The observed delay is related to the string tension and allows bounds to be placed on $G\mu$.

²²This l denotes CMB power-spectrum multipole and is not to be confused with the l which labels the angular momentum in the compact space (see chapter 3).

²³This was true even for $n_s > 1$, which is otherwise ruled out by existing data. The inclusion of cosmic strings into the Λ CDM paradigm (taking n_s as a free parameter) shows that no pressure is placed on such models.

2.3. THE KLEBANOV-STRASSLER GEOMETRY AS AN EXAMPLE OF A FLUX-COMPACTIFICATION AND BRANE INFLATION

of $G\mu < 10^{-7}$, while future CMBpol [227] data should improve this to $G\mu < 10^{-9}$. Specific calculations for Abelian-Higgs strings suggest that, taking a null hypothesis (i.e. that strings make no contribution), observations from the *Clover* experiment [228] will limit the string tension to $G\mu < 0.12 \times 10^{-6}$, above which detection should be possible [129]. Whatever the technical difficulties, similar calculations may, in principle, be performed for more exotic strings species (including (p, q) -strings and necklaces in warped throat scenarios - see section 5.10) and the possibility of detection remains.

As we shall see in the next section, in flux-compactified models the warping caused by the back-reaction of the fluxes on the large dimensions may *reduce* the effective tension of the strings, allowing existing observational bounds to be avoided. This possibility was first suggested in [191, 193], and the current bounds from brane inflation on the *warped* tension of F/D -strings are $10^{-11} \leq G\mu \leq 10^{-6}$ [201]-[203].

Although DBI inflation is by no means the only cosmological paradigm that leads to the production of string-like defects - indeed, different string species arise in many other string theory and field theory models of the early universe - the prediction of potentially copious numbers of F - and D -strings does seem to be a specific feature of the model. Hence the phenomenology and cosmological consequences of (p, q) -string networks in the warped throat background are worth investigating as a potential means of providing evidence for or against the theory.

As mentioned above, recent analysis of the CMB power spectrum using a Λ CDM model with Abelian-Higgs strings suggested that this provides a *better* fit to the current data than stringless Λ CDM models, with strings obeying the bound (2.60) contributing around ten percent of the primordial fluctuations [126, 127]. Theoretically it is therefore possible that other string species, for example (p, q) -strings with warped tension, or stringy objects such as networks of necklaces and cycloops, may yet provide an even better fit to the data. This is likely to prompt renewed interest in cosmological models which generate such defects, including DBI inflation. In particular, extra-dimensional effects may prove to be crucial in distinguishing different theories. Therefore, although a fit to CMB data using necklace/cycloop models is not attempted here, this thesis contributes to the analysis of the cosmological effects of exotic stringy objects in viable cosmological models.

2.4 Topological defect strings vs “stringy strings”: (p, q) -strings in the KS throat

2.4.1 String species, internal structure and effective actions

In the preceding sections of this chapter we have introduced the notion of cosmic strings as topological defects formed during symmetry-breaking phase transitions, given a brief overview of string evolution, and developed the idea of wound strings in theories with compact extra dimensions. In particular we have introduced generic phenomenological models of two types of qualitatively different winding configuration - strings with “smooth” windings, which we term cycloops, and strings with step-like windings, which we refer to as cosmic necklaces. However, as these terms refer only to the winding state of the string (i.e. its geometric embedding in the spacetime background) and not to its *nature*, it is clear that, even in a single background geometry, many possible cycloop/necklace models are possible for different string species.

We must first draw the distinction between field-theoretic strings (i.e. topological defects) and “stringy strings”, i.e. macroscopic string networks which play the role of defects in models of string cosmology. It is important to remember that field-theoretic strings are essentially field configurations and *not* string-like objects in their own right, even though they may be treated as such once formed. One consequence of this is that field-theoretic strings always possess some degree of internal structure - at least radially, though not along their length - due to the vortex configuration of the field(s).

However, when analysing the dynamics of free string loops, it is common to ignore the thickness of the vortex core and to approximate the string as a truly one-dimensional object. The key parameter is the ratio of the vortex width δ to the curvature radius of the string \mathcal{R} , so that for $\delta \ll \mathcal{R}$ the string thickness may be neglected [15, 114]. To lowest order in δ/\mathcal{R} , the effective action for a topological defect string is then

$$S = -\mu \int d^2\zeta \sqrt{-\gamma} \quad (2.61)$$

where $\mu \sim \eta^2$ is the string tension (in units of $[E][l]^{-1}$) and γ is the determinant of the induced metric on the resulting worldsheet:

$$\gamma_{ab}(\zeta) = \frac{\partial X^\mu}{\partial \zeta^a} \frac{\partial X^\nu}{\partial \zeta^b} g_{\mu\nu}(X(\zeta)) \quad (2.62)$$

where $\mu, \nu \in \{0, 1, \dots, d\}$ label the coordinates of the background and $a, b \in \{0, 1\}$ label the worldsheet coordinates.

Thus the integrand $d^2\zeta\sqrt{-\gamma}$ is simply the worldsheet area dA and (2.61) is the generalisation for a one-dimensional object of the action for a zero-dimensional relativistic point-particle, $S = -m \int ds$. This is known as the Nambu or Nambu-Goto action [229, 230] and is the fundamental action which describes the dynamics of a free F -string. However, in this case the string tension depends directly on a fundamental constant, i.e. the slope parameter/fundamental string scale $l_s \sim \sqrt{\alpha'}$, not on the integration of an energy density over a vortex, and we must perform an appropriate replacement, $\mu \rightarrow \mathcal{T} \sim \alpha'^{-1}$, in the action. For an F -string in flat space the fundamental tension is

$$\mathcal{T} = \frac{1}{2\pi\alpha'} \quad (2.63)$$

but in general the effective tension will depend upon the background geometry such that $\mathcal{T} = \mathcal{T}(g)$, although in *all* cases $\mathcal{T} \propto \alpha'^{-1}$ is required to ensure that the action is dimensionless.

However, unlike single F -strings (and defect strings such as the flux-confining vortex-line strings considered in section 2.2.1, to which they are dual in the KS geometry [5]), D -branes may carry an additional world-volume gauge field $A_a(\zeta)$ and an antisymmetric tensor field $B_{ab}(\zeta)$ (see [155]) so that for D -strings

$$S = -\mathcal{T} \int d^2\zeta \sqrt{-\det(\gamma_{ab} + B_{ab} + \lambda F_{ab})}. \quad (2.64)$$

Here F_{ab} is analogous to the usual EM field tensor $F_{\mu\nu}$ (discussed earlier), but is now defined only on the world-sheet by

$$F_{ab} = \partial_a A_b - \partial_b A_a \quad (2.65)$$

where $a, b \in \{0, 1\}$ and λ is a constant with dimensions of $[l]^2$.²⁴ It may be shown that the appropriate multiplying constant for the field tensor is [155]

$$\lambda = 2\pi\alpha' = \mathcal{T}^{-1}. \quad (2.66)$$

The antisymmetric tensor field B_{ab} is given by the pull-back of the bulk space Kalb-Ramond field $B_{\mu\nu}$ (see footnote 13 on page 41)

$$B_{ab}(\zeta) = \frac{\partial X^\mu}{\partial \zeta^a} \frac{\partial X^\nu}{\partial \zeta^b} B_{\mu\nu}(X(\zeta)) \quad (2.67)$$

²⁴This λ is not to be confused with the dimensionless coupling constant of the scalar field in the Abelian-Higgs model, which was introduced in chapter 2.

and, although $B_{\mu\nu}$ is Abelian, we note that its pull-back to the world-sheet (or world-volume) B_{ab} is not. For a general D_p -brane this gives the following lowest order action:

$$S_p = -T_p(g) \int d^{p+1}\zeta e^{-\Phi} \sqrt{-\det(\gamma_{ab} + B_{ab} + \lambda F_{ab})} \quad (2.68)$$

where λF_{ab} is defined according to (2.65) and (2.66), and we have accounted for the change from the two-dimensional worldsheet to the - possibly higher-dimensional - worldvolume coordinates, labelled by the indices $a, b \in \{0, 1 \dots p + 1\}$.

This is known as the Abelian Dirac-Born-Infeld (DBI) action, as mentioned previously, and is a modification of the Born-Infeld action used in the study of non-linear electrodynamics [231]. However, this “simple” action may also couple to the closed string R - R fields in the background, resulting in an additional contribution which is proportional to the vector potential. Specifically, the interaction term is proportional to the anti-symmetrised combination of the gauge potential with each of the field strengths taking part in the interaction and is given by the pull-back of the R - R form in the bulk space to the world-sheet [152]. The correction is known as a CS term as it is a geometric invariant of the worldvolume, that is, independent of the relation between the embedding and the background space [232]. For simplicity, we chose to ignore such corrections in the analysis that follows (see chapters 3-5) but it is important to appreciate that in an extended analysis such problems may need to be addressed. For the Abelian DBI action, we expect that the additional CS term will also be Abelian, for any string background, so this problem should at least be tractable.

The dynamics of the basic one-dimensional objects in string theory, the fundamental string (or F -string) and the D_1 -brane (or D -string), may therefore differ considerably. In general we would expect the dynamics of an F -string to correspond more to those of a topological defect string (in the same background), at least within the limit for which the Nambu-Goto action is a valid approximation for the latter, though differences between field-theoretic strings and stringy strings still exist. In particular we note that *unwound* F/D -strings possess no characteristics which are determined by a single dimensionless integer n , unlike defect strings, whose properties depend on the winding number.²⁵

However, as also mentioned above, the worldsheet of the D -string may carry a $U(1)$ gauge field flux and bound states of F/D -strings may form to create generic objects known as (p, q) -strings. Here both p and q are integers and refer to the number of F -strings and D -strings in the bound state, respectively. It has also been shown that forming a (p, q) bound state is equivalent to dissolving p units of “electric” flux and q units of “magnetic”

²⁵In chapter 5 we investigate a possible relation between the topological winding number n of a defect string and the *physical* winding number n_w of an F/D -string wrapping the compact space. In the former case, n denotes an “internal” property of the string, whereas in the latter, n_w is a geometric property determined by the embedding.

flux on the worldsheet of a single F -string (see [193] and [201, 233]). This is due to the presence of an $SL(2, Z)$ symmetry which interchanges the B_2 field with the R - R 2-form C_2 , hence transforming F -strings into D -strings and vica-versa [234]. The correct action to describe the dynamics of (p, q) -strings is therefore the full non-Abelian DBI action for coincident D_p -branes, where in this case $p = 1$, which here refers to the *dimensionality* of the branes.²⁶ We now briefly discuss the origin of this action.

2.4.2 The non-Abelian DBI action

It is known that the coalescing of multiple branes generates enhanced symmetry in the gauge fields on the worldsheet of the resulting bound state. For example, when N D_p -branes, each carrying a $U(1)$ gauge field, reach a brane separation of the order of the string scale $l_s \sim \sqrt{\alpha'}$, the massive modes of the independent world-sheet fields become massless, resulting in the symmetry enhancement

$$U(1)^N \rightarrow U(N) \tag{2.69}$$

as the branes coalesce [235, 236]. This is a non-Abelian gauge group and hopes that the gauge group of the standard model, or supersymmetric extensions of the standard model, may be constructed from coincident D -branes are based on such interesting and promising results, though a full string/brane description of standard particle physics has not yet been realised [237]-[239].²⁷

The appropriate transformation for the worldvolume vector field is

$$\begin{aligned} A_a &= A_\mu^i T_i \\ F_{ab} &= \partial_{[a} A_{b]} + i[A_a, A_b] \end{aligned} \tag{2.70}$$

where $\{T_i\}$, $i \in \{1, 2, \dots, N^2\}$ are the $U(N)$ group generators, which satisfy the standard relation

$$Tr(T_i T_j) = N \delta_{ij}. \tag{2.71}$$

The scalar fields must also transform under the gauge group and choosing them to transform under the adjoint (Lie algebra) representation allows us to write the covariant derivative in

²⁶We must not confuse *this* p with the number of F -strings.

²⁷We also note that, just as symmetry enhancement and the conversion of massive to massless modes occurs as branes coalesce, brane separation results in symmetry-*breaking* and in previously massless string modes acquiring mass. D -brane dynamics therefore provide an exact analogue of the Higgs process in field theory, though here the symmetry-breaking is *dynamic*, rather than “static” as it is when mediated by the presence of a Higgs field. Further remarks on possible dynamical methods of breaking symmetry are also given at the end of chapter 5.

terms of the Lie bracket:

$$D_a \phi^i = \partial_a \phi^i + i[A_a, \phi^i] \quad (2.72)$$

where ϕ^i are the world-volume scalars. If the scalars commute, they may be simultaneously diagonalised with respect to the position operator and the corresponding N eigenvalues interpreted as the positions of the N individual D_p -branes. Thus we see that, despite the non-Abelian nature of the gauge group for the worldvolume of coincident branes, and the resulting complexity of the action, we may still interpret the worldvolume scalars ϕ^i by analogy with the case of a single D_p -brane, in which they represent the embedding coordinates $X^i(\tau, \sigma)$.

Although their matrix-valued nature allows the scalar fields to be interpreted intuitively, in practice it makes calculating the *exact* form of the action for N coincident branes of arbitrary dimensionality p very difficult. However, this has been achieved by Tseytlin [240] using scattering amplitudes, and the resulting action can be transformed using T-duality (see [155]) to interchange the scalar and vector fields such that

$$\begin{aligned} \phi^{(p+1)} &\rightarrow A_{(p+1)} \\ A_p &\rightarrow \phi^p. \end{aligned} \quad (2.73)$$

This technique was used by Myers [241, 242] and the resulting form of the non-Abelian DBI action for N coincident D_p -branes, given below, is known as the Myers action:

$$S = -T_p \int d^{(p+1)}\zeta STr \left[e^{-\Phi} \sqrt{\det(Q_j^i)} \sqrt{-\det(\widehat{E}_{ab} + \widehat{E}_{ai}(Q^{-1} - \delta)^{ij}\widehat{E}_{jb} + \lambda F_{ab})} \right]. \quad (2.74)$$

Here \widehat{E}_{ab} denotes the pull-back of the spacetime metric $G_{\mu\nu}$ and Kalb-Ramond field $B_{\mu\nu}$ to the worldvolume

$$\widehat{E}_{ab} = \mathcal{P}[G_{\mu\nu} + B_{\mu\nu}] \quad (2.75)$$

and we have defined the tensor Q_j^i by

$$Q_j^i = \delta_j^i + i\lambda[\phi^i, \phi^k]\widehat{E}_{kj}. \quad (2.76)$$

The notation STr indicates that the trace is completely symmetric with respect to all non-Abelian terms of the form F_{ab} , $D_a \phi^i$ and $i[\phi^i, \phi^j]$ [241]. In (2.75) and (2.76) $\mu, \nu \in \{0, 1, \dots, p\}$ label the worldvolume coordinates ζ , as before, and $i, j, k \in \{1, 2, \dots, N^2\}$, whereas T_p now represents the *total* tension of the brane, which again in general depends on both the geometry of the embedding space and on the properties of the D_p -branes which coalesce to create the bound state [243]. There is also a CS term, as in the case of a single D_p -brane, though this too is generally non-linear.

In the rest of this thesis, we restrict our detailed analysis to the cosmological consequences

of cycloops/necklace loops formed from single F - and D -strings (when dealing specifically with string theory models). This allows us to model the dynamics using the standard Abelian DBI/Nambu-Goto actions, which we will see reduce to the same form at the tip of the warped throat where $B_2 \sim 0$ (see chapter 3). However, for general (p, q) -strings the analysis is far more complicated as we must use the full non-Abelian DBI action to model the string dynamics. In the case of the warped throat geometry, there is an important caveat: It has been shown that, in the large p or large q limit, general (p, q) -strings “blow up” and become dual to D_3 -branes at the tip of the throat [244, 245]. This occurs when the non-Abelian DBI action couples to R - R forms with dimensionality greater than one, allowing a brane-dielectric effect which causes the lower dimensional brane to expand into a higher-dimensional one (in this case $D_p \rightarrow D_{p+2}$, [246]). These D_3 -branes wrap 2-cycles in the throat geometry, so that the brane still behaves like a one-dimensional string close to the tip. Mathematically we “recover” the Abelian DBI action in $D = 3 + 1$ dimensions from its non-Abelian counterpart (including the CS term) in $D = 1 + 1$ dimensions as $p, q \rightarrow \infty$, so that the analysis again becomes simplified in this limit.

Although it is also possible to investigate the consequences of cycloop/necklace formation from (p, q) -strings with high p and/or q within our analysis, we do not pursue this here as the formation probability for such bound states remains extremely uncertain. Although much work has been done to determine the tension spectrum of (p, q) -strings in a variety of backgrounds, including the KS throat (see [245]), comparatively little is known about the relative abundances of the (p, q) species. Even if the overall spectrum of number densities could be normalised somehow, it is still not clear how to determine the *probability* of forming a general (p, q) bound state.

We therefore assume $(1, 0)$ -strings (F -strings) and $(0, 1)$ -strings (D -strings) to be the most common stringy objects able to play the role of cosmic strings. However, other authors, notably Sarangi and Tye [247], have suggested that the most common stringy objects in any geometry are likely to be D_p -branes wrapping $(p - 1)$ -dimensional cycles in the compact space. In a more refined analysis, it would, in principle, be possible to perform some kind of weighted summation over all string species with respect to the calculations which determine their impact on cosmologically observable parameters (for example with respect to PBH and DM formation, as investigated in the following chapters). In this case, the relative abundance of each type of (p, q) -string could be estimated by their relative formation probabilities. However, as the full non-Abelian action would be needed to determine the dynamics of the higher order contributions, the resulting analysis is likely to be complicated considerably by the addition of each new string species.

Despite this, the non-Abelian DBI (Myers) action is still of importance to our model in one other respect as yet another complication arises from the fact that each species has its

own specific effective tension for a given background. Even if we restrict ourselves to single F - and D -strings, we still need a way to calculate the tension $\mathcal{T}(g)$ for these objects in the warped deformed conifold. For “macroscopic” (p, q) -strings, i.e. strings with high p /high q ,²⁸ this may be calculated relatively easily by considering the dual D_3 -brane wrapped on a 2-cycle within the S^3 [245], but for strings with small p and/or small q it remains an open problem. In order for the description of (p, q) -strings to arise naturally from the hybrid $D3 - \bar{D}3$ inflation scenario, we also need a “microscopic” theory for the lowest lying string modes. This can only be achieved by considering the effective action of the strings themselves. Thankfully, some progress has been made in this direction, at least in the large q limit [248].

In the following sections we outline the origin of the existing formulae for the tensions of macroscopic and microscopic (p, q) -strings in the warped deformed conifold. We then return to considering the differences and similarities between field-theoretic and stringy strings, in light of our knowledge concerning their respective effective actions and tensions. The chapter concludes with a discussion of questions which may arise in the context of “model mixing”, where defect strings wrap non-trivial cycles in extra-dimensional scenarios which are often (though not exclusively) motivated by string theory.

2.4.3 Macroscopic and microscopic (p, q) -strings

For the D_3 -brane dual of a macroscopic (p, q) -string to behave as a one-dimensional object in the warped throat geometry it must wrap a *stable* 2-cycle in the three-sphere which regularises the tip. This implies that we must switch on a non-zero magnetic flux on the worldvolume in order to stabilise the brane [245, 248].²⁹

For simplicity we may assume that this flux is parallel to the $U(1)$ gauge field and we are free to choose a gauge such that only two components of F_{ab} , F_{01} and F_{23} , are non-zero. If the brane is extended in two of the non-compact directions (i.e. if the three-dimensional brane behaves like a one-dimensional string with respect to the non-compact space) and is wrapped on an S^2 within the S^3 , it may be shown that the Hamiltonian density takes the form

$$\mathcal{H} = \frac{a_0^2}{\lambda} \sqrt{\frac{q^2}{g_s^2} + \frac{b_0^2 M^2}{\pi^2} \sin^4(\psi)} + \left[\frac{M}{\pi} \left(\psi - \frac{\sin(2\psi)}{2} \right) - (p - qC_0) \right] \quad (2.77)$$

²⁸Note that here “macroscopic” does not refer to the physical size of the string.

²⁹Although the formula for the effective tension of a wrapped brane was derived separately in each of these references, we follow [248] in the analysis that follows for the sake of notational convenience.

where $\psi \in [0, 4\pi)$ is the azimuthal angle on the three-sphere and C_0 is the R - R scalar charge, which is simply a numerical constant (as are a_0 and b_0 , introduced earlier). However, as mentioned earlier, C_0 is trivial in the KS background. We may therefore set $C_0 = 0$ without loss of generality, though we choose to keep it as a free parameter in the discussion that follows, in order to ensure consistency with the results presented in [248, 255]. If we then minimise the energy with respect to the radius of the S^2 , we find that

$$\psi_{min} \sim \frac{b_0^2 - 1}{2} = \frac{(p - qC_0)\pi}{M}. \quad (2.78)$$

This yields the following value for the S^2 radius:

$$R_{S^2} = R \left| \sin \left(\frac{\pi(p - qC_0)}{M} \right) \right| \quad (2.79)$$

where R is the radius of the S^3 . Substituting this back into the Hamiltonian density then gives the effective tension for a macroscopic (p, q) bound state (see also [249, 250])

$$\mathcal{H}_{min} \equiv T_{(p,q)} = \frac{a_0^2}{\lambda} \sqrt{\frac{q^2}{g_s^2} + \left(\frac{b_0 M}{\pi} \right)^2 \sin^2 \left(\frac{\pi(p - qC_0)}{M} \right)}. \quad (2.80)$$

Strictly speaking we would expect this simple macroscopic description to be in need of modification, as Witten showed that turning on fluxes introduces non-commutative effects on the brane worldvolume [251]. Following on from this work, Seiberg and Witten identified the limit in which the string dynamics in the warped throat are described by a non-commutative gauge theory. They showed that a formal equivalence exists between the ordinary (dual) commutative gauge theory and the new non-commuting gauge fields, whereby the non-commutative effects may be incorporated into the model by defining a suitable Hodge-star product in place of the usual product function [252]. For large fluxes the non-commutative effects are negligible, but for small fluxes they result in important corrections to the string dynamics.

Ward and Thomas used the Myers action together with a “fuzzy sphere” ansatz for the worldvolume scalars [253, 254] to incorporate some of these effects, though their results were consistent with the macroscopic description [245] and the resulting string tension (2.80), as well as with the previous results in [252] in that the non-commutative corrections were “washed out” in the large flux/large string number limit. They began by constructing the appropriate form of the Myers action for q coincident D -strings with non-zero electric flux on the worldvolume.³⁰ At the tip of the throat the Kalb-Ramond field tends to zero

³⁰In this description q is already quantised and the $U(1)$ worldvolume flux is characterised by some real number p . We will later find that this too is quantised naturally in the context of q coincident D -strings, leading to a dual description of (p, q) -strings.

and in the strongly coupled regime

$$g_s = e^\Phi \sim 1 \quad (2.81)$$

the string frame then coincides with the Einstein frame. Taking the non-commutative coordinates ϕ^i to be non-vanishing in the directions of the S^3 and expanding the determinant of the potential term in the action, they found

$$\det(Q_j^i) = 1 - \frac{\lambda^2}{2} [\phi^a, \phi^b] [\phi^c, \phi^d] \Omega_{ac}^3(y) \Omega_{bd}^3(y) + \dots \quad (2.82)$$

and hence

$$S = -\mathcal{T} \int d^2\zeta \text{STr} \left(a_0^2 \sqrt{1 - \mathbb{I} \cdot \frac{\lambda^2 \epsilon^2}{a_0^4}} \sqrt{1 - \frac{\lambda^2}{2} [\phi^a, \phi^b] [\phi^c, \phi^d] \Omega_{ac}^3(y) \Omega_{bd}^3(y)} \right) \quad (2.83)$$

to lowest order, where $\Omega^3 \equiv \Omega_3$ is the metric on the unit three-sphere, whose coordinates are labelled by $\{y^a\}$, $a \in \{1, 2, 3\}$.³¹ ³² For simplicity, the dynamic part of the action was neglected.

A “fuzzy sphere” ansatz for the transverse scalars (see [253]-[256]) was then introduced so that

$$\phi^a = \hat{R} e_i^a \alpha^i \quad (2.84)$$

where α^i are the generators of the $SU(2)$ algebra,³³ e_i^a are the vielbeins on the three-sphere and \hat{R} is the so-called “canonical radius” of the fuzzy sphere, which is related to the physical radius R_F via

$$R_F^2 = \hat{R}^2 \lambda^2 \hat{C}. \quad (2.85)$$

Here \hat{C} represents the quadratic Casimir invariant of the representation, which is related to the R - R 2-form and the transverse scalars by

$$\hat{C} = \lambda \partial_c C_{ab} \phi^c. \quad (2.86)$$

³¹Here we have fixed the gauge such that $A_0 = 0$, which is equivalent to setting $F_{01} = \epsilon$, so that the gauge field is proportional to the identity matrix \mathbb{I} . This breaks the original symmetry of the coincident branes, so that $U(q) \rightarrow SU(q) \times U(1)$, where the $U(1)$ field now commutes with the $SU(q)$ sector.

³²See [255] for a summary of the main results of [253, 254] as applied specifically to (p, q) -strings in the KS geometry. See also [256] for a related article.

³³Recall that $SU(2)$ is the double cover of $SO(3) \equiv S^3$

Expanding the R - R 2-form C_2 in the CS contribution gives

$$S_{CS} = \mathcal{T} g_s \int d^2\zeta \text{STr} \left(\mathcal{P}[C_0 + e^{i\lambda i_\phi C_2}] \right) \quad (2.87)$$

where i_ϕ denotes the interior product by ϕ^i , regarded as a vector in the transverse space [241, 242] and the symmetrised trace operation may be approximated by a trace over the gauge group in the large q limit, i.e. neglecting terms in $1/q^2$ and higher order powers³⁴ [255]. This yields a field strength F_{abc} which gives rise to quantised flux when integrated over the S^3 . Hence it is possible to write

$$F_{abc} = f \Omega_{abc} \quad (2.88)$$

where Ω_{abc} is the volume element on the S^3 and $f \in \mathbb{R}$. After imposing the usual flux normalisation condition (2.41), this gives

$$f = \frac{2}{b_0 g_s R}. \quad (2.89)$$

The canonical momentum of the EM field may then be determined by varying the total Lagrangian density (including the CS term) for the fuzzy-sphere ansatz. The resulting displacement field (i.e. p) is now quantised in terms of the string tension, such that

$$p = q\mathcal{T} \left(a_0^2 \sqrt{1 + 4R_F^2 \hat{R}^2} \frac{\lambda^2 \epsilon^2}{a_0^4} \left(1 - \frac{\lambda^2 \epsilon^2}{a_0^4} \right)^{-\frac{1}{2}} + g_s \lambda C_0 + \frac{4\lambda}{3b_0} \frac{R_F^2 \hat{R}}{R} \right) \quad (2.90)$$

(see [255]). Substituting this into the appropriate expression for the Hamiltonian density and minimising with the respect to the fuzzy sphere radius (as we did in the macroscopic case with the radius of the 2-cycle for the D_3 -brane, R_{S^2}), we obtain

$$R_F \sim \pi \left(\frac{g_s}{b_0} \right) (p - qC_0) \left(\frac{R}{\alpha'} \right)^{-1} \quad (2.91)$$

in the large M limit, which is in agreement with the equivalent Abelian expression (2.79) to leading order $\sim \mathcal{O}(1/M)$. The resulting expression for the string tension is then

$$\begin{aligned} \mathcal{H}_{min} &\equiv T_{(p,q)} \\ &= \frac{a_0^2}{\lambda} \sqrt{\frac{q^2}{g_s^2} \left(1 + \frac{1}{4} \left(\frac{g_s}{b_0} \right)^4 \frac{(p - qC_0)^4 \lambda^2}{R^4 \hat{C}} \right)} + (p - qC_0)^2 \left(1 - \frac{1}{4} \left(\frac{g_s}{b_0} \right)^4 \frac{(p - qC_0)^4 \lambda^2}{R^4} \right) \end{aligned} \quad (2.92)$$

³⁴Due to the inclusion of the S^3 vielbeins in the fuzzy sphere ansatz, we may rewrite the Casimir invariant directly in terms of the matrix representation of the $SU(2)$ group elements, i.e. $\hat{C}\mathbb{I}_q = \alpha^i \alpha^j \delta_{ij}$ where \mathbb{I}_q is the rank q identity matrix. This feature simplifies the calculation of the symmetrized trace for both large and finite q , though the form is especially simple in the limit $q \rightarrow \infty$.

which agrees with the equivalent Abelian expression (2.80) up to $\sim \mathcal{O}(1/M^2)$. Thus we have an expression for the tension in the large q and large M limits, but which is valid for finite and potentially small p . Progress towards an expression which is also valid for small M may be made by first taking the large M limit, as above, and then expanding the general expression for the Hamiltonian density in powers of $1/M$ *before* minimising the energy. Taking the SUGRA approximation $g_s M \gg 1$, (2.55) allows us to ignore large corrections to the S^3 metric caused by the back-reaction and this ensures the validity of the effective action on which the resulting analysis is based. However, it has been suggested that further perturbative analysis of \mathcal{H} may provide a reasonably good approximation for the effective tension even in the limit $g_s M \sim \mathcal{O}(1)$ [255].

To account properly for microscopic strings an exact prescription for the symmetrized trace of the Myers action integrand is needed, though this is unknown in the general case. However, a prescription for the symmetrized trace of $SO(3)$ was proposed in [257] and this was later used by Ward to construct a preliminary investigation in the case of two coincident D -strings, i.e. $q = 2$ [255]. He found that, even in this simple case, the resulting minimisation conditions for \mathcal{H} were highly non-linear and difficult to solve analytically, though the expression for \mathcal{H} itself was relatively simple and dependent on an overall factor of a_0^2/λ , as in (2.80) and (2.92) above.

The important point is that there is very strong evidence to suggest that

$$T_{(p,q)} \sim \frac{a_0^2}{\lambda} [\dots] \quad (2.93)$$

for *all* values of p and q . Perhaps even more importantly, all known expressions for the effective tension agree with one another in both the $p = 0$ and $q = 0$ cases, so that

$$T_{(1,0)} \sim \frac{a_0^2}{\lambda} \times \mathcal{O}(1) \quad (2.94)$$

and

$$T_{(0,1)} \sim \frac{a_0^2}{\lambda} \times \mathcal{O}\left(\frac{1}{g_s}\right), \quad (2.95)$$

irrespective of the precise ansatz for the worldvolume scalars. As we shall see in the following chapter, using the Nambu-Goto action or Abelian form of the DBI action (i.e. the appropriate actions for F - and D -strings), with an ansatz describing wound strings at the tip of the throat, leads to a similar dependence of the effective tension on the warp factor. In other words, $T_1 \rightarrow a_0^2 T_1$ where T_1 labels the “fundamental” tension of the string species (i.e. either $T_{(1,0)}$ or $T_{(0,1)}$) *in the warped throat*, and the factor of a_0^2 arises from the pull-back of the spacetime metric to the worldsheet.

In this case the “fundamental” tension of the string species in the background geometry is

2.4. TOPOLOGICAL DEFECT STRINGS VS “STRINGY STRINGS”: (p, q) -STRINGS
IN THE KS THROAT

always *proportional* to the truly fundamental string tension $\mathcal{T} = \lambda^{-1}$, from (2.63), but contains additional metric-dependent factors, so that $T_1 = T_1(g)$. For the warped throat geometry these corrections will, in general, depend on the parameters which control the blow-up of the S^3 , i.e. $b_0 \sim \mathcal{O}(1)$, g_s and M (regarding $l_s = \sqrt{\alpha'}$ as the fundamental unit) and on the values of p and q themselves (as in equations (2.94)-(2.95)). We therefore expect similar criteria to hold for more general (p, q) -strings ($p, q > 1$), with $T_{(p,q)} = T_{(p,q)}(p, q, g_s, M)$, $T_{(p,q)} \propto \mathcal{T} = \lambda^{-1}$ in *all* cases and $T_{(p,q)} \rightarrow a_0^2 T_{(p,q)}$ in the final action. This suggests that equation (2.93) provides a *reasonably* good order of magnitude estimate for the effective tension of all (p, q) -string species. In turn, this suggests that our results provide a reasonably accurate picture of certain cosmological consequences of (p, q) -string networks *in general*, even though we restrict our analysis to the lowest lying string modes.

The main point is that, although branes composed of p F -strings and q D -strings “blow up” for $p, q \gg 1$, we may continue to use string-like ansatz for the embedding if the extra “blown up” dimensions wrap stable cycles in the transverse space. *All* effects of the string’s “expansion” into a higher-dimensional brane may then be incorporated into the dynamics simply by replacing the original flat-space string tension, $\mathcal{T} = \lambda^{-1}$, with an appropriate formula depending on p, q and the parameters which define the metric $g_{\mu\nu}$.

Finally, we turn our attention to certain problems which may arise in the context of “model mixing”. We will argue in chapter 5 that the effective action for so-called “pinched” field-theoretic strings is equivalent to the Nambu action with a worldsheet-coordinate-dependent tension. Building on previous results in chapter 3, we will see that this is also one way of interpreting the four-dimensional effective action for a wound F - or D -string in an extra-dimensional background. Thus we see that two types of structure - one a geometric property of the embedding and one internal to the string itself - appear, phenomenologically, to be equivalent. The fundamental result of chapter 5 implies that extra-dimensional effects involving strings with *no* internal structure are able to “mimic” field-theoretic structure in defect strings. One particularly important aspect of this correspondence is an interpretation of the topological winding number n of an unwound vortex string in terms of the physical winding number n_w of a wound string with no internal structure.

The question then arises: what happens if we place a field-theoretic string in an extra-dimensional background? Although such scenarios are *often* motivated by string theory, which is mathematically inconsistent in $(3+1)$ -dimensions, they are not exclusive to it, and it is reasonable to ask what happens if a vortex string wraps windings in the internal space. One possible answer is that, for $R \leq r_s$ ($r_s \leq r_v$)³⁵ such windings are unphysical and that, for $R \gg r_v$, the Nambu action provides an adequate approximation. In this case, the

³⁵i.e. if the length scale of the compact space is less than or comparable to the size of the vortex core(s).

internal structure of the field-theoretic string may be neglected. However, although this seems plausible in the case of an $n = \pm 1$ string (as considered as an F -string dual in the original paper by Nielsen and Olesen [15]) it is unclear whether a vortex string with topological winding $|n| > 1$ and physical winding $|n_w|$ *also* admits a dual string-theory model in which $|n|$ may be interpreted as a purely geometric effect.

The situation is even less clear if we imagine a *pinched* string wrapping windings in the internal space. In both cases, two phenomenologically equivalent but physically different types of structure are combined, and it is by no means clear what the resulting phenomenology may be, or how it may relate to the phenomenology of more complex string species, such as (p, q) -strings in higher dimensional scenarios. Although we do not investigate this possibility in great detail, a preliminary answer to these questions is suggested at the end of chapter 5, where it is argued that *all* field-theoretic strings - even those embedded in higher-dimensional geometries - may admit dual models in terms of wound strings with no internal structure. We note however, that an extended analysis of this problem may provide interesting avenues for future research, and help to shed further light on the relation between field theory and string theory strings.

The preceding sections conclude our discussion of the relevant background material for this thesis. We now move on to consider the formation of necklace loops and non-topological cycloids in chapters 3 and 4, before considering the relation of wound F/D -strings to pinched vortex strings in chapter 5.

CHAPTER 3

PRIMORDIAL BLACK HOLES AND DARK MATTER FROM NECKLACE COLLAPSE

3.1 Introduction

There has, in recent years, been a renewed effort to test string theory in a cosmological context. This is due in part to the availability of increasingly precise data from experiments such as WMAP [258, 259] and SDSS [260, 261]. However, it is also due to theoretical advances which have resulted in a better understanding of the compactifications of the theory down to $(3 + 1)$ -dimensions. Since such compactifications are typically warped, this means that mass-scales in the effective theory can be significantly reduced. One important consequence of this is that superstrings may have a much smaller tension than first realised [191, 193].

Originally Witten [196] ruled out the notion that F -strings could play the role of cosmic-strings because of their extremely high mass density. The unwarped string tension is so large that the presence of cosmic F -strings (formed after inflation) would be immediately evident in the CMB. This effectively killed the subject until GKP (Giddings-Kachru-Polchinski) [262] showed, in the context of type IIB strings, that by turning on non-trivial fluxes threading cycles in a class of compact manifolds one could obtain highly warped four-dimensional backgrounds. The warping then acts in such a way as to reduce the overall tension of any object, allowing observational bounds to be evaded.

Simultaneously, there has also been renewed interest in models of open string inflation. In such models the energy density of the inflaton field(s) is provided by the geometric distance between the D_3 -brane of our universe and parallel branes or anti-branes. Since such branes/anti-branes are charged under massless R - R form fields, it is expected that large numbers of F - and D -strings will be produced at the end of inflation [191, 245, 247], as well as (p, q) bound states of multiple strings [234, 248, 256]. Observationally, however, this raises a potential problem as these strings are not redshifted away and therefore (presumably) fine-tuning is required to restrict their number to $\mathcal{O}(1)$ per Hubble volume. In the following analysis we will simply assume that some phase of open string inflation has occurred, though it remains an open problem to generate such a configuration in an explicit model of string theory inflation.

Given that these strings exist in a higher-dimensional theory, one could also imagine that they wrap cycles within the internal space [154]. Such cycles could be either “smooth” or “lumpy” from a four-dimensional perspective. A string that wraps a series of internal cycles at separate points in four-dimensional space would appear as a necklace: that is, as a system of monopoles or “beads” connected by string segments. Alternatively, strings which wrap the compact directions smoothly along their four-dimensional length would appear to have a continuously varying mass density in the case of non-geodesic windings (as considered in the present chapter), or a constant mass density in the case of geodesic windings (as considered in chapter 4). The exact nature of the variation depends on the geometry of the compact space, as well as the string embedding, though in general we would expect the effective tension to be periodic.

Matsuda proposed that a necklace structure may form from a smoothly varying configuration as the string relaxes to a quasi-stable state [6]. In this case the periodic variation of effective string tension is viewed as the sum of the standard string tension plus a lifting potential in the (angular) compact directions. If the angular directions are flat, the energy of the string is minimised for a smoothly varying configuration, but in the presence of a potential a necklace structure is energetically favoured. Furthermore, the existence or absence of a potential affects the stability of the extra-dimensional windings when strings chop off from the network to form loops. In the absence of a lifting potential, windings must be stabilised topologically giving rise to objects called “cycloops”. This is not true for necklace solutions which may exist, at least over cosmologically relevant time scales, even if the compact space is simply connected. The quasi-stability of the necklace solution is discussed in greater detail in section 3.5.

The cosmological consequences of cycloops were first investigated by Avgoustidis and Sheldard [16]. They showed that, unlike an ordinary string loop, a decaying cycloop leaves a topologically trapped remnant when it reaches zero radius. This remnant appears as a monopole to a four-dimensional observer and may be interpreted as a DM particle. Like ordinary string loops, cycloops also have a small probability ($f \sim 10^{-20}$) of collapsing to form PBHs in the course of their first oscillation [115]. These PBHs may then decay to leave topologically stable Planck-mass relics. Although many authors have considered the production of Planck-mass relics from decaying black holes (beginning with MacGibbon [96]) the possibility that these relics may be topologically trapped string remnants has not been thoroughly investigated [6, 16].

By contrast, Matsuda has claimed that a large fraction $f \sim 1$ of all necklace loops eventually collapse to form PBHs via a separate necklace-specific process. This claim is based on the assumption that mass-energy may only be lost, via GW emission, from the four-dimensional

string segments, leaving the bead mass unchanged. Thus when the necklace loop reaches its minimum radius, it will undergo collapse if the mass of the beads is large enough to produce a Schwarzschild radius greater than the string width.¹ He therefore proposed that small loops produced at very early times may form stable relics which also act as DM candidates. Conversely, he argued that loops created at later times would be larger and hence likely to contain enough mass in their beads to cause them to collapse into PBHs [8].

However, this original schematic analysis involved a number of simplifying assumptions, such as the existence of a time-independent lifting potential and hence a constant bead mass for necklace loops formed at different epochs. The initial inter-bead spacing was also assumed to scale like the entropy distance at the time of network formation² and the dynamical evolution of the inter-bead distance was modeled by the standard string-monopole network evolution equations, originally proposed by Berezinsky and Vilenkin [263].

In the following analysis we attempt to construct a more concrete model of necklace formation, based on ideas from type IIB string theory. We calculate the explicit form of the lifting potential for a loop of string with extra-dimensional windings in the KS geometry [5, 169]. Using realistic models of winding and loop formation, we see that the potential itself evolves dynamically, resulting in a time-dependent bead mass. This shows that the first of these assumptions must be modified, at least for certain backgrounds.

Additionally, the decay signature of necklace loops in our model is in many ways the opposite of what Matsuda predicted. We find that PBH formation is favoured at early times, with potential DM relics forming later. This is indeed an unexpected result (c.f. [8]), though one which appears to follow naturally from the consideration of monopole/bead formation as a *dynamical* process rather than as the result of a separate phase transition prior to string formation. We argue that this is the correct approach to take when considering “monopoles” which form from extra-dimensional windings and a comparison of our results with field-theoretic string-monopole networks is given in section 3.6. This suggests that the usual evolution equations for string-monopole networks do not apply to necklaces formed from wound-strings.

In addition to a renewed interest in the role of F/D -string networks in cosmology, many physicists are still devoted to the study of field-theoretic cosmic strings [124, 264, 265]. Whilst a stringy origin of the CMB perturbations has been ruled out by observation, the best Λ CDM model fit to the data suggests that these strings may contribute at the level of

¹We assume here that the minimum radius of the loop is determined by the effective width of the string, $\delta \sim l_s = \sqrt{\alpha'}$.

²The entropy distance is defined to be $d_S(t_s) \sim t_M^{\frac{1}{2}} t_s^{\frac{1}{2}}$, where t_s is the formation time of the string network and $t_M \leq t_s$ is the time of monopole formation [6].

$\sim 10\%$ [126, 127] (for a review see also [266]), making them extremely important objects to study. Unfortunately, a best fit for (p, q) -strings, necklaces or cycloids has not yet been investigated [267].

However, recent discoveries of dualities between gauge field strings and F/D -strings have raised the possibility of unifying these two approaches. Indeed, if string theory really is a theory of everything (TOE), and if we accept QFTs to be valid low-energy approximations, we may also hope to find string theory analogues of all field theory phenomena. If therefore we expect topological defects, including strings, to arise generically in symmetry-breaking processes, we must investigate the relationship between fundamental strings and field theory strings in much more detail. This forms the motivation behind our identification of the inter-bead distance with the correlation length of a field-theoretic string network, $\xi(t)$, in section 3.4, though the possible relationship between wound F/D -strings and field-theoretic strings is investigated in greater depth in chapter 5 through the introduction of the notion of a “pinched” string.

The aim of this chapter is to consider a simple model of wound-string necklaces in a well understood SUGRA background using type IIB string theory, thereby extending the initial phenomenological approach begun in [8]. Following the considerations above, we also consider the possible relation of these objects to field-theoretic strings, restricting ourselves to generic considerations. Since the background yields an explicit form for the lifting potential in terms of the number of extra-dimensional windings, we may compute the bead mass precisely if this number is known for a string loop formed at any epoch. Following [16], we assume that the motion of a string in the compact space, prior to the chopping off of a loop, is random. This allows us to estimate both the time-dependent bead mass and the average inter-bead distance. We find that the results depend on the definition of the parameter ω_l , which gives the fraction of the total string length contained in the extra-dimensional windings. Two definitions are suggested: Identifying the inter-bead distance in the string picture with the correlation length in the field theory picture, we see that the first definition leads naturally to a scaling solution - similar to that for field theoretic strings but with a correlation length $\xi(t) \sim \gamma t$ ($0 < \gamma \leq 1$) much smaller than the horizon. The second definition leads to a sub-scaling solution $\xi(t) \sim t^{\frac{3}{4}}$.

More importantly, we are able to compute the PBH mass spectrum produced by collapsing necklaces. Since the mass of an individual necklace depends upon the structure of the internal manifold as well as the string tension, the resulting PBH spectrum yields information about the size of the extra dimensions and the warp factor. This influences the background cosmic ray flux via the Hawking radiation of PBHs expiring at the present epoch. We are thus able to provide observational bounds on string theory parameters using measurements of the extragalactic gamma-ray flux at 100MeV from EGRET [13].

An interesting result is that both definitions of ω_l give the same qualitative behaviour, with PBH formation occurring only over a limited time period in the early universe. However, the upper and lower limits of this window - and hence the resulting bounds on the model parameters - do vary significantly in each case.

The layout of this chapter is as follows: In section 3.2 we construct the worldvolume action for string loops before analysing their stability in section 3.3. Section 3.4 deals with the formation of these loops and their cosmological impact, focusing on the predictions for PBH abundance and section 3.5 contains a brief discussion of our main results and suggestions for future work.

We conclude this introduction with a note regarding terminology. The “necklaces” which are the subject of the present chapter and of Matsuda’s original work should not be confused with “necklaces” formed via other string-monopole interactions. For example, Leblond and Wyman [268] have shown that D_0 -branes (monopoles) may be formed at junctions between strings in a (p, q) -string network. The resulting necklaces are of no relation to the ones considered here. Related work can be found in [269]-[272].

3.2 Strings with non-trivial windings in the internal space

The background we wish to consider is that of the KS throat [5, 169] since it is one of the better understood backgrounds of the type IIB theory.³ Recall that conical singularities are the most generic kind of singularities arising within compactifications of IIB string theory on manifolds of $SU(3) \times SU(3)$ structure [164]. Since explicitly realistic compactifications are difficult to construct, we will take a more phenomenological approach by considering (non-compact) conical backgrounds such as the conifold $T^{1,1}$ that can be glued to a (conformal) CY manifold. Provided we work in a region far from this gluing, we can (locally) work with the conifold geometry without worrying too much about the precise details of the compactification mechanism. With this in mind, we can regularise the singular conifold by allowing the S^2 to shrink to zero size. This is just the deformation of the conifold, which is topologically equivalent to the cotangent bundle over the three-sphere T^*S^3 , where the S^3 has some minimal size.⁴

³Our choice for the background is also inspired in part by the AdS/CFT duality, since the KS geometry is known to be dual to an $\mathcal{N} = 1$ confining gauge theory (see section 2.3). Viewed from this perspective, the strings are effectively the confining strings of the gauge theory with non-trivial wrapping. Whilst this is interesting in its own right, our motivation here will be to model cosmic necklaces rather than gauge theory necklaces. As we will demonstrate in chapter 5, it may be possible to generate necklace-type objects from gauge theory strings *without* requiring them to adopt non-trivial winding configurations.

⁴We should also point out that there is nothing special about the deformed conifold solution. One could equally well use the resolved conifold where the S^2 is blown up instead [273, 274]. Indeed the resulting string

Recall that in canonical coordinates the metric at the tip is

$$\begin{aligned}
 ds^2 &= a_0^2 \eta_{\mu\nu} dx^\mu dx^\nu + R^2 (d\psi^2 + \sin^2 \psi (d\theta^2 + \sin^2 \theta d\phi^2)) \\
 \psi &\in [0, 4\pi), \quad \theta \in [0, \pi), \quad \phi \in [0, 2\pi)
 \end{aligned} \tag{3.1}$$

where the square of the warp factor, $0 < a_0^2 < 1$, is inversely proportional to the square of the three-sphere radius, R^2 , (with a constant of proportionality determined by the deformation parameter of the conifold) and that the latter is proportional to the number of units of quantised R - R 3-form flux, M and the string coupling g_s . The basic point is that the warping varies like $1/g_s M$, where we are assuming the SUGRA limit $g_s M \gg 1$, so that, for fixed R , constraints on the warping can be interpreted as directly constraining the background geometry. In what follows we will assume that (3.1) is representative of a large class of warped geometries, without necessarily having an explicit realisation in a fully UV complete construction.

The action for both fundamental strings (F -strings) and D_1 -branes (D -strings) - or in more general (p, q) notation $(1, 0)$ - and $(0, 1)$ -strings respectively - in the warped deformed conifold is the Nambu-Goto action with additional worldsheet flux, plus a possible CS term for the D -string,

$$S = -T_1 \int d\sigma dt \sqrt{-X} + S_{CS} \tag{3.2}$$

where T_1 denotes either $T_{(1,0)}$ or $T_{(0,1)}$ and $X = \det X_{ab}$ with

$$X_{ab} = \gamma_{ab} + \lambda F_{ab}, \quad a, b \in \{0, \sigma\} \tag{3.3}$$

where γ_{ab} is the usual induced metric on the worldsheet

$$\gamma_{ab} = G_{MN}(X(\sigma, t)) \partial_a X^M(\sigma, t) \partial_b X^N(\sigma, t), \quad M, N \in \{0, \dots, 9\}, \tag{3.4}$$

and $\lambda = 2\pi l_s^2$. The simple form of the Lagrangian density $\sqrt{-X}$ arises because we are neglecting the coupling of the worldsheet to the NS - NS 2-form field, which is vanishing in our background (at least in the limit we are considering). The flux tensor is anti-symmetric in that $\lambda F_{00} = \lambda F_{\sigma\sigma} = 0$ and $\lambda F_{0\sigma} = -\lambda F_{\sigma 0}$, $\lambda F_{0\sigma} \geq 0$. Note that we are absorbing the definition of the string coupling into the field-strength tensor, since this allows us to identify the string frame with the Einstein frame. The CS coupling is given by the integral of the pull-back of the R - R 2-form over the worldsheet for the case of D -strings:

$$S_{CS} = T_1 \int M \alpha' (\psi - \sin \psi \cos \psi) d\theta \wedge d\phi. \tag{3.5}$$

tension scales directly with the resolution parameter and is therefore highly constrained by observations. The resulting solution is then very similar to the model considered in [276].

However, for simplicity we choose to ignore this correction in the following analysis and instead concentrate solely on the Nambu-Goto component of the action.

We wish to take the following general ansatz for the string embedding:

$$X^M = (t, r(t) \sin \sigma, r(t) \cos \sigma, z_0, \tau \rightarrow 0, 0, 0, \psi(\sigma, t), \theta(\sigma, t), \phi(\sigma, t)) \quad (3.6)$$

where $\psi \in [0, 4\pi)$, $\theta \in [0, \pi)$ and $\phi \in [0, 2\pi)$, as before. This describes a circular string in the Minkowski directions which is wrapped over the S^3 in the internal space.⁵ Using the metric (3.1) and the embedding ansatz (3.6), the action becomes

$$S = -T_1 a_0^2 \int d\sigma dt \sqrt{(1 - \dot{r}^2)(r^2 + a_0^{-2} R^2 s'^2) - a_0^{-2} r^2 R^2 \dot{s}^2 - a_0^{-4} \lambda^2 F_{0\sigma}^2 - a_0^{-4} R^4 \dot{s}^2 s'^2 + a_0^{-4} R^4 (\dot{s} s')^2} \quad (3.7)$$

where we have introduced the slightly abusive notation

$$\begin{aligned} \dot{s}^2 &= \dot{\psi}^2 + \sin^2 \psi (\dot{\theta}^2 + \sin^2 \theta \dot{\phi}^2) \\ s'^2 &= \psi'^2 + \sin^2 \psi (\theta'^2 + \sin^2 \theta \phi'^2) \\ (\dot{s} s') &= \dot{\psi} \psi' + \sin^2 \psi (\dot{\theta} \theta' + \sin^2 \theta \dot{\phi} \phi'). \end{aligned} \quad (3.8)$$

Here a dot or dash indicates differentiation with respect to t or σ , respectively, and we have chosen the gauge so as to identify the worldsheet time coordinate with the proper time in the Lorentz frame of the loop, t . We have also included a non-zero “electric” gauge field contribution for generality. For the D -string case, this corresponds to the dis-solving of F -string charge on the worldsheet and the strings are essentially superconducting.

There are two constants of motion for this configuration, the total energy of the string H and the angular momentum l , due to the motion of the string in the internal dimensions.^{6, 7} We parameterise these conserved charges as [276]

$$H = \frac{\partial L}{\partial \dot{q}^I} \dot{q}^I - L, \quad l = \frac{\partial L}{\partial \dot{q}^I} q'^I \quad (3.9)$$

⁵In this model the strings sit at the tip of the warped throat, which is also a choice made for the sake of simplicity. However, there is no a priori reason why we should make this assumption and a more general analysis would follow the lines of [275].

⁶Note that although the string “rotates” around the S^3 , no centripetal force is acting upon it. The internal (compact) dimensions are parameterised in terms of the angular variables ψ , θ and ϕ and so the motion through the S^3 is measured in $rad \times [t]^{-1}$, the units of angular velocity.

⁷We have not here considered the more general case of a loop with non-trivial windings in the internal manifold which also rotates in Minkowski space. Such a scenario would require the action of a genuine centripetal force provided by the string effective tension.

where L is the Lagrangian and q^I are the canonical coordinates, which are themselves functions of the world-volume coordinates through $q^I = (r(t), \sigma, \psi(\sigma, t), \theta(\sigma, t), \phi(\sigma, t), A_a(\sigma, t))$. Using (3.7) and neglecting the CS term, we find the following expressions for these conserved charges

$$\begin{aligned}
 H &= T_1 \int d\sigma \frac{a_0^2(r^2 + a_0^{-2}R^2s'^2)}{\sqrt{(1 - \dot{r}^2)(r^2 + a_0^{-2}R^2s'^2) - a_0^{-2}r^2R^2\dot{s}^2 - a_0^{-4}\lambda^2F_{0\sigma}^2 - a_0^{-4}R^4\dot{s}^2s'^2 + a_0^{-4}R^4(\dot{s}s')^2}} \\
 l &= T_1 \int d\sigma \frac{R^2r^2(\dot{s}s')}{\sqrt{(1 - \dot{r}^2)(r^2 + a_0^{-2}R^2s'^2) - a_0^{-2}r^2R^2\dot{s}^2 - a_0^{-4}\lambda^2F_{0\sigma}^2 - a_0^{-4}R^4\dot{s}^2s'^2 + a_0^{-4}R^4(\dot{s}s')^2}}.
 \end{aligned}$$

However, it is more useful to rewrite the Hamiltonian in canonical form using the momenta

$$\begin{aligned}
 P^2 &= \left(\frac{\partial L}{\partial \dot{r}}\right)^2, & \Pi^2 &= \left(\frac{\partial L}{\partial \dot{A}}\right)^2 \\
 L_\psi^2 &= \left(\frac{\partial L}{\partial \dot{\psi}}\right)^2, & L_\theta^2 &= \left(\frac{\partial L}{\partial \dot{\theta}}\right)^2, & L_\phi^2 &= \left(\frac{\partial L}{\partial \dot{\phi}}\right)^2.
 \end{aligned} \tag{3.10}$$

This will simplify the form of our solutions for stable string windings with non-zero world-sheet flux ($\lambda F_{0\sigma} \neq 0$). This is especially true in the static ($l = 0$) case, which we will consider in section 3.3.

After a long but straightforward calculation we find that the canonical form of the Hamiltonian reduces to

$$H = \int d\sigma \sqrt{r^2 + a_0^{-2}R^2s'^2} \sqrt{T_1^2 a_0^4 + \frac{P^2}{(r^2 + a_0^{-2}R^2s'^2)} + \frac{\Pi^2}{a_0^{-4}\lambda^2} + \tilde{L}_\psi^2 + \tilde{L}_\theta^2 + \tilde{L}_\phi^2} \tag{3.11}$$

where we have written

$$\begin{aligned}
 \tilde{L}_\psi^2 &= \frac{a_0^4 \dot{\psi} L_\psi^2}{T_1^2 a_0^2 R^2 r^2 \dot{\psi} + \sin^2 \psi [\theta' (\dot{\psi} \theta' - \dot{\theta} \psi') + \sin^2 \theta \phi' (\dot{\psi} \phi' - \dot{\phi} \psi')]} \\
 \tilde{L}_\theta^2 &= \frac{a_0^4 \dot{\theta} L_\theta^2}{T_1^2 a_0^2 R^2 \sin^2 \psi r^2 \dot{\theta} + [\psi' (\dot{\theta} \psi' - \dot{\psi} \theta') + \sin^2 \psi \sin^2 \theta \phi' (\dot{\theta} \phi' - \dot{\phi} \theta')]} \\
 \tilde{L}_\phi^2 &= \frac{a_0^4 \dot{\phi} L_\phi^2}{T_1^2 a_0^2 R^2 \sin^2 \psi \sin^2 \theta r^2 \dot{\phi} + [\psi' (\dot{\phi} \psi' - \dot{\psi} \phi') + \sin^2 \psi (\dot{\phi} \theta' - \dot{\theta} \phi')]}
 \end{aligned} \tag{3.12}$$

In the next section we will specify the ansatz (3.6) completely by identifying the functions $\psi(\sigma, t)$, $\theta(\sigma, t)$ and $\phi(\sigma, t)$. We will then use equation (3.11) to determine the stability conditions in the static case by minimising the total energy of the string. Finally, we see how this leads naturally to a concrete model of necklace loops in the warped throat scenario when these solutions are perturbed.

3.3 Stability analysis for string loops in the static ($l = 0$) case and necklace formation

In the static case we assume that there is no motion in the compact dimensions and that the loop is neither expanding nor contracting in Minkowski space. Setting $\dot{\psi} = \dot{\theta} = \dot{\phi} = 0$ and $\dot{r} = 0$ (or equivalently $L_\psi^2 = L_\theta^2 = L_\phi^2 = 0$ and $P^2 = 0$) gives the static potential

$$V = \int d\sigma a_0^2 \sqrt{T_1^2 + \frac{\Pi^2}{\lambda^2}} \sqrt{r^2 + a_0^{-2} R^2 s'^2} \quad (3.13)$$

and $l = 0$, as expected. Even static strings of this kind may lose mass-energy over time due to the emission of gravitational radiation, causing them to shrink. However, we refer here to the stability of extra-dimensional windings in the static gauge over an epoch in which the loop size r and energy V are roughly constant. The shrinking of necklace loops over cosmological time scales and its implications are dealt with explicitly in section 3.4.

We must now complete the ansatz (3.6). Choosing $\psi(\sigma, t)$, $\theta(\sigma, t)$ and $\phi(\sigma, t)$ so that the angular winding is linear in σ ⁸

$$\begin{aligned} \psi(\sigma, t) &= 2n_\psi \sigma + \psi(t), \\ \theta(\sigma, t) &= n_\theta \sigma + \theta(t), \\ \phi(\sigma, t) &= n_\phi \sigma + \phi(t). \end{aligned} \quad (3.14)$$

with $n_\psi, n_\theta, n_\phi \in \mathbb{N}$ and $0 < \sigma \leq 2\pi$, this gives

$$V = \int d\sigma a_0^2 T_1 \sqrt{1 + \frac{\Pi^2}{T_1^2 \lambda^2}} \sqrt{r^2 + a_0^{-2} R^2 (4n_\psi^2 + \sin^2 \psi (n_\theta^2 + \sin^2 \theta n_\phi^2))} \quad (3.15)$$

where ψ and θ are themselves functions of σ and we have set $\dot{\psi}(\sigma, t) = \dot{\psi}(t) = 0$ etc in (3.14). Here n_ψ, n_θ and n_ϕ represent the number of physical windings in each of the ψ, θ and ϕ -directions respectively. The factor of two in the ansatz for $\psi(\sigma, t)$ is an artifact of the coordinate system and is due to the fact that the principle range of ψ is twice that of the polar angle ϕ .

We see immediately that $V = V(\psi, \theta)$, indicating that the ϕ -direction is flat, whereas the ψ and θ -directions are “lifted” by the presence of a potential energy density \mathcal{V} , which is the integrand in (3.15). It is now possible to make a connection between wound-strings

⁸This configuration corresponds to a situation in which the end point of the string is equally likely to move in each of the angular directions prior to the moment of loop formation. As we shall see in section 3.4, when we consider the random walk regime, this assumption is well motivated from a physical point of view. We also note for future reference that in canonical coordinates, windings of this form do not wrap geodesics in the S^3 . This has important implications for the σ -dependence of both H and l .

3.3. STABILITY ANALYSIS FOR STRING LOOPS IN THE STATIC ($l = 0$) CASE AND NECKLACE FORMATION

at the tip of the conifold throat and the cosmic necklaces predicted generically by Matsuda [9]. First we must determine the conditions under which the wrappings described above are stable, which is done by minimising the total energy V . Perturbations of this configuration are then seen to give rise to beads, whose mass can be estimated from the functional form of the potential.

However, rather than simply minimising the potential, it is useful (and easier) at this point to develop a physical intuition for the string configuration. Treating ψ and θ as independent variables, we may sketch the lifting potential (strictly speaking, the lifting potential energy density, but from here on these two terms will be used interchangeably) which the string “sees” throughout the whole S^3 . This is done by plotting the integrand \mathcal{V} in (3.15) and is shown for the range ($0 \leq \psi < 4\pi$, $0 \leq \theta < 2\pi$) in figure 3.1.

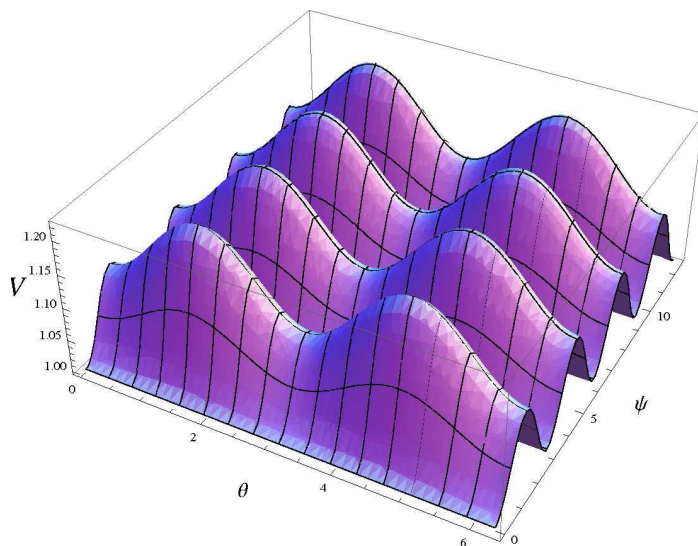


Figure 3.1: Plot of the static potential \mathcal{V} , setting the tension pre-factor term to unity and also $r^2 = 1$, $a_0^{-2}R^2 = 1$ and $n_\psi^2 = n_\theta^2 = n_\phi^2 = 1$.

The critical points and associated field masses may be found by diagonalising the corresponding Hessian matrix. We verify that \mathcal{V} has equal local maxima at $(\psi = (2n+1)\pi/2, \theta = (2m+1)\pi/2)$, saddle points of equal magnitude at $(\psi = (2n+1)\pi/2, \theta = m\pi)$ and flat directions which are also local minima (i.e. “troughs” not “ridges” or points of inflection) given by $(\psi = n\pi, \theta)$, where $m, n \in \mathbb{Z}$. This gives rise to two local maxima, two saddle points and two flat directions in the principle range. The associated field masses are given below,

- $\psi = \frac{(2n+1)\pi}{2}, \theta = \frac{(2m+1)\pi}{2}$ (local maxima)

$$m_\theta^2 = -\frac{T_1 R^2 n_\phi^2}{\sqrt{r^2 + a_0^{-2} R^2 (4n_\psi^2 + n_\theta^2 + n_\phi^2)}}, m_\psi^2 = -\frac{T_1 R^2 (n_\theta^2 + n_\phi^2)}{\sqrt{r^2 + a_0^{-2} R^2 (4n_\psi^2 + n_\theta^2 + n_\phi^2)}} \quad (3.16)$$

3.3. STABILITY ANALYSIS FOR STRING LOOPS IN THE STATIC ($l = 0$) CASE AND NECKLACE FORMATION

- $\psi = \frac{(2n+1)\pi}{2}$, $\theta = m\pi$ (saddle points)

$$m_\theta^2 = \frac{T_1 R^2 n_\phi^2}{\sqrt{r^2 + a_0^{-2} R^2 (4n_\psi^2 + n_\theta^2)}}, m_\psi^2 = -\frac{T_1 R^2 n_\theta^2}{\sqrt{r^2 + a_0^{-2} R^2 (4n_\psi^2 + n_\theta^2)}} \quad (3.17)$$

- $\psi = n\pi$, θ (flat directions)

$$m_\theta^2 = 0, m_\psi^2 = \frac{T_1 R^2 (n_\theta^2 + \sin^2 \theta n_\phi^2)}{\sqrt{r^2 + 4a_0^{-2} R^2 n_\psi^2}}. \quad (3.18)$$

It is now intuitively clear that minimal energy configurations correspond to strings wrapping flat directions in the two-dimensional submanifold described by ψ and θ . Physically this corresponds to strings wrapping some point in the S^3 which is uniquely determined by the condition $\psi = n\pi$ for some $n \in \mathbb{Z}$. This may be seen from the metric (3.1) and is the reason why n_θ and n_ϕ do not contribute to the total energy. Even though, technically, $n_\theta, n_\phi \geq 0$, windings around points have zero length and are not physically meaningful. This result is precisely what we should expect, since the minimum energy configuration corresponds to a situation in which the string has zero length contained in extra-dimensional windings.

We may verify this by substituting $\psi = n\pi$ and setting $\Pi^2 = 0$ in (3.15), showing that the total energy of a string wrapping flat directions in the potential \mathcal{V} is given by

$$V = 2\pi a_0^2 r T_1, \quad (3.19)$$

which is simply the rest mass of a string loop with radius r in warped Minkowski space.

This is certainly a very complicated way of verifying an intuitively obvious result but the above analysis will prove useful when we consider perturbations which result in different sections of a single string lying along equivalent local minima, that is, when the string interpolates between degenerate minima (flat directions) in the (ψ, θ) submanifold, resulting in the formation of beads.

The flat directions in figure 3.1 effectively define degenerate vacuum states for the string. For this reason we propose identifying the inter-bead distance in the string picture with the correlation length of field-theoretic strings. This forms the basis for identifying the field-theoretic parameter γ (which defines the correlation length as a fraction of the horizon distance) with the parameters which define the KS geometry in the following section. Also, though we refer to the bead-forming states as perturbations from the minimum energy (zero winding) configuration, this is true only in an energetic sense. Such states differ locally from the minimum energy configuration only in the vicinity of a bead.

3.3. STABILITY ANALYSIS FOR STRING LOOPS IN THE STATIC ($l = 0$) CASE AND NECKLACE FORMATION

Indeed, it is unclear whether it is possible to create a necklace from a standard F - or D -string loop via physical perturbations of a section of the string *after* the formation of the loop. This is the same as asking whether it is meaningful for an open string section (which may itself form part of a string loop or part of a string section connected to the network) to contain fractional windings which result in the formation of beads.

It is subtle point but in his generic argument Matsuda [9] predicted that, due to the presence of the lifting potential, integer windings would *not* be necessary for stability. In principle, this should allow for the formation of beads in open string sections due to local fractional windings. Though there is no reason why this could not happen generically, the possibility is not explicitly realised in our model. As discussed in the following section, we assume that any small-scale structure due to local partial windings will quickly disappear due to the annihilation of beads/anti-beads.

In our model the existence of the potential barrier which stabilises the windings after the loop chops off from the network (and which allows for the formation of beads) depends upon the presence of non-zero integer windings *at the moment of loop formation*. What is more, this may be generally true in this class of models since the form of the lifting potential in the extra dimensions ought always to be determined by the parameters that characterise the internal windings. Alternatively, however, it may be possible to account for the stabilisation of fractional windings in an extended analysis by allowing non-integer values of n_ψ , n_θ and n_ϕ . Appropriate boundary conditions for the functions $\psi(\sigma, t)$, $\theta(\sigma, t)$ and $\phi(\sigma, t)$ would then have to be fixed to ensure that the general ansatz (3.6) described a *continuous* string. Though this is an interesting question, and one which merits further investigation, we restrict ourselves here to considering configurations containing integer windings.⁹

What happens physically is the following: Before the loop chops off from the network, the string is free to move and create windings in the compact dimensions. If the internal manifold were not simply connected, these would become topologically trapped, resulting in the formation of cycloops [16]. However, as the S^3 is simply connected, these windings cannot be topologically stabilised. Instead they are stabilised by the presence of the lifting

⁹In addition, the dual field theory model for wound-strings developed in chapter 5 strongly suggests that - in the KS geometry at least - fractional windings are *unstable*. In order to create a fractional winding within a sub-section of the string (in a closed string loop the net number of windings along the total string length must of course be integer) it is necessary for the winding direction to change by $\pm\pi$ (i.e. from clockwise to anti-clockwise or vica-versa), at some point in the compact space which is *not* a pole of the S^3 . In the field picture this represents a discontinuous change from positive to negative topological winding number in the dual vortex string, so that vortices and anti-vortices of finite size then directly neighbour one another. Clearly, such a situation would lead to an instability as we would expect such configurations to immediately annihilate. As we expect duality to hold even in the case of long strings, this then suggests that fractional windings are generically unstable. In the string picture, an argument for the instability of non-integer windings can also be obtained from considering the interaction of the string tension (viewed as vector quantity) with the lifting potential (see section 5.9.2).

3.3. STABILITY ANALYSIS FOR STRING LOOPS IN THE STATIC ($l = 0$) CASE AND NECKLACE FORMATION

potential \mathcal{V} , which is itself a function of the number of windings.

We may imagine that, at the moment of loop formation, the string ansatz is described accurately by (3.14) as sketched in figure 3.2a. However, as soon as the string chops off from the network to form a loop, the total energy (V) is no longer minimised for such a smoothly varying configuration. Although windings may continue to vary smoothly in the ϕ -direction, they will then adopt a step-like configuration in the (ψ, θ) sub-manifold, as illustrated in figure 3.2b.

This is only an approximation. Technically, if the string configuration (i.e. the ansatz) changes, then the form of the lifting potential also changes. This results in a complicated iterative process with complicated string dynamics before the eventual formation of a steady state.

However, if we consider \mathcal{V} to be approximately constant, we see that the integral $V = \int d\sigma \mathcal{V}$ is minimised precisely for the step-like configuration shown in figure 3.2b, in which the string interpolates between degenerate minima by crossing the potential barrier perpendicularly at its lowest point, i.e. at a saddle point ($\psi = (2n + 1)\pi/2$, $\theta = m\pi$). This may be thought of energetically as a series of small perturbations away from the genuine minimum energy configuration of zero-windings (described above), which is equivalent to a string wrapping a single flat direction in the (ψ, θ) sub-manifold. Looking at it from this perspective helps us to justify our original assumption that \mathcal{V} remains approximately constant, so long as we remember to set $n_\psi = 0$ in (3.15).

This leads to an apparent contradiction. We may assume, at the moment of loop formation, that $n_w \sim n_\psi \sim n_\theta \sim n_\phi > 0$. After this, windings in the ϕ -direction will still be able to vary smoothly, though they will not be stable and may in principle contract until they are point-like. This possibility is discussed in detail in section 3.4.6.

Nevertheless, so long as $n_\phi > 0$, windings in the (ψ, θ) sub-manifold will relax into the step-like configuration shown in figure 3.2b, resulting in the formation of approximately $2n_\psi$ beads. This forces us to view the configuration as a series of small perturbations (in fact, a series of $2n_\psi$ perturbations) away from the configuration described by $\psi = n\pi$ and $n_\psi = 0$. We must therefore continue to regard $n_\psi > 0$ (the number of windings in the ψ -direction at the moment of loop formation) as physically meaningful when estimating the number of beads, but we must regard it as approximately zero when estimating the bead mass. This is a little strange but it is quite consistent with the physical picture we have been sketching.

To obtain our estimate for the bead mass (M_b), we first expand (3.15) with n_ψ set equal

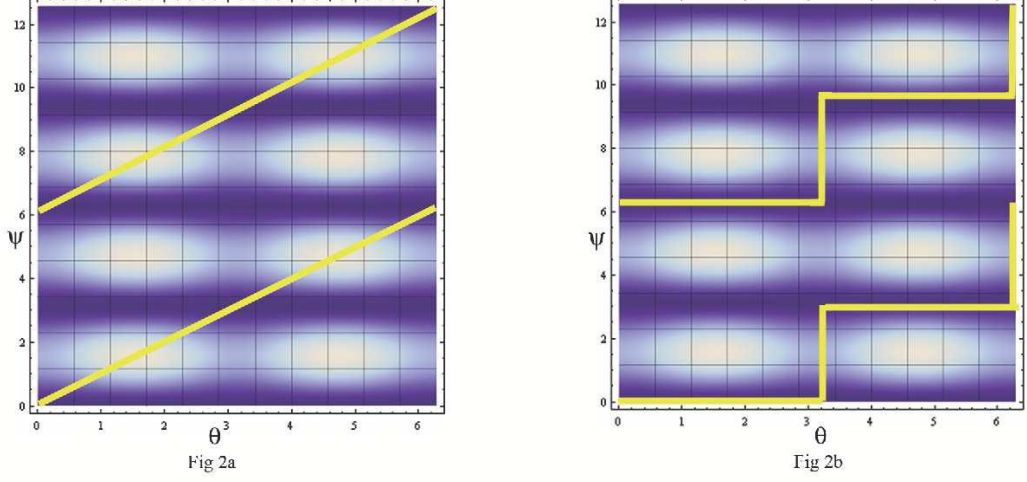


Figure 3.2: (a) shows strings winding smoothly across the effective potential \mathcal{V} on the (θ, ϕ) sub-manifold. (b) shows step-like configurations which minimise the total string energy within \mathcal{V} .

to zero. Assuming $a_0 r \gg n_w R$ at the moment of loop formation, which corresponds to a large loop in the Minkowski directions, we obtain the approximate expression

$$V \sim \sqrt{1 + \frac{\Pi^2}{T_1^2 \lambda^2}} \left(2\pi a_0^2 r T_1 + T_1 \int_0^{2\pi} d\sigma \frac{R^2 \sin^2 \psi (n_\theta^2 + \sin^2 \theta n_\phi^2)}{r} \right). \quad (3.20)$$

We then move from the smooth windings picture shown in figure 3.2a to the step-like configuration in figure 3.2b by setting $\psi = m\pi$ globally, except in the vicinity of a bead, where $\theta = m\pi$, $m\pi \leq \psi \leq (m+1)\pi$ and

$$d\psi \sim d\sigma. \quad (3.21)$$

Our expression for the total energy is then

$$\begin{aligned} V &\sim \sqrt{1 + \frac{\Pi^2}{T_1^2 \lambda^2}} \left(2\pi a_0^2 r T_1 + 2n_\psi \times \frac{1}{2} T_1 \frac{R^2}{r} n_\theta^2 \int_{\psi_i=m\pi}^{\psi_f=(m+1)\pi} \sin^2 \psi d\psi \right) \\ &\sim \sqrt{1 + \frac{\Pi^2}{T_1^2 \lambda^2}} \left(2\pi a_0^2 r T_1 + 2n_\psi \times \frac{\pi}{4} T_1 \frac{R^2 n_\theta^2}{r} \right). \end{aligned} \quad (3.22)$$

As the first term is simply the rest mass of the string in the Minkowski directions, the second term corresponds to the rest mass of $N_b = 2n_\psi$ beads. Finally, setting $n_\psi \sim n_\theta \sim n_w$ explicitly, we have the following estimates for the initial number of beads N_b and the bead

mass M_b :

$$N_b \sim 2n_w$$

$$M_b \sim \frac{\pi}{4} T_1 \sqrt{1 + \frac{\Pi^2}{T_1^2 \lambda^2}} \left(\frac{R^2 n_w^2}{r} \right) \quad (3.23)$$

That the bead mass is inversely proportional to r makes sense on the assumption that the total length of the string remains constant so that if there is less string length involved in internal windings (resulting in less massive beads), more length is added to the ordinary four-dimensional part of the loop. The converse is also true. Thus the first term in the expression for the *total* string mass-energy increases in magnitude as the second decreases and vice-versa. Interestingly, M_b is effectively quantised in terms of the number of windings present in the θ -direction.

Let us now also consider the full expression for the bead mass. One can integrate the potential over the above range and the result is roughly the sum of the bead mass and the rest mass associated with an unwound string (with $n_w = 0$). We can then rewrite the bead mass, including all the higher order terms, with an appropriate normalisation to yield

$$M_b \sim 2a_0^2 T_1 r \sqrt{1 + \frac{\Pi^2}{T_1^2 \lambda^2}} \left(\text{EllipticE} \left(\frac{n_w R i}{a_0 r} \right) - \frac{\pi}{2} \right) \quad (3.24)$$

which is valid for non-zero winding number n_w .¹⁰ One can easily check that in the limit where $n_w R \ll a_0 r$ the mass reduces exactly to (3.23).

3.4 Cosmological implications of necklace loops

We now investigate the cosmological implications of necklace loops based on the assumption that they retain their necklace structure after formation. As we have already seen, the θ -dependence of the lifting potential depends on the presence of windings in the ϕ -direction ($n_\phi > 0$) and its ψ -dependence requires the presence of windings in the θ -direction ($n_\theta > 0$). However, since the ϕ -direction is flat, windings along this direction are unstable. If these windings contract, this “flattens” the θ -direction, leaving the θ -windings free to contract as well. This in turn flattens the ψ -direction and necklace structure disappears as the bead mass (which comes from extra-dimensional windings) is converted into the ordinary rest mass of a loop in Minkowski space. Due to the presence of single flat direction in the S^3 , the entire necklace structure of the loop is therefore unstable and may unravel in time.

We consider this possibility later in this section where we introduce a time-dependent model

¹⁰The EllipticE function used here is defined via the elliptic integral of the second kind, $\text{EllipticE}(\beta, k) = \int_0^\beta \sqrt{1 - k^2 \sin^2 \theta} d\theta$ where $k^2 = \sin^2(\alpha)$ ($0 < k^2 < 1$) is known as the elliptic modulus and α is the modular angle [277].

for the number of windings. For the moment we will consider $n_w \sim n_\psi \sim n_\theta \sim n_\phi$ to be roughly constant. We can now use Matsuda's original assumption that the four-dimensional part of the loop loses mass-energy via the emission of gravitational radiation in Minkowski space (just like an ordinary cosmic string in four dimensions) but that the bead-mass which is formed from the winding of the string in internal space is unaffected by this process.

To investigate the cosmological implications of necklace loops, we must therefore modify equation (3.22) by inserting a time-dependent radius $r(t, t_i)$ into the first term of the expansion (the loop mass in Minkowski space) and the initial radius $r(t_i)$ into the second term (the bead mass). The time-dependent radius of a shrinking loop in warped Minkowski space is given by

$$a_0 r(t, t_i) = a_0 (\alpha t_i - \Gamma \mathcal{G} T_1 (t - t_i)) \quad (3.25)$$

where t_i is the time of loop formation and $t \geq t_i$ is the cosmic time coordinate. The parameter Γ is a measure of the rate of energy loss due to the emission of gravitational radiation, \mathcal{G} is Newton's constant (which is determined by the volume of the S^3) and $0 < a_0 \alpha < a_0$ determines the characteristic initial loop radius as a fraction of the horizon, $d_H \sim a_0 c t$. The initial loop radius as a function of t_i is then

$$a_0 r(t_i) = a_0 \alpha t_i. \quad (3.26)$$

The bead mass now explicitly depends on the time of loop formation, t_i via (3.26). However, we also expect that the initial number of beads, N_b , to depend in some way on t_i . We therefore need some way of estimating the initial number of windings in each direction $n_w = n_w(t_i)$.

Following Avgoustidis and Shellard [16] (and taking into account the warp factor a_0), we use the random walk regime to estimate the initial number of windings present in each angular direction, $n_w(t_i)$, as ¹¹

$$n_w(t_i) = \frac{\sqrt{a_0 \alpha \omega_l \epsilon_l t_i}}{R} \quad (3.27)$$

¹¹Although in general a random walk will not give rise microscopically to completely smooth windings, as described by the embedding ansatz, it should on average produce something similar from a macroscopic point of view. Any extra beads formed by microscopic structure would quickly annihilate one another if we assume that they are free to move around the *shrinking* loop in a random walk. This random motion occurs when small sections of the string momentarily acquire enough energy to jump between adjacent minima in the effective potential causing the bead to move from a four dimensional perspective. In his original paper [8] Matsuda predicted that, based on the idea of a random walk, approximately $\sqrt{n_w(t_i)}$ beads/anti-beads created in pair formation would survive until late times. However, we contest that this is valid only for a *static* loop. For a shrinking loop it seems clear that all bead-anti-bead pairs will eventually collide and annihilate, at least if the minimum radius of the string (\sim string thickness) is comparable to or less than the initial spacing. This implies that only beads formed from *net* windings will contribute to the mass of any PBHs/DM relics eventually created. Further discussion of this point is given in section 3.5.

where $0 \leq \omega_l < 1$ is the fraction of the total string length l (not to be confused with the angular momentum) contained in the windings and ϵ_l is the step length. This definition tells us that string-necklace networks will tend to form once the correlation length becomes larger than the scale of the internal dimensions.

The parameter ω_l may be defined as the ratio of the string length in the internal dimensions to the total length of the string in all dimensions. Following [154], but using the notation defined earlier, the concise definition is

$$\omega_l = \sqrt{\int \left(\frac{R^2 s'^2}{a_0^2 r^2 + R^2 s'^2} \right) \mathcal{V} d\sigma} / \int \mathcal{V} d\sigma \quad (3.28)$$

where $\mathcal{V}(\sigma)$ denotes the integrand in (3.15). In order to simplify the above expression, we make the approximation

$$\begin{aligned} \omega_l &\sim \sqrt{\frac{\int R^2 s'^2 d\sigma}{\int (a_0^2 r^2 + R^2 s'^2) d\sigma}} \int \mathcal{V} d\sigma / \int \mathcal{V} d\sigma \\ &\sim \sqrt{\frac{n_w^2 R^2 \int (4 + \sin^2(n_w \sigma) + \sin^4(n_w \sigma)) d\sigma}{a_0^2 r^2 + n_w^2 R^2 \int (4 + \sin^2(n_w \sigma) + \sin^4(n_w \sigma)) d\sigma}} \end{aligned} \quad (3.29)$$

where in the second step we have ignored the numerical coefficient in front of the r^2 term, and again assumed $n_w \sim n_\psi \sim n_\theta \sim n_\phi$. Finally, it is straightforward to show that

$$\int (4 + \sin^2(n_w \sigma) + \sin^4(n_w \sigma)) d\sigma \sim O(10) \quad (3.30)$$

for all possible values of $n_w(t_i)$. Therefore, ω_l can be well approximated by

$$\omega_l \sim \frac{n_w R}{\sqrt{a_0^2 r^2 + n_w^2 R^2}} \quad (3.31)$$

up to various numerical factors which would have appeared in the above expression if the integral in (3.28) been performed in full. It is clear, however, that ω_l has the correct functional dependence on both n_w and r . This means that, whatever time-dependent models we use for $r(t_i)$, $n_w(t_i)$ and $\omega_l(t_i)$, they must satisfy (3.31) for consistency. At this stage we are not imposing any additional conditions on $a_0 r$ and therefore ω_l is just a parameter of the theory.

If we use (3.26) as our model for $r(t_i)$ and substitute ω_l from (3.31) into our previous expression for $n_w(t_i)$ (which also uses the approximation $r(t_i) \sim \alpha t_i$), we find a cubic equation in the variable $(n_w R)^2$,

$$(n_w R)^6 + a_0^2 (\alpha t_i)^2 (n_w R)^4 - a_0^2 (\alpha t_i)^2 \epsilon_l^2 (n_w R)^2 = 0. \quad (3.32)$$

This has the trivial solution $(n_w R)^2 = 0$ (no windings) and the more physically relevant solution

$$(n_w R)^2 = \frac{a_0^2 (\alpha t_i)^2}{2} \left(-1 \pm \sqrt{1 + \frac{4\epsilon_l^2}{a_0^2 (\alpha t_i)^2}} \right), \quad (3.33)$$

although the reality of n_w requires us to take the positive sign before the square root. The time-dependence of $n_w(t_i)$ in the expression above is then consistent with the definition of ω_l in (3.31).

Next we move on to consider to size of the step length ϵ_l . The maximum velocity of the string in the compact dimensions is c (where $c = 1$ in natural units), which corresponds to a step length per unit time ($\Delta t = a_0^{-1} t_s = a_0^{-1} \sqrt{\alpha'}$) of $\epsilon_l = a_0^{-1} l_s = a_0^{-1} \sqrt{\alpha'}$.¹² However, only the end points of the string at the horizon move at the speed of light. For two points on the string within the horizon, separated by a distance $d \sim \alpha t$, the relative velocity between them is $v \sim \alpha c$ which corresponds to an effective step length of

$$\epsilon_l \sim \alpha a_0^{-1} \sqrt{\alpha'}. \quad (3.34)$$

This definition also implies $n_w(t_i) \propto \alpha$, as we would expect. This ensures that the number of beads on a long string, which stretches across the entire horizon $n_H(t_i)$, is independent of α . In fact, the assumption of a constant step length ϵ_l at all points along the string (as in [16]) is problematic, as this leads to a measure of $n_H(t_i)$ which is proportional to $1/\sqrt{\alpha}$.

Using (3.34) and (3.33) the condition for bead formation, $n_w(t_i)^2 \geq 1$, is equivalent to

$$t_i \geq \frac{R^2}{\alpha \sqrt{\alpha^2 \alpha' - a_0^2 R^2}} \quad (3.35)$$

and the reality of the above solution translates into the constraint

$$a_0^2 \leq \frac{\alpha^2 \alpha'}{R^2}. \quad (3.36)$$

Strictly speaking, a_0^2 is fixed by the ratio of the fluxes arising in a full string compactification and is therefore highly sensitive to the magnitude of string coupling, the string scale and the flux parameters. In the non-compact case which we are considering we also require

¹²Here we have used the fact that the standard string tension $T_1 \sim \alpha'^{-1}$ is given by the fundamental string mass divided by the fundamental string length $T_1 = \frac{m_s}{l_s} \sim \frac{\sqrt{\alpha'^{-1}}}{\sqrt{\alpha'}} \sim \alpha'^{-1}$ together with the fact that the *effective* tension of the string in the warped throat is $\tilde{T}_1 \sim a_0^2 T_1$. We then treat this as the division of the “warped” string mass $\tilde{m}_s \sim a_0 \sqrt{\alpha'}^{-1}$ by the “warped” string scale $\tilde{l}_s \sim a_0^{-1} \sqrt{\alpha'}$, so that the velocity of light is given by $c = \frac{\tilde{l}_s}{\tilde{t}_s} = \frac{a_0^{-1} \sqrt{\alpha'}}{a_0^{-1} \sqrt{\alpha'}} \equiv \frac{l_s}{t_s} = \frac{\sqrt{\alpha'}}{\sqrt{\alpha'}} = 1$. In the next chapter we will see that there may be good reason to suppose that the end points of the string at the horizon move at some velocity $v \sim \sqrt{1 - a_0^2} c < c$. However, for phenomenologically favoured small values of a_0^2 , this overall factor is close to unity and makes little difference to the results of the argument presented here.

$a_0^2 < 1$ in order to ensure that the solution is warped. Therefore the existence condition for beads appears to impose a strict upper bound on the value of a_0^2 , which imposes a strong constraint on the deformation parameter of the conifold geometry. If $a_0^2 = \alpha^2 \alpha' / R^2$, this allows necklaces to form only at infinity, and so only the strict inequality in (3.36) is physically meaningful.

One can now substitute the solution for $n_w R$ into the generalised mass function in (3.24). If we define the function

$$G(t_i) = -1 + \sqrt{1 + \frac{4\alpha'}{a_0^4 t_i^2}}, \quad (3.37)$$

then we see that there is a remarkable cancellation of terms and we are left with

$$M_b \sim 2a_0^2 T_1 \alpha t_i \sqrt{1 + \frac{\Pi^2}{T_1^2 \lambda^2}} \left(\text{EllipticE} \left(i \sqrt{\frac{G(t_i)}{2}} \right) - \frac{\pi}{2} \right), \quad (3.38)$$

which is *not* a monotonic function of time. For vanishingly small t_i , the mass is increasing until it reaches a maximum value, before decreasing monotonically. This leads to the interesting possibility that one can have sustained PBH formation during a “window”, where the mass function is greater than the critical value required to produce a gravitational radius larger than the string width. This possibility is dealt with in section 3.4.2. The explicit form of $\omega_l(t_i)$ is

$$\omega_l \sim \frac{a_0^2 t_i}{2\sqrt{\alpha'}} \left(-1 + \sqrt{1 + \frac{4\alpha'}{a_0^4 t_i^2}} \right) = \frac{a_0^2 t_i}{2\sqrt{\alpha'}} G(t_i) \quad (3.39)$$

which tends to unity as $t_i \rightarrow 0$ and zero as $t_i \rightarrow \infty$, as we would expect.

To aid visualisation in the discussions that follow, we plot the functions $M_b(t_i)$, $N_b = 2n_w(t_i)$ and $\omega_l(t_i)$ and the inter-bead distance $d(t_i)$ in figure 3.3, for fixed values of our model parameters, in order to illustrate the qualitative behaviour of each.

What is clear from these plots is that, assuming no gravitational emission, there are initially a few beads per loop, with large mass. However, as t_i increases, the number of beads and the average inter-bead distance increase, while their corresponding mass decreases. The total mass lost due to the decreasing mass of individual beads outweighs the mass gained by the increase in bead number, which eventually tends to a constant value. Therefore, one expects the system to eventually become dominated by a large number of (almost) massless beads. Of course, including the effects of gravitational emission from the beads, as well as from the connecting string segments (or equivalently, considering the string as “structureless”, so that it must contract equally along its entire length, including the wound sections), may change this result significantly. In this case, the heavier beads will lose mass more quickly and the resulting spectrum of necklace bead masses will depend on both t_i and t explicitly. It is an interesting open question as to how this emission affects PBH formation.

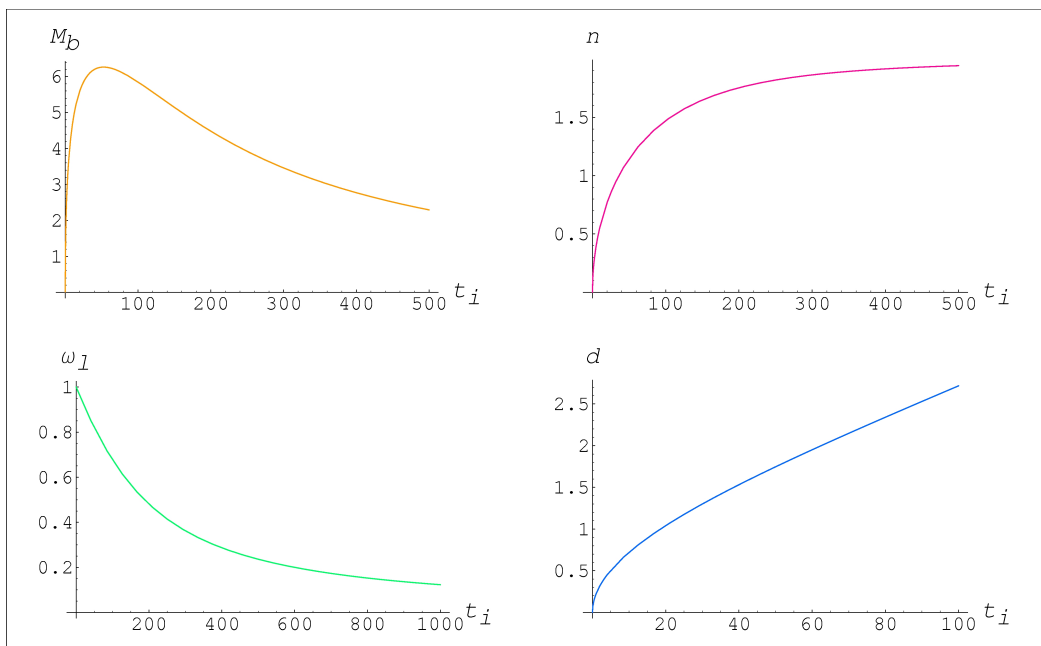


Figure 3.3: Plots of the dynamic variables associated with winding formation as a function of the time of loop formation, t_i . The bead mass $M_b(t_i)$, number of beads $N_b(t_i) \sim 2n_w(t_i)$, fraction of the total string length contained in the windings $\omega_l(t_i)$, and the average inter-bead distance $d(t_i)$ are shown. In all plots model parameters have been set such that $a_0 = 0.1$, $\alpha' = 1$, $R = 5$, $\alpha = 0.8$ and $T_1 \sqrt{1 + \frac{\Pi^2}{T_1^2 \lambda^2}} = 1$.

3.4.1 Late time formation - the scaling regime

Using the fact that the product $n_w R$ is fixed by the parameters of the theory, let us consider the asymptotics to better understand the physics at early and late epochs. Let us initially focus on the late-time regime where

$$t_i \gg \frac{2\sqrt{\alpha'}}{a_0^2} \quad (3.40)$$

which, using (3.33), implies that the initial number of windings per loop (for a loop formed at late t_i) is constant,

$$n_w^2 \sim \frac{\alpha^2 \alpha'}{a_0^2 R^2}. \quad (3.41)$$

The condition for bead formation $n_w(t_i)^2 \geq 1$ simply reproduces (3.36), ensuring the reality of $t_i^{(min)}$ - the minimum time at which necklaces formation begins - and is consistent with our expectations. Assuming, however, that the strict inequality in (3.36) is almost saturated, so that necklaces are able to form at (large) finite time, we are able to estimate the average inter-bead distance for necklaces formed at late times,

$$d(t_i) \sim \frac{a_0 r(t_i)}{N_b} \sim \frac{a_0^2 R t_i}{2\sqrt{\alpha'}}. \quad (3.42)$$

Identifying this with the correlation length along the string, $\xi(t_i)$, as mentioned in the previous section, we see that our solution corresponds to a scaling regime in which we may identify the scaling parameter γ with the KS parameters, i.e.

$$d(t_i) \sim \xi(t_i) \sim a_0 \gamma t_i, \quad (3.43)$$

implying

$$\gamma \sim \frac{a_0 R}{2\sqrt{\alpha'}}. \quad (3.44)$$

This might be compared with the result of field theory calculations, where the initial number of beads on a loop of radius $r(t_i)$ in the scaling regime is given by [114]

$$N_b(t_i) \sim \frac{r(t_i)}{\xi(t_i)} \sim \frac{\alpha}{\gamma}. \quad (3.45)$$

Hence we see that the condition for bead formation at late times in the string picture (3.43) is equivalent to the condition for bead formation in the scaling regime of the field theory, $\gamma \leq \frac{1}{2}\alpha$. Both conditions ensure $N_b \geq 2$, implying that beads come in pairs. This is also consistent with the identification of the inter-bead distance with the correlation distance of the degenerate vacuum states along the string. Thus we see that a scaling solution arises naturally at late times in the string picture, allowing us to identify various string parameters with their field theory counterparts.

Using the condition on γ and α for bead formation, i.e. $0 < \gamma \leq \frac{1}{2}\alpha$, this simply recovers our previous constraint on $a_0 R$ (3.36). However, by setting α to the maximum value allowed by causality ($\alpha = 1$) we may place a maximum upper bound on the radius of the S^3 ,

$$R \leq a_0^{-1} \sqrt{\alpha'}. \quad (3.46)$$

This means that beads/windings will not form unless the radius of the S^3 is smaller than the warped string scale, irrespective of the value of α . It also implies

$$a_0^2 \leq \frac{1}{Mg_s}, \quad b_0 \sim \mathcal{O}(1) \quad (3.47)$$

in order for windings to form. We now ask what happens to the time-dependence of the mass function in the late-time limit. The argument of the EllipticE term becomes small and therefore we may expand the mass term to obtain

$$M_b(t_i) \sim T_1 \sqrt{1 + \frac{\Pi^2}{T_1^2 \lambda^2} \frac{\pi \alpha^2 \alpha'^{\frac{3}{2}}}{2 a_0^3 t_i}} \left(1 - \frac{3}{16} \frac{\alpha'}{a_0^4 t_i^2} + \dots \right), \quad (3.48)$$

from which we see that the mass is inversely proportional to t_i and that $M_b \rightarrow 0$ as $t_i \rightarrow \infty$. This implies that any necklace structure should disappear at sufficiently late times. In other words, it is unlikely that any necklaces formed at late times would be distinguishable from ordinary string loops. One should quantify this by noting that the mass is also inversely proportional to the scale of the warping, so that for highly warped throats the mass will be approximately constant over a much longer time scale.

3.4.2 Early time formation

Returning now to the cubic solution for $(n_w R)^2$, let us consider early time formation subject to the condition $t_i \leq \frac{2\sqrt{\alpha'}}{a_0^2}$. This gives

$$n_w^2(t_i) \sim \frac{(\alpha t_i) \sqrt{\alpha'}}{R^2} - \frac{1}{2} \left(\frac{a_0}{R} \right)^2 (\alpha t_i)^2 \quad (3.49)$$

to second order, which also implies

$$\omega_l(t_i) \sim 1 - \frac{1}{2} \frac{a_0^2}{\sqrt{\alpha'}} (\alpha t_i) \quad (3.50)$$

from the definition of ω_l . Clearly therefore $\omega_l \rightarrow 1$ as $t_i \rightarrow 0$, that is, as $a_0 r(t_i) \rightarrow \mathcal{O}(n_w R)$. Utilising the bead-formation condition then allows us to place a bound on the bead formation time via

$$\frac{R^2}{\alpha \sqrt{\alpha^2 \alpha' - a_0^2 R^2}} \leq t_i \leq \frac{2\sqrt{\alpha'}}{a_0^2}. \quad (3.51)$$

The average distance between beads, should necklaces begin to form,¹³ may then be approximated by

$$d(t_i) \sim \frac{a_0 R \sqrt{t_i}}{2\alpha'^{1/4}} \left(1 + \frac{a_0^2 t_i}{4\sqrt{\alpha'}} + \dots \right) \quad (3.52)$$

which, unlike the the late-time approximation, does not correspond to any known regime in the field theory if we continue to identify $d(t_i)$ with the correlation distance $\xi(t_i)$. However, the second term is sub-dominant at very early times when $t_i \leq \frac{4\sqrt{\alpha'}}{a_0^2}$, suggesting that it may be reasonable to keep only first order terms in the expansion especially if $t_i \ll \frac{2\sqrt{\alpha'}}{a_0^2}$. Such a very early time approximation may correspond to a damping regime in the field theory picture. The above equation would then represent an intermediate regime, where damped and scaling solutions can be joined together. Assuming now that $t_i \ll \frac{2\sqrt{\alpha'}}{a_0^2}$ and keeping only the first order term in (3.49), we see that the condition for bead formation $n_w^2(t_i) \geq 1$ is equivalent to

$$t_i \geq \frac{R^2}{\alpha^2 \sqrt{\alpha'}}. \quad (3.53)$$

This is consistent with our previous estimates and shows that bead formation will occur in the very early time regime¹⁴ only when $a_0^2 R^2 \ll \alpha^2 \alpha'$. With this in mind, we see that the inter-bead distance is set by the leading factor in (3.52), which is consistent with the field theory picture at early times during the damping regime, where we expect the correlation distance $\xi(t_i)$ to be given by a power-law solution of the form [114]

$$\xi(t_i) \sim t_d^{\frac{1}{2}} t_i^{\frac{1}{2}} \quad (3.54)$$

with t_d corresponding to the characteristic damping time of small-scale oscillations on the string (and where we have effectively identified $t_d \sim a_0^2 R^2 / 4\sqrt{\alpha'}$).

However, a damping regime is usually obtained by considering collisions of the string with an external plasma. In this case the damping term comes from the internal dynamics of the model, suggesting that the inertia of the beads (when M_b is large) is sufficient to cause the correlation length to scale as $\xi(t_i) \sim \sqrt{t_i}$ at very early times.

Furthermore, unless the warping is extraordinarily large, the time-scales over which this effect takes place are likely to be insignificant compared to the cosmological timescale. As a future amendment to the current work it will be useful to impose an external damping regime and to study the effect of the interaction of the windings with the external plasma. Naively we may expect collisions of the string with particles in the compact space to inhibit the formation of windings, resulting in the delayed on-set of a scaling regime. This to is

¹³We have assumed $t_i^{(min)} \sim \frac{R^2}{\alpha \sqrt{\alpha^2 \alpha' - a_0^2 R^2}} \leq \frac{2\sqrt{\alpha'}}{a_0^2}$, which is equivalent to assuming $a_0^2 R^2 \leq 0.83 \alpha^2 \alpha'$.

¹⁴The condition $t_i^{(min)} \sim \frac{R^2}{\alpha^2 \sqrt{\alpha'}} \leq \frac{2\sqrt{\alpha'}}{a_0^2}$ implies that $a_0^2 R^2 \leq 2\alpha^2 \alpha'$, which is automatically satisfied by (3.36).

likely to mirror the field theory case, though further investigation is needed to establish whether the correlation distance scales according to (3.54).

Once again, for the sake of completeness, we consider how the mass function changes as a function of time in this epoch. The elliptic integral is actually divergent in this limit, but we can consider the leading order divergence which will dominate the spectrum. The resulting expression for the mass function is

$$M_b(t_i) \sim 2T_1 \sqrt{a_0 \alpha'^{1/4}} \sqrt{1 + \frac{\Pi^2}{T_1^2 \lambda^2} (\alpha t_i)^{3/4}}, \quad (3.55)$$

which tends to zero as $t_i \rightarrow 0$. This is within the regime where we may expect PBH formation to occur, since the mass of the necklace plus beads steadily increases with time.

3.4.3 PBH formation

We now calculate the contribution to the PBH mass spectrum from collapsing necklace loops, based on the assumption that loops which chop off from the string network retain their necklace structure indefinitely. We will initially take the number of beads per loop to be constant from the time of formation.

The minimum radius to which a contracting loop may shrink, δ_l , is limited by the string width, which we assume to be comparable to the inverse of the symmetry-breaking scale η_s [6, 8], that is, $\delta_l \sim \eta_s^{-1}$.¹⁵ The condition for gravitational collapse then becomes

$$R_S > \eta_s^{-1} \quad (3.56)$$

where R_S is the Schwarzschild radius of the loop. We may estimate the Schwarzschild radius using the spherically symmetric approximation

$$R_S(t_i) \sim 2\mathcal{G}M_T(t_i) \quad (3.57)$$

where \mathcal{G} is the modified Newton's constant (see later) and $M_T(t_i)$ is the total mass of the necklace. A necklace formed at time t_i will therefore collapse to form a PBH if

$$M_T(t_i) \geq \frac{\eta_s^{-1}}{2\mathcal{G}}. \quad (3.58)$$

¹⁵Recall that for Abelian field theories the tension of a string is proportional to the square of the symmetry-breaking scale, $\mu \sim \eta^2$. An Abelian F/D -string with the same assumption gives $\eta_s \sim \sqrt{\alpha'}^{-1}$. However, we will leave η_s as a free parameter in the discussion that follows.

Assuming that δ_l is small, the bead mass will provide the dominant contribution to $M_T(t_i)$ so that

$$\begin{aligned} M_T(t_i) &\sim N_b(t_i)M_b(t_i) \\ &\sim \frac{8T_1a_0^3}{\sqrt{2}R} \sqrt{1 + \frac{\Pi^2}{T_1^2\lambda^2}(\alpha t_i)^2} \sqrt{G(t_i)} \left(\text{EllipticE} \left(i\sqrt{\frac{G(t_i)}{2}} \right) - \frac{\pi}{2} \right), \end{aligned} \quad (3.59)$$

which is a non-monotonic function. We can approximate the solution at early times by

$$M_T(t_i) \sim T_1 \sqrt{1 + \frac{\Pi^2}{T_1^2\lambda^2} \frac{\pi}{4} \frac{\alpha^2 \sqrt{\alpha'}}{R} a_0 t_i} + \dots \quad (3.60)$$

and late times by

$$M_T(t_i) \sim T_1 \sqrt{1 + \frac{\Pi^2}{T_1^2\lambda^2} \frac{\pi}{2} \frac{\alpha^2 \alpha'^{\frac{3}{2}}}{a_0^3 R} \frac{1}{t_i} \left(1 - \frac{3\alpha'}{16a_0^4 t_i^2} \right)}. \quad (3.61)$$

We note that M_T is linearly increasing with $a_0 t_i$ at very early times, whilst we find that it scales as $1/(a_0^3 t_i)$ at late times. Thus the sensitivity to the warp factor is most pronounced at late times, since a vanishingly small value of a_0 means that the total mass remains larger over a wider time-scale. Ultimately however, the total mass will tend to zero asymptotically. The complete mass function $M_T(t_i)$, using the definition of the elliptic integral, is sketched in figure 3.4 to illustrate the time-dependence. In figure 3.5 this is shown together with the early and late-time approximations.

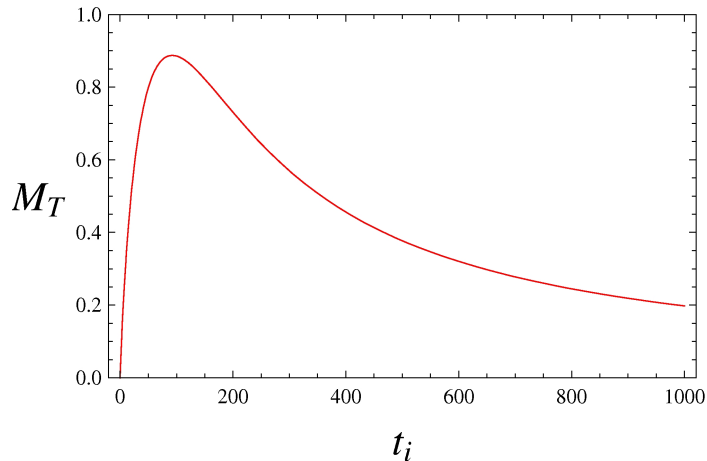


Figure 3.4: The total mass M_T contained within the beads of a necklace as a function of t_i . The model parameters have been fixed so that $a_0 = 0.1$, $\alpha' = 1$, $R = 5$, $\alpha = 0.8$ and $T_1 \sqrt{1 + \frac{\Pi^2}{T_1^2\lambda^2}} = 1$.

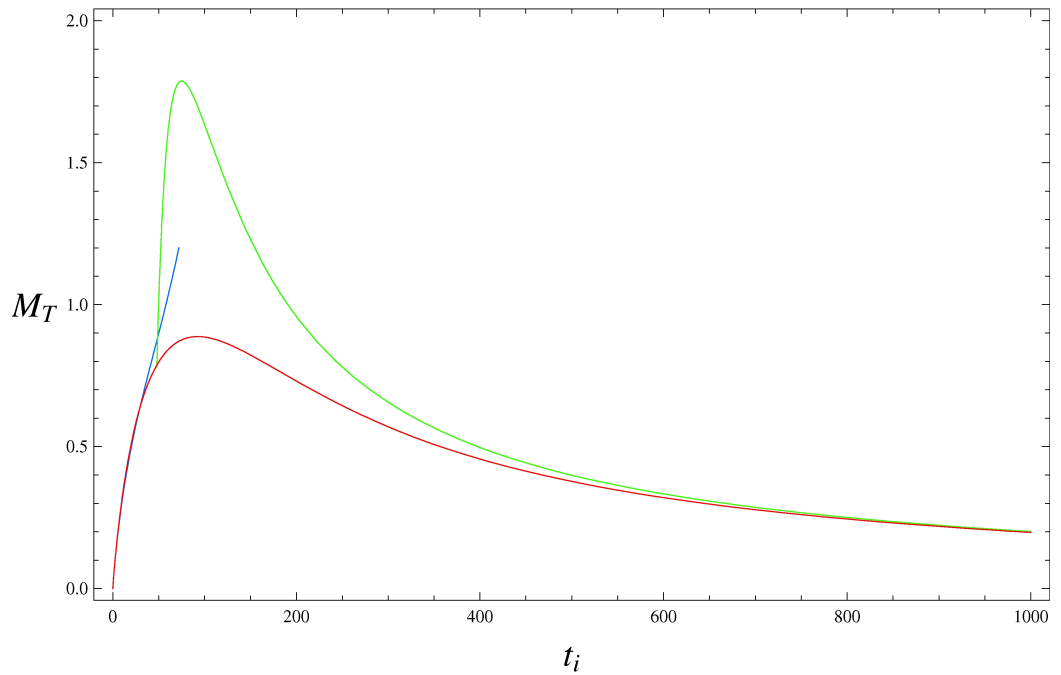


Figure 3.5: The total mass M_T contained within the beads of a necklace as a function of t_i , together with the early and late-time approximations given by (3.60)/(3.61), respectively. The same parameter choices were made as in figure 3.4. The blue (green) curves are the early (late) time approximations respectively. Note that the late time approximation seems to over-estimate the maximum mass.

Without precise values for the model parameters, it is difficult to determine the accuracy (as a percentage estimate) of either the early or late-time approximations. However, it is interesting that the late-time approximation also qualitatively captures the behaviour of $M_T(t_i)$ in the early-time regime. In fact, the peaks of the two functions are in approximately the same position, although the peak of the approximation is roughly twice as high as the peak of the true curve.

It is also clear that the peak of the full mass function, which is potentially the region of greatest interest with respect to PBH formation, lies between the regions in which either the early or late-time approximations are valid. As we shall see, in order to calculate the PBH spectrum analytically in terms of our model parameters, we must integrate over the region of the curve (3.59) which satisfies (3.58). This is not possible in general, as any such region (if it exists) will certainly include the peak itself. We must therefore find some way of approximating the elliptic integral in this crucial region.

While this can be done in many ways, we will use the following method. To begin with, we estimate the maximum height of the full mass function by utilising the fact that the peak of the late-time approximation lies at roughly the same value of t_i . Differentiating the second equation in (3.60) and solving the resulting expression $dM_T/dt_i = 0$ gives

$$t_i^{(peak)} \sim \frac{3}{4a_0^2}. \quad (3.62)$$

Substituting this back into (3.59) then gives

$$M_T^{(peak)} = M_T(t_i^{(peak)}) \sim 5.47 T_1 \sqrt{1 + \frac{\Pi^2}{T_1^2 \lambda^2} \frac{\alpha^2 \alpha'^{\frac{3}{2}}}{8a_0 R}}. \quad (3.63)$$

Substituting the full expression for $n_w(t_i)$ (3.33) into (3.23) and using $M_T(t_i) \sim N_b(t_i)M_b(t_i)$ from (3.59) also gives a function which shows the same qualitative behaviour as the true $M_T(t_i)$ curve (as we would expect). Taking this approach corresponds to expanding the elliptic integral only to first order in $n_w(t_i)$, but keeping the full time dependence of this function (which is valid even at early times) as opposed to keeping higher order terms in the expansion of the elliptic integral and using the late-time approximation $n_w(t_i) \sim \alpha\sqrt{\alpha'}/a_0 R$ as in (3.60). The resulting expression for $M_T(t_i)$ is

$$M_T(t_i) \sim \frac{\pi}{\sqrt{32}} T_1 \sqrt{1 + \frac{\Pi^2}{T_1^2 \lambda^2} \frac{a_0^3 (\alpha t_i)^2}{R}} \left(-1 + \sqrt{1 + \frac{4\alpha'}{a_0^4 t_i^2}} \right)^{\frac{3}{2}}. \quad (3.64)$$

Although this is still highly inaccurate within the region of the peak, a function *of this form* may be used to capture the behaviour of the full expression down to all but the earliest

times (where the early-time expansion above must again be used).¹⁶ We may then fit a curve of the form

$$M_{T\text{approx}}(t_i) \sim A T_1 \sqrt{1 + \frac{\Pi^2}{T_1^2 \lambda^2} \frac{a_0^3 (\alpha t_i)^2}{R}} \left(-1 + \sqrt{1 + \frac{C \alpha'}{a_0^4 t_i^2}} \right)^{\frac{3}{2}} \quad (3.65)$$

where A and C are free parameters, to the true $M_T(t_i)$ curve by demanding that the approximate function satisfies the following conditions:

- It passes through the point $(t_i^{(peak)}, M_T^{(peak)}) = \left(\frac{3}{4a_0^2}, 5.47 T_1 \sqrt{1 + \frac{\Pi^2}{T_1^2 \lambda^2} \frac{\alpha^2 \alpha'^{\frac{3}{2}}}{8a_0 R}} \right)$
- It has the same asymptotic behaviour as the full elliptic integral. This is equivalent to the requirement that $A = \frac{\pi}{\sqrt{32}} C^{-\frac{3}{2}}$.

These two conditions are sufficient to fix A and C uniquely, giving

$$\begin{aligned} A &\rightarrow 0.368657, \\ C &\rightarrow 5.25648. \end{aligned} \quad (3.66)$$

The resulting fit is remarkably good both at late times and in the vicinity of the peak and is shown for a selection of parameter values in figure 3.6. Only at very early times does the approximation appear to break down, which becomes clear if we “zoom in” near $t_i = 0$, as shown in figure 3.7. However, if we *are* required to integrate over a time range that includes a region in which (3.65) becomes invalid, we may always split the resulting integral into two parts. It would then be necessary to integrate, using the early-time approximation in (3.60) expanded to arbitrary order, over some range $0 \leq t_i \leq t_E$ (where t_E marks the time at which the approximation starts to break down), whilst using the expressions (3.65)-(3.66) over the remainder of the range $t_E \leq t_i \leq t_F$.

Starting with (3.56) we may now estimate the range of time over which necklaces will form that will eventually collapse to produce black holes, i.e necklaces with sufficiently high mass contained in their beads to produce a Schwarzschild radius larger than the string width. From our previous discussion we see that the mass function peaks at earlier times, therefore favouring PBH formation in this regime - that is, from the collapse of small necklace loops with a relatively low number of high mass beads.

In fact, it is clear from the plots of $N_b(t_i)$ and $M_b(t_i)$ in figure 3.3, and especially from the plot of $M_T(t_i) \sim N_b(t_i)M_b(t_i)$ in figure 3.4, that the increase in bead number at late times is *insufficient* to compensate for the reduction in the mass of individual beads. Simi-

¹⁶It is more useful in this respect to keep the full time dependence in $n_w(t_i)$, while expanding to only first order in n_w , than it is to expand to two or more orders in the argument of the EllipticE for large t_i .

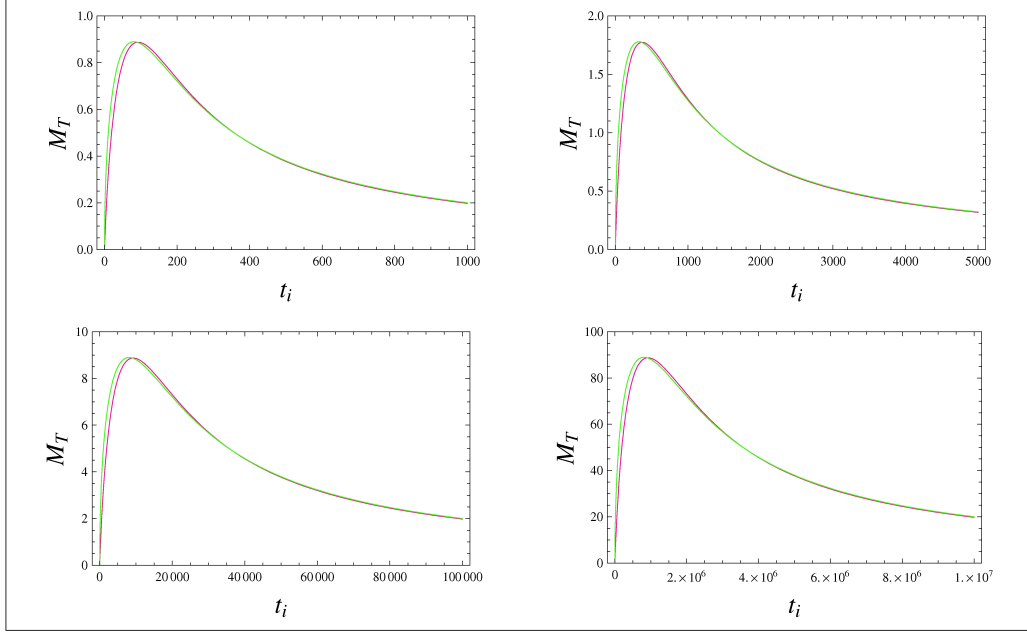


Figure 3.6: Plot of the exact necklace mass M_T (red curve) and the approximate fit function $M_{T_{approx}}$ (green curve) as a function of t_i for $a_0 = 0.1, 0.05, 0.01, 0.001$ (top left to bottom right). In all the plots $\alpha' = 1$, $R = 5$, $\alpha = 0.8$ and $T_1 \sqrt{1 + \frac{\Pi^2}{T_1^2 \lambda^2}} = 1$.

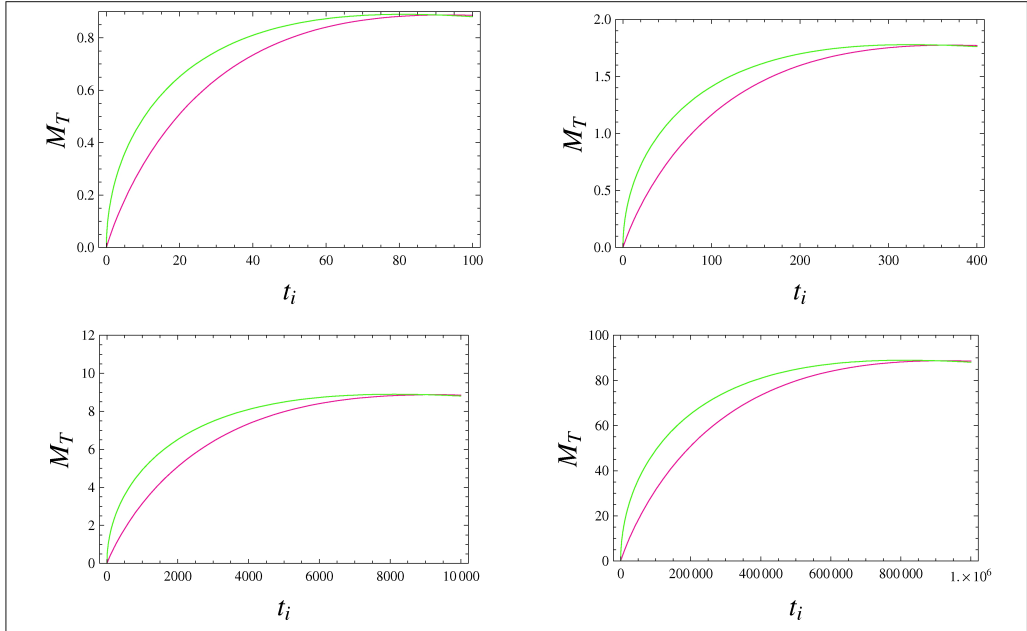


Figure 3.7: Zoom in of the four plots shown in figure 3.6, clearly exhibiting the early-time breakdown of the fit function $M_{T_{approx}}(t_i)$

larly, at very early times, there are an insufficient number of extra-dimensional windings to produce enough beads to create a large Schwarzschild radius, even though the individual bead mass is high. This results in the formation of a window in the early universe, during which necklaces suitable for PBH formation are produced.

The limits of this window, t_{PBH}^{\pm} , may be estimated by solving (3.58) with the appropriate expression for $M_T(t_i)$. Let us assume that the energy scale of the symmetry-breaking process which gives rise to the (p, q) -string network is the *unwarped* string energy scale

$$\eta_s \sim \sqrt{\alpha'}^{-1} \quad (3.67)$$

and consider the limits which arise from inserting (3.65) with the values of A and C given above. The resulting time bounds can be solved for analytically but yield rather complicated expressions which we do not give here.

These analytic expressions are valid so long as the (3.65) provides a relatively good approximation to the true $M_T(t_i)$ curve. However, the validity of the lower bound, t_{PBH}^- , should always be checked (for a given set of parameter values) by plotting the full mass function together with the PBH formation bound

$$\frac{\eta_s^{-1}}{2\mathcal{G}} \sim \frac{R^3(\alpha')^2}{2} \frac{1}{G_{(10)}}, \quad (3.68)$$

where we have used the fact that the effective four-dimensional gravitational coupling is related to the ten-dimensional one through

$$\mathcal{G} = \frac{G_{(10)}}{\text{Vol}(X_6)}, \quad (3.69)$$

where X_6 is the internal manifold. We can approximate the coupling via

$$\mathcal{G} \sim \frac{G_{(10)}}{R^3(\alpha')^{3/2}}, \quad (3.70)$$

although we will typically assume $G_{(10)} \sim \mathcal{O}(1)$ (in units where $\alpha' = 1$) for simplicity. If this forms a poor estimate of the true t_{PBH}^- , it is necessary to expand the early-time approximation given in (3.60) to as many orders as required to reach an accurate value and to resolve (3.58).

For the sake of completeness, we note that the early-time expansion given to first order in (3.60) remains reasonably accurate up to

$$t_E \sim \frac{\sqrt{\alpha'}}{2a_0^2}, \quad (3.71)$$

beyond which the function (3.65) is undoubtedly valid. The resulting estimate of t_{PBH}^- (where $t_{PBH}^- < t_E \sim \frac{\sqrt{\alpha'}}{2a_0^2}$) is

$$t_{PBH}^- \sim \frac{R^4}{8a_0\alpha'^{5/2}\alpha^2 T_1 \sqrt{1 + \frac{\Pi^2}{T_1^2 \lambda^2}}}. \quad (3.72)$$

In order to be safe, therefore, we may choose to split up any integral involving the necklace mass $M_T(t_i)$ into two pieces: the first using the early-time approximation (3.60) between the limits $0 \leq t_i \leq t_E$ and the second using (3.65) between $t_E \leq t_i \leq t_F$ where t_E is given by (3.71).

An estimate for t_{PBH}^+ can also be obtained using the late-time expansion for $M_T(t_i)$ and this yields the simple expression

$$t_{PBH}^+ \sim \frac{\pi\alpha'^{7/2}\alpha^2 T_1 \sqrt{1 + \frac{\Pi^2}{T_1^2 \lambda^2}}}{a_0^3 R^4}. \quad (3.73)$$

The next step towards calculating the necklace contribution to the present day PBH spectrum is to estimate the time at which a collapsing loop reaches its minimum radius $\delta_l \sim \eta_s^{-1} \sim \sqrt{\alpha'}$. This depends on t_i via

$$t'(t_i) \sim \left(1 + \frac{\alpha}{\Gamma \mathcal{G} T_1}\right) t_i - \frac{\eta_s^{-1}}{\Gamma \mathcal{G} T_1}. \quad (3.74)$$

Our approximations suggest that δ_l will be small and therefore the second term will be sub-dominant. This implies that the corresponding time range over which PBHs actually form from the collapse of these loops is $t_{PBH}^- \leq t'(t_i) \leq t_{PBH}^+$ where

$$t'_{PBH}^\pm \sim \left(1 + \frac{\alpha}{\Gamma \mathcal{G} T_1}\right) t_{PBH}^\pm. \quad (3.75)$$

The initial mass of a black hole forming at $t'(t_i)$ is therefore $M_T(t_i)$, which can be compared with the mass of a black hole formed from an ordinary string loop, $M_{PBH}(t_i) \sim \mu\alpha t_i$, which yields the present day mass spectrum [118]

$$\frac{dn_{PBH}(M)}{dM} \propto M^{-2.5}. \quad (3.76)$$

Clearly the mass spectrum for PBHs formed via the collapse of necklaces is far more complicated, although the relevant calculation of the present day spectrum proceeds in a similar fashion. Firstly, we identify

$$M_{PBH}(t'(t_i)) = M_T(t_i). \quad (3.77)$$

Assuming also that the PBH formation window lies in the radiation-dominated epoch, the number density of string loops with initial length $r(t_i) = \alpha t_i$ which chop off from the

network at time t_i is

$$n(r(t_i), t_i) \sim \frac{\nu_r}{t_i^{\frac{3}{2}} r(t_i)^{\frac{3}{2}}} = \frac{\nu_r}{\alpha^{\frac{3}{2}} t_i^3} \quad (3.78)$$

where ν_r is the number of long strings per Hubble volume. Now, in field theoretic models

$$\nu_r = g\gamma^{-3}\tilde{c} \quad (3.79)$$

where g is a Lorentz factor, γ is the scaling parameter (which we identify with the KS parameters so that $\gamma \sim a_0 R/2\sqrt{\alpha'}$) and \tilde{c} is the loop production parameter. For ordinary four-dimensional strings, \tilde{c} is extracted from simulations and is of order unity. For higher-dimensional strings it is suppressed by a factor

$$P \sim \left(\frac{\delta}{R}\right)^{d-3} \quad (3.80)$$

where δ is the string thickness and d is the number of *spatial* dimensions. In our model $\delta \sim \eta_s^{-1} \sim \sqrt{\alpha'}$ and $d = 6$, giving

$$P \sim \left(\frac{\sqrt{\alpha'}}{R}\right)^3 \quad (3.81)$$

and hence

$$\nu_r \sim \frac{8g}{a_0^3} \left(\frac{\sqrt{\alpha'}}{R}\right)^6. \quad (3.82)$$

In higher-dimensional theories the scaling parameter γ (which determines the correlation length) is also expected to be suppressed by a factor of P during the scaling regime, but small-scale structure on the strings is likely to lead to weaker P -dependence, $P_{\text{eff}} = f(P)$ [16, 154]. However, as the correlation length has already been determined directly in terms of the model parameters, it is likely that this effect has already been accounted for. In the warped geometry it also appears consistent to account for the warping of both space *and* time by introducing the transformations $t_i \rightarrow a_0 t_i$, $r(t_i) \rightarrow a_0 r(t_i)$ into the expression (3.78), yielding an additional factor of a_0^{-3} . However, we believe this effect too is already incorporated via the derivation of ν_r in terms of the warped throat model parameters. In fact, such an explanation gives a nice interpretation of the formula (3.82), which is then seen as the product of three terms: a ‘‘warping term’’ which accounts for the back-reaction on the large dimensions a_0^{-3} , a term accounting for extra-dimensional effects $(\sqrt{\alpha'}/R)^3$ and a standard Lorentz factor $\sim g$.

The PBH formation rate at $t'(t_i)$ is (minus) the rate of necklace formation at t_i

$$\frac{dn_{PBH}(t'(t_i))}{dt'(t_i)} = -\frac{dn(r(t_i), t_i)}{dt_i} \sim \frac{3\nu_r}{\alpha^{\frac{3}{2}} t_i^4}, \quad (3.83)$$

so finally we may use the relation

$$\begin{aligned} \frac{dn_{PBH}(t'(t_i))}{dM_{PBH}(t'(t_i))} &= \frac{dn_{PBH}(t'(t_i))}{dt'(t_i)} \times \frac{dt'(t_i)}{dM_{PBH}(t'(t_i))} \\ &\sim \frac{3\nu_r}{\alpha^{\frac{3}{2}} t_i^4} \times \left(\frac{dM_T(t_i)}{dt_i} \right)^{-1} \end{aligned} \quad (3.84)$$

to find the contribution to the PBH mass-spectrum from collapsing necklaces by substituting for $t'(t_i)$ and redshifting to the current epoch. However, the expression is extremely complex and is not given here.

Of more interest is the calculation of the total contribution of the spectrum to the fraction of the critical density of the universe at the current epoch, $\Omega_{PBH}(t_0)$. The standard formula for $\Omega_{PBH}(t_0)$ from collapsing cosmic string loops is [8]

$$\Omega_{PBH}(t_0) = \frac{1}{\rho_{crit}(t_0)} \int_{\max(t_c, t_*)}^{t_0} dt \frac{dn_{PBH}}{dt} M(t, t_0) \quad (3.85)$$

where t_* is the formation time of a black hole with mass $M_* \approx 4.4 \times 10^{14} h^{-0.3}$ gm ($\sim 10^{20}$ in Planck units for $h = 0.72$ [279]), whose lifetime would be the present age of the universe.¹⁷ The variable $M(t, t_0)$ is the current mass of a black hole that formed at a time t , and t_c is the time at which loops first begin to form.

Again assuming that most of the loop production occurs in the radiation dominated era, the rate of black hole formation is then given by,

$$\frac{dn_{PBH}}{dt} = \frac{3\nu_r f}{\alpha^{\frac{3}{2}} t^4} \frac{a(t)^3}{a(t_0)^3} \quad (3.86)$$

where f is the fraction of loops which collapse on the first oscillation, which is expected to be small. In the standard calculations it is typical to neglect the effect of Hawking radiation by making the approximation $M(t, t_0) \sim M(t) \sim \mu G t$, which has been shown to make a difference of less than six per cent to the final value of $\Omega_{PBH}(t_0)$ [118], though in our model the difference may be substantially greater and is therefore something which should be checked for completeness.

Adjusting the standard calculations to account for the effect of necklace formation, we expect there to be contributions to $\Omega_{PBH}(t_0)$ from two qualitatively different sources: First, we expect to find a spike in PBH formation in the very early universe due to the gravita-

¹⁷This value was calculated in a four-dimensional FRW model using the standard value of $G = 6.67 \times 10^{-11} \text{Nm}^2\text{kg}^{-2}$. But, in a higher-dimensional model, gravity is expected to become much stronger on very small scales, resulting in a significantly higher rate of Hawking evaporation for the smallest PBHs. However, for simplicity, we will neglect such small corrections.

tional collapse of necklace loops which shrink to their minimum radius $\delta_l \sim \eta_s^{-1}$ within a time $t' \sim \left(1 + \frac{a_0 \alpha}{\Gamma \mathcal{G} T_1}\right) t_i$, although on cosmological time-scales we may simply assume $t' \sim t_i$. The total mass of all the beads contained in these loops is large and therefore dominates the contribution to the initial mass of the black hole. This corresponds to the first term in (3.87).

The second contribution to $\Omega_{PBH}(t_0)$ comes from loops which collapse *before* shrinking to their minimum size, by adopting a sufficiently compact and spherically symmetric configuration on their first oscillation [114, 115]. In principle, this process is continuous through the history of the universe, although at late times we may neglect the contribution of the beads to the masses of black holes formed in this way, leaving just the first term in the second integral. At early times the beads must be included and therefore both terms become important.

The expression for the (approximate) contribution of PBHs formed from collapsing loops to the current mass-density of the universe is therefore

$$\begin{aligned} \Omega_{PBH}(t_0) \approx & \frac{1}{\rho_{crit}(t_0)} \int_{t_*^-}^{t_*^+} dt_i \frac{3\nu_r}{\alpha^{\frac{3}{2}} t_i^4} \frac{a(t_i)^3}{a(t_0)^3} M_T(t_i) \times \left(\frac{t_*^+}{t_r}\right)^{\frac{1}{2}} \left(\frac{t_r}{t_0}\right)^{\frac{3}{2}} \\ & + \frac{1}{\rho_{crit}(t_0)} \int_{t_*^+}^{t_0} dt_i \left(\frac{6\pi\nu_r f T_1 \sqrt{1 + \frac{\Pi^2}{T_1^2 \lambda^2}}}{\alpha^{\frac{1}{2}} t_i^3} + \frac{3\nu_r f M_T(t_i)}{\alpha^{\frac{3}{2}} t_i^4} \right) \frac{a(t_i)^3}{a(t_0)^3} \end{aligned} \quad (3.87)$$

where t_*^\pm are the times between which the necklace mass exceeds M_* . In practice, however, the factor $f \sim 10^{-20}$ multiplying the integral on the second line indicates that (without fine tuning of the parameters) by far the largest contribution will come from the first integral between t_*^- and t_*^+ . In other words, we expect the necklace-specific channel to dominate the production of PBHs and therefore choose to neglect the latter two terms.

The two factors in large brackets outside the first integral account for the redshifting from the *end* of PBH production (with $M_{PBH} \geq M_*$) from necklace collapse to the present day. For our purposes it is convenient to use the parameterisation,

$$\rho_{crit}(t_0) \sim 3H_0^2 m_p^2, \quad t_0 \sim \frac{2}{3} H_0^{-1}. \quad (3.88)$$

For PBHs to form via the necklace-specific process outlined above *and* to survive to the present day, thus contributing to the current mass density of the universe, we require

$$M_T(t_i) \geq M_* \quad (3.89)$$

for at least some range of t_i within $t_{PBH}^- \leq t_i \leq t_{PBH}^+$. There are then three possible scenarios:

- $M_* \leq \frac{\eta_s^{-1}}{2\mathcal{G}}$. If this condition is satisfied for all t_i in which black holes are produced, we can integrate the first term in (3.87) over the range $t_{PBH}^- \leq t_i \leq t_{PBH}^+$.
- $\frac{\eta_s^{-1}}{2\mathcal{G}} < M_* < M_T^{(max)}$. With M_* in this range, the expression above will automatically be satisfied for times between $t_*^- \leq t_i \leq t_*^+$.
- $M_* > M_T^{(max)}$. All PBHs formed by this process will evaporate long before the present epoch.

In reality the first of these scenarios will not occur if $\eta_s \sim \sqrt{\alpha'}^{-1}$ ($\equiv m_p$) *unless* R is hierarchically larger than the fundamental string scale. This is theoretically compatible with the bound (3.36) for small enough values of the warp factor, though we need not assume that the bound is close to saturation. Working in Planck units and using (3.69) together with $\eta_s \sim \sqrt{\alpha'}^{-1} \sim m_p$, it is possible to show that $M_* > \eta_s^{-1}/2\mathcal{G}$, so we need only “tune” the values of our model parameters so that $M_T(t_i) > M_*$ for at least *some* range of t_i . It turns out that the most important parameters for ensuring this condition are the warp factor a_0 and the worldsheet flux momentum Π . We shall discuss later a (somewhat restrictive) region of the whole parameter space of a_0, R, Π for which this condition is met. But it seems that one is either required to have small values of a_0 and/or large values of Π . That large Π should help ensure PBH production is understandable since the pre-factor $\sqrt{1 + \frac{\Pi^2}{T_1^2 \lambda^2}}$ simply multiplies the expression for $M_T(t_i)$, whereas increasing worldsheet flux does not affect the value of M_* . However, the relation between $M_T(t_i)$ and a_0 is more complicated as this factor appears in a complex way inside the Elliptic function.

For the sake of completeness, we calculate $t_*^\pm(M_*)$ explicitly by setting $M_T(t_i) = M_*$. We then use the early-time expansion of $M_T(t_i)$, given previously, to estimate t_*^- and the late-time approximation to $M_T(t_i)$ to obtain t_*^+ . The result is

$$\begin{aligned}
 t_*^-(M_*) &\sim \frac{M_* R}{4T_1 a_0 \alpha^2 T_1 \sqrt{1 + \frac{\Pi^2}{T_1^2 \lambda^2}}} \alpha'^{-\frac{1}{2}} \\
 t_*^+(M_*) &\sim \frac{\pi \alpha^2 T_1 \sqrt{1 + \frac{\Pi^2}{T_1^2 \lambda^2}}}{2a_0^3 M_* R} \alpha'^{\frac{3}{2}}.
 \end{aligned} \tag{3.90}$$

Although one could also obtain t_*^+ by equating $M_{T_{approx}}(t_i)$ with M_* , the resulting expression for t_*^+ is rather unwieldy and does not significantly differ in its value from the approximate form given here. The evaluation of (3.87) between the limits t_*^- and t_*^+ (given by (3.90)) is then obtained by integrating between t_*^- and t_E using the early-time approximation (3.71) and between t_E and t_*^+ using the numerical fit. The full expression is well approximated by

$$\begin{aligned}
 \Omega(t_0) \sim & \\
 & \frac{10^{-25} g \sqrt{\alpha} \sqrt{\Pi^2 + \lambda^2 T_1^2}}{\pi a_0 R^7 t_0^{3/2} \rho_{crit}} [-4AC^{\frac{1}{4}}(F-1)^{-\frac{1}{4}} \left\{ \frac{F+5}{(F-1)^{\frac{1}{4}}} - 3 \times 2^{\frac{3}{4}} {}_2F_1 \left(\frac{1}{4}, \frac{1}{4}; \frac{5}{4}; \frac{1}{2}(1-F) \right) \right\} \\
 & - (2 \left(\frac{32}{\pi} \right)^{\frac{1}{2}} (F^2-1)^{-\frac{1}{4}} - \frac{1}{384} (\text{Log}(256) - 3) (F^2-1)^{\frac{3}{4}} + \sqrt{2\pi} (1 + \text{Log}(16)) (F^2-1)^{\frac{1}{4}} \\
 & - \pi \text{Log} \left(\frac{1}{8a_0} (F^2-1)^{\frac{1}{2}} \right) - 8\pi \text{Log} \left(\frac{1}{2a_0^2} \right) - 19.312]
 \end{aligned}$$

where ${}_2F_1$ is the usual hypergeometric function and we have defined

$$F(a_0, R, M_*, \alpha, \lambda T_1, \Pi) \equiv \frac{16a_0^2 M_*^2 R^2}{\alpha^4 (\Pi^2 + \lambda^2 T_1^2)}. \quad (3.91)$$

As noted above, the fulfillment of the condition $M_T(t_i) \geq M_*$ requires small values of the warp factor and/or large values of the flux parameter Π , though the exact relationship between $M_T(t_i)$ and a_0 is complex. We must also ensure, for consistency, that $t_*^-(M_*) < t_*^+(M_*)$ (where these values are given by (3.90)). Exactly how small a_0 is required to be in order to fulfill both of these requirements depends on how large Π is. We see from the explicit expression

$$\Pi = \frac{2T_1 \lambda^2 F_{0\sigma}^2}{a_0^2 \sqrt{r^2 + a_0^{-2} R^2 s'^2 - a_0^{-4} \lambda^2 F_{0\sigma}^2}} \quad (3.92)$$

that, in principle, $0 \leq \Pi \leq \infty$ for a flux $\lambda F_{0\sigma}$ in the allowable range $0 \leq \lambda^2 F_{0\sigma}^2 \leq a_0^2 (a_0^2 r^2 + R^2 s'^2)$. As causality requires that $F_{0\sigma}^2 < a_0^4 \lambda^{-2} (r^2 + a_0^{-2} R^2 s'^2)$ we may assume

$$F_{0\sigma}^2 = \beta a_0^4 \lambda^{-2} (r^2 + a_0^{-2} R^2 s'^2) \quad (3.93)$$

where $0 \leq \beta < 1$. Equation (3.92) may then be rewritten in terms of β as

$$\Pi = \frac{2T_1 \sqrt{\beta} \lambda}{\sqrt{1-\beta}}, \quad (3.94)$$

from which it is clear that $\beta = 0$ corresponds to $\Pi = 0$ and that $\Pi \rightarrow \infty$ as $\beta \rightarrow 1$. However, the bound for PBH formation is not the only condition we must consider, as the predictions of our model must also be consistent with observational bounds. Current observational constraints on the PBH energy density come from the EGRET experiment, which measures the extragalactic gamma ray flux at 100MeV [13, 63]. By calculating the expected contribution to this flux from black holes expiring at the present epoch [118, 278] (see also [63, 280] for bounds derived for the standard PBH spectrum using the latest data),

it has been shown that the current PBH density created from the collapse of cosmic strings is bounded by

$$\Omega_{PBH}(t_0) < 10^{-9}. \quad (3.95)$$

This bound is based on the prediction that the PBH mass spectrum follows the profile predicted by the standard Hawking collapse process, such that $M_{PBH}(t) \sim t$ and the number density per mass interval is given by (3.76). Technically, one should recalculate this bound using the spectrum predicted by the necklace-specific collapse channel in order to place bounds on the model parameters from experimental data. Although it would be fruitful to recalculate the bound on $\Omega_{PBH}(t_0)$ at a later date, we use $\Omega_{PBH}(t_0) < 10^{-9}$ as a “ball park” figure with which to proceed.

Not *all* the region of parameter space allowing PBH production is compatible with observation. For example, “typical” values of $a_0 \sim 10^{-11}$ and $\Pi \sim 10^{12}$ are sufficient to ensure $M_T(t_i) > M_*$ for at least some t_i but the resulting value of the $\Omega_{PBH}(t_0)$ integral (3.91) is *huge* ($\Omega_{PBH}(t_0) \sim 10^3 \gg 1$) if R is comparable to the string scale. However, due to the large R -dependence in the denominator caused by the extra-dimensional contribution to ν_r we (happily) see that values of $R \sim \mathcal{O}(10^2)$ are sufficient to bring $\Omega_{PBH}(t_0)$ within the observable bound $\Omega_{PBH}(t_0) < 10^{-9}$. Thus the dimensions of the compact space need not be hierarchically larger than the string scale in order for the predictions of our model to be consistent with observational constraints.

To systematically explore the values of a_0, R and Π which are consistent with all the constraints above, we can express the value of the peak of the necklace mass function, $M_{T_{approx}}$ given by (3.65), in terms of M_* :

$$M_T^{peak} \sim 5.47 T_1 \sqrt{1 + \frac{\Pi^2}{T_1^2 \lambda^2} \frac{\alpha^2 \alpha'^{\frac{3}{2}}}{8a_0 R}} = \kappa M_* \quad (3.96)$$

where $\kappa > 1$ is a parameter that for given values of $(a_0, \alpha, R, \Pi, T_1, \alpha')$ expresses how far the peak value of M_T is above the mass scale M_* . Using this definition we can express the quantity $\sqrt{1 + \frac{\Pi^2}{T_1^2 \lambda^2}}$ in terms of $(a_0, \alpha, R, \kappa, T_1, \alpha')$ and the above terms for t_*^\pm simplify considerably to

$$t_*^- = \frac{0.171 \alpha'^{-1/2}}{a_0^2 T_1 \kappa}, \quad t_*^+ = \frac{2.297 T_1 \kappa \alpha'^{3/2}}{a_0^2}. \quad (3.97)$$

It is interesting that both t_*^- and t_*^+ depend on the warp factor as a_0^{-2} . It may be thought that the times t_*^- and t_*^+ should approach one another for $\kappa = 1$, since the definition of t_* requires values of t_i for which $M_T = M_*$. However, we have assumed the early-time approximation for M_T in determining t_*^- , and not the late-time approximation $M_{T_{approx}}$. This assumption then requires that we take $\kappa > 1$. We could, of course, consider situations where κ is closer to unity, but then one has to use $M_{T_{approx}}$ in the determination of both

t_*^- and t_*^+ , which is technically complicated.

Now evaluating (3.91) using the above, we obtain an expression that depends on the parameters $(a_0, \alpha, R, \Pi, T_1, \alpha', t_0, \rho_{crit})$. In figure 3.8 we present a contour plot showing the values of R, κ that are consistent with the condition $\Omega_{PBH}(t_0) < 10^{-9}$. In this plot we have taken, as typical values, $a_0 = 0.1$ and $\alpha = 0.8$, set $T_1 = \alpha'^{-1} = 1$ and input the standard values of ρ_{crit} , t_0 and M_* . The resulting bounds on $\{R, \kappa\}$ are remarkably insensitive to the actual value of a_0 because the latter only appears in $\Omega_{PBH}(t_0)$ via logarithmic factors. For given (allowed) values of $\{R, \kappa\}$ we can then deduce the value for Π via (3.96), which is of course sensitive to the value of a_0 .

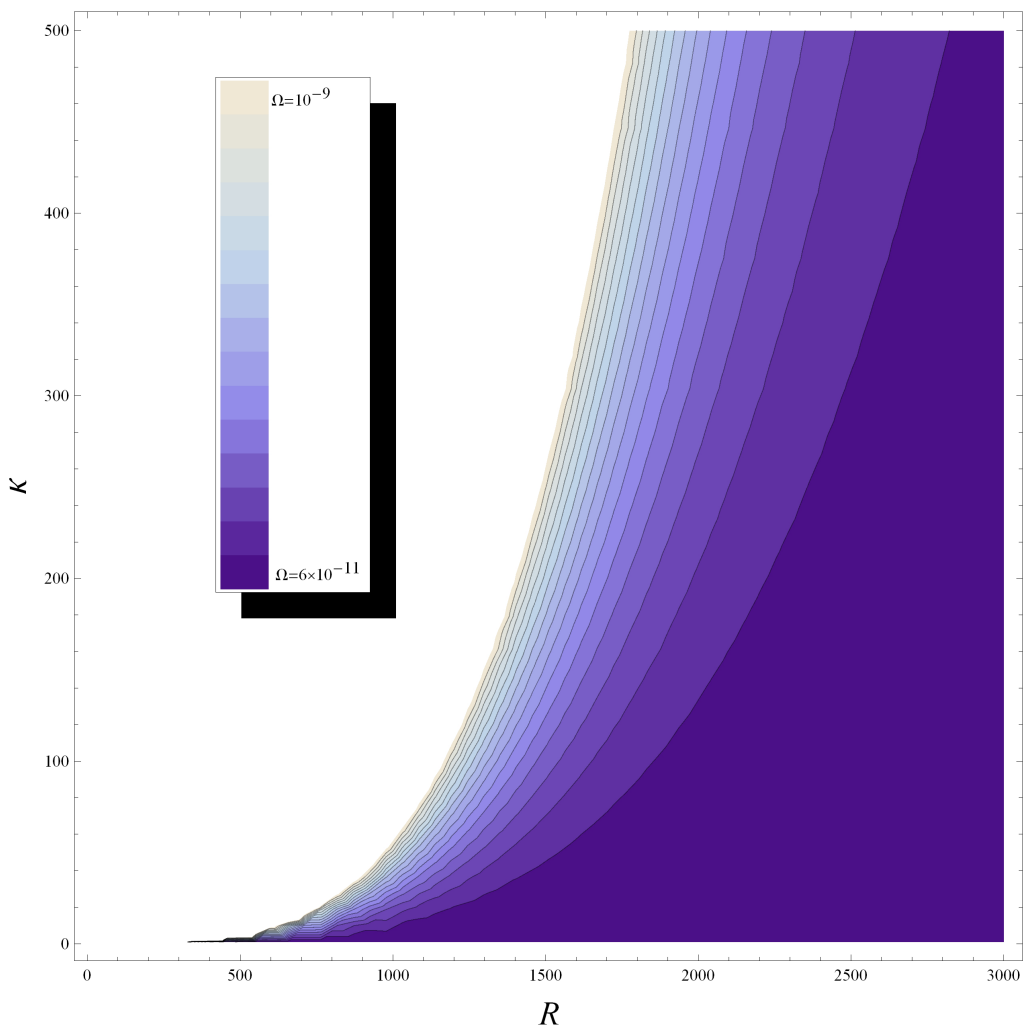


Figure 3.8: Contour plot showing the allowed regions of $\{R, \kappa\}$ consistent with the bound $\Omega(t_0) < 10^{-9}$. Only a few contours are plotted. We have chosen $a_0 = 0.1$, $\alpha' = 1$, $\alpha = 0.8$ and $T_1 = 1$.

To visualize the allowed values of Π corresponding to those of a_0 , R and κ , we use the three-dimensional contour plot shown in figure 3.9. We illustrate six typical surfaces in the $\{\text{Log}[a_0], R, \kappa\}$ plane, corresponding to $\Pi = 10^{12}, 10^{10}, 10^8, 10^6, 10^4, 10^2$ (from front to back). These surfaces also take into account the observational allowed values of $\{R, \kappa\}$ illustrated in figure 3.8.

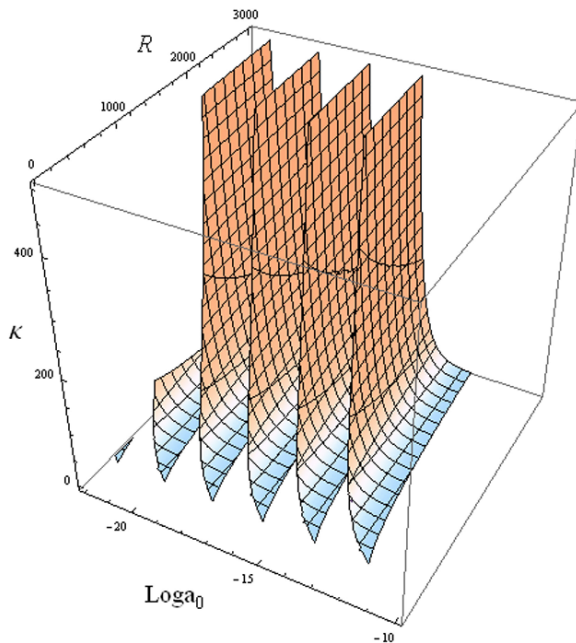


Figure 3.9: Three-dimensional contour plots showing values of the flux parameter Π in the $(\text{Log}[a_0], R, \kappa)$ plane. Six surfaces are shown corresponding (from front to rear) to the values of $\Pi = 10^{12}, 10^{10}, 10^8, 10^6, 10^4, 10^2$. These plots take into account the observational bounds on $\{R, \kappa\}$ shown in figure 3.8. The remaining choice of parameters are as in figure 3.8.

3.4.4 Quasi-stable necklaces

Let us now drop the assumption that the loops retain their necklace structure indefinitely. As outlined earlier, it is reasonable to expect that wrappings in the flat ϕ -direction may unwind over time leading to the “flattening” of the θ -direction. This in turn flattens the ψ -direction, and so on, until the whole necklace structure unravels.

Assuming that the motion of the string in the ϕ -direction remains random *after* the formation of a loop, and that the motion is also random in any newly flattened direction, we should expect the characteristic lifetime of the beads in any necklace to be comparable to the formation time, t_i . This is because the average warped time taken for a single ϕ -winding

to contract to a point is $a_0 t_1 \sim \frac{R^2}{a_0^{-1} \sqrt{\alpha'}}$.¹⁸ The warped time taken for $n_w(t_i)$ windings to contract is therefore

$$a_0 t_{n(t_i)} \sim \frac{n_w^2(t_i) R^2}{a_0^{-1} \sqrt{\alpha'}} \quad (3.98)$$

As we are only considering that part of the string which forms the extra-dimensional windings, we may compare the expression above with (3.27), in which ω_l and α have been set to unity. We then see that

$$t_{n_w(t_i)} \sim t_i. \quad (3.99)$$

This implies that the number of necklaces originally formed at t_i which survive for a time $\Delta t \gg t_i$ after formation will be negligible, with most having become standard string loops. However, it is difficult to estimate the fraction of necklaces surviving for an arbitrary length of time Δt using such generic arguments, though this is exactly what we must calculate to determine the true contribution of necklace collapse to the PBH mass spectrum. In particular, we must calculate the fraction of loops which retain their necklace structure for an interval $\Delta t \sim \frac{\alpha}{\Gamma \bar{G} T_1} t_i$. To do this, we consider the probability distribution which describes fluctuations of the radial coordinate. For a random walk this is simply a Gaussian distribution with mean $\mu = 0$ and variance

$$\sigma^2(\Delta t) \sim a_0^{-1} \frac{\Delta t}{\delta t} \epsilon_l^2 \sim a_0^{-2} \sqrt{\alpha'} \Delta t \quad (3.100)$$

where $\delta t \sim a_0^{-1} \sqrt{\alpha'}$ is the time interval between steps, $\epsilon_l \sim a_0^{-1} \sqrt{\alpha'}$ is the step length and Δt is the total (unwarped) time elapsed. The total probability density function is

$$\begin{aligned} \Phi(t, \sigma(\Delta t)) &\sim \frac{1}{\sqrt{2\pi}\sigma(\Delta t)} e^{-\frac{1}{2} \frac{t^2}{\sigma^2(\Delta t)}} \\ &\sim \frac{a_0}{\sqrt{2\pi}(\sqrt{\alpha'} \Delta t)^{\frac{1}{2}}} \exp\left(-\frac{a_0^2 t^2}{2\sqrt{\alpha'} \Delta t}\right). \end{aligned} \quad (3.101)$$

Since a loop forming at time t_i has $n_w(t_i)$ windings to lose, the radial coordinate must “travel” a distance approximately equal to $n_w(t_i)R$ in order for the loop to lose its necklace structure. The fraction of necklaces $f(\Delta t)$ which survive for an interval Δt after t_i is then given by the integral of the above expression between $t \sim \pm a_0^{-1} n_w(t_i)R \sim \pm a_0^{-1} (\sqrt{\alpha'} t_i)^{\frac{1}{2}} \sim$

¹⁸Here we have used the fact that the radius of the winding must contract by a distance $\sim R$. Assuming a step length $\epsilon_l \sim a_0^{-1} \sqrt{\alpha'}$ for the change in the radial coordinate, this requires a total displacement of $\sim \frac{R}{a_0^{-1} \sqrt{\alpha'}}$ steps. This requires on average $\sim R^2/a_0^{-2} \alpha'$ random steps, which takes (warped) time $a_0 t \sim \frac{R^2}{a_0^{-2} \alpha'} \times a_0^{-1} \sqrt{\alpha'} = \frac{R^2}{a_0^{-1} \sqrt{\alpha'}}$.

$\pm\sigma(t_i)$, which can be well approximated using the error function,

$$\begin{aligned} f(\Delta t) &\sim \text{Erf} \left(\frac{\sigma(t_i)}{\sqrt{2}\sigma(\Delta t)} \right) \sim \text{Erf} \left(\frac{1}{\sqrt{2}} \frac{a_0^{-1}(\sqrt{\alpha'}t_i)^{\frac{1}{2}}}{a_0^{-1}(\sqrt{\alpha'}\Delta t)^{\frac{1}{2}}} \right) \\ &\sim \text{Erf} \left(\sqrt{\frac{t_i}{2\Delta t}} \right). \end{aligned} \quad (3.102)$$

Thus when $\Delta t \sim t_i$ the fraction of loops which have retained their extra-dimensional windings is approximately

$$f(t_i) \sim \text{Erf} \left(\frac{1}{\sqrt{2}} \right) \sim 0.68, \quad (3.103)$$

which matches well with our result (3.99).¹⁹ The fraction of necklaces which survive until they reach the minimum radius is

$$f \left(\Delta t \sim \frac{\alpha}{\Gamma\mathcal{G}T_1} t_i \right) \sim \text{Erf} \left(\frac{1}{\sqrt{2}} \left(\frac{\alpha}{\Gamma\mathcal{G}T_1} \right)^{-\frac{1}{2}} \right). \quad (3.104)$$

Strictly speaking, therefore, the integral (3.87) should be multiplied by the additional numeric factor above to account for the the loss of necklaces which unravel before reaching the point at which they can undergo gravitational collapse.

Since $f \left(\Delta t \sim \frac{\alpha}{\Gamma\mathcal{G}T_1} t_i \right) \leq 10^{-20}$, the necklace-specific channel becomes comparable (or subdominant) to the standard Hawking process when when $\alpha \geq 1.591 \times 10^{39} \Gamma\mathcal{G}T_1$. Practically, however, the values of α , Γ , \mathcal{G} and T_1 here are such that this is unlikely to occur without significant fine-tuning.

3.4.5 Comparison with the standard string-monopole network

The dynamics of string-monopole network evolution depends crucially upon the ratio of the monopole energy density to the string tension [6, 263]. This dimensionless parameter, denoted \mathcal{R} in the literature, is

$$\mathcal{R} = \frac{m}{\mu d} \quad (3.105)$$

where m is the the monopole mass, μ is the tension and d is the distance between monopoles. For $\mathcal{R} \ll 1$ the network behaves like an ordinary string network, reaching a scaling solution at late times, but for $\mathcal{R} \gg 1$ the mass of the beads dominates the dynamics of the evolution. In our case, these energy scales are time-dependent and the corresponding parameter is

$$\mathcal{R}(t_i) = \frac{M_b(t_i)}{T_1 d(t_i)}, \quad (3.106)$$

¹⁹We see that $f(\Delta t) < 0.68$ for all $\Delta t > t_i$. In fact, $\text{Erf}(1/2) \sim 1/2$, so the *majority* of loops ($f(\Delta t) > 1/2$) will have lost all their windings by $\Delta t \sim 2t_i$. This helps to quantify our earlier result (3.99) more precisely.

which scales as $\mathcal{R} \sim t_i^{-2}$ for $t_i \gg \frac{2\sqrt{\alpha'}}{a_0^2\alpha}$ and $\mathcal{R} \sim t_i^{-\frac{1}{2}}$ for $t_i \ll \frac{2\sqrt{\alpha'}}{a_0^2\alpha}$. Thus, as $t_i \rightarrow \infty$, $\mathcal{R} \rightarrow 0$ and vice-versa. Our results are therefore consistent with the standard analysis in that the necklaces behave like an ordinary string network for $\mathcal{R} \ll 1$ but like a string-monopole network when $\mathcal{R} \gg 1$ since the mass of the beads becomes significant.

However, the dynamics of \mathcal{R} differ profoundly in our model. This indicates that the effect of beads formed from extra-dimensional windings is different to the effect created by monopoles²⁰ with regard to network evolution. To understand this in more detail let us consider the latter. The standard equation for the evolution of \mathcal{R} is [7]

$$\frac{\dot{\mathcal{R}}}{\mathcal{R}} = -\kappa_s t^{-1} + \kappa_g t^{-1} \quad (3.107)$$

where the first term on the right-hand side describes the stretching of the string due to the cosmic expansion and the the second term describes the contraction due to emission of gravitational radiation. It is a reasonable to assume that

$$\kappa = \kappa_g - \kappa_s > 0 \quad (3.108)$$

which allows us to solve (3.107) up to some constant of integration,

$$\mathcal{R} \sim t^\kappa. \quad (3.109)$$

Using (3.105) the evolution of the inter-monopole distance then scales like

$$d \sim \mathcal{R}^{-1} \sim t^{-\kappa}. \quad (3.110)$$

This was the crucial assumption Matsuda used to identify $d(t)$ with the step length of the random walk $\chi(t)$ of the monopole along the string [8]. From this point, the estimated initial number of beads per loop is taken to be

$$N_b(t_i) \sim n_w(t_i) \sim \frac{r(t_i)}{d(t_s) \times \left(\frac{t}{t_s}\right)^{k-1}} \quad (3.111)$$

where $d(t_s) \sim (t_M t_s)^{\frac{1}{2}}$ is the initial bead spacing in the *network* at the time of string formation t_s (where $t_s \sim \sqrt{\alpha'}$) and $k = 0$ corresponds to the (natural) $\kappa = 1$ solution of (3.107).²¹

²⁰For example, monopoles formed after a separate phase transition at some temperature $T_M > T_s$.

²¹The initial conditions of Matsuda's model *are* consistent with ours if we identify the initial damping time $t_d \sim a_0^2 R^2 / 4\sqrt{\alpha'}$ with the time of initial monopole formation t_M and the time of initial loop formation t_i with the initial string formation time t_s . The difference between the two models is that, while both t_M and t_s are fixed parameters related to a single *specific* time of string-monopole network formation, t_i is continuous a paramter which defines a continuously varying bead mass, determined by the dynamical evolution of the windings. In addition, as mentioned earlier, in an extended analysis the collision of the string network

Assuming that $\sim \sqrt{n_w}$ beads would survive without annihilation (as in [6]), we find that $m_{coil} \propto \sqrt{n_w}$ and hence

$$m_{coil} \sim t_i^{\frac{2-k}{2}}, \quad (3.112)$$

which favours black hole production at late times and DM production for small t_i . This is the standard result assuming that necklaces which reach their minimum radius but which have insufficient mass to undergo collapse to form PBHs can only interact with other matter gravitationally, leading to the production of Planck-scale DM relics. In Matsuda’s original scenario, based on the assumptions above, large numbers of Planck-scale DM “particles” are formed at early times with smaller numbers of increasingly massive black holes formed at later times. In our model this process is essentially reversed with a window of PBH production in the early universe (though potentially this window may be quite large for small a_0 , so the last epoch of PBH formation is not necessarily “early”, even on cosmological time-scales) when $M_T(t_i) > M_*$, with potential DM candidates forming well into the scaling regime when $M_T(t_i) < M_*$.

Physically the above equations describe the shrinking of the string sections connecting neighbouring monopoles. Effectively the contraction of the string is able to pull these monopoles through the horizon at an ever increasing rate.²² Hence we find that the early and late-time limits of \mathcal{R} , as defined above, are opposite to those obtained from (3.106), namely that $\mathcal{R} \rightarrow \infty$ as time increases, while $\mathcal{R} \rightarrow 0$ as $t_i \rightarrow 0$. Similarly the natural solution, $\kappa = \kappa_g - \kappa_s \sim 1$, obtained from an order of magnitude estimate, gives $d \sim t^{-1}$ in the standard case as opposed to $d \sim t$ in our case. In yet another respect, therefore, we have obtained the opposite results to the standard analysis.

Again it is not immediately obvious that what applies to monopoles formed in a separate phase transition also applies to beads formed by extra-dimensional windings. Although a contracting string may pull ordinary monopoles through the horizon at an ever increasing rate, a winding may not cross the horizon “ready-made” and concentrated at a point from a four-dimensional perspective. This is because insufficient time will have elapsed to establish correlations in the compact dimensions. Put another way, if the horizon advances by a distance $a_0 c \delta t$, the end point of the string formerly localised at the horizon, can move by at most a distance $c \delta t$ from its original position in the compact space. Causality therefore places a limit on the rate at which new windings can enter the horizon, whereas no such

with the background plasma should be taken into account implying that t_d should become temperature (and hence time) dependent. Ultimately, therefore, it would seem that the idea of a fixed bead formation time is inappropriate in the context of beads formed dynamically from wound-strings over an extended period of time, rather than from a phase transition at a specific time, as in field-theoretic models.

²²Alternatively this can be viewed as the expanding horizon uncovering monopoles, separated by increasingly short distances, the distances having been shortened by the contraction of the string.

limit exists for ordinary monopoles.²³

In fact, the considerations above help to explain why the number of windings $n_w(t_i)$ is proportional to the ratio a_0/R not simply to $1/R$ in the warped throat model. Although larger R results in a slower rate of winding formation (as we would expect) this effect is, at least potentially, dwarfed by the effect of the warp factor a_0 (c.f. (3.41)) which is related to R via the deformation parameter, $a_0^2 \sim \tilde{\epsilon}^{\frac{4}{3}} R^{-2}$. This is because a_0 limits the increase of the horizon distance in the infinite directions (but not in the compact space) via

$$d_H(\delta t) = a_0 c \delta t. \quad (3.113)$$

As the *resultant* velocity of the end point of the string is $c = 1$, smaller a_0 results in a greater velocity in the compact spaces and hence a larger limiting value for $n_w(t_i)$ (c.f. the introduction of the factor $\sqrt{1 - a_0^2}$ into the formula for $n_w(t_i)$ in the velocity correlations regime in the next chapter).

In general, however, beads may enter the horizon more rapidly the smaller their effective radii. In fact, this at least partially accounts for the falling bead mass at late times: since $t_i \rightarrow \infty$, we expect that $\omega_l \rightarrow 0$ for a random walk in the extra dimensions. This could be achieved through either:

- Falling number density (per unit distance along the string), at late times, $n_w \sim d^{-1}$
- Windings wrapping ever smaller effective radii in the S^3 .

The fact that $d^{-1} \sim t_i^{-1}$ at late times highlights the first effect and $M_b \sim t_i^{-1}$ indicates the second. In practice, however, we would expect both effects to play some role.

The question then arises, does the shrinking bead mass have a counterpart in field theory? It is natural to consider whether the arguments for the limitation of windings entering the horizon hold true for the “bead-equivalents” of field-theoretic strings in the dual Abelian (or non-Abelian) Higgs models. This question is addressed in chapter 5.

Finally we note that the predictions of our model (specifically that PBH production is favoured at early times with potential DM production at later epochs, in contrast to previous predictions) are highly dependent on the assumption of a random walk regime which produces the extra-dimensional windings. It is not immediately clear how this behaviour might be modified by the introduction of a velocity correlations regime, though it is possible that the results may be more in line with those of previous studies. It is also highly

²³An alternative way to view this result is to consider windings as correlations in the compact space. All windings must therefore form within the horizon to preserve the causal structure.

dependent upon the assumption that only beads formed from *net* windings, not from bead-anti-bead ($b-\bar{b}$) pair formation, contribute to the mass of PBH/DM relics. As we have seen, assuming that $\sim \sqrt{n_w} b/\bar{b}s$ survive until the string reaches its minimum radius (where n_w must be taken to include *all* beads/anti-beads created from random steps along the string, not simply those formed by net displacement in the compact space) leads to (3.112) and to qualitative behaviour which is the very opposite to that obtained in our model. However, as stated previously, we believe that such an argument is valid only for a *static* string and that in a contracting loop all beads will eventually collide with their anti-bead counterparts before the minimum radius is reached. In particular, in our model we may expect the initial $b-\bar{b}$ spacing to be approximately equal to the step length $\epsilon_l \sim a_0^{-1}\alpha\sqrt{\alpha'}$, which is most certainly greater than the minimum radius $\delta_l \sim \eta_s^{-1} \sim \sqrt{\alpha'}$ for all reasonable values of α and a_0 .

3.5 Discussion

In this chapter we have investigated a simple cosmic string model using several key ideas from string theory. Our starting point was the assumption that there is some initial stage of inflation that leads to the creation of strings (along the lines of [247]) and that these strings may undergo dynamical evolution leading to the creation of non-zero windings in the internal space. We argued that the string feels a lifting potential due to the non-trivial geometry of the background, causing it to form a step-like winding configuration which appears as a necklace from a four-dimensional perspective. By estimating the mass of such a string configuration we were able to show that formation at late times reduces to a scaling solution, which one may hope to identify with a relic DM phase. We also note in passing that, in principle, we require DM production from necklaces between t_{PBH}^+ and t_0 not to over-close the universe. However, as the present day DM density bound is (approximately) $\Omega_{DM}(t_0) < 0.3$ and because of the t^{-3} suppression of the loop production function, we find that in all but pathological cases the PBH density bound $\Omega_{PBH}(t_0) < 10^{-9}$ is by far the most stringent constraint.

In some sense, this has been a bottom-up approach to the problem. The warp factor is simply a parameter of the metric, depending only on the extra-dimensional flux and the deformation parameter of the (non-compact) SUGRA background. A fully realised UV approach will precisely fix the warping as a function of the closed-string moduli VEVs and the flux, thereby leading to a more tightly constrained theory. However, the general features of our approach should remain intact. In particular, the formation window for PBHs at early times contrasts strongly with the original field theory/string necklace model proposed by Matsuda [8]. Although we initially feared that this result may be in some sense disappointing, due to the likelihood of PBHs formed at early times having evaporated by the present epoch, we have shown that it is possible to satisfy the condition $M_T(t_i) > M_*$ and current

observational constraints within the model constructed here.

It is worth stressing that, for very small a_0 , the window of black hole formation may be sufficiently large for the assumption of a constant M_* to become inaccurate. A more detailed analysis would therefore take into account the rate of black hole evaporation in the extra-dimensional background by introducing a time-dependent lower bound on the PBH mass $M_*(t_i)$. An improved analysis would also consider how the abundance of PBHs formed through necklace collapse in the very early universe affects BBN and subsequent structure formation. In fact, there are *many* theoretical and observational constraints which any such model must satisfy concurrently (see [63] for a recent review), thereby potentially allowing the KS model parameters to be bounded with even greater precision.

It is clear from our model that generating *any* PBHs of mass M_* restricts us to a small region of the (a_0, R, Π) parameter space, as is shown in figures 3.8 and 3.9. This is not surprising if we recall that $M_* \sim 10^{20}$ in Planck units and so there is a hierarchy issue here. On the other hand, since the warp factor a_0 depends exponentially on background fluxes, obtaining small enough values to generate a hierarchically large M_T is not so unnatural.

In order to satisfy the PBH observational bounds, one requires larger background flux M if there is larger worldvolume flux Π . This is inherently obvious, since the additional worldvolume flux can be treated as an effective mass correction to the necklace. This additional mass will back-react on the solution and the probe limit will be rendered invalid, unless the background flux is also increased to compensate. What is interesting is that, for fixed warping, there is a large parameter space where bounds are satisfied. Another interesting feature is that, as is clear from figure 3.8, the allowed values of R for regions where $M_T \gg M_*$ (corresponding to large κ) are still in the “mild” hierarchy region $R \sim 10^3 l_s$. Indeed, the only way a value of $R \sim l_s$ may be consistent with observational evidence is if the peak of M_T is fine-tuned so as to be very close to, but just above, M_* . This reduces the time interval between t_*^- and t_*^+ , which can be made small enough to allow the value of R to be reduced while still obtaining $\Omega_{PBH}(t_0) < 10^{-9}$.

Our construction is very model-dependent in some sense, since it is only valid for a special class of SUGRA backgrounds of the type IIB string. Another interesting class of cosmic string models arises from considering heterotic M-theory on the orbifold $CY_3 \times S^1/\mathbb{Z}_2$. The strings in this case can arise from wrapping membranes (or five-branes) over various cycles within the internal space [281, 282]. Topologically stable strings are only possible for five-branes wrapping a complete four-cycle within the CY space [283]. However, other wrappings are potentially possible if there is a lifting potential and a similar analysis could, in principle, be performed.

One other issue that remains is the validity of substituting the expression $r(t_i) = \alpha t_i$ for the variable r in the bead mass terms of the EllipticE expansion and $r(t, t_i) = \alpha t_i - \Gamma T_1 \mathcal{G}(t - t_i)$ into the leading order term representing the mass of the four-dimensional sections of the string. As stated previously, this is entirely consistent with Matsuda’s original assumption that the bead mass remains constant after loop production due to the “trapping” effects of the lifting potential, whereas the sections of string not contained in the extra-dimensional windings shrink through the emission of gravitational radiation. However, the reparametrisation invariance of the Nambu-Goto action implies that it may not be possible to talk of one “section” of the string expanding/contracting while other sections remain fixed. By definition strings have no substructure which seem to imply that they must expand or contract along their entire length. In our model this would mean that the contraction of the string due to gravitational radiation in the warped Minkowski directions in fact produces a contraction of the string along the internal direction as well. If true, this implies that the expression $r(t, t_i)$ should be substituted in *both* the bead-mass and four-dimensional parts of the string mass integral, creating an explicitly time dependent bead-mass $M_b(t, t_i)$ for $t > t_i$. Potentially this may alter the present results significantly, as we would expect the number of necklaces which retain sufficient mass in their extra-dimensional windings to produce PBHs when reaching their minimum radius to diminish sharply. This is therefore likely to lead to a much smaller amount of black hole production and greatly increased DM/stable relic formation. It is hoped that the question of the explicit time-dependence of the bead mass may be resolved conclusively by investigating field theory duals of the string necklaces discussed here and some preliminary work aimed at answering this important question is presented in chapter 5. Interestingly though, this work also suggests necklace relics may be dual to topological defect strings containing gauge field vortices. This, in turn, implies that such relics do not represent viable DM candidates, as we therefore expect them to emit/absorb gauge field radiation.

A further aside concerns the question of binding energy between $b - b$ or $\bar{b} - \bar{b}$ pairs which coalesce, or of the related “anti-binding” energy between $b - \bar{b}$ pairs (i.e. the energy released when they annihilate). In field-theoretic models the situation is essentially reversed and a binding energy exists between neighbouring monopoles/anti-monopoles (which attract one another) while an “anti-binding” energy exists between true monopole or anti-monopole pairs (which repel each other). However, these energies (and the strengths of the attractive/repulsive forces they generate) may be calculated if the topological charges of the monopoles and field couplings are known (see [114]). We may suspect that, if similar but somehow *opposite* binding energies exist between beads formed from extra-dimensional windings, their presence may alter the string dynamics so that the evolution of a string configuration with N_b “one step” beads into a single bead formed from N_b steps will be energetically favoured. Once formed, it is also possible that such a configuration may unwind more rapidly than its corresponding N_b -bead counterpart, leading to a necessary modifica-

tion of the arguments in section 3.4.3.

In such a scenario we may also expect an attractive force to operate between neighbouring $b-b$ or $\bar{b}-\bar{b}$ pairs, and a repulsive force to operate between neighbouring sets of $b-\bar{b}$. While for true monopoles these forces are caused by the interaction of the fields resulting from the topological charge, it is not difficult to imagine an explicitly stringy origin for forces which behave in a qualitatively similar manner: In this case the attraction/repulsion may be seen to result from the action of the string tension (viewed as a vector quantity in the compact space) in a manner similar to that which results in the formation of step-like winding configurations. In effect, a section of string lying between two beads formed from opposing windings is “pulled” from either end, or equivalently the beads are “pushed” further apart (though the total string length remains constant), whereas a section of string lying between two beads formed from like windings is “pushed” from either side, while the beads are “pulled” closer together (again the total string length is constant). This possibility, and its relation to beads formed from “pinched” strings, is also discussed further in chapter 5, though the argument presented is schematic and no specific calculations are performed.

As a first approximation then we have assumed in the analysis above that there is *no* binding energy between the winding states. We note also that, in the absence of a full Boundary Superstring Field Theory (BSFT) picture [284], this seems intuitively likely given that the string configuration must be considered as a collective phenomena, which suggests that the unwinding of N_b single steps will be just as hard as unwinding a single N_b -step wrapping. However, it is not clear how one can really understand this problem without a more detailed analysis of the boundary theory and, by contrast, the arguments above would seem to suggest that an adequate boundary theory *must* include a description of the forces between similar and dissimilar winding pairs.

Finally, it is interesting to speculate further on the recent result implied by the PAMELA experiment [285, 286], which suggests that there is an over-abundance of high energy positrons in the cosmic background. Rather than interpreting this as a signal for DM, it has also been suggested that this is in agreement with predictions from cosmic strings [287]. It would certainly be interesting to extend the present analysis along those lines.

CHAPTER 4

NON-TOPOLOGICAL CYCLOOPS

4.1 Introduction

In this chapter we propose a mechanism for the creation of cosmic string loops with dynamically stabilised windings in the internal space. Assuming a velocity correlations regime in the post-inflationary epoch, such windings are seen to arise naturally in string networks prior to loop formation. The angular momentum of the string in the compact space may then be sufficient to ensure that the windings remain stable *after* the loop chops off from the network, even if the internal manifold is simply connected. For concreteness we again embed our model in the KS geometry, with strings lying at the tip. Our results may therefore be compared with those of the previous chapter, in which we saw that the adoption of a random walk regime led to the creation of static loops with step-like windings, i.e. cosmic necklaces. This work represents a direct extension of the previous $l = 0$ case to a scenario where $l > 0$.

We see that, in contrast to the static case, energy minimisation of the string loop in the dynamical case favours a smoothly varying winding configuration, so that the resulting object resembles a cycloop [16] as opposed to a necklace [8]. However, as the internal space at the conifold tip is simply connected, the loops do not contain topologically stabilised windings. In their original conception, Avgoustidis and Shellard used this term to refer only to loops with windings which are topologically trapped and we therefore propose the term “non-topological cycloops” to refer to string loops with dynamically stabilised smooth windings around a simply connected compact manifold.

One of the most interesting results of this investigation is the discovery of the interaction between the string tension and the angular momentum in the compact space which, as we shall see, causes the loop to oscillate between alternate phases of expansion and contraction. We note that this, in principle, should give rise to a distinct GW signature, the future detection of which could provide indirect evidence for the existence of extra dimensions. Unfortunately, it is not possible to investigate this idea within the scope of this thesis, though some preliminary remarks regarding future work in this direction are given in the discussion section at the end of this chapter.

The existence of string loops with dynamically stabilised windings in the KS geometry

[5] was first demonstrated by Iglesias and Blanco-Pillado [276] and the following work contains significant overlap with their paper. They considered strings at the tip of the throat, with geodesic wrappings in the S^3 which regularises the conifold singularity. In particular, in considering geodesic windings, we will find it convenient to use so-called Hopf coordinates, as they did, to describe the geometry of the three-sphere.

Although they derived a lower bound for the angular momentum of a loop with a given number of windings - below which the windings became unstable - the result must remain of purely theoretical interest to cosmology as long as a specific mechanism for winding formation (and hence for string angular momentum formation) is not considered. The purpose of the following work is to find a mechanism which leads to the formation of string configurations such as those investigated in [276] and to investigate the resulting string dynamics with specific reference to their cosmologically observable consequences.

Assuming that a velocity correlations regime in the post-inflationary epoch leads naturally to the formation of geodesic windings [16], we show that the winding number (n_w), total energy (E) and angular momentum (l) of the string are specified precisely by the model parameters, that is, by the parameters which define the KS geometry (i.e. the value of the warp factor a_0 and the radius of the three-sphere R) and those which determine the characteristic scale of the string loops (α, t_i).¹ Substituting for l and n_w in the bound referred to above then demonstrates the stability of these windings, at least under the assumption that l remains approximately constant over small time scales after the moment of loop formation. By assuming also that the total energy of the string remains approximately constant (i.e. by neglecting the loss of E and l via GW emission), we then determine the equation of motion (EOM) for the four-dimensional string radius $r(t)$, and solve it to find a (generically) oscillating solution.

Crucially, we observe that the qualitative behaviour of the loop depends on the value of the warp factor a_0 , with $a_0^2 < 1/2$ leading to an initial expansion phase and $a_0^2 > 1/2$ to an initial contraction phase. The fixed point solution $a_0^2 = 1/2$ is a static, non-oscillatory solution. In both oscillatory modes (initially contracting *and* expanding) we find that the period of the oscillation is inversely proportional to a_0^2 , and proportional to the initial size of the loop $r(t_i) = (\alpha t_i)$.

The layout of the chapter is as follows: In section 4.2 we briefly review the relevant KS background, focusing in particular on the description of the tip geometry in our new coordinate system. In section 4.3 we show how the assumption of a velocity correlations regime

¹However, this assumption may be questioned. Unfortunately, the analysis of the string dynamics in the case of non-geodesic windings is extremely complicated and must be omitted here. Further discussion of this point is given in section 4.6.

yields a dynamical model of winding formation after the end of inflation. Section 4.4 recaps the generic results of [276] which we then combine with the results of the previous section to give explicit expressions for n_w , E and l at the moment of loop formation. The EOM for the loop radius is then derived and solved in section 4.5. A brief summary of the main results, together with a discussion of their cosmological implications and possible consequences for experimental observations, is presented in section 5.6. Finally, the two appendices at the end of this thesis deal with issues arising in the current chapter: Appendix A outlines the method of Eulerian substitution of the third kind, which is used to integrate the differential equation involving $\dot{r}(t)$ and $r(t)$ derived in section 4.5. Appendix B gives a detailed description of the Hopf fibration of the three-sphere, which is introduced briefly in section 4.2 and used throughout the following analysis.

4.2 Description of the tip geometry in Hopf coordinates

The KS geometry is the canonical example of a background which resolves a conifold singularity in type IIB string theory. As we have already given an extended discussion of this geometry in chapter 2, we refer the interested reader to the original paper [5] for further details. As noted previously, the essential point is that the conifold is the cone over an $S^2 \times S^3$ base space. When we deform the conifold, the S^2 shrinks to zero size, and the ten-dimensional metric factorises into the (warped) product $\mathbb{R}_{1,3} \times S^3$.

To recap: In canonical coordinates the effective metric of the KS geometry at the tip of the warped throat takes the form

$$ds^2 = a_0^2 \eta_{\mu\nu} dx^\mu dx^\nu + R^2 (d\psi^2 + \sin^2 \psi (d\theta^2 + \sin^2 \theta d\phi^2))$$

$$\psi \in [0, 4\pi), \quad \theta \in [0, \pi), \quad \phi \in [0, 2\pi)$$
(4.1)

where $\eta_{\mu\nu}$ is the usual four-dimensional Minkowski metric, a_0^2 is the square of the warp factor ($0 < a_0^2 < 1$) and the radius of the three-sphere is defined by

$$R^2 = b_0 M g_s \alpha'. \tag{4.2}$$

Here M is the number of units of flux wrapping the internal space, which is also the number of fractional D_3 -branes at the bottom of the throat, g_s is the string coupling, $l_s = \sqrt{\alpha'}$ is the fundamental length scale of the string, and b_0 is a numerical constant of order one. The relation between the size of the S^3 and the warp factor induced by the back reaction of the fluxes is

$$a_0^2 \sim \frac{\tilde{\epsilon}^{-4/3}}{R^2} \tag{4.3}$$

where the constant $\tilde{\epsilon}^{-4/3}$ is related to the deformation parameter of the conifold.

Of course, the relations (4.2) and (4.3) remain true in any coordinate system and, as mentioned above, we will find it convenient to use the Hopf fibration of the three-sphere when considering the formation of geodesic windings. These are the kind of windings we expect to form in the presence of velocity correlations which imparts an initial (constant) angular momentum density to each point along the string. In Hopf coordinates the S^3 is described as a one-parameter family of flat two-tori (to which it is topologically equivalent) [288] and the canonical metric (4.1) reduces to a much simpler form,

$$ds^2 = -a_0^2 \eta_{\mu\nu} dx^\mu dx^\nu + R^2 (d\theta^2 + (d\psi + \cos\theta d\phi)^2) \quad (4.4)$$

where ψ , θ and ϕ retain their original principle ranges, $\psi \in [0, 4\pi)$, $\theta \in [0, \pi)$ and $\phi \in [0, 2\pi)$.

The Killing vectors also adopt a simple form and are always parallel to the unit vectors in the ψ , θ and ϕ -directions. Fixing the value of the θ -coordinate such that $\theta = \theta_0$ then selects a flat T^2 sub-manifold and windings which follow the Killing directions in this manifold are necessarily geodesic in the full S^3 . However, the choice of gauge in this respect is somewhat arbitrary and we are free to choose $\theta_0 = 0$. This simplifies both the resulting metric and the Killing vectors of the T^2 , the latter now being *identical* to the unit vectors in the remaining ψ and ϕ -directions. Although it may be shown explicitly that the Lagrangian density \mathcal{L} for a string loop with geodesic windings in the S^3 is σ -independent in *any* coordinate system, the simple form of the Killing vectors in Hopf coordinates allows us to more easily calculate $L = \int d\sigma \mathcal{L} = 2\pi \mathcal{L}$. A thorough treatment of the Hopf fibration of the three-sphere, and a full description of geodesic windings in both canonical and Hopf coordinates, is given in Appendix B, along with a coordinate-independent geometric analysis.

4.3 A dynamical model of winding formation

We now proceed to construct our dynamical model of winding formation. In the velocity correlations regime the initial number of windings per loop, for a loop of size $r(t_i) = \alpha t_i$, is [16]

$$n_w(t_i) \sim \frac{\omega_l \alpha t_i}{R} \quad (4.5)$$

where ω_l is the fraction of the total string length which lies in the extra dimensions and is defined via [1]

$$\omega_l \sim \frac{n_w R}{\sqrt{a_0^2 r^2 + n_w^2 R^2}}. \quad (4.6)$$

Substituting this back into the expression above gives a unique physical physical solution,

$$n_w(t_i) \sim \frac{\sqrt{1 - a_0^2} \alpha t_i}{R}. \quad (4.7)$$

The condition $a_0^2 < 1$ ensures that $n_w(t_i) > 0$ for all $t_i > 0$. Also important is that the number of windings increases linearly with time, with an overall coefficient modulated by the presence of the warp factor.

Alternatively, one can choose to solve for w_l rather than the winding number, where

$$\omega_l(t_i) \sim \sqrt{1 - a_0^2}, \quad (4.8)$$

indicating that the magnitude of the warping imposes a physical constraint on the length of the string in the extra dimensions. We can also identify this quantity with the velocity of the string in the compact space. Imagine that the “end point” of the string at the horizon moves with a fixed velocity $v < 1$ in the extra dimensions. Then at time t_i there will be approximately

$$n_w(t_i) \sim \frac{vt_i}{R} \quad (4.9)$$

windings within the horizon and the number of windings within a fraction α of the horizon distance is therefore

$$n_w(t_i) \sim \frac{v\alpha t_i}{R}. \quad (4.10)$$

This is equal to the number of windings per loop for loops formed at time t_i in the scaling regime. With this identification we see that

$$\omega_l(t_i) \sim v(t_i) \sim \sqrt{1 - a_0^2} \quad (4.11)$$

and the physical conditions $0 < v < 1$ and $0 < \omega_l < 1$ are automatically satisfied by the condition $0 < a_0^2 < 1$. Furthermore, it is intuitively obvious that $\omega_l(t_i), v(t_i), n_w(t_i) \rightarrow 0$ as $a_0^2 \rightarrow 1$ because the $a_0^2 = 1$ solution of the KS model corresponds to Minkowski space in $(9 + 1)$ dimensions.² In this case, there are no internal fluxes and thus no compact extra dimensions, implying that no windings can exist.

We can also understand why $\omega_l(t_i), v(t_i) \rightarrow 1$ as $a_0^2 \rightarrow 0$ if we realise that windings are effectively correlations which can only form *within* the horizon (see sections 3.4 and 3.5). The horizon in the infinite dimensions advances according to

$$d_H^\infty(t) = a_0 t, \quad (4.12)$$

²Although this is not obvious from (4.3), the rationale behind this statement is the following; if no fluxes exist to provide an effective potential with which to compactify the extra dimensions, there can be no back-reaction on the ordinary four-dimensional Minkowski manifold. Hence $a_0^2 = 1$ and $R^2 \rightarrow \infty$ automatically, leading to a flat six-dimensional space in place of the metric (4.1)/(4.4). Similarly the other dimensions of the bulk CY space are no longer flux-compactified. In such a scenario, the formula (4.3) would not be valid as, by definition, it holds only for $a_0^2 < 1$.

whereas in our background the horizon distance in CY space (S^3) is

$$d_H^{CY}(t) = t. \quad (4.13)$$

Although the expression $a_0^2 = 0$ is strictly unphysical (corresponding to an extremal horizon), the limit $a_0^2 \rightarrow 0$ corresponds to a situation in which the infinite dimensions are ‘‘closed off’’ so that the string exists only in the compactified space (hence $\omega_l = 1$). In a time interval δt , the value of a_0^2 limits the increase of the horizon distance in the infinite directions (but not in the compact space) via

$$\delta d_H^\infty = a_0 \delta t, \quad (4.14)$$

which places a limit on how fast the correlations can form. Strictly speaking, the horizon in the infinite direction advances by a distance $a_0 \delta t$ when the horizon in the compact space advances by δt . The end point of the string, which must move with resultant velocity $v_{res} = 1$, must therefore cover a total distance *in the compact space* given by

$$\delta d = \sqrt{1 - a_0^2} \delta t, \quad (4.15)$$

which limits the effective velocity of the string in the extra dimensions to $v \sim \frac{\delta d}{\delta t} = \sqrt{1 - a_0^2}$. The parameter $\omega_l(t_i)$ is then given by the ratio of the string velocity in the compact space to the speed of light, $\omega_l(t_i) \sim v(t_i) \sim \sqrt{1 - a_0^2}$. Happily we find that the details of the compactification scheme determine $v(t_i)$, $\omega_l(t_i)$ and $n_w(t_i)$ uniquely.³

4.4 Comparison with the results of Blanco-Pillado and Iglesias

We wish to consider a string loop which has windings over the full S^3 . In a previous study [276], Euler variables were used to describe the S^3 as an $SU(2)$ group manifold. This foliates the three-sphere into a one-parameter set of flat tori, so that, for fixed angle θ_0 , the metric reduces to that of a flat two-torus. The strings therefore wrap only a two-dimensional sub-manifold of the full three-sphere.

We wish to generalize this result to consider windings over the full S^3 using the Hopf map.

³In the preceding section it could be argued that, accounting for the effects of warping, the original formula for $n_w(t_i)$ in unwarped space (4.5) (which was taken directly from [16]) should be modified to give $n_w(t_i) \sim \frac{\omega_l a_0(\alpha t_i)}{R}$. However, using this in conjunction with (4.6) gives $n_w(t_i) = \omega_l(t_i) = 0$ as the only possible solution. As there are good physical grounds (outlined above) for believing that the identification $\omega_l(t_i) \sim v(t_i) \sim \sqrt{1 - a_0^2}$ is valid, we therefore choose to leave the formula (4.5) unchanged, even in the presence of warped space. However, this approach does conflict with the method used in chapter 3, where we assumed that the standard formula for $n_w(t_i)$ in the random walk regime (in unwarped space, [16]) should be modified to include the effect of the warping via $n_w(t_i) \sim \frac{\sqrt{\alpha \omega_l \epsilon_l t_i}}{R} \rightarrow \frac{\sqrt{a_0 \alpha \omega_l \epsilon_l t_i}}{R}$. This is based on the substitution $r(t_i) \rightarrow a_0 r(t_i)$. We must therefore admit that, at present, it remains unclear exactly *how* to incorporate the effects of warping in the infinite dimensions into the existing dynamical models.

We therefore use the following ansatz to describe a string loop, with general, non-specific windings around the S^3 ,

$$X^M(\sigma, t) = (t, r(t) \sin(\sigma), r(t) \cos(\sigma), z_0, 0, 0, 0, \psi(\sigma, t), \theta(\sigma, t), \phi(\sigma, t)) \quad (4.16)$$

Here we have again chosen our gauge so as to identify the worldsheet time coordinate with the proper time in the Lorentz frame of the loop. In keeping with the physical scenario we are considering, we now specify the ansatz more completely, so that $\psi(\sigma, t)$, $\theta(\sigma, t)$ and $\phi(\sigma, t)$ describe *geodesic* windings. As previously stated, in Hopf coordinates the Killing vectors of the three-sphere take a particularly simple form and are parallel to the unit vectors $(1, 0, 0)$, $(0, 1, 0)$ and $(0, 0, 1)$, so that geodesic windings are described by

$$\begin{aligned} \psi(\sigma, t) &= 2n_\psi \sigma + \psi(t), \\ \theta(\sigma, t) &= n_\theta \sigma + \theta(t), \\ \phi(\sigma, t) &= n_\phi \sigma + \phi(t), \end{aligned} \quad (4.17)$$

where $n_\psi, n_\theta, n_\phi \in \mathbb{Z}$ represent the number of physical windings in each angular direction. As in canonical coordinates, the factor of two in front of the n_ψ term results from the fact that the principle range of ψ is twice that of the polar angle ϕ . Even though (technically) we have retained exactly the same ansatz used to describe *non-geodesic* windings in the previous chapter, its *meaning* in the new coordinate system is now completely different. It is a strange but convenient coincidence that the same choice of ansatz in different coordinate systems describes appropriately the different kinds of windings we expect to form in both the random walk regime ($l = 0$) and velocity correlations regime ($l > 0$).

Plugging (4.16) and (4.17) into the standard Nambu-Goto term of the F/D -string action (and ignoring the topological CS term in the case of the D -string, and other flux-dependent contributions), we then have

$$S = -T_1 \int d\sigma dt \sqrt{a_0^2(1 - \dot{r}^2)(a_0^2 r^2 + R^2 s'^2) - a_0^2 r^2 R^2 \dot{s}^2} \quad (4.18)$$

where $s = \psi + \theta + \phi$ and T_1 denotes either the F - or D -string tension, as before. In fact, we may simplify our result even further by an appropriate gauge choice with respect to the angular coordinates. Since we know that geodesics of the compact space correspond to great circles on the S^3 , we may set either of the winding numbers n_θ or n_ϕ to zero without loss of generality. The resulting string action with geodesic windings on the S^3 (in Hopf coordinates) is

$$S = -T_1 \int d\sigma dt \sqrt{a_0^2(1 - \dot{r}^2)(a_0^2 r^2 + R^2(2n_\psi + n_\phi)^2) - a_0^2 r^2 R^2(\dot{\psi} + \dot{\phi})^2}. \quad (4.19)$$

The constants of motion are again given by

$$E = \frac{dL}{dq^I} \dot{q}^I - L, \quad l = \frac{dL}{dq^I} q^I, \quad (4.20)$$

where $q^I \in \{t, \sigma, \psi, \theta, \phi\}$ (and we have now assumed that $\vec{A} = 0$, c.f. chapter 3). The first expression is the Hamiltonian and the second corresponds to the total angular momentum of the string in the compact directions, which we now expect to be non-zero.⁴ Again, using our ansatz (4.16)-(4.17) we see that these expressions become

$$\begin{aligned} E &= 2\pi T_1 \frac{a_0^2(a_0^2 r^2 + R^2(2n_\psi + n_\theta)^2)}{\sqrt{a_0^2(1 - \dot{r}^2)(a_0^2 r^2 + R^2(2n_\psi + n_\phi)^2) - a_0^2 r^2 R^2(\dot{\psi} + \dot{\phi})^2}}, \\ l &= 2\pi T_1 \frac{a_0^2 r^2 R^2(2n_\psi + n_\theta)(\dot{\psi} + \dot{\theta})}{\sqrt{a_0^2(1 - \dot{r}^2)(a_0^2 r^2 + R^2(2n_\psi + n_\phi)^2) - a_0^2 r^2 R^2(\dot{\psi} + \dot{\phi})^2}}. \end{aligned} \quad (4.21)$$

Iglesias and Blanco-Pillado [276] have shown that, for a loop which is stationary in (3+1)-dimensions (i.e. for $\dot{r} = 0$), the energy of the string configuration is minimised precisely for

$$r^2 = \frac{l}{2\pi T_1 a_0^2} \quad (4.22)$$

and

$$\dot{s}^2 = (\dot{\psi} + \dot{\theta})^2 = \frac{a_0^2}{R^2}. \quad (4.23)$$

These results are obtained by first rewriting $\dot{s}^2 = (\dot{\psi} + \dot{\theta})^2$ in terms of l , r , R and $s'^2 = (2n_\psi + n_\theta)^2$ and substituting into the expression for E (so that $E = E(r, l, R, s')$), before minimising with respect to r . This gives the first condition (4.22), and the second condition (4.23) is obtained by further substitution into the expression for l .

Any dynamical model we construct for the formation of geodesic windings *and* for the motion of the string after loop formation must be consistent with these general results. At first sight our model suggests $v^2(t_i) = \dot{s}^2(t_i)R^2 \sim (1 - a_0^2)$, which does not correspond (in general) to the energy minimisation condition $v^2 = \dot{s}^2 R^2 = a_0^2$. In fact, these two conditions only coincide for the specific value $a_0^2 = 1/2$, where the velocity in both compact and non-compact dimensions is $v \sim 1/\sqrt{2}$. We would not expect such a string configuration to undergo time evolution under the influence of its own internal dynamics, although it may

⁴Recall that, although the string “rotates” around the S^3 , no centripetal force is acting upon it. The internal (compact) dimensions are parameterised in terms of the angular variables ψ , θ and ϕ , and so the motion through the S^3 may be measured in $rad \times [t]^{-1}$. As the effective radius of “rotation” for any point along the string is simply the radius of the three-sphere, multiplication by R converts this “angular velocity” into the “true velocity” of the string. However, even here we must be careful - as the string has no internal structure, the “velocity” of the string parallel to itself (in this case parallel to the geodesic windings) is not clearly defined. It is therefore possible (in principle) to have $v(t) \sim \dot{s}(t)R > 1$ though this does *not* violate causality due to the boost invariance of the string along its length.

still shrink via the loss of mass-energy (and angular momentum) due to GW emission and this possibility is discussed in section 4.6. We conclude that if the value of the warp factor is exactly $a_0 = 1/\sqrt{2}$, the energy of the string configuration will be automatically minimised from the moment of loop formation, i.e. the initial radius of the string loop $r(t_i)$ and the initial angular momentum $l(t_i)$ will be related via $r^2 = l/2\pi T_1 a_0^2$, and the velocity of the string in the compact space will be $v \sim \sqrt{1 - a_0^2} = a_0 = 1/\sqrt{2}$ for all $t \geq t_i$.

However, when $a_0^2 > 1/2$, the string velocity in the compact space is too small to provide enough angular momentum to “match” the radius of the loop, that is, the angular momentum required for a cycloop of radius r to minimise the energy of its configuration. Alternatively, one can understand this as a string loop with fixed energy changing configuration in order to minimise the surface-to-energy ratio. Hence, from the arguments in [276], we expect that $a_0^2 > 1/2$ implies $l < 2\pi T_1 a_0^2 r^2$. Similarly, if $a_0^2 < 1/2$, this should imply that the initial angular momentum of the loop exceeds the optimum value for a loop of that size and we find the converse result, $l > 2\pi T_1 a_0^2 r^2$. In a full string theory compactification, the warp factor is exponentially small and therefore this would appear to be the dominant string channel. However, we will take a more phenomenological approach and consider the full range of values for the warping. Furthermore, as stated above, these results should hold true for any physically viable dynamical model. It is therefore worth testing the theory developed in section 4.2 to ensure consistency in this matter. In short, the arguments of Iglesias and Blanco-Pillado regarding the energy minimisation condition (for all r and l) [276], ought to be consistent with our own dynamical model of $l(t_i)$ and $r(t_i)$ outlined above.

Because we are dealing with geodesic windings, we may always redefine our coordinate system so as to identify the variable n_w from (4.5) with the variable s' , both of which represent the total number of *physical* windings in the compact space. Hence $n_w \sim 2n_\psi + n_\theta$. We now insert the expressions for $n_w(t_i)$, $v^2 = \dot{s}^2 R^2 = a_0^2$ and $r(t_i) = \alpha t_i$ into (4.21) (with $\dot{r}(t_i) = 0$) to find ⁵

$$\begin{aligned} E(t_i) &= 2\pi T_1 \frac{a_0(\alpha t_i)}{\sqrt{1 - a_0^2}}, \\ l(t_i) &= 2\pi T_1 a_0^2 (\alpha t_i)^2. \end{aligned} \tag{4.24}$$

Hence the second part of the energy minimisation condition (4.23) implies the first, and vice-versa, as expected for consistency. However, as noted above, in general we have $v^2(t_i) = \dot{s}^2(t_i)R^2 = (1 - a_0^2)$ from (4.11), which is not equal to a_0^2 unless $a_0^2 = (1 - a_0^2) = 1/2$ giving

⁵We could have substituted $n(t_i) = a_0^2(\alpha t_i)^2/R^2$ in place of the usual expression (4.5), taking advantage of the fact that $v^2 \sim a_0^2 R^2$ in this case. This leads to the expression $E(t_i) = 2\pi T_1 \times 2a_0^2(\alpha t_i)$, which is equivalent to (4.24) for $a_0^2 = (1 - a_0^2) = 1/2$. We therefore see that the total energy is split equally between the rest mass of the loop in warped Minkowski space and the kinetic energy due to motion in the S^3 .

the *constant* values:

$$\begin{aligned} E &= E(t_i) = 2\pi T_1(\alpha t_i), \\ l &= l(t_i) = \pi T_1(\alpha t_i)^2. \end{aligned} \tag{4.25}$$

Under such special circumstances we would not expect the string configuration to evolve due to its own internal dynamics, though the emission of GWs due to accelerated motion of the string and the resulting shrinkage of the loop radius r must still be accounted for, as mentioned previously.

Considering the more general case ($a_0^2 \neq 1/2$) and substituting (4.5), (4.11) and $r(t_i) = \alpha t_i$ into (4.21) (keeping $\dot{r}(t_i) = 0$) gives

$$\begin{aligned} E(t_i) &= 2\pi T_1(\alpha t_i) \\ l(t_i) &= 2\pi T_1(1 - a_0^2)(\alpha t_i)^2, \end{aligned} \tag{4.26}$$

which implies

$$\begin{aligned} l(t_i) &> 2\pi T_1 a_0^2 (\alpha t_i)^2 && (a_0^2 < 1/2), \\ l(t_i) &< 2\pi T_1 a_0^2 (\alpha t_i)^2 && (a_0^2 > 1/2). \end{aligned} \tag{4.27}$$

We find that the total energy of a cycloop with radius $r(t_i) = \alpha t_i$ is independent of a_0^2 . At first glance this seems nonsensical: the value of the warp factor determines the velocity in the compact space at the moment of loop formation via $v(t_i) \sim \dot{s}(t_i)R \sim \sqrt{1 - a_0^2}$, which in turn determines the initial number of loops via $n_w(t_i)R \sim v(t_i)r(t_i) \sim \sqrt{1 - a_0^2}(\alpha t_i)$. A cycloop moving with greater velocity in the compact space would therefore have a greater number of windings than a slower moving string with the same radius in the non-compact directions. Consequently, an increase in the kinetic energy of the loop would seem to go hand in hand with an increase in the total rest mass. However, although this is clearly true in *unwarped* space, we must remember that the presence of the warp factor *also* reduces the four-dimensional energy density via the effective tension $\tilde{T}_1 = a_0^2 T_1$. Equation (4.26) suggests that, even though a smaller warp factor implies a greater rate of winding formation and a greater kinetic energy for the windings in the compact space, the would-be increase in the total energy of the cycloop is completely off-set by the reduction in four-dimensional energy density. This is yet another example of the subtleties involved in transferring ideas and results which are intuitively obvious in flat space to highly warped backgrounds.

The question then remains: what happens if the energy minimisation conditions are not automatically satisfied at the moment of loop formation? This is equivalent to the question: What happens dynamically when either $a_0^2 < 1/2$ or $a_0^2 > 1/2$? Intuitively, we would expect that if $l(t_i) > 2\pi T_1 a_0^2 r(t_i)^2$ ($a_0^2 < 1/2$), the radius of the loop would rapidly expand,

introducing a non-zero $\dot{r}(t)$ term for $t > t_i$.⁶ Physically, this corresponds to the conversion of kinetic energy from the motion of the string in the compact space into rest-mass energy in four dimensions. The conservation of angular momentum also suggests that any fraction of $l(t_i)$ “lost” in this process is carried away by the gravitational radiation produced by the accelerating loop, though as a first approximation we may neglect this. Hence we must allow for the most general case by including the explicitly time-dependent term $\dot{r} = \dot{r}(t)$ in the expressions for E and l , whose derivative $\ddot{r}(t)$ we expect to be initially positive for an expanding loop (i.e. $\ddot{r}(t_i) > 0$). We must also reintroduce a time-dependent velocity term $v(t) = \dot{s}(t)R$ for $t > t_i$, whose derivative $\dot{v}(t)$ we expect initially to be negative in this case ($\dot{v}(t_i) = \ddot{s}(t_i)R < 0$).

Similarly, if $l(t_i) < 2\pi T_1 a_0^2 r(t_i)^2$ ($a_0^2 > 1/2$), we expect the opposite process to occur - with rest-mass energy of the loop being converted into kinetic energy in the extra dimensions. For $t > t_i$, we again introduce the extra dynamical terms $\dot{r}(t)$, whose derivative $\ddot{r}(t)$ we now expect to be initially negative ($\ddot{r}(t_i) < 0$), and $v(t) = \dot{s}(t)R$, whose derivative $\dot{v}(t)$ we now expect to be initially positive ($\dot{v}(t_i) = \ddot{s}(t_i)R > 0$). Again we face the possibility that a significant proportion of the initial angular momentum of the loop will eventually be lost through the emission of gravitational radiation during dynamical evolution.

As a first approximation, however, we will assume the loss of angular momentum via gravitational wave emission to be negligible, taking $l \approx l(t_i)$ for all $t > t_i$. We will also assume that the total energy lost via GW emission during the dynamical evolution of the loop is negligible, i.e. that $E \approx E(t_i)$ for $t > t_i$. What drives the evolution in this case is not changes in the energy of the system to “match” the conditions, but changes in the conditions to match the given energy, that is, the mutual and interdependent evolution of $r(t)$ and $\dot{s}(t)$ toward a loop configuration which meets the energy minimisation criteria (4.22)-(4.23).

The approach outlined above has the added advantage that in both cases we may assume that the number of windings remains fixed. As we shall see in the next section, the stability of the extra-dimensional windings places a lower bound on the value of l . If l remains constant, all that is required to ensure stability of the windings throughout dynamical evolution towards the minimum energy state is that the string have sufficient angular momentum to stabilise its windings *at the moment of loop creation*. In the next section we will demonstrate (following the analysis in [276]) that the stabilisation of windings places a bound on l , with more windings requiring a larger angular momentum to remain stable.⁷ Thus, if

⁶This inequality is strict since at $t = t_i$ we still have that $\dot{r}(t_i) = 0$. If this were not the case, then the energy minimisation condition (4.22) would itself be different.

⁷We will also see that angular momentum required for the stability of the string configuration is proportional to the number of windings in the loop. The angular momentum required *per winding* is therefore constant.

the value of l were to change significantly during the evolution process, the dynamics of the loop may be considerably more complicated, with windings “falling off” the S^3 as the loop expands/contracts.

4.5 Loop dynamics after formation

We now investigate the stability requirements for the extra-dimensional windings, both generically and in light of our specific dynamical model. We find that the rate of winding production in our model ensures the stability of the ansatz (4.16)-(4.17) at the moment of loop creation for all possible formation times t_i . We then leave this result and consider the loop dynamics in each of the regimes ($l(t_i) > 2\pi T_1 a_0^2 r(t_i)^2$, $a_0^2 < 1/2$ and $l(t_i) < 2\pi T_1 a_0^2 r(t_i)^2$, $a_0^2 > 1/2$) discussed above, on the assumption that the loops retain their windings during the evolution towards an energy-minimising state,⁸ which is equivalent to the assumption that $l = l(t_i)$ for all $t > t_i$.

By introducing a small perturbation in one of the bulk-space directions perpendicular to the S^3 , it is possible to show, from the resulting expansion for the ten-dimensional action, that the string configuration (4.16)-(4.17) is stable [276] (this corresponds to moving the entire string “up” from the bottom of the throat by a small amount). The ansatz (4.17) (with $n_\theta = 0$) also implicitly assumes that the motion of the string in the compact space is parallel to the direction of the windings, so it is not physically meaningful to perturb the string in either the ψ or ϕ -directions. We may, however, investigate the effect of perturbing the string in the θ -direction in order to determine the stability of the winding configuration. Turning on a small perturbation $\delta\theta$ results in the following perturbation of the Lagrangian [276]:

$$\delta L = \left(\frac{l}{2\pi T_1 a_0^2} + R^2(2n_\psi + n_\theta)^2 \right) \delta\dot{\theta}^2 - \frac{a_0^2}{R^2} \left(\frac{l}{2\pi T_1 a_0^2} - R^2(2n_\psi + n_\theta)^2 \right) \delta\theta^2 \quad (4.28)$$

which results in the stability condition

$$l > 2\pi T_1 a_0^2 R^2 (2n_\psi + n_\theta)^2. \quad (4.29)$$

In other words, the total angular momentum must satisfy this bound (note the strictness of the inequality) in order for the number of windings ($2n_\psi + n_\theta$) to remain stable. Again, identifying $n_w \sim 2n_\psi + n_\theta$ and substituting for $n_w(t_i)$ using (4.7) and $l(t_i)$ using (4.24), we may investigate the stability of the windings in our dynamical model *at the moment of loop*

⁸We will also find, in the next section, that the loop does not remain stable at the energy-minimising configuration. However, it still evolves from the initial radius *towards* such a configuration. As we will show, the loop actually “overshoots” its own energy-minimising configuration due to the non-zero velocity of the radial coordinate at that point, leading to an oscillating solution.

formation. The resulting condition reduces to

$$a_0^2 < 1, \quad (4.30)$$

which is automatically satisfied by the definition of a_0^2 in the KS geometry. Thus we see that the stability condition is satisfied and that *all* windings are stable at the time of loop formation for *all* t_i and for all physical values of a_0^2 , R^2 and α .

We now introduce non-zero time-dependent terms $\dot{r}(t)$ and $v(t) = \dot{s}(t)R$ for $t > t_i$ in (4.21), which initially satisfy

$$\begin{aligned} \ddot{r}(t_i) &> 0 & (a_0^2 < 1/2) \\ \ddot{r}(t_i) &< 0 & (a_0^2 > 1/2) \end{aligned} \quad (4.31)$$

$$\begin{aligned} \ddot{s}(t_i)R &= \dot{v}(t_i) < 0 & (a_0^2 < 1/2) \\ \ddot{s}(t_i)R &= \dot{v}(t_i) > 0 & (a_0^2 > 1/2) \end{aligned} \quad (4.32)$$

and the boundary conditions

$$\dot{s}(t_i)R = v(t_i) \sim \sqrt{1 - a_0^2}, \quad \dot{r}(t_i) = 0. \quad (4.33)$$

Henceforth we assume that the number of windings remains constant from the moment of loop formation, $n_w = n_w(t_i)$, and attempt to determine the corresponding dynamical evolution of the loop in the warped Minkowski directions. Using $l = l(t_i)$ and $E = E(t_i)$, we then have

$$\begin{aligned} l = l(t_i) &= 2\pi T_1(1 - a_0^2)(\alpha t_i)^2 \\ &= \frac{2\pi T_1 a_0^2 \sqrt{1 - a_0^2} (\alpha t_i) r^2(t) \dot{s}(t) R}{\sqrt{a_0^2(1 - \dot{r}^2(t))(a_0^2 r^2(t) + (1 - a_0^2)(\alpha t_i)^2) - a_0^2 R^2 r^2(t) \dot{s}^2(t)}} \end{aligned} \quad (4.34)$$

and

$$\begin{aligned} E = E(t_i) &= 2\pi T_1(\alpha t_i) \\ &= \frac{2\pi T_1 a_0^2 (a_0^2 r^2(t) + (1 - a_0^2)(\alpha t_i)^2)}{\sqrt{a_0^2(1 - \dot{r}^2(t))(a_0^2 r^2(t) + (1 - a_0^2)(\alpha t_i)^2) - a_0^2 R^2 r^2(t) \dot{s}^2(t)}}. \end{aligned} \quad (4.35)$$

Rearranging (4.34) gives

$$a_0^2 r^2 \dot{s}^2 R^2 = a_0^2 (1 - a_0^2) (1 - \dot{r}^2) (\alpha t_i)^2 \quad (4.36)$$

and rearranging (4.35) gives

$$a_0^2 r^2 \dot{s}^2 R^2 = \frac{a_0^2 (a_0^2 r^2(t) + (1 - a_0^2)(\alpha t_i)^2) [(1 - \dot{r}^2)(\alpha t_i)^2 - a_0^2 (a_0^2 r^2(t) + (1 - a_0^2)(\alpha t_i)^2)]}{(\alpha t_i)^2}, \quad (4.37)$$

so that equating these two expressions yields a non-linear first order differential equation in $r(t)$:⁹

$$\dot{r}^2 + \frac{a_0^4}{(\alpha t_i)^2} r^2 + (-1 + 2a_0^2(1 - a_0^2)) + (1 - a_0^2)^2 (\alpha t_i)^2 \frac{1}{r^2} = 0. \quad (4.38)$$

We note that the constant terms involving a_0^2 and the terms involving powers of r form a perfect square, so that this equation may be rewritten as

$$\dot{r}^2 - 1 + \left(\frac{a_0^2}{(\alpha t_i)} r + \frac{(1 - a_0^2)(\alpha t_i)}{r} \right)^2 = 0. \quad (4.39)$$

It is then explicitly clear that there exist two critical values of r at which $\dot{r} = 0$, i.e. at which the expansion of the loop (at least momentarily) comes to a halt. These are

$$r_{c1} = (\alpha t_i) \quad (4.40)$$

and

$$r_{c2} = \frac{(1 - a_0^2)}{a_0^2} (\alpha t_i). \quad (4.41)$$

Although it is not possible to show this directly without the explicit form of the solution $r(t)$, the first of these values must correspond to the boundary condition $\dot{r}(t_i) = 0$, which we imposed when calculating $E(t_i)$ and $l(t_i)$, as well as when determining the energy-minimisation conditions (4.22)-(4.23). However, the second of these values is intriguing as it does *not* correspond to the minimum energy condition. We can tell immediately therefore that the dynamical evolution of the loop will not lead to a steady energy-minimising state, and we may instead expect a solution which oscillates between the two values $r_{c1} = (\alpha t_i)$ (the initial radius of the loop) and $r_{c2} = \frac{(1 - a_0^2)}{a_0^2} (\alpha t_i)$.

To see if such a solution is consistent with the physical arguments above, i.e that $a_0^2 < 1/2$ leads to an *initially* expanding loop, $a_0^2 > 1/2$ to an *initially* contracting loop and $a_0^2 = 1/2$ to a static loop of radius $r(t) = (\alpha t_i)$ for all $t > t_i$, we must now ask two questions: First, which is greater, the initial radius or the second critical value? This will determine whether the loop initially expands or contracts; Second, which is greater, the second critical value or the radius corresponding to the energy-minimisation condition? This will determine

⁹Alternatively we may substitute either of the expressions (4.37) or (4.36) into the original string action (4.19) and then determine the Euler-Lagrange equations. The resulting equations must necessarily have the same solution as (4.38) but the method adopted here, which utilises the string constants of motion, is far simpler.

whether the behaviour of the loop is in accordance with our assumptions.

Whether $r_{c1} = r(t_i) < (>)r_{c2}$ depends on whether $(1 - a_0^2)/a_0^2 > (<)1$, or equivalently whether $a_0^2 < (>)1/2$, with $a_0^2 < 1/2$ implying that the loop must *expand* from its initial value $r(t_i) = (\alpha t_i)$ to $r = \frac{(1-a_0^2)}{a_0^2}(\alpha t_i) > (\alpha t_i)$ and $a_0^2 > 1/2$ implying that the loop must *contract* from its initial value $r(t_i) = (\alpha t_i)$ to $r = \frac{(1-a_0^2)}{a_0^2}(\alpha t_i) < (\alpha t_i)$.

The second question may be answered as follows: By equating our expression for $l(t_i)$ (4.26) with the second part of the energy-minimisation conditions (4.23), the critical radius corresponding to the fulfillment of this condition on r_{min} may be written in terms of a_0^2 and the initial radius $r(t_i) = (\alpha t_i)$, as

$$r_{min} = \frac{\sqrt{1 - a_0^2}}{a_0}(\alpha t_i). \quad (4.42)$$

Whether $r_{c2} < (>)r_{min}$ then depends on whether $(1 - a_0^2)/a_0^2 < (>)\frac{\sqrt{1-a_0^2}}{a_0}$, which is also equivalent to the condition $a_0^2 > (<)1/2$.

Therefore, $a_0^2 < 1/2$ implies that the loop *expands* from its initial value $r(t_i) = (\alpha t_i)$ towards the radius corresponding to the energy-minimising configuration $r_{min} = \frac{\sqrt{1-a_0^2}}{a_0}(\alpha t_i) > r(t_i)$ but overshoots it and continues expanding to the second critical value $r_{c2} = \frac{(1-a_0^2)}{a_0^2}(\alpha t_i) > r_{min}$. Similarly, $a_0^2 > 1/2$ implies that the loop *contracts* from its initial value $r(t_i) = (\alpha t_i)$ towards the radius corresponding to the energy-minimising configuration $r_{min} = \frac{\sqrt{1-a_0^2}}{a_0}(\alpha t_i) < r(t_i)$ but overshoots it and continues contracting to the second critical value $r_{c2} = \frac{(1-a_0^2)}{a_0^2}(\alpha t_i) < r_{min}$. In both cases, we expect the loop to oscillate back and forth between $r_{c1} = r(t_i)$ and r_{c2} but our findings are consistent with the assumptions about the initial behaviour of the loop expressed in the boundary conditions (4.31)-(4.33). For $a_0^2 = 1/2$, $r(t_i) = r_{c2} = r_{min} = (\alpha t_i)$ and the loop remains static in four dimensions.

Interestingly, there is also another way to interpret both the fixed point and oscillatory solutions in terms of the distance between neighbouring windings, $d \sim a_0 r/n_w$. At the first critical radius (corresponding to $t = t_i$) we have

$$d_{c1} = \frac{a_0}{\sqrt{1 - a_0^2}}R, \quad (4.43)$$

whereas at the second critical radius

$$d_{c2} = \frac{\sqrt{1 - a_0^2}}{a_0}R. \quad (4.44)$$

For $a_0^2 > 1/2$ we have $d_{c1} > d_{c2}$, whereas for $a_0^2 < 1/2$ we have $d_{c1} < d_{c2}$ (as expected), and the fixed point solution $a_0^2 = 1/2$ corresponds to $d_{c1} = d_{c2} = R$. The stability of the string configuration therefore appears to depend on the ratio of the inter-winding distance to the radius of the compact space, with $d/R = 1$ giving rise to an equilibrium position, where the string tension exactly balances the effects of the angular momentum.

The parameter $\omega_l \sim \frac{n_w R}{\sqrt{a_0^2 r^2 + n_w^2 R^2}} \sim \frac{R}{d} \left(1 + \frac{R^2}{d^2}\right)^{-\frac{1}{2}}$ also undergoes dynamical evolution between the two critical values

$$\omega_{l(c1)} \sim \sqrt{1 - a_0^2} \tag{4.45}$$

and

$$\omega_{l(c2)} \sim a_0 \sim \sqrt{1 - \omega_{l(c1)}^2}. \tag{4.46}$$

Here $a_0^2 > 1/2$ implies $\omega_{l(c1)} < \omega_{l(c2)}$, $a_0^2 < 1/2$ implies $\omega_{l(c1)} > \omega_{l(c2)}$ and $a_0^2 = 1/2$ implies $\omega_{l(c1)} = \omega_{l(c2)} = 1/\sqrt{2}$.

It is interesting to speculate that, from a four-dimensional perspective, the value of ω_l is somehow related to a measure of *torsion*. If this is so, the successive phases of loop expansion and contraction may be viewed as the string “winding” and “unwinding” (or “twisting” and “untwisting”) in the process of evolving between equivalent (i.e. degenerate) energy states. Intuitively, this would seem to be the analogue of the motion of a loop of elastic band, with an intrinsic tension and an initial number of “twists” along its length: The tension of the band acts to contract the loop radius, whereas the torsion resulting from the presence of the twists acts to make the loop expand. Whether the loop expands or contracts (initially) then depends on which of these forces dominates the dynamics.¹⁰

Having now determined the general behaviour of our solution in each of the three cases $a_0^2 < 1/2$, $a_0^2 = 1/2$ and $a_0^2 > 1/2$, we now find the explicit form of $r(t)$. By making the substitution $y = r^2$, (4.38) may be rearranged to give

$$dt = \pm \frac{1}{2} \frac{dy}{\sqrt{-ay^2 + by - c}} \tag{4.47}$$

¹⁰The suggestion that ω_l is related to a measure of torsion is also supported by the dual defect-string model proposed in chapter 5. Under the proposed duality, ω_l is related to the topological winding number via $|n| \sim 1/\sqrt{1 - \omega_l^2}$, so that a change in the fractional string length contained in the extra-dimensional windings - either over a region of space or through evolution in time (or both) - corresponds also to a change in vorticity (or “winding”/“twisting”) from a field-theoretic perspective. This appears to be a natural definition of torsion in such models.

where we have defined the coefficients a, b and c to be explicitly positive for a_0^2 in the range $0 < a_0^2 < 1$:

$$\begin{aligned} a &= \frac{a_0^4}{(\alpha t_i)^2}, \\ b &= 1 - 2a_0^2(1 - a_0^2), \\ c &= (1 - a_0^2)^2(\alpha t_i)^2. \end{aligned} \quad (4.48)$$

The discriminant of the quadratic,

$$\Delta = b^2 - 4ac = 1 - 4a_0^2(1 - a_0^2) = (1 - 2a_0^2)^2, \quad (4.49)$$

is positive for all $0 < a_0^2 < 1$, except at $a_0^2 = 1/2$, where $\Delta = 0$. Integrating (4.47) yields the following explicit expression for t in terms of y , where K is the usual integration constant and A, B are the *real* roots of the equation $-ay^2 + by - c = 0$:¹¹

$$t = \mp \frac{1}{\sqrt{a}} \tan^{-1} \left(\pm \sqrt{\frac{B - y}{y - A}} \right) \mp K, \quad (4.50)$$

which may be rearranged to give

$$y(t) = \frac{B + A \tan^2(\sqrt{a}(t + K))}{1 + \tan^2(\sqrt{a}(t + K))}. \quad (4.51)$$

The roots of the quadratic $-ay^2 + by - c = 0$ are

$$\begin{aligned} y &= (\alpha t_i)^2 \\ y &= \frac{(1 - a_0^2)^2}{a_0^4} (\alpha t_i)^2 \end{aligned} \quad (4.52)$$

but choosing $A = (\alpha t_i)^2$ and $B = \frac{(1 - a_0^2)^2}{a_0^4} (\alpha t_i)^2$ does not allow us to fix K in order to satisfy the boundary conditions. We must therefore choose $B = (\alpha t_i)^2$ and $A = \frac{(1 - a_0^2)^2}{a_0^4} (\alpha t_i)^2$ in (4.51) before setting $y(t_i) = (\alpha t_i)^2$ to determine

$$K = -t_i. \quad (4.53)$$

Our final solution for $r(t)$ is given by taking $r = +\sqrt{y}$

$$r(t) = \sqrt{\frac{(\alpha t_i)^2 + \frac{(1 - a_0^2)^2}{a_0^4} (\alpha t_i)^2 \tan^2 \left(\frac{a_0^2}{(\alpha t_i)} (t - t_i) \right)}{1 + \tan^2 \left(\frac{a_0^2}{(\alpha t_i)} (t - t_i) \right)}}, \quad (4.54)$$

¹¹This solution was obtained by performing a Eulerian transformation of the third kind. A brief sketch of this method is given in Appendix A.

which may be rewritten in terms of basic trigonometric functions:

$$r(t) = (\alpha t_i) \sqrt{1 + \left(\frac{1 - 2a_0^2}{a_0^4} \right) \sin^2 \left(\frac{a_0^2}{(\alpha t_i)} (t - t_i) \right)}. \quad (4.55)$$

It is clear that for $a_0^2 \neq 1/2$, the solution (4.54)/(4.55) oscillates between $r(t_i) = (\alpha t_i)$ at $t = n\pi \frac{(\alpha t_i)}{a_0^2}$ for $n \in \mathbb{Z}^+$ and $r_{c2} = \frac{(1-a_0^2)}{a_0^2}(\alpha t_i)$ at $t = (2m+1)\frac{\pi}{2} \frac{(\alpha t_i)}{a_0^2}$, $m \in \mathbb{Z}^+$. For $a_0^2 = 1/2$ we have $A = B$ ($\Delta = 0$) and $r(t) = (\alpha t_i)$ for all $t > t_i$, as expected. It is tedious but straightforward to twice differentiate (4.54) in order to verify the boundary conditions (4.31). We obtain

$$\begin{aligned} \dot{r}(t) &= \frac{(1 - 2a_0^2)}{a_0^2} \sin(x) \cos(x) \left\{ 1 + \left(\frac{1 - 2a_0^2}{a_0^4} \right) \sin^2(x) \right\}^{-\frac{1}{2}}, \\ \ddot{r}(t) &= \frac{(1 - 2a_0^2)}{(\alpha t_i)} \left\{ 1 + \left(\frac{1 - 2a_0^2}{a_0^4} \right) \sin^2(x) \right\}^{-\frac{1}{2}} \\ &\quad \times \left[\cos^2(x) - \sin^2(x) - \left(\frac{1 - 2a_0^2}{a_0^4} \right) \sin^2(x) \cos^2(x) \left\{ 1 + \left(\frac{1 - 2a_0^2}{a_0^4} \right) \sin^2(x) \right\}^{-\frac{3}{2}} \right], \end{aligned} \quad (4.56)$$

where we have defined $x \equiv \frac{a_0^2}{(\alpha t_i)}(t - t_i)$, from which it can be seen that $\dot{r}(t_i) = 0$ and $\ddot{r}(t_i) = \frac{(1-2a_0^2)}{(\alpha t_i)}$, and hence $\ddot{r}(t_i) > 0$ for $a_0^2 < 1/2$ and $\ddot{r}(t_i) < 0$ for $a_0^2 > 1/2$, in accordance with the boundary conditions (4.31).

Figure 4.1 illustrates the qualitatively different behaviour of the solution (4.55) for different values of a_0^2 . The three curves show the three different types of dynamical evolution that a loop (formed with initial radius $r(t_i) = \alpha t_i$) may undergo in the $a_0^2 < 1/2$, $a_0^2 = 1/2$ and $a_0^2 > 1/2$ cases. We plot the behaviour of $v(t) \sim \dot{s}(t)R$ for the same test values of a_0^2 , α and t_i in figure 4.2. The full expression for $v(t)$ may be obtained by taking either (4.36) or (4.37) and substituting for $r(t)$ from (4.55) and $\dot{r}(t)$ from (4.56), though we omit it here for the sake of brevity. As expected, the behaviour of $\dot{v}(t)$ satisfies the boundary conditions (4.32). Even though, for any given model, the values of a_0^2 and α are constant, string loops are continuously formed throughout the history of the universe, meaning that t_i will be a free parameter. In each of the oscillating regimes we would therefore expect to see a *spectrum* of oscillation periods, with smaller loops formed at earlier epochs oscillating more rapidly between their initial and maximum radii than larger loops formed at late times. This is illustrated for the $a_0^2 < 1/2$ regime in figure 4.3. The corresponding behaviour of $v(t) \sim \dot{s}(t)R$ is shown in figure 4.4, using the same values for the parameters.

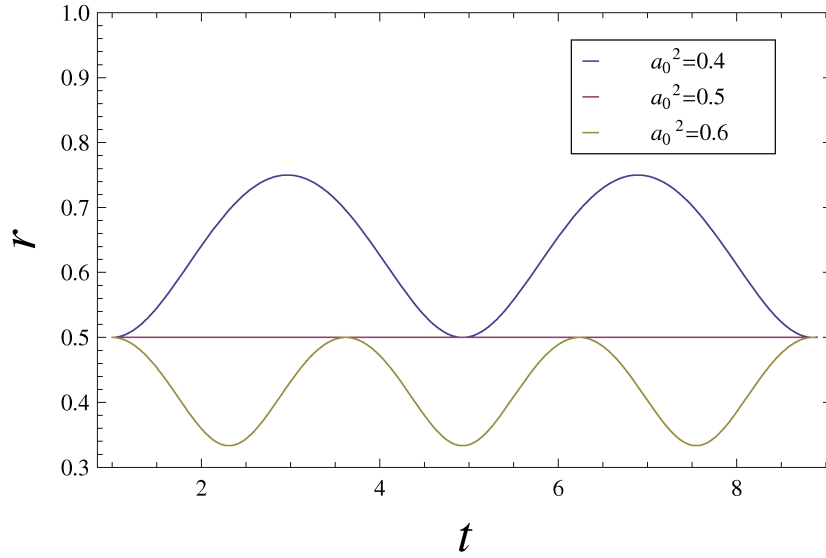


Figure 4.1: This figure illustrates the behaviour of the solution (4.55) in the three qualitatively different regimes. For convenience, we have chosen $t_i = 1$, $\alpha = 0.5$ for all three curves and set $a_0^2 = 0.4, 0.5$ and 0.6 .

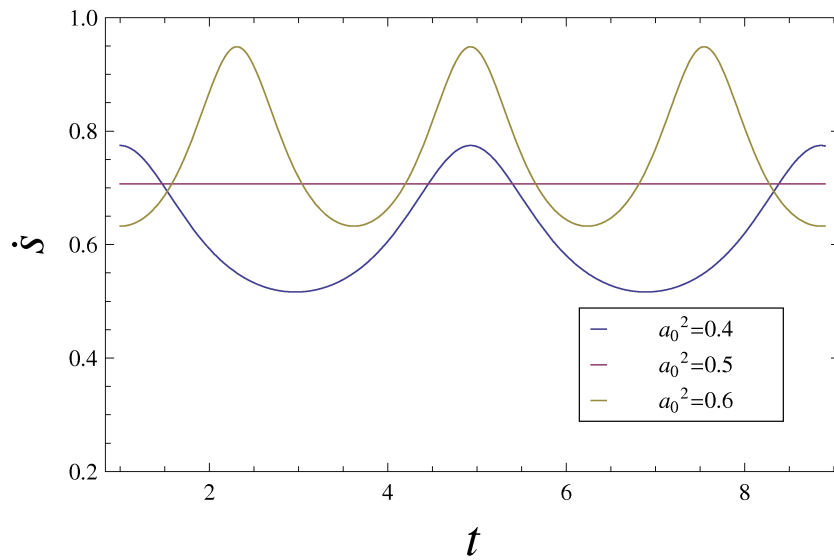


Figure 4.2: This figure illustrates the behaviour of $v(t) \sim \dot{s}(t)R$ in the three qualitatively different regimes. Again we have chosen $t_i = 1$, $\alpha = 0.5$ for all three curves and the values $a_0^2 = 0.4, 0.5$ and 0.6 .

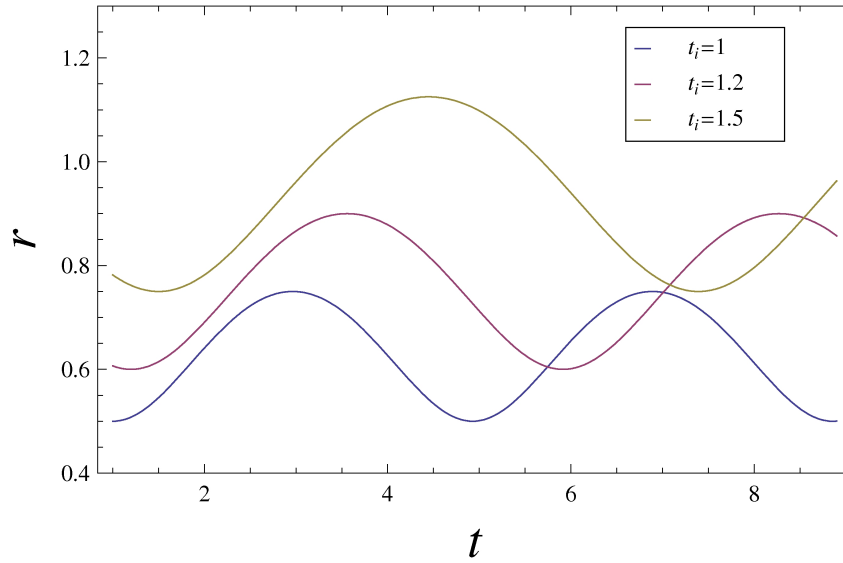


Figure 4.3: This figure illustrates the behaviour of $r(t)$ for loops formed at three different epochs in the $a_0^2 < 1/2$ regime. For the sake of convenience we have fixed $a_0^2 = 0.4$ and $\alpha = 0.5$ for all three curves and set $t_i = 1$, $t_i = 1.2$, and $t_i = 1.5$.

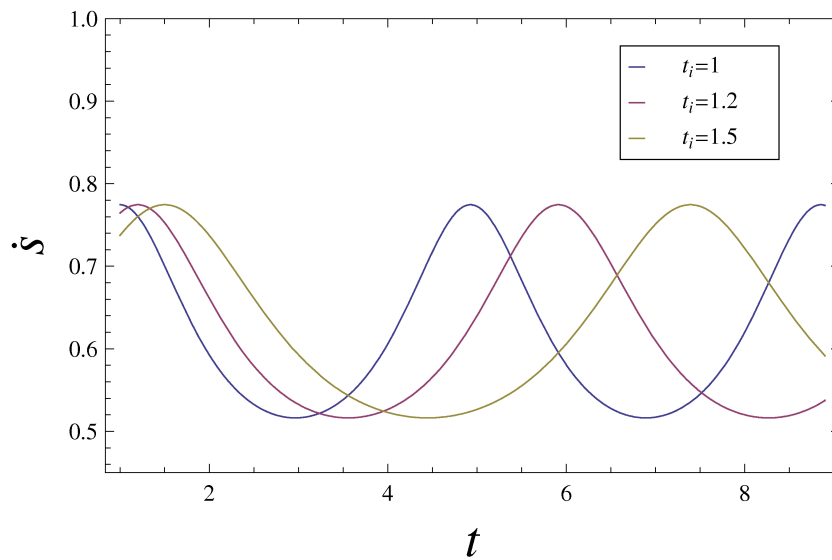


Figure 4.4: This figure illustrates the behaviour of $v(t) \sim \dot{s}(t)R$ for loops formed at three different epochs in the $a_0^2 < 1/2$ regime. As in figure 4.3 we choose to set $a_0^2 = 0.4$ and $\alpha = 0.5$ for all three curves and consider $t_i = 1$, $t_i = 1.2$, and $t_i = 1.5$.

4.6 Discussion

In this chapter we have argued that a velocity correlations regime in the post-inflationary epoch leads naturally to the formation of string loops with geodesic windings in the compact space. For strings at the tip of the conifold throat of the KS geometry, we were able to show that the quantities which determine the dynamical evolution of a circular loop (i.e. the initial winding number $n_w(t_i)$, energy $E(t_i)$ and string velocity/angular momentum in the compact space, $\dot{s}(t_i)/l(t_i)$), are *uniquely* determined by the parameters a_0^2 , R , α and t_i . Crucially, these windings were found to have sufficient angular momentum in the compact directions to remain stable after the string chops off from the network to form a loop.

The interaction between the tension and the angular momentum in the compact space was found to play a significant role in the dynamical evolution of the string, including, perhaps surprisingly, the evolution in four dimensions. By assuming energy and angular momentum loss via gravitational radiation to be negligible, we determined EOM for the four-dimensional radius $r(t)$ and the string velocity $v(t) \sim \dot{s}(t)R$, which we believe to be valid over small time scales after loop formation.

We found that the qualitative behaviour of the string depends crucially on the square of the warp factor, $0 < a_0^2 < 1$, with $a_0^2 < 1/2$ leading to an oscillatory solution characterised by an initial expansion phase and $a_0^2 > 1/2$ to oscillations with an initial contracting phase. In each case the string was seen to oscillate between its initial radius $r(t_i) = (\alpha t_i)$ and a secondary critical value defined by $r_{c2} = \frac{(1-a_0^2)}{a_0^2}(\alpha t_i)$, with period of oscillation $T = \frac{(\alpha t_i)}{a_0^2}$.

In the two oscillatory regimes, it is the interaction of the angular momentum with the string tension which “drives” the dynamical evolution, converting kinetic energy into rest mass during expansion (with the inverse process occurring in the contracting phase). The string is seen to evolve *towards* a static minimum energy configuration where $l = 2\pi a_0^2 T_1$ and $\dot{s}^2 = a_0^2/R^2$, but is unable to satisfy these two conditions simultaneously at a point where $\dot{r}(t) = 0$. By contrast, in the $a_0^2 = 1/2$ case we find that the energy-minimising conditions *are* satisfied simultaneously at the moment of loop formation. In this case the tension exactly offsets the effect of the angular momentum, so the string remains static at its original radius $r(t_i) = (\alpha t_i)$.

The meaning of the term “small” above is somewhat ambiguous, but it seems reasonable to assume that our solution will provide a valid approximation over at least one full oscillatory cycle of the loop, that is, over a period $\Delta t \sim T = \frac{(\alpha t_i)}{a_0^2}$. For periods $\Delta t \gg T$ our analysis must be extended to include the effects of GW emission on $E(t)$ and $l(t)$ (or equivalently on $r(t)$ and $\dot{s}(t)$). We may expect the qualitative effect of energy and angular momentum loss to be relatively simple, as long as the string retains sufficient angular momentum for the

extra-dimensional windings to remain stable. In this case, it is likely that the loss of E and l due to GW emission will act to damp the oscillations of $r(t)$ and $\dot{s}(t)$. What is unclear, however, is whether the damping coefficient itself will be time-dependent. For example, it is possible that smaller oscillations lead to greater rates of emission per unit length (as the rate of acceleration $\ddot{r}(t)$ is higher in this case), so that the damping itself increases with time (for an individual loop).

In the case that the windings eventually become unstable (as $l(t)$ drops below the threshold for ensuring their stability), the string dynamics are likely to become complicated and it is not clear whether the process of winding contraction (i.e. of windings “falling off” the S^3) may even be accommodated within an analysis which uses an ansatz of the form (4.16) to describe the string configuration. This is because the coordinates $r(t) \sin \sigma$, $r(t) \cos \sigma$, $\psi(\sigma, t)$, $\theta(\sigma, t)$ and $\phi(\sigma, t)$ are treated as *independent* variables with respect to the the EOM. We are therefore unable to take account of the continuously connected nature of the string when string sections “move” from one direction to another (e.g. in “falling off” the S^3 to form part of the four-dimensional rest mass).

The present analysis could still be improved by accounting for the effects of GW emission under the assumption that that loops retain their windings, which would indeed be valid up to the point where $l(t)$ drops below the critical value (which may also be calculated). Such an improved analysis could proceed as follows: one could compute the stress-energy tensor for an oscillating loop and look for solutions with this as a source to the Einstein equations. This should allow us to estimate the rate of loss of E and l via GW emission and, as stated, we expect this to produce a damping term in the equations for $r(t)$ and $\dot{s}(t)$.

Calculating the emission spectrum for an oscillating loop would also be of immense practical interest. The GW signature of such a loop, whose self-oscillation is caused by the presence of angular momentum in the compact space, may differ significantly from that of a string whose oscillations, though superficially similar, do not result from self-interaction. GW emission from loops oscillating with period $\omega \sim L^{-1}$ (where L is the loop size) have been studied in four dimensions [289]-[292]. However, in such cases the loop is not undergoing *genuine* phases of expansion and contraction, but rather experiencing “wiggles” of a size comparable to its own length. Although Weinberg [293] has shown that (in an FRW universe) the power of a weak, isolated, periodic source (to lowest order in G) may be given by a single formula *regardless* of the exact nature of the source, it is not immediately clear that this should hold in extra-dimensional scenarios.

Additionally, such sources (i.e. loops) have no angular momentum to shed in the process of emission. In fact, even if we were to study loops whose self-oscillation was due to their “rotational” motion in Minkowski space (see [114, 294]), we would expect the angular

momentum carried away by gravitational radiation to be very different from that lost via emission from oscillating cycloops.¹² In particular, we expect the gravitons emitted from oscillating cycloops to carry momentum in the *compact* directions. This implies that their associated wavelengths must be quantized in terms of integer multiples of the length-scale of the compact space. It is this crucial fact that would allow us to distinguish between “extra-dimensional” and “four-dimensional” GW spectra and may enable us to extract information about compact dimensions in future observations: for example, using data from the forthcoming LISA [295]-[299] or existing LIGO experiments [300]-[301].

However, a note of caution must be added. We have shown that the interaction between the string tension and the angular momentum term which causes the string to oscillate mediates the interconversion of potential and kinetic energy. In addition, as noted previously, the “angular momentum” in the compact space is not “true” angular momentum, in the sense that it is not associated with a centripetal force. It is *linear* momentum defined on a space with periodic boundary conditions. It is therefore possible to imagine that, during the period of loop oscillation, the momentum in the compact space is converted - via the action of the string tension - into momentum in the Minkowski directions, and vice-versa. Although we would expect gravitons emitted at an arbitrary point in the cycle to carry some combination of “extra-dimensional” and ordinary momentum, it is at present unclear how the former could be measured experimentally.¹³

Although the full string theory compactification favours exponentially small values of a_0^2 , there is also the possibility of obtaining evidence from the GW signature of wound strings exists even in the case of static loops (i.e. the $a_0^2 = 1/2$ case). These loops, which form automatically with a configuration which meets the energy minimising-conditions, look just like ordinary string loops from a four-dimensional perspective. However, they contain an “unseen” angular momentum which is not directly manifested in their dynamical evolution in Minkowski space. As stated above, we expect that even ordinary four-dimensional string loops may undergo periodic oscillations with $\omega \sim L^{-1}$, creating ripples in spacetime and giving rise to GWs. Such fluctuations *along* the length of the string - though not in the total four dimensional length itself - would likely still occur in this case (though it is possible that the existence of the angular momentum term may lend a certain “rigidity” to the circular string configuration, making it more resistant to deformation) but the string must also now

¹²One possible further extension of the current analysis would be to consider a wound string with rotational motion in both the compact *and* Minkowski directions.

¹³See [302]-[306] for articles on the detection of general periodic sources using LIGO. Reference [307] also gives an overview of how GW signatures from the inflationary stage of string cosmology scenarios may be detected using the same experiment (though periodic sources are not considered). More general material on sources and spectra of GWs in string cosmology scenarios are given in [308]-[315], while [316] deals specifically with expected dilation contributions. Much of this material is also presented in Gasperini [317]. The review by Cline [318] specifically covers GW emission from strings in warped throat models as well as providing an excellent introduction to many areas of string cosmology.

shed its angular momentum. The GW signature of even a non-self-oscillating loop in the extra-dimensional scenario is therefore also likely to differ significantly from the standard case of an unwound string, though perhaps to a lesser degree than in the self-oscillating case. Nonetheless, the possibility of the indirect detection of compact dimensions from cosmic strings remains, even in the absence of self-oscillating loops.

Finally, we conclude this discussion by outlining some of the possible limitations of the above analysis. We have assumed throughout the present work that the velocity correlations regime leads naturally to (a) geodesic windings and (b) movement of the string parallel to itself (i.e. along the geodesics). However, *both* these assumptions may be questioned. The rationale for adopting such an approach (which simplified the resulting analysis considerably) was that velocity correlations should impart a constant angular momentum density to each point along the string. Therefore we expect each “point” (or infinitesimal string segment) to travel along a geodesic curve, both before and after loop formation. However, it has not been proven that each point along the string traversing a separate geodesic leads to a winding configuration that is itself geodesic. Likewise, it does not necessarily follow that the resulting motion of the string as a whole is parallel to itself. In general, we may expect that the geometry of the internal space plays a role in determining the exact nature of the winding configuration and the resulting string motion. Moreover, we have not included the contribution from the Ramond-Ramond (R - R) sector which, in principle, will couple to the string. This charge term may also be ultimately crucial for distinguishing between cosmic strings and cosmic superstrings.

While, in principle, motion of the string perpendicular to its length may easily be accounted for (see end of Appendix B), the most significant problem in the analysis of string loops with non-geodesic windings arises from the resulting σ -dependence of the integrands in the expressions for E and l . The present analysis may therefore be improved by a more thorough investigation of the winding process itself and, though we expect our expressions for $n_w(t_i)$ and $v(t_i) \sim \dot{s}(t_i)R$ to remain valid in the KS case, the appropriate string ansatz may well be more complicated. Although it seems unlikely that the qualitative behaviour of the string will differ significantly from that described in the scenarios above, finding analogous (and *quantitatively* different) results may be extremely difficult. But, ultimately, exact quantitative predictions will be needed for any comparison with future experimental data and such a project would be extremely worthwhile.

CHAPTER 5

PINCHED STRINGS IN A MODIFIED ABELIAN-HIGGS MODEL

5.1 Introduction

Having investigated the possibility of dynamically stabilised windings in the internal space, we now return to our discussion of quasi-stable static configurations. In chapter 3 it was shown that such windings may remain stable (or quasi-stable) only by adopting a step-like winding configuration, leading to the production of “cosmic necklaces”. This is due to the existence of a “lifting potential” in the internal space, which arises from the geometric embedding of the the worldsheet.

From a four-dimensional perspective the windings appear as a series of monopoles or “beads” connected by ordinary sections of string. Superficially these resemble the standard string-monopole networks found in field-theoretic models [114] but their behaviour is in many ways fundamentally different. In contrast to previous predictions based on field theory defects, it is found that the gravitational collapse of necklaces formed in the class of backgrounds defined by the KS geometry [5] leads to the formation of PBHs during a window in the early universe, followed by the formation of *potential* DM relics in the scaling regime [1]. This is almost the complete reverse of the standard predictions for string-monopole networks [263].

The root cause of this difference appears to be the existence of a time-dependent bead mass in the necklace model, as opposed to the constant bead mass of true monopoles connected by strings. This arises from the time-dependence of the lifting potential and is a somewhat unexpected result. Initial investigations of string necklaces assumed the existence of a constant potential and hence a constant bead mass, though these were based solely on generic arguments [6]-[9]. The summary in chapter 3, based on the work presented in [1], represents the first explicit realisation of necklace formation in string theory, in which it was shown that these assumptions must be modified, at least for the class of backgrounds considered.

As mentioned previously, this raises two interesting possibilities: Either the formation of necklace-like objects is possible only in string theory, or there exist previously unknown solutions in dual gauge theory models which are equivalent to the objects described by strings

with step-like windings.

At present there is no *known* field theory analogue of necklaces formed from extra-dimensional windings. In particular, there is no known way to produce string-monopole networks with time-varying bead masses. The question as to whether a dual field theory model exists is therefore important because, if the formation of necklace-type objects *is* a string-specific (or specifically extra-dimensional) effect, then their predicted effects on observable cosmological parameters could be used to obtain experimental evidence in favour of string theory (or at least in favour of higher-dimensional models).

The aim of this chapter is to investigate the possibility of such a dual configuration. A crude way to understand this would be to say that we seek to establish a relation between the topological winding number n of a defect string (in four space-time dimensions) and the physical winding number, n_w , of an F/D -string (or (p, q) bound state) in an extra-dimensional scenario. We also seek to establish a field-theoretic model in which “bead” formation occurs dynamically as the configuration “relaxes” to an energy-minimising state in which mass density becomes highly localised in spatially separated regions along the string.

For simplicity, we take the simplest of all field-theoretic models of string formation - the Abelian-Higgs model - as our starting point. As we shall see, it is possible to propose a relatively natural model for such a “pinched” string (based on a generalisation of the well known Nielsen-Olesen vortex [15]) after introducing an appropriate modification of the usual Abelian-Higgs action to include coordinate-dependent couplings in both the scalar and vector fields (i.e. $\sqrt{\lambda}^{eff}(z)$ and $e^{eff}(z)$ in our gauge choice). This then appears to mimic the behaviour of the wound-string necklaces discussed in chapter 3.

We propose the pinched string solution as a dual necklace model and argue that a time-dependent bead mass may be obtained, though this possibility is not rigorously analysed here and uncertainties remain which must be addressed in future publications. The main basis for the proposed correspondence is an analysis of the four-dimensional effective tension of the wound strings, together with the periodically varying tension of the pinched string, which may be made to take the same form for appropriate ansatz choices. Following the correspondence between string theory and field theory parameters suggested by this comparison, an argument is then put forward for a geometric interpretation of the field-theoretic terms, such as gauge flux and topological winding number, in the string picture. Furthermore, we find that, although the introduction of z -dependence in the original field couplings may seem somewhat strange and even “unnatural”, it has a very natural interpretation in the dual string picture due to the relation between the three-sphere radius R and the string coupling g_s ($R^2 \sim b_0 M g_s \alpha'$).

As the interchange between vortices and anti-vortices in the field-theoretic model necessarily involves the consideration of sub-Planck scales, we present a hypothetical model for discretising the Planck-scale structure of the vortex. Though such discretisation is necessary to prevent the emergence of divergences in the Euler-Lagrange equations, it is not intended as a literal, but only as an effective model. Whatever the exact nature of the physical limit imposed by the Planck scale it is likely that it determines some sort of limit on the process of *measurement*¹ rather than implying the outright discretisation of spacetime or of fields on a spacetime background. We adopt this method only as an *approximation* to an (as yet) unknown theory of the quantum structure of fields on the smallest scales and present an argument for its validity (as an effective/approximate model) based on matching solutions at the boundary of Planck-sized regions to well known solutions valid on scales Δr , $\Delta z \geq l_p$. However, we find that the localisation of the (classical) field-theoretic string core on scales $r \geq \mathcal{O}(l_p)$ admits a very natural interpretation in terms of the quantum constraints on the dual wound F/D -strings.

The structure of this chapter is as follows: In section 5.2 we present a brief overview of the Abelian-Higgs model, including the general (covariant) form of the Euler-Lagrange equations. We then determine their specific form for a cylindrically symmetric ansatz. However, the covariant equations we obtain differ from those given in the standard literature (c.f. [15, 114, 124]), which we believe to be a consequence of confusion regarding the appropriate metric terms to include in the action. One consequence of this is that the gauge field ansatz we must adopt in order to obtain consistency differs from that found in the usual references, though the net effect is to obtain equations very similar to the standard EOM quoted for the functions which characterise the scalar/vector field solutions, $f(r)$ and $\alpha(r)$. We take this opportunity to review the current literature, including the covariant form of

¹The general uncertainty principle for any two quantum mechanical operators acting on a system described by the wavevector $\vec{\psi}$ (i.e. corresponding to physical observations made on that system), \hat{O}_1 and \hat{O}_2 , is $\Delta_\psi O_1 \Delta_\psi O_2 \geq \frac{1}{2} |\langle \vec{\psi}, [\hat{O}_1, \hat{O}_2] \vec{\psi} \rangle|$, where the notation $\langle \vec{A}, \vec{B} \rangle$ represents the overlap between the vectors \vec{A} and \vec{B} [319]. As the commutator may be written in the general form $[\hat{O}_1, \hat{O}_2] = i\hbar + \hat{O}_3$, this may then be rewritten as $\Delta_\psi O_1 \Delta_\psi O_2 \geq \hbar/2 + |\langle \vec{\psi}, \hat{O}_3 \vec{\psi} \rangle|$, i.e. $\Delta_\psi O_1 \Delta_\psi O_2 \sim \hbar/2 + f(\vec{\psi})$ where $f(\vec{\psi})$ is the wavefunction-dependent part. However, setting $\hat{O}_1 = \hat{x}$ and $\hat{O}_2 = \hat{p}$ (so that $[\hat{O}_1, \hat{O}_2] = [\hat{x}, \hat{p}] = i\hbar$) and $\Delta_\psi O_1 = \Delta_\psi x = l_p$, $\Delta_\psi O_2 = \Delta_\psi p = m_p/c$ gives $\Delta_\psi x \Delta_\psi p = \hbar/2$, *regardless* of the state vector $\vec{\psi}$. This implies that, regardless of the system in question, it is meaningless to *simultaneously* probe length/energy scales smaller than the Planck length/Planck energy. In addition, we note that a Planck-mass object has a gravitational radius of order $R_S \sim \mathcal{O}(l_p)$, so that a critical energy-density for any physical system *not* sheathed within an event horizon is $\rho_c \sim m_p/l_p \sim 1$. Combining these two results then suggests that it is impossible to define the wavefunction of a quantum mechanical system (other than a black hole) on a length scale less than $\sim l_p$. Furthermore, in the condensed matter (superconductor) analogue of the Abelian-Higgs model, the specific analogue of the phase θ (which acts as an order parameter in the theory of symmetry-breaking) is the so-called Bogolubov wave-function (see [114]). As we expect *all* order parameters to have characteristic physical scales, below which they cannot be consistently defined, we infer that the correct “cut-off” below which the phase in the Abelian-Higgs model (and hence the vorticity/winding number $|n|$ of an Abelian-Higgs vortex) becomes undefined, is $\sim l_p$.

the Euler-Lagrange equations, the usual scalar and gauge field ansatzes, the resulting specific form of the EOM and their asymptotic and small r solutions in the both the uncoupled and coupled regimes (following [320] for the latter). Despite subtle differences, our results largely agree with those quoted in the literature, though we believe the approach outlined here contains a greater degree of mathematical rigour. For completeness, and in order to allow easy comparison with later calculations of the z -dependent tension of the “pinched” string $\mu_{|n|}(z)$, explicit calculations of the constant string tension $\mu_{|n|}$ for the cylindrically symmetric ansatz are given in section 5.3.

In section 5.4 we introduce a non-cylindrically-symmetric ansatz for the scalar and gauge field contributions, based on a specific discretisation scheme in the Planck-scale region of the vortex core (in which vorticity itself may no longer be defined) and introducing the z -dependent couplings $\sqrt{\lambda}^{eff}(z)$ and $e^{eff}(z)$. From this, we derive the specific form of the Euler-Lagrange equations in the non-cylindrically-symmetric case in order to verify that the pinched string configuration is a valid solution of the EOM. For certain physically reasonable assumptions these are found to reduce to simplified forms which, for a given value of z , are structurally equivalent to the EOM for the cylindrically symmetric case obtained in section 5.2. This allows analogous large and small r solutions for the scalar and gauge fields but the behaviour of these fields is now, in general, z -dependent. These results are given in sections 5.5 and 5.6 and the resulting z -dependent tension of the string is calculated in section 5.7. We show that this new z -dependent tension depends crucially on the form of a generic, dimensionless, periodic function $G(z)$, which varies between zero and one but is, to good approximation, independent of the exact physics of the vortices in the Planck-scale regions.

In section 5.8 the effective four-dimensional tension of an F/D -string with linear winding ansatz at the tip of the KS throat is compared with the previous result for the pinched string. For an appropriate and natural choice of $G(z)$, this enables a correspondence between the field theory and the string theory parameters to be drawn. This section also contains a deeper analysis of the relation between the scalar and vector fields in the Higgs model and their geometric interpretation in the theory of wound strings. A brief argument for a time-dependent bead mass in the former, which is equivalent to that of the latter, is also presented. Finally, section 5.9 addresses a number of minor points which arise throughout the previous analysis and section 5.10 contains a brief summary of the main conclusions and a discussion of proposals for future work.

5.2 Revisiting the Abelian-Higgs model

In much of the standard literature on cosmic strings the EOM for the Abelian-Higgs model are obtained by treating the Lagrangian density as fundamental, that is, by setting $\delta\mathcal{L} = 0$.

However, it is the covariant form of the action which truly determines the dynamics of the system, so that we must set $\delta S = \int d^4x \delta(\sqrt{-g}\mathcal{L}) = 0$ in order to determine the EOM. Looking directly at the action, we see that, for fields in Minkowski space which are described in terms of the usual Cartesian coordinates, $x^\mu \in \{t, x, y, z\}$, these two approaches lead to the same set of EOM since $\sqrt{-g} = 1$. In this case $\sqrt{-g}$ is dimensionless, d^4x has units of $[l]^4$ and \mathcal{L} has units of $[E][l]^{-3} = [l]^{-4}$ so that the action is also dimensionless, as required. However, when describing field configurations in cylindrical polar coordinates where $x^\mu \in \{t, r, \theta, z\}$, d^4x has dimensions of $[l]^3$ and the square root of the determinant becomes $\sqrt{-g} = r$, with dimension $[l]$. Technically, it is always the covariant product $d^4x\sqrt{-g}$ which has dimensions $[l]^4$, so the Lagrangian density cannot be taken to be fundamental unless all four of the coordinate labels have dimension $[l]$ and $\sqrt{-g}$ is a dimensionless constant.

One way to interpret the tendency in the existing literature to treat \mathcal{L} as fundamental is to say that, in doing so, we simply neglect the coupling of the Abelian-Higgs field to gravity. This would seem to be a valid approximation, even for strings in highly curved backgrounds, as for any reasonable values of r_s and r_v (c.f. equation (2.23)), the widths of both the scalar and vector cores occupy only small portion of the total spacetime manifold and local flatness may be assumed. The effects of macroscopic curvature on the string dynamics may then be incorporated into the string effective action (i.e. the Nambu action) in the usual way, by using the full space-time metric $g_{\mu\nu}$ to determine the intrinsic metric on the worldsheet, $\gamma_{ab} = g_{\mu\nu}\partial_a X^\mu\partial_b X^\nu$, before contracting to find the determinant term $dA = \sqrt{-\gamma}$.

When working in global Minkowski space - as in this chapter - it is possible to put forward this argument and to assume that the coupling to the background does not influence the structure of the vortices which make up the string core. However, since it is just as convenient to work with the full covariant action as the Lagrangian density, we choose to adopt the former approach for the sake of thoroughness. We will also opt to work in polar coordinates, so that, as noted above, our metric determinant is non-trivial. This implies that our gauge connection must be dimensionless, since the only non-zero component of the vector field in the vortex ansatz is the angular part, A_θ .

Using the (+ - - -) metric convention, and introducing the covariant derivative $D_\mu = \partial_\mu + ieA_\mu$ (together with its conjugate), the covariant form of the Abelian-Higgs action is

$$S = \int d^4x \sqrt{-g} \left(D_\mu \phi g^{\mu\nu} \bar{D}_\nu \bar{\phi} - \frac{1}{4} F_{\mu\nu} F^{\mu\nu} - \frac{1}{4} \lambda (\phi \bar{\phi} - \eta^2)^2 \right). \quad (5.1)$$

Varying this action with respect to the scalar and gauge fields yields the resultant EOM, assuming that the gauge field and scalar derivatives vanish at the boundary,

$$\begin{aligned} 0 &= \frac{1}{\sqrt{-g}} D_\mu (\sqrt{-g} g^{\mu\nu} D_\nu \phi) + \frac{\lambda}{2} \phi (\phi \bar{\phi} - \eta^2) \\ 0 &= \frac{1}{\sqrt{-g}} \bar{D}_\mu (\sqrt{-g} g^{\mu\nu} \bar{D}_\nu \bar{\phi}) + \frac{\lambda}{2} \bar{\phi} (\bar{\phi} \phi - \eta^2), \end{aligned} \quad (5.2)$$

with the corresponding Maxwell equation now taking the form

$$\frac{1}{\sqrt{-g}} \partial_\mu (\sqrt{-g} F^{\mu\nu}) = j^\nu. \quad (5.3)$$

The $U(1)$ current is

$$j^\nu = -ie g^{\mu\nu} (\bar{\phi} D_\mu \phi - \phi \bar{D}_\mu \bar{\phi}), \quad (5.4)$$

where we have defined

$$F_{\mu\nu} = \partial_\mu A_\nu - \partial_\nu A_\mu, \quad (5.5)$$

and

$$F^{\mu\nu} = g^{\mu\alpha} g^{\nu\beta} F_{\alpha\beta}, \quad (5.6)$$

as usual. The static, cylindrically symmetric ansatz then takes the form

$$\begin{aligned} \phi_n(R_s, \theta) &= \eta f(R_s) e^{in\theta} \\ A_{n\theta}(R_v) &= -\frac{n}{e} \alpha(R_v) \end{aligned} \quad (5.7)$$

where

$$R_s = \frac{r}{r_s}, \quad R_v = \frac{r}{r_v} \quad (5.8)$$

are dimensionless variables and r_s, r_v are the length scales of the scalar and vector cores, respectively. These are fixed by the Compton wavelengths of the associated scalar and vector bosons to be

$$\begin{aligned} r_s &= (m_s)^{-1} \approx (\sqrt{\lambda}\eta)^{-1} \\ r_v &= (m_v)^{-1} \approx (2e\eta)^{-1}, \end{aligned} \quad (5.9)$$

as noted previously. Here $f(R_s)$ and $\alpha(R_v)$ are dimensionless real functions satisfying the conditions

$$f(R_s) = \begin{cases} 0 & \text{if } R_s = 0 \quad (r = 0) \\ 1 & \text{if } R_s \rightarrow \infty \quad (r \gg r_s) \end{cases} \quad (5.10)$$

and

$$\alpha(R_v) = \begin{cases} 0 & \text{if } R_v = 0 \quad (r = 0) \\ 1 & \text{if } R_v \rightarrow \infty \quad (r \gg r_v). \end{cases} \quad (5.11)$$

We also note that the definition of the ansatz (5.7) corresponds to the definition of the physical field \vec{A} according to

$$\vec{A} = A_\mu \hat{e}^\mu = A_\theta \hat{e}^\theta = A_\theta g^{\theta\theta} \hat{e}_\theta = \frac{A_\theta}{r^2} \hat{e}_\theta \equiv A^\theta \hat{e}_\theta = A^\mu \hat{e}_\mu. \quad (5.12)$$

Or, equivalently, using $A^\theta = \frac{A_\theta}{r^2}$ and $\vec{A}^2 = A^\theta A_\theta = g^{\theta\theta} A_\theta$, so that

$$A_n^\theta = -\frac{n}{er^2} \alpha(R_v) \quad (5.13)$$

and

$$\vec{A}^2 = \frac{n^2}{e^2 r^2} \alpha^2(R_v). \quad (5.14)$$

We can then define the scalar and gauge field equations by

$$0 = \frac{d^2 f}{dR_s^2} + \frac{1}{R_s} \frac{df}{dR_s} + \frac{n^2 f}{R_s^2} (\alpha^2 - 1) + \frac{f(f^2 - 1)}{2}, \quad (5.15)$$

$$0 = \frac{d^2 \alpha}{dR_v^2} - \frac{1}{R_v} \frac{d\alpha}{dR_v} - f^2 (\alpha - 1), \quad (5.16)$$

where we have manipulated the original forms of the EOM (which come from substituting the ansatz (5.7) into (5.2)-(5.3)) by multiplying the original scalar equation by r_s^2 to get (5.15) and the original vector equation by $r^2 r_v^2$ in order to get (5.16). This allows us to define both the scalar and vector EOM purely in terms of the dimensionless variables R_s and R_v .

Although multiplying the original form of our equations by powers of r is potentially hazardous in the asymptotic limit, as the resulting mathematics may become meaningless or trivial (e.g. “ $\infty = \infty$ ”), multiplying the vector EOM through by r^2 causes no problems for $r \rightarrow \infty$ as each term in the equation still goes to zero independently. In fact, each term in *both* the scalar and vector EOM goes to zero as $R_s, R_v \rightarrow \infty$, and $f(R_s), \alpha(R_v) \rightarrow 1$.

However, defining the parameter

$$\beta = \left(\frac{r_v}{r_s} \right)^2 \quad (5.17)$$

allows us to rewrite the scalar equation as

$$0 = \frac{d^2 f}{dR_v^2} + \frac{1}{R_v} \frac{df}{dR_v} + \frac{n^2 f}{R_v^2} (\alpha^2 - 1) + \frac{1}{2} \beta f (f^2 - 1). \quad (5.18)$$

and treating the ratio β as a numerical constant allows us to rewrite both the scalar and vector EOM in terms of a single dimensionless variable R_v . Adopting the form (5.18) for the scalar EOM is then equivalent to assuming $f = f(R_v)$ instead of $f = f(R_s)$ in the ansatz (5.7). This would seem to be counter-intuitive as, physically, we expect the length scale r_s to determine the width of the scalar core (i.e. the region over which $f \approx 0 \rightarrow f \approx 1$), as stated above. However, the fact that (5.15) and (5.18) are *algebraically equivalent* shows that we may assume *either* functional form for f in our initial ansatz. Both equations have the same approximate solutions in the large and small r limits. As we shall see, it is the value of r_s which characterises the small r solution, though both scales r_s and r_v play a role in the asymptotics, at least when the EOM are solved as a coupled pair.

We will find it convenient to use the form (5.18) instead of (5.15) for the scalar EOM, though “large” and “small” r for *both* forms of the equation must still be defined with respect to r_s , rather than r_v as for the vector EOM (5.16).

Reviewing the literature

At this stage it is useful to comment on our EOM, as they are slightly different to the ones quoted in the standard literature. Taking the Lagrangian density as fundamental, the “covariant” form of the scalar EOM is quoted in the review by Hindmarsh and Kibble (HK) [124] as

$$\left[D^2 + \lambda \left(|\phi|^2 - \frac{1}{2}\eta^2 \right) \right] = 0. \quad (5.19)$$

This equation differs from that given in (5.2) because of the exclusion of factors of $\sqrt{-g}$ and $\frac{1}{\sqrt{-g}}$ from the derivative term but is otherwise identical, if we use the definition $D^2 = D_\mu D^\mu$ and account for the differing numerical factor used in front of the potential term of the Lagrangian (which is arbitrary).² It is therefore equivalent to that used in Vilenkin and Shellard (VS) [114];

$$D^\mu D_\mu \phi + \frac{\lambda}{2} \phi (\phi \bar{\phi} - \eta^2) = 0. \quad (5.20)$$

The vector EOM is also given as

$$\partial_\nu F^{\mu\nu} = j^\nu \quad (5.21)$$

in both sources, which again differs from the expression given in (5.3) because of the exclusion of factors of $\sqrt{-g}$ and $\frac{1}{\sqrt{-g}}$ in the derivative. VS [114] then go on to define the $U(1)$

²In other words, setting $\sqrt{-g} = 1$ in (5.2) and exchanging $\lambda \rightarrow -\lambda$ recovers the scalar EOM (5.19).

current as

$$j^\nu = 2e \text{Im}[\bar{\phi} D^\nu \phi]. \quad (5.22)$$

Accounting for the difference in notation, this is again equivalent to that given in HK [124]

$$j^\nu = -ie(\phi^* D^\nu \phi - \phi D^\nu \phi^*), \quad (5.23)$$

and to the expression (5.4) where we recognise that $D^\nu \phi^* \equiv \overline{D^\nu \phi}$. The specific forms of the scalar and vector EOM are not quoted explicitly in [124], though [114] uses a vector equation equivalent to (5.16) and a scalar equation equivalent to

$$0 = \frac{d^2 f}{dR_v^2} + \frac{1}{R_v} \frac{df}{dR_v} - \frac{n^2 f}{R_v^2} (\alpha - 1)^2 + \frac{1}{2} \beta f (f^2 - 1), \quad (5.24)$$

which still differs from the scalar EOM (5.18) by the interchanging of the terms $+\frac{n^2 f}{r^2}(\alpha^2 - 1)$ and $-\frac{n^2 f}{r^2}(\alpha - 1)^2$. Although this will effect the numerical solution in the intermediate range $r_s < r \ll \infty$, it is clear that (5.18) and (5.24) have the same approximate forms for both $r \leq r_s$ and $r \rightarrow \infty$ ($r \gg r_s$), so that their respective analytic solutions remain the same in both these limits.

In order to obtain the derivative term in (5.24) from that in (5.20) it is necessary to define

$$\begin{aligned} D_\mu D^\mu \phi &= \partial_\mu \partial^\mu \phi - 2ie A_\mu \partial^\mu \phi - e^2 A_\mu A^\mu \\ &\equiv \nabla^2 \phi - 2ie A_\theta \partial_\theta \phi - e^2 (A_\theta)^2 \phi. \end{aligned} \quad (5.25)$$

However, the covariant expression $\partial_\mu \partial^\mu = g^{\mu\nu} \partial_\mu \partial_\nu$ is only equivalent to the ∇^2 operator in a *Cartesian* coordinate system. Covariantly, ∇^2 is defined as

$$\nabla^2(\cdot) = \frac{1}{\sqrt{-g}} g^{\mu\nu} \partial_\mu (\sqrt{-g} \partial_\nu (\cdot)). \quad (5.26)$$

Likewise, although we may consistently define $A_\theta \partial^\theta \phi = A^\theta \partial_\theta \phi = g^{\theta\theta} A_\theta \partial_\theta \phi$ and $A_\theta A^\theta = g^{\theta\theta} A_\theta A_\theta = \frac{n^2}{e^2 r^2} \alpha^2$ using the definition (5.7) together with the standard definition of metric contraction, it is the practice in the usual literature to define

$$A_n^\theta \equiv A_{n\theta} = -\frac{n}{er} \alpha \quad (5.27)$$

and to use the ‘‘ad hoc’’ definitions

$$\vec{A}^2 = A_n^\theta A_{n\theta} = \frac{n^2}{e^2 r^2} \alpha^2 \quad (5.28)$$

and

$$\partial^\theta = \partial_\theta \equiv \frac{1}{r} \frac{\partial}{\partial \theta}. \quad (5.29)$$

This corresponds to defining the covariant derivative *not* by its individual covariant components (i.e. $D_\mu = \partial_\mu - ieA_\mu$) but by

$$D = \nabla - ie\vec{A} \quad (5.30)$$

where ∇ represents the gradient operator *in any coordinate system*. This is the same as defining $\nabla(\cdot) = \partial_\mu(\cdot)\hat{e}^\mu = \partial^\mu(\cdot)\hat{e}_\mu$ (i.e. covariantly) but then “absorbing” one factor of r^{-1} into the “component” part $\partial_\mu(\cdot)$ and one factor of r^{-1} into the vector part \hat{e}_μ . It is then *not* possible to define the gradient operator consistently in terms of its components, $\nabla_\mu(\cdot) \equiv \partial^\mu(\cdot) \neq \partial_\mu(\cdot)$. Likewise, we must then use the “ad hoc” definition of the θ -component of the vector field in order to maintain consistency in the units so that $\vec{A} \equiv A_{n\theta} \propto \frac{1}{r}$, though this is strictly inconsistent with the covariant definition $\vec{A} = A_\mu \hat{e}^\mu = A^\mu \hat{e}_\mu$. Finally, an appropriate covariant modification to the formula for the quantised flux Φ_n given by (2.14) (following VS [114])³ may be defined via either

$$\Phi_n = \oint_B |\vec{A}| r d\theta = \oint_B \sqrt{\vec{A}^2} r d\theta = \oint_B \sqrt{A_\mu A^\mu} r d\theta, \quad (5.31)$$

which in our case implies

$$\Phi_n = \oint_B \sqrt{A_\theta A^\theta} r d\theta = \oint_B \sqrt{\frac{n^2}{e^2 r^2}} r d\theta = \frac{2\pi n}{e}, \quad (5.32)$$

as expected, or

$$\Phi_n = - \oint_B A_\mu dx^\mu = - \oint_B A_\theta d\theta = \frac{2\pi n}{e}, \quad (5.33)$$

where again B denotes the boundary at radial infinity.

Turning our attention now to the solutions of the EOM given in the usual literature, we consider (5.18)/(5.24) and (5.16) in both the small and large r limits. As stated above, we may in principle take *either* (5.18) or (5.24), as their small and large r forms are equivalent. Hence the solutions to our EOM do not differ substantially to those given in the usual sources.⁴

³ $\Phi_n = \oint_B A_{n\theta} r d\theta = \frac{2\pi n}{e}$

⁴We do later uncover a minor discrepancy between the sub-leading order term in the small r expansion for α quoted in [124] and the one obtained independently here. However, such considerations are of minor importance.

We may choose to solve these equations, in either limit, as either a coupled pair or using the uncoupled approximation. Specifically, we may “uncouple” the scalar EOM from the vector EOM (or equivalently f from α in the scalar EOM) in either the small or large r limit by assuming the boundary condition $\alpha \sim 0$ or $\alpha \sim 1$, respectively, and solving for f . Similarly we may “uncouple” the vector EOM from the scalar EOM (or equivalently α from f in the vector EOM) by assuming the boundary condition $f \sim 0$ or $f \sim 1$ and solving for α .

Alternatively, we may solve the EOM as a coupled pair by substituting appropriate ansatzes for both f and α in the small and large r limits and setting the coefficients of the leading order terms to zero. This approach was first adopted (for $r \rightarrow \infty$) by Perivarpoulos [320] and we review his results (which are also quoted in HK [124]), together with the “uncoupled” solutions given in VS [114] and in the original paper by Nielsen and Olesen [15]. In the small r limit, coupling the equations has no effect (to first order) on the approximate solutions for f and α but, in the large r limit, the value of β plays a role in determining the asymptotics of f . In particular, it is found that a critical value of β exists which separates two qualitatively different asymptotic regimes.

Beginning with the assumption $f = f(R_s)$, the asymptotic form of f in the uncoupled regime (i.e. setting $\alpha \rightarrow 1$ in the scalar EOM), is given by VS [114] as

$$\begin{aligned} f(R_s) &\approx 1 - K_0(R_s) \\ &\approx 1 - \mathcal{O}(\exp(-R_s)) \end{aligned} \tag{5.34}$$

where K_0 is the zero-order modified Bessel function of the second kind. This form comes directly from solving (5.15), whereas solving the alternative form (5.18) gives $f(R_v) \approx 1 - K_0(\sqrt{\beta}R_v)$, which is equivalent.

However, beginning with the assumption that $f = f(R_v)$, HK [124] give the expansion in this limit (for $\beta \leq 2$)⁵ as

$$\begin{aligned} f(R_v) &\approx 1 - f_1 R_v^{-\frac{1}{2}} \exp(-\sqrt{\beta}R_v) \\ &= f(R_s) \approx 1 - f_1 \left(\frac{R_s}{\sqrt{\beta}} \right)^{-\frac{1}{2}} \exp(-R_s) \end{aligned} \tag{5.35}$$

⁵Here we are using the definition $\beta = r_v^2/r_s^2 \equiv (\sqrt{\lambda}\eta)^2/(\sqrt{2}\eta e)^2 = \lambda/2e$, following VS [114], but Perivarpoulos [320] and HK [124] use the definition $\beta = r_v^2/r_s^2 \equiv (\sqrt{\lambda}\eta)^2/(\eta e)^2 = \lambda/e$, so that $\beta = 2$ in our units is equivalent to $\beta = 4$ (the quoted critical value) in theirs. The definition of β and the critical value of $\beta = 4$ given in [114] (citing [320]) are in fact inconsistent. However, the situation is complicated even further by the fact that VS [114] and HK [124] use one definition of the Lagrangian density (i.e. that defined above in (5.1)), whereas Nielsen and Olesen [15] and Perivarpoulos [320] use another, including a factor of 1/2 in front of the derivative term. The asymptotic form of f quoted in [320] (i.e. $f(R_v) \approx 1 - f_1 R_v^{-\frac{1}{2}} \exp(-\sqrt{2\beta}R_v)$) is therefore similar, but not identical to (5.35) given above, but the difference is easily accounted for. HK [124] also adopts a factor of $1/\sqrt{2}$ in front of the scalar field ansatz, though this is optional, and makes no difference to any results of physical importance.

where f_1 is an arbitrary constant (necessarily in the range $0 < f_1 < 1$ and typically assumed to be of order one). We therefore see that the long-range behaviour is determined to some extent by r_v as well as r_s (or equivalently by the value of the ratio β). Physically, this may be understood intuitively as we would expect the long range fall-off of the scalar field to be determined, at least in part, by the gauge field contribution to the energy density which ‘‘cancels’’ the logarithmic divergence of the global string energy density on scales $r > r_v$.

As stated above, mathematically our freedom to choose either $f = f(R_s)$ or $f = f(R_v)$ comes from the fact that they give rise to *algebraically equivalent* EOM, with both the resulting equations being structurally equivalent to the *un*-rescaled scalar EOM derived from assuming $f = f(r)$. As also stated above, and as we shall see later, assuming either $f = f(R_s)$ or $f = f(R_v)$ gives rise to the *same* small r solution for f , which is characterised by the length-scale r_s rather than r_v , again in accord with our physical intuition. The real difference between the asymptotic solution (5.34) and (5.35) is that (5.34) is obtained by assuming $\alpha \rightarrow 1$ in (5.51) (which effectively decouples the gauge field contribution α from the scalar EOM in the asymptotic limit), whereas (5.35) represents a solution to the genuinely coupled EOM.

Perivolaropolous’ [320] approach to solving the equations of motion (perturbatively) as a coupled pair in the large r limit involved adopting the ansatz

$$\begin{aligned} f &\rightarrow 1 + \delta f \\ \alpha &\rightarrow 1 + \delta\alpha. \end{aligned} \tag{5.36}$$

Substituting (5.36) and assuming $|\delta\alpha| > |\delta f|$ (given that $r_v > r_s$) allows us to keep terms in δf , $\delta\alpha$ and $(\delta\alpha)^2$ but to ignore terms in $(\delta f\delta\alpha)$, $(\delta f)^2$ and $(\delta f)^3$, so that the EOM reduce to,⁶

$$0 = \delta f'' + \frac{1}{R_v}\delta f' - \frac{(\delta\alpha)^2}{R_v^2} + \beta\delta f \tag{5.37}$$

$$0 = \delta\alpha'' - \frac{1}{R_v}\delta\alpha' - \delta\alpha \tag{5.38}$$

where a dash represents differentiation with respect to R_v . The resulting vector EOM contains no terms in δf , so it may be solved directly by substituting the following ansatz

⁶The original EOM quoted in Perivolaropolous’ paper are $\delta f'' + \frac{1}{R_v}\delta f' - \frac{(\delta\alpha)^2}{R_v^2} - 2\beta\delta f = 0$ and $\delta\alpha'' - \frac{1}{R_v}\delta\alpha' - 2\delta\alpha = 0$, *not* those quoted here. This results from the differing definitions of the Lagrangian density and the parameter β . Although we have followed exactly the same approach to that used in [320], we have modified our results to ensure consistency with the definitions of \mathcal{L} and r_v used throughout this work.

for $\delta\alpha$,

$$\alpha = c_1 e^{-\gamma R_v} R_v^\chi + c_2 e^{-\gamma R_v} R_v^{\chi-1}, \quad c_1, c_2 \sim \mathcal{O}(1), \quad (5.39)$$

and setting the coefficients of the two leading order terms to zero. This yields two constraint equations which allow the values of γ and χ to be fixed:⁷

$$\begin{aligned} \delta\alpha &= c_1 e^{-R_v} R_v^{\frac{1}{2}} + c_2 e^{-R_v} R_v^{-\frac{1}{2}} \\ &\approx c_1 e^{-R_v} R_v^{\frac{1}{2}}. \end{aligned} \quad (5.40)$$

Using a similar ansatz for f ,

$$f = c_0 e^{-a R_v} R_v^b, \quad c_0 \sim \mathcal{O}(1), \quad (5.41)$$

and performing the same procedure for both the homogenous and particular forms of the resulting equation, then gives

$$f(R_v) \approx 1 - f_1 R_v^{-\frac{1}{2}} \exp(-\sqrt{\beta} R_v) - f_2 R_v^{-1} (\beta - 2)^{-1} e^{-2R_v} \quad (5.42)$$

where f_2 is a constant satisfying the same conditions as f_1 .⁸ Hence, for $\beta \leq 2$, equation (5.35) is valid, whereas for $\beta > 2$ we have

$$f(R_v) \approx 1 - \mathcal{O}(R_v^{-1} e^{-2R_v}). \quad (5.43)$$

It had previously been assumed that the solution given in the original paper by Nielsen and Olesen [15],

$$\begin{aligned} f(R_v) &\approx 1 - K_0(R_v) \\ &\approx 1 - \mathcal{O}\left(R_v^{-\frac{1}{2}} \exp(-R_v)\right), \end{aligned} \quad (5.44)$$

was roughly valid in all cases, though like the solution (5.34) quoted in [114] (which possibly contains a misprint in neglecting the factor of $\sim R_v^{-\frac{1}{2}}$ in front of the exponential, but which is correct in replacing R_v by R_s in the argument of the exponential), this is essentially a solution to the *uncoupled* scalar EOM. Reference [320] was the first to demonstrate conclusively that the coupling of the gauge field to the scalar field is capable of modifying the asymptotics of the latter. Perhaps surprisingly, this work showed that the modification depends on a critical value of β which separates two qualitatively different regimes.

⁷Perivapoulos' original paper uses $\delta\alpha = c_1 e^{-\sqrt{2} R_v} R_v^{\frac{1}{2}}$.

⁸The method adopted here is identical to that in [320] but takes into account our redefinition of the parameter β , which differs from the one used in that paper. The critical value of β given here, i.e. $\beta = 2$, therefore corresponds to the value $\beta = 4$ quoted as the critical value by Perivapoulos.

Turning our attention now to the vector EOM, the asymptotic solution to the uncoupled vector EOM (5.16) (i.e. assuming $f \rightarrow 1$), is quoted by both VS [114] and Nielsen and Olesen [15] as

$$\begin{aligned}\alpha(R_v) &\approx 1 - a_1 R_v K_1(R_v) \\ &\approx 1 - a_1 R_v^{\frac{1}{2}} \exp(-R_v)\end{aligned}\tag{5.45}$$

where K_1 is the first order modified Bessel function of the second kind and a_1 is a constant such that $0 < a_1 < 1$, which we typically assume to be of order one (like f_1 and f_2). This is also in agreement with Perivarpoulous's results [320] (again accounting for the differing definition of the action) and hence with those quoted in HK [124], which we expect, as Perivarpoulous' approach shows that δf has no effect on the vector EOM to lowest order.

Turning our attention now to the $r \rightarrow 0$ limit, both VS [114] and HK [124] agree in citing, $f \propto r^{|n|}$ and $\alpha \propto r^2$ (to first order) for small r . However, again we are faced with the problem of defining "small" with reference to a single length scale for each function. Taking both f and α to be functions of R_v , HK use

$$f(R_v) \approx f_0 R_v^{|n|},\tag{5.46}$$

$$\alpha(R_v) \approx a_0 R_v^2 - \frac{|n| f_0^2}{4(|n| + 1)} R_v^{2|n|+2},\tag{5.47}$$

where f_0 and a_0 are again constants of order one,⁹ whereas defining $f = f(R_s)$, $\alpha = \alpha(R_v)$ leads to

$$f(R_s) \approx R_s^{|n|}\tag{5.48}$$

$$\alpha(R_v) \approx R_v^2 + \mathcal{O}(R_v^{2|n|+2})\tag{5.49}$$

instead. It may then be argued that there exists a contradiction between the small and large r forms of f , with one taking the functional form $f = f(R_s)$ and the other taking (almost) the form $f = f(R_v)$. However, as argued previously, this contradiction is only apparent. On the other hand, these results do conform to our intuition that $r_s = m_s^{-1}$ should set the length-scale for the scalar core (at small r), whereas the large-scale fall-off for f should to some extent be controlled by the gauge field and hence the parameter $r_v = m_v^{-1}$.

By contrast, the results given in (5.46) imply that $r_v = m_v^{-1}$ also sets the scale for the

⁹Here $a_0 \sim \mathcal{O}(1)$ must *not* be confused with the warp factor of the KS metric.

scalar field core, which seems counter-intuitive. However, for $r \ll r_v$, equation (5.24) reduces to

$$0 = \frac{d^2 f}{dR_v^2} + \frac{1}{R_v} \frac{df}{dR_v} - \frac{n^2 f}{R_v^2} + \frac{1}{2} \beta f \quad (5.50)$$

whose true solution is

$$\begin{aligned} f(R_v) &\approx (\sqrt{\beta} R_v)^{|n|} \\ &= f(R_s) \approx R_s^{|n|} \end{aligned} \quad (5.51)$$

(see later) which leads us to question the result given in HK [124].

Clearly, in either case, the approximate forms of f and α for small r depend on the absolute value of the winding number $|n|$. Realistically though, we might also expect $|n|$ to have some influence on the asymptotics of either of these functions. However, we see that the reason why $|n|$ plays no part in determining the long-range behaviour of f is that the term containing n^2 in (5.24) is proportional to $(\alpha - 1)^2$, which goes to zero for large r . A similar result also holds, even for the corresponding scalar EOM derived from the action (5.15), in which the term containing n^2 is proportional to $(\alpha^2 - 1)$. In addition, the function α cannot depend on $|n|$ in the asymptotic limit, as n does not appear even in the coupled vector EOM.

Finally, we note that the first term $\sim \mathcal{O}(R_v^2)$ in (5.47) comes from solving the vector EOM using the uncoupled approximation (i.e. setting $f^2 \approx 0$), whereas a second term in the expansion $\sim \mathcal{O}(R_v^{2|n|+2})$ (which satisfies $\mathcal{O}(R_v^{2|n|+2}) \geq \mathcal{O}(R_v^4)$ for $|n| \geq 1$) comes from solving the EOM as a coupled pair in the small r limit. This is done by substituting $f \sim f_0 R_s^{k_f} = (f_0 \sqrt{\beta} R_v)^{k_f}$ and $\alpha \sim a_0 R_v^{k_\alpha}$, $k_f, k_\alpha > 0$ into (5.18) and (5.16), giving

$$\begin{aligned} 0 &= f_0 \sqrt{\beta}^{k_f} [k_f^2 - n^2] R_v^{k_f-2} + f_0 \sqrt{\beta}^{k_f} n^2 R_v^{k_f+2k_\alpha-2} \\ &+ f_0 \sqrt{\beta}^{k_f} n^2 R_v^{k_f+2k_\alpha-2} - \frac{1}{2} f_0 \sqrt{\beta}^{k_f+2} R_v^{k_f} + \frac{1}{2} (f_0)^3 \sqrt{\beta}^{3k_f+2} R_v^{3k_f} \end{aligned} \quad (5.52)$$

and

$$0 = a_0 [k_\alpha^2 - 2k_\alpha] R_v^{k_\alpha-2} - (f_0)^2 \sqrt{\beta}^{2k_f} R_v^{2k_f+k_\alpha} + (f_0)^2 \sqrt{\beta}^{2k_f} R_v^{2k_f}. \quad (5.53)$$

Beginning with (5.52) and requiring that the leading order terms (i.e. those with the *smallest* exponents) cancel *exactly* implies

$$k_f = |n|. \quad (5.54)$$

5.3. CALCULATION OF THE (CONSTANT) STRING TENSION FOR A
CYLINDRICALLY SYMMETRIC STRING $\mu_{|n|}$

Equation (5.53) then implies either $k_\alpha - 2 < 2k_f$, and hence $k_\alpha = 2$, or

$$k_\alpha = 2|n| + 2 \tag{5.55}$$

and

$$a_0 = -\frac{(f_0^2)\beta^{|n|}}{4|n|(|n| + 1)}, \tag{5.56}$$

which differs from the result quoted in (5.47) by the interchange of terms $\beta^{|n|}/|n|$ and $|n|$. Using (5.24) instead of (5.18) gives rise to identical results.

5.3 Calculation of the (constant) string tension for a cylindrically symmetric string $\mu_{|n|}$

The formula for the tension of an Abelian vortex string is given in VS [114] (quoting Preskill [321]) as

$$\mu = \int r dr d\theta \left\{ \left| (\nabla - ie\vec{A})\phi \right|^2 + \frac{1}{2}(\vec{E}^2 + \vec{B}^2) + V(|\phi|) \right\} \tag{5.57}$$

where the three terms inside the curly brackets correspond to the gradient energy density, the electromagnetic energy density and the potential energy density, respectively. However, again accounting for differences in notation and recognising that $D^\mu\phi^* \equiv \bar{D}_\mu\bar{\phi}$, Preskill's original lecture notes give

$$\mu = \int r dr d\theta \left\{ D_\mu\phi\bar{D}^\mu\bar{\phi} + \frac{1}{2}(\vec{E}^2 + \vec{B}^2) + V(|\phi|) \right\} \tag{5.58}$$

where D denotes the covariant derivative, with components $D_\mu = \partial_\mu - ieA_\mu$. The ‘‘derivative’’ term in (5.59) therefore corresponds to the incorrect definition $D = \nabla - ie\vec{A}$ (5.30) given earlier, where $\nabla = \frac{\partial}{\partial r} + \frac{1}{r}\frac{\partial}{\partial\theta} + \frac{\partial}{\partial z}$ in cylindrical polars and \vec{A} is taken to be proportional to r^{-1} , as in (5.27), though this is not consistent with the proper *covariant* definition of the gauge field.

Although using (5.59) together the ‘‘ad hoc’’ definition of vector multiplication and the ansatz (5.27) gives rise to the same expression for the final tension as using Preskill's original formula (5.58), the gauge field ansatz (5.7) and the standard definition of metric contraction, the latter is more rigorous from a mathematical perspective.

Despite this, for $|n| \sim 1$ VS [114] give the resulting tension as

$$\mu \approx 2\pi\eta^2 \ln\left(\sqrt{\beta}\right) \tag{5.59}$$

5.3. CALCULATION OF THE (CONSTANT) STRING TENSION FOR A
CYLINDRICALLY SYMMETRIC STRING $\mu_{|n|}$

which, as we shall see, is the correct result. They again attribute this to Preskill [321], whose original lectures give

$$\begin{aligned}\mu &\approx \pi\eta^2 \left[\ln(\sqrt{\beta}) + \frac{1}{e^2\eta^2 r_v^2} + \lambda\eta^2 r_s^2 \right] \\ &\approx 2\pi\eta^2 + \pi\eta^2 \ln(\sqrt{\beta}),\end{aligned}\tag{5.60}$$

which is approximately equivalent to (5.59) for $\ln(\sqrt{\beta}) \gg 1$.

We now verify these results explicitly using the formula (5.58) together with the ansatz (5.7), though we include the most general case $|n| \geq 1$, which we will need for comparison with the *general* case of wound F/D -strings with $n_w \geq 0$ in section 5.7. The calculations are shown in full, so that they may be compared with the calculations to determine the z -dependent tension $\mu_{|n|}(z)$ for the pinched string, given in section 5.6.

The correct definitions of D and A_θ lead to the gradient term

$$\begin{aligned}D_\mu\phi\bar{D}^\mu\bar{\phi} &= (\partial_\mu - ieA_\mu)\phi g^{\mu\nu}(\partial_\nu + ieA_\nu)\bar{\phi} \\ &= \partial_r\phi g^{rr}\partial_r\bar{\phi} + (\partial_\theta - ieA_\theta)\phi g^{\theta\theta}(\partial_\theta + ieA_\theta)\bar{\phi} \\ &= \eta\frac{\partial f}{\partial r}e^{in\theta}\eta\frac{\partial f}{\partial r}e^{-in\theta} + \frac{1}{r^2}\left(\frac{\partial}{\partial\theta} + in\alpha\right)\eta f e^{in\theta}\left(\frac{\partial}{\partial\theta} - in\alpha\right)\eta f e^{-in\theta} \\ &= \eta^2\left(\frac{\partial f}{\partial r}\right)^2 + \frac{\eta^2|n|^2}{r^2}f^2(\alpha - 1)^2.\end{aligned}\tag{5.61}$$

The resulting integral may then be split into three parts. Within the scalar core region, $0 \leq r \leq r_s$, we may approximate the functions f and α by $f \sim \frac{r^{|n|}}{r_s^{|n|}}$ and $\alpha \sim \frac{r^2}{r_v^2}$, giving

$$\begin{aligned}\int_0^{2\pi} d\theta \int_0^{r_s} D_\mu\phi\bar{D}^\mu\bar{\phi} r dr &= \int_0^{2\pi} d\theta \int_0^{r_s} \eta^2 \left(\frac{\partial f}{\partial r}\right)^2 r dr + \int_0^{2\pi} d\theta \int_0^{r_s} \frac{\eta^2|n|^2}{r^2} f^2(\alpha - 1)^2 r dr \\ &\approx 2 \times 2\pi \frac{\eta^2|n|^2}{r_s^{2|n|}} \int_0^{r_s} r^{2|n|-1} dr \approx 2\pi\eta^2|n|.\end{aligned}\tag{5.62}$$

In the region $r_s \leq r \leq r_v$, we may assume $\alpha \sim \frac{r^2}{r_v^2}$ and $f \sim 1$, giving

$$\begin{aligned}\int_0^{2\pi} d\theta \int_{r_s}^{r_v} D_\mu\phi\bar{D}^\mu\bar{\phi} r dr &= \int_0^{2\pi} d\theta \int_{r_s}^{r_v} \eta^2 \left(\frac{\partial f}{\partial r}\right)^2 r dr + \int_0^{2\pi} d\theta \int_{r_s}^{r_v} \frac{\eta^2|n|^2}{r^2} f^2(\alpha^2 - 1)^2 r dr \\ &\approx 0 + 2\pi\eta^2|n|^2 \int_{r_s}^{r_v} \frac{dr}{r} \approx 2\pi\eta^2|n|^2 \ln(\sqrt{\beta}).\end{aligned}\tag{5.63}$$

On scales $r > r_v$, we may assume $f \sim 1$ and $\alpha \sim 1$, so that $D_\mu\phi\bar{D}^\mu\bar{\phi} \sim \left(\frac{\partial f}{\partial r}\right)^2 + \frac{f^2(\alpha-1)^2}{r^2} \sim 0$ and the gauge field contribution effectively ‘‘cancels’’ the energy density contribution of the scalar field gradient. The overall contribution to the energy density of the covariant gradient

5.3. CALCULATION OF THE (CONSTANT) STRING TENSION FOR A
CYLINDRICALLY SYMMETRIC STRING $\mu_{|n|}$

term is therefore

$$\int_0^{2\pi} d\theta \int_0^\infty D_\mu \phi \bar{D}^{\mu} \bar{\phi} r dr \approx 2\pi\eta^2 |n| + 2\pi\eta^2 |n|^2 \ln(\sqrt{\beta}). \quad (5.64)$$

Turning our attention to the gauge field flux term, we see that $\vec{E} = 0$ and that the only non-zero component of \vec{B} is

$$B_z = F_{r\theta} = \partial_r A_\theta = -\frac{n}{e} \frac{d\alpha}{dr}, \quad (5.65)$$

so that

$$\vec{B}^2 = F_{r\theta} F^{r\theta} = g^{rr} g^{\theta\theta} F_{r\theta} F_{r\theta} = \frac{n^2}{e^2 r^2} \left(\frac{d\alpha}{dr} \right)^2. \quad (5.66)$$

Integrating over the vector core region, $0 \leq r \leq r_v$, for which $\alpha \sim \frac{r^2}{r_v^2}$ then gives

$$\int_0^{2\pi} d\theta \int_0^{r_v} \frac{1}{2} \vec{B}^2 r dr \approx \frac{2\pi |n|^2}{e^2 r_v^4} \int_0^{r_v} r dr = 2\pi\eta^2 |n|^2 \quad (5.67)$$

where we have used the definition $r_v \approx (\sqrt{2}e\eta)^{-1}$. For $r > r_v$ we may take $\alpha \sim 1$ so that $\vec{B}^2 \propto \left(\frac{d\alpha}{dr} \right)^2 \rightarrow 0$.

Finally, we consider the potential term. Within the scalar core the potential energy density may be approximated by

$$V(|\phi|) = \frac{\lambda\eta^3}{2} f(f^2 - 1) \approx \frac{1}{2} \eta^2 \frac{r^{|n|}}{r_s^{|n|+2}}, \quad (5.68)$$

so the contribution to the tension becomes

$$\int_0^{2\pi} d\theta \int_0^{r_s} V(|\phi|) r dr \approx \frac{\pi\eta^2}{r_s^{|n|+2}} \int_0^{r_s} r^{|n|+1} dr = \frac{\pi\eta^2}{|n| + 2}, \quad (5.69)$$

whereas for $r > r_s$ we can assume $f \sim 1$ and $V(|\phi|) \propto (f^2 - 1) \rightarrow 0$.

Summing *all* the contributions, the total tension is

$$\mu_{|n|} \approx 2\pi\eta^2 |n|^2 \left(1 + \ln(\sqrt{\beta}) + \frac{1 + 4|n| + 2|n|^2}{2|n|^2(2 + |n|)} \right), \quad (5.70)$$

which is clearly dominated by the terms proportional to $|n|^2$, (i.e. higher order terms are suppressed by the $1/|n|$ expansion) and which, to leading order, gives

$$\mu_{|n|} \approx 2\pi\eta^2 |n|^2 \left(1 + \ln(\sqrt{\beta}) + \dots \right). \quad (5.71)$$

5.3. CALCULATION OF THE (CONSTANT) STRING TENSION FOR A
CYLINDRICALLY SYMMETRIC STRING $\mu_{|n|}$

At critical coupling, $\beta = 1$, we may approximate $\mu_{|n|}$ by

$$\mu_{|n|} \approx 2\pi\eta^2 |n|^2. \quad (5.72)$$

The leading order contribution arises from the gauge field component. However, we note that this result is dependent upon the form of $\alpha(r)$ (and hence also $f(r)$, since the two must be related in a way which ensures the cancellation of the gauge field and scalar gradient contributions to the energy density on large scales). When $\beta = 1$ the general ansatz for $A_{n\theta}$ and ϕ_n remains valid but the the solutions for $\alpha(r)$ and $f(r)$ used here ($\alpha(r) \sim (r/r_v)^2$ ($r \leq r_v$)), $f(r) \sim (r/r_s)^{|n|}$ ($r \leq r_s$)), do not minimise the energy of the field configuration for $|n| > 1$. Bogomol'nyi [322, 323] showed that $\alpha(r)$ and $f(r)$ which satisfy

$$\begin{aligned} \frac{df}{dr} &= \frac{nf}{r}(1 - \alpha), \\ \frac{1}{r} \frac{d\alpha}{dr} &= \mp \frac{1}{n}(f^2 - 1) \end{aligned} \quad (5.73)$$

automatically satisfy the Euler-Lagrange equations and also minimise the vortex energy, giving

$$\mu_{|n|} = 2\pi|n| \quad (5.74)$$

instead of (5.72). Explicit solutions of these equations were later found by de Vega and Shaposnik [324] who showed that the energy-minimising form of $\alpha(r)$ is

$$\alpha(r) = -\frac{1}{n} \sum_{k=1}^{\infty} \beta_k \left(\frac{r}{\sqrt{2}} \right)^{2k} \quad (5.75)$$

where the coefficients β_k are given by the recursion relation

$$\beta_k = \frac{1}{k(k-2)} \sum_{l=2}^{k-1} l\beta_l\beta_{k-l}, \quad \beta_1 = -1, \quad \beta_2 \approx 0.7279. \quad (5.76)$$

The function f can then easily be found by inverting the vector equation in (5.73) to make f the subject and substituting (5.75)-(5.76).

The string described here is therefore unstable and may decay into $|n|$ strings with unit windings. Alternatively, the fields may undergo dynamical evolution (while maintaining a single n -vortex string configuration) towards a state in which the energy-minimising conditions are satisfied. Whether it is possible for an n -vortex string with tension $\mu_{|n|} = 2\pi|n|^2$ to dynamically evolve into a static state in which $\mu_{|n|} = 2\pi|n|$ is an interesting open question and it at least conceivable that such an instability would result in an oscillating solution, similar to that encountered in chapter 4 for wound strings. Furthermore, as our main purpose in constructing the string described above (with $\mu_{|n|} = 2\pi|n|^2$, rather than $\mu_{|n|} = 2\pi|n|$)

5.3. CALCULATION OF THE (CONSTANT) STRING TENSION FOR A CYLINDRICALLY SYMMETRIC STRING $\mu_{|n|}$

is to be able to generalise this result to the non-cylindrical case in which $\mu_{|n|} = 2\pi|n|^2$ is simply the leading-order contribution to the tension and there exists an additional periodic part.

Although the Bogomol'nyi result demonstrates that the pinched string described in sections 5.4-5.7 is unstable for $|n| > 1$ and must therefore break apart or undergo dynamical evolution to a stable state, our purpose in constructing it is (at least in part) to demonstrate its equivalence to the wound-string states considered earlier in this thesis. In chapters 3 and 4 we found string configurations with $\omega_l > 0$ which were generically unstable (i.e. not static, as in chapter 4, or quasi-stable as in chapter 3), which, according to the duality proposed in section 5.8, correspond to field-theoretic strings with $|n| > 1$. It is therefore unlikely that the solutions presented here are in conflict with existing results, though it is clear that more work is needed to clarify the relation between the energy-minimising (stable) vortex-line string (with $|n| > 1$, $\beta = 1$) and the corresponding energy-minimising (stable) F/D -string configuration with $\omega_l > 0$. Ideally we would like to develop a fully dynamical theory of both wound-string and vortex-line string evolution and to study the dynamics of both F/D -strings with non-zero windings and field-theoretic strings with topological charge greater than unity that begin life in a non-energy-minimising state. If the duality suggested in section 5.8 is valid, full dynamical equivalence must also be demonstrated. Unfortunately, such work is beyond the scope of this thesis, though some further remarks on possible extensions of the current work to the fully dynamical case are given in section 5.10.

In the following section we introduce a non-cylindrically symmetric ansatz for the pinched string and the resulting EOM are then solved in section 5.5. We show that, for a set of reasonable physical assumptions, these equations and their solutions take on exactly analogous forms to those of the more familiar cylindrical case, but with the substitution $r_s \rightarrow r_s^{eff}(z)$, $r_v \rightarrow r_v^{eff}(z)$. In other words, the structure of the vortices remains essentially the same, except that the radii of the scalar and vector cores become functions of their position along the string. Therefore, the calculation of the tension *for a given value of z* also remains substantially the same as that outlined above, apart from the introduction of a new radial magnetic flux term $\sim F_{z\theta}F^{z\theta}$ (associated with the z -dependent variation of A_θ) and of a new z -derivative component in the $D\phi\overline{D}\phi$ term, which give rise to an *additional* periodic part.

Although the resulting tension $\mu_{|n|}(z)$ is periodic in z , it still carries a leading order constant term $\sim 2\pi\eta^2|n|^2$ (as mentioned above), derived in an analogous fashion to that in (5.72), which may be identified with a similar leading order constant term $\sim 2\pi a_0^2 T_1$ in the expression for the effective four-dimensional tension of a wound F/D -string. In addition, although the analogue of the parameter $\beta = (r_v/r_s)^2$ can clearly be defined (i.e.

$\beta^{eff}(z) \equiv (r_v^{eff}(z)/r_s^{eff}(z))^2$, it may be shown that, for an appropriate choice of ansatz for $r_s^{eff}(z)$ and $r_v^{eff}(z)$, $\beta^{eff}(z) = \beta = 1$ for $r_s = r_v$ and the resulting analogue of the logarithmic term $\ln(\sqrt{\beta})$ (i.e. $\ln(\sqrt{\beta^{eff}(z)})$) also vanishes.

5.4 Introduction of the modified action and pinched string ansatz

We now introduce z -dependent couplings in both the scalar and vector fields of the standard Abelian-Higgs model. However, although the couplings are coordinate dependent, they are *not* treated as fundamental fields in the same way as ϕ and \vec{A} .¹⁰

We are interested in static, non-cylindrically-symmetric solutions to the resulting covariant EOM¹¹ and must therefore modify the ansatz (5.7) to include some form of z -dependence. Crucially, we wish our new solution to represent a string which interpolates between energetically degenerate regions of vortex/anti-vortex solutions to the EOM and hence we anticipate the existence of Planck-sized regions in which vorticity itself cannot be defined and which separate neighbouring string sections labelled by $\pm |n|$. To this end, we find it necessary to parameterise our new couplings in terms of the winding number, such that¹²

$$\begin{aligned}\sqrt{\lambda} &\rightarrow \sqrt{\lambda}_{|n|}^{eff}(z) = \sqrt{\lambda} G_{\sqrt{\lambda}_{|n|}}(z) \\ e &\rightarrow e_{|n|}^{eff}(z) = e G_{e_{|n|}}(z)\end{aligned}\tag{5.77}$$

where $G_{\sqrt{\lambda}_{|n|}}(z) \in [1, r_s/|n|l_p]$ and $G_{e_{|n|}}(z) \in [1, r_v/|n|l_p]$ are dimensionless functions.

This implies the existence of z -dependent scalar and vector boson masses (also parameterised by $|n|$) and hence of z -dependent effective radii for the scalar and vector cores. In other words, a non-cylindrical string can be found from the correspondence

$$\begin{aligned}r_s &\rightarrow r_{s|n|}^{eff}(z) = (\sqrt{\lambda}_{|n|}^{eff}(z)\eta)^{-1} \\ r_v &\rightarrow r_{v|n|}^{eff}(z) = (\sqrt{2}e_{|n|}^{eff}(z)\eta)^{-1}.\end{aligned}\tag{5.78}$$

¹⁰We will see later that this ‘‘phenomenological device’’ admits a relatively natural interpretation in the proposed dual wound-string picture.

¹¹Following some reasonable simplifying assumptions, these solutions become formally equivalent to the cylindrically symmetric vortex solutions of the standard Abelian-Higgs model, using the substitutions $\sqrt{\lambda} \longleftrightarrow \sqrt{\lambda}_{|n|}^{eff}(z)$ and $e \longleftrightarrow e_{|n|}^{eff}(z)$ (see section 5.5).

¹²We will later see that the approximation $r_s, r_v \gg |n|l_p$ allows us to dispense with the parameterisation of the couplings in terms of $|n|$ when calculating the periodic tension (i.e. so that $\sqrt{\lambda}_{|n|}^{eff}(z) \rightarrow \sqrt{\lambda}^{eff}(z)$ and $e_{|n|}^{eff}(z) \rightarrow e^{eff}(z)$). For now though, we must retain them in order to demonstrate the validity of our solution.

By analogy with the cylindrically symmetric case, we may define new dimensionless variables by

$$\begin{aligned} R_s &\rightarrow R_{s|n|}^{eff}(z) = \frac{r}{r_{s|n|}^{eff}(z)} \\ R_v &\rightarrow R_{v|n|}^{eff}(z) = \frac{r}{r_{v|n|}^{eff}(z)} \end{aligned} \quad (5.79)$$

and new r and z -dependent functions (also paramaterised in $|n|$) $F_{|n|}(r, z)$ and $A_{|n|}(r, z)$ via

$$\begin{aligned} F(r) &\equiv F(R_s) \rightarrow F_{|n|}(r, z) \equiv F(R_{s|n|}^{eff}(z)) \\ A(r) &\equiv A(R_v) \rightarrow A_{|n|}(r, z) \equiv A(R_{v|n|}^{eff}(z)). \end{aligned} \quad (5.80)$$

However, for now we leave the form of the z -dependence in these functions *unspecified* and deal with the most general EOM.

In order to describe the existence of regions of $+|n|$ and $-|n|$ winding, as well as to account for the Planck-sized regions which mark the transitions and in which $|n|$ itself becomes *undefined*, we must introduce a step-like function $H_{|n|}(z)$ into the scalar and gauge field ansatzes, with three discrete ranges

$$H_{|n|} : z \rightarrow \{-1, 0, +1\} \forall z \in \mathbb{R}. \quad (5.81)$$

Our general modified ansatz then takes the form

$$\begin{aligned} \phi_{|n|}(r, \theta, z) &= F_{|n|}(r, z) e^{i|n|H_{|n|}(z)\theta} \\ A_{|n|\theta}(r, z) &= -\frac{|n| H_{|n|}(z)}{e_{|n|}^{eff}(z)} A_{|n|}(r, z). \end{aligned} \quad (5.82)$$

Specifically, we choose to define the function $H_{|n|}(z)$ as

$$H_{|n|}(z) = \begin{cases} 0 & \text{if } m\Delta - |n|l_p \leq z \leq m\Delta + |n|l_p \\ +1 & \text{if } 2m\Delta + |n|l_p < (2m+1)\Delta - |n|l_p \\ -1 & \text{if } (2m+1)\Delta - |n|l_p < (2m+1)\Delta + |n|l_p, \end{cases}$$

where $m \in \mathbb{Z}$ and Δ is some scale characterising the length of a section of $\pm |n|$ string (which we expect to satisfy $\Delta \geq r_s, r_v$). We then see that $H_{|n|}(z)$ admits a representation in terms of a superposition of Heaviside step functions $\Theta(z)$, specified over appropriate ranges, such

that

$$H_{|n|}(z) = \begin{cases} \Theta(z - 2m\Delta - |n|l_p), & 2m\Delta - |n|l_p \leq z < (2m+1)\Delta - |n|l_p \\ \Theta(-(z - (2m+1)\Delta - |n|l_p)), & 2m\Delta + |n|l_p < z \leq (2m+1)\Delta + |n|l_p \\ -\Theta(z - (2m+1)\Delta - |n|l_p), & 2(m+1)\Delta - |n|l_p \leq z < 2(m+1)\Delta - |n|l_p \\ -\Theta(-(z - 2(m+1)\Delta - |n|l_p)), & (2m+1)\Delta + |n|l_p < z \leq 2(m+1)\Delta + |n|l_p. \end{cases}$$

For future reference we note that the square of $H_{|n|}(z)$ is

$$H_{|n|}^2(z) = \begin{cases} 0 & \text{if } m\Delta - |n|l_p \leq z \leq m\Delta + |n|l_p \\ 1 & \text{if } (m+1)\Delta + |n|l_p \leq z \leq (m+1)\Delta - |n|l_p \end{cases}$$

or equivalently

$$H_{|n|}^2(z) = \begin{cases} 0 & \text{if } \Theta(z - m\Delta - |n|l_p), \quad m\Delta - |n|l_p \leq z < (m+1)\Delta - |n|l_p \\ 1 & \text{if } \Theta(z - m\Delta + |n|l_p), \quad m\Delta + |n|l_p < z \leq (m+1)\Delta + |n|l_p. \end{cases}$$

and that its first derivative, the square of its first derivative and its second derivative, are defined as

$$\begin{aligned} \frac{dH_{|n|}(z)}{dz} &= \sum_{m=-\infty}^{\infty} [\delta(z - 2m\Delta - |n|l_p) + \delta(z - 2m\Delta + |n|l_p)] \\ &- \sum_{m=-\infty}^{\infty} [\delta(z - (2m+1)\Delta - |n|l_p) + \delta(z - (2m+1)\Delta + |n|l_p)], \end{aligned} \quad (5.83)$$

$$\left(\frac{dH_{|n|}(z)}{dz}\right)^2 = \sum_{m=-\infty}^{\infty} [\delta^2(z - m\Delta - |n|l_p) + \delta^2(z - m\Delta + |n|l_p)], \quad (5.84)$$

and

$$\begin{aligned} \frac{d^2H_{|n|}(z)}{dz^2} &= \sum_{m=-\infty}^{\infty} [\delta'(z - 2m\Delta - |n|l_p) + \delta'(z - 2m\Delta + |n|l_p)] \\ &- \sum_{m=-\infty}^{\infty} [\delta'(z - (2m+1)\Delta - |n|l_p) + \delta'(z - (2m+1)\Delta + |n|l_p)], \end{aligned} \quad (5.85)$$

where the prime represents differentiation with respect to z . Although the mathematical definition of $H_{|n|}(z)$ is complicated, the function itself is easy to visualise and is shown in figure 5.1.

Note that the Planck-sized regions where $H_{|n|}(z) = 0$ do *not* represent genuine discontinuities in the phase of the complex field or in the rotational direction of the gauge current. Rather they represent regions where both the phase θ and the winding number $|n|$ (or

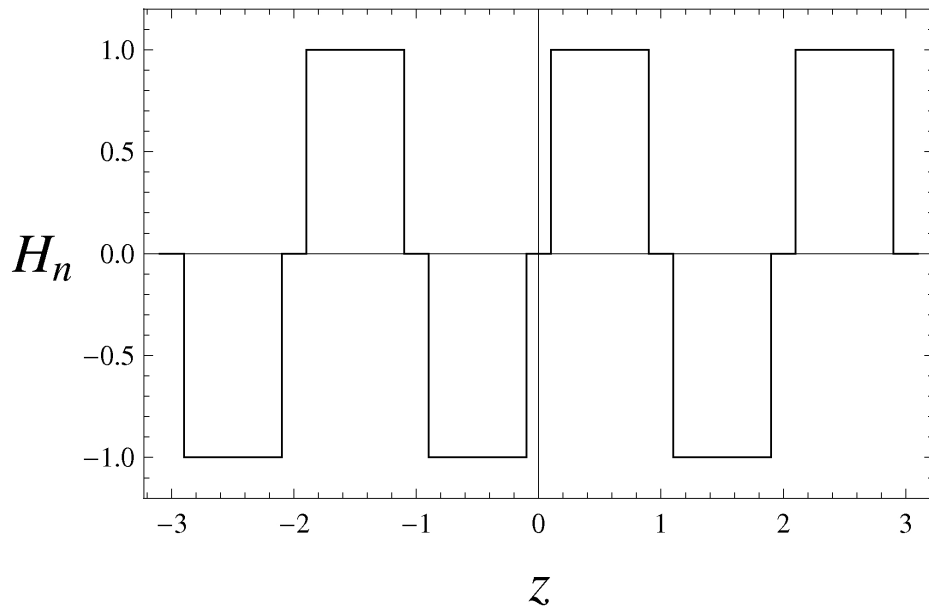


Figure 5.1: $H_{|n|}(z)$ in the range $-3\Delta \leq z \leq 3\Delta$ with $\Delta = 1$ and $|n|l_p = 0.1$.

equivalently the magnetic flux quantum number) are *undefined*. We may therefore set

$$\theta = |n| = A_{|n|}(r, z) = 0 \quad \forall r \leq |n|l_p, z \in [m\Delta \pm |n|l_p] \quad (5.86)$$

without loss of generality.¹³ It is not possible (or meaningful) to localise the string core on length scales $\Delta r < \mathcal{O}(l_p)$ or $\Delta z < \mathcal{O}(l_p)$. Furthermore, we may assume that only a change in topological number of ± 1 will occur (on average) within a Planck-sized region, so that it is not possible to define continuous changes in $|n|$ over scales of $\Delta r < l_p$ or $\Delta z < l_p$, though we propose that this does *not* necessarily mean that discrete jumps in the topological winding number cannot take place over Planck-sized distances.¹⁴ The change from a $+|n|$ to a $-|n|$ winding state must therefore take place over a distance $\Delta z \approx 2|n|l_p$. The winding number $|n|$ is still undefined over the *entire* range $\Delta z \approx 2|n|l_p$, but a change in winding number of $\pm 2|n|$ cannot take place over a smaller distance. It is not, however, meaningful to ascribe a definite change in topological winding number of ± 1 to a *specific* Planck length within Δz .

¹³This is like setting $\theta = 0$ when $r = 0$ in a polar coordinate system. Technically, an angular position may only be defined for $r > 0$, so that assigning θ a value at $r = 0$ is not physically meaningful. By convention, it may be set equal to zero.

¹⁴Topological considerations prevent an $|n_1|$ vortex from morphing continuously into an $|n_2|$ vortex ($|n_1| \neq |n_2|$) over length scales $\Delta z \gg l_p$, as there exists no diffeomorphism which *smoothly* maps one state to the other. Discontinuities are also usually considered unphysical. However, on distances $\Delta z \sim l_p$ there exist no *smooth* maps at all! We argue that there is nothing, in principle, to prevent the topological winding number from changing discontinuously as long as it does so in a region where the discontinuity of space is also manifest, i.e. over $\Delta z \sim \mathcal{O}(l_p)$.

It therefore seems natural to assume that $|n|$ may change (on average) by at most ± 1 over a single Planck length l_p and that the winding number is *genuinely* undefined at $r = 0$ (where θ is also undefined), so that it may be set equal to zero without loss of generality. This implies that, as we traverse the *fundamental* string core, the absolute value of the winding number changes from $|n|$ to zero and then back up to $|n|$. This requires a distance of $\Delta r = 2|n|l_p$, so that

$$r_s, r_v \geq |n|l_p. \quad (5.87)$$

The same bound can also be obtained in a different way. If we assume that is not meaningful for the phase of a complex field θ to vary continuously over Planck sized distances, we may estimate the maximum rate of change with respect to the physical angular coordinate ϑ at the string core boundary r_i , $i \in \{s, v\}$, via $|\frac{d\theta}{d\vartheta}|_{r=r_i} \approx \frac{\Delta\theta}{\Delta\vartheta} \leq \frac{2\pi r_i}{l_p}$. But when $\Delta\vartheta = 2\pi$, we have $\Delta\theta = 2\pi|n|$, which recovers the relation above (5.87). This is the same as the statement that if the natural unit of phase is one radian, a *phase change* of $\Delta\theta = 1 \text{ rad}$ cannot take place over a distance $\Delta s = r\Delta\theta < l_p$ on the circumference of a circle. ¹⁵

5.5 Equations of motion for a pinched string

Turning our attention now to the EOM for the non-cylindrical string, we see that substituting the ansatz (5.82) into the appropriately modified versions of (5.2)-(5.4) gives rise to the following scalar and vector equations

$$\begin{aligned} 0 &= \frac{\partial^2 F_{|n|}}{\partial r^2} + \frac{1}{r} \frac{\partial F_{|n|}}{\partial r} + \frac{|n|^2 H_{|n|}^2}{r^2} (A_{|n|}^2 - 1) + \frac{1}{(r_{s|n|}^{eff})^2} \cdot \frac{1}{2} F_{|n|} (F_{|n|}^2 - 1) + \frac{\partial^2 F_{|n|}}{\partial z^2} \\ &- i|n|\theta \left\{ F_{|n|} \frac{d^2 H_{|n|}}{dz^2} + 2 \frac{\partial F_{|n|}}{\partial z} \frac{dH_{|n|}}{dz} \right\} - |n|^2 \theta^2 F_{|n|} \left(\frac{dH_{|n|}}{dz} \right)^2 \end{aligned} \quad (5.88)$$

¹⁵The fact that, for a string with winding number $\pm|n|$, it is not possible to localise the string core on scales $\Delta r < 2|n|l_p$ may also be explained in yet another way. As stated in the first footnote of this chapter, the Abelian-Higgs model has a condensed matter analogue [325]-[331] in the field of superconductivity [332, 333]. In this analogue system (see [114]), symmetry is broken *dynamically* when free electrons “coalesce” to form Cooper pairs, resulting in a transition to a lower energy (superconducting) state with degenerate *effective* vacua in which magnetic flux lines (from any external magnetic field) are confined within highly localised flux tubes (see also [332, 333]). This implies that the Higgs field which mediates spontaneous symmetry-breaking *statically* may not be fundamental, and may instead be interpreted as a phenomenological device which effectively models some underlying (but as yet unknown) dynamical process. Formally, the order parameter of the Abelian-Higgs model (i.e. the phase θ) is equivalent to the Cooper pair (Bogolubov) wavefunction of a superconducting fluid. Considering this in conjunction with the uncertainty principle (including wavefunction-dependent terms) suggests that the minimum scale on which θ can be defined is $\sim l_p$. We take this to imply that the minimum range over which graduated changes in the scalar field ϕ may occur is *also* $\sim l_p$. This applies equally to the real and imaginary parts, or equivalently to both the phase *and* the magnitude of the complex field. In addition, the natural unit for the phase θ is one radian, which together with the considerations above, implies that a phase change of $\Delta\theta = \pm 1$ may not take place over a distance $\Delta r < l_p$ and hence gives rise to the condition (5.87).

and

$$\begin{aligned}
 0 &= H_{|n|} \left(\frac{\partial^2 A_{|n|}}{\partial r^2} - \frac{1}{r} \frac{\partial A_{|n|}}{\partial r} - \frac{1}{(r_{v|n|}^{eff})^2} (A_{|n|} - 1) \right) \\
 &+ \frac{1}{r_{v|n|}^{eff}} \left\{ r_{v|n|}^{eff} H_{|n|} \frac{\partial^2 A_{|n|}}{\partial z^2} + r_{v|n|}^{eff} \frac{d^2 H_{|n|}}{dz^2} A_{|n|} + \frac{d^2 r_{v|n|}^{eff}}{dz^2} H_{|n|} A_{|n|} \right\} \\
 &+ \frac{2}{r_{v|n|}^{eff}} \left\{ r_{v|n|}^{eff} \frac{dH_{|n|}}{dz} A_{|n|} + \frac{dr_{v|n|}^{eff}}{dz} H_{|n|} A_{|n|} + r_{v|n|}^{eff} H_{|n|} \frac{\partial A_{|n|}}{\partial z} \right\}. \quad (5.89)
 \end{aligned}$$

Considering (5.88) first, we see that the imaginary part must be set equal to zero independently. However, the considerations above imply that the phase θ is effectively *undefined* not only at $r = 0$ but *for all* $r \leq |n| l_p$ over the Planck-sized regions in which $H_{|n|}(z) = 0$, $z \in [m\Delta - |n| l_p, m\Delta + |n| l_p]$. We may therefore set $\theta = 0$ in this region without loss of generality, according to (5.86).

In the regions where $H_{|n|}(z) = \pm 1$ ($z \notin [m\Delta - |n| l_p, m\Delta + |n| l_p]$), θ may be defined consistently but each term in the curly brackets goes to zero independently and so the imaginary component vanishes for all z . This argument is equivalent to multiplying the entire equation by $H_{|n|}(z)$ and setting either $H_{|n|}(z) = 0$ or the sum of terms which it multiplies equal to zero in alternate regions. Similar considerations hold for the term proportional to θ^2 on the third line, so the final form of the scalar EOM is

$$0 = \frac{\partial^2 F_{|n|}}{\partial r^2} + \frac{1}{r} \frac{\partial F_{|n|}}{\partial r} + \frac{|n|^2}{r^2} (A_{|n|}^2 - 1) + \frac{1}{(r_{s|n|}^{eff})^2} \cdot \frac{1}{2} F_{|n|} (F_{|n|}^2 - 1) + \frac{\partial^2 F_{|n|}}{\partial z^2} \quad (5.90)$$

where we consider *only* the regions in which $H_{|n|}^2 = 1$.

We may adopt the same strategy when dealing with the vector EOM, which shows that *all* the terms in the curly brackets go to zero for *all* z except the term proportional to $H_{|n|} \frac{\partial^2 A_{|n|}}{\partial z^2}$. This must be included in the final form of the EOM,

$$0 = \frac{\partial^2 A_{|n|}}{\partial r^2} - \frac{1}{r} \frac{\partial A_{|n|}}{\partial r} - \frac{1}{(r_{v|n|}^{eff})^2} (A_{|n|} - 1) + \frac{\partial^2 A_{|n|}}{\partial z^2} \quad (5.91)$$

where again we need only consider regions in which $H_{|n|}^2 = 1$.

This approach is equivalent to treating the Planck-scale regions as a “black box” for which we have no effective theory in the field picture. Although we have no explicit expressions for the scalar and vector field functions $F_{|n|}$ and $A_{|n|}$ with which to calculate the tension of the string within the ranges $z \in [m\Delta \pm |n| l_p]$, we will later *assume* a tension of $\sim 2\pi\eta^2 |n|^2$

in these regions to ensure the continuity of $\mu_{|n|}(z)$. Although this is somewhat unsatisfactory, we will see that both the assumed tension for the Planck-scale sections and the spatial localisation of the string core on scales $\sim |n|l_p$ admit natural explanations in the string picture (see section 5.7), which we propose as a justification for the assumptions made here.

However, we must acknowledge that, using our current approach, it is impossible to obtain solutions for $F_{|n|}(r, z)$ and $A_{|n|}(r, z)$ in the regions for which $H_{|n|}^2 = 0$ and that these remain essentially untreated in our present analysis. Clearly, if the solutions we obtain in the regions where $H_{|n|}^2 = 1$ are to be viewed as physical, the Planck-sized regions which connect sections of vortex/anti-vortex string must be dealt with independently, in such a way as to ensure continuity with respect to the string tension $\mu_{|n|}(z)$. This problem will be dealt with in the following section, in which $\mu_{|n|}(z)$ is calculated explicitly.¹⁶

Although we have yet to specify the exact form of the z -dependence of $F_{|n|}(r, z)$ and $A_{|n|}(r, z)$ (in the regions for which $H_{|n|}^2 \neq 0$), we may still use our physical intuition to impose appropriate boundary conditions. It is reasonable to assume that boundary conditions analogous to those imposed on $f(r)$ and $\alpha(r)$ still hold for *any* value of z - just as they did in the cylindrically symmetric case - so

$$F_{|n|}(r, z) = \begin{cases} 0 & \text{if } r = 0 \quad \forall z \\ 1 & \text{if } r \rightarrow \infty \quad \forall z \end{cases} \quad (5.92)$$

and

$$A_{|n|}(r, z) = \begin{cases} 0 & \text{if } r = 0 \quad \forall z \\ 1 & \text{if } r \rightarrow \infty \quad \forall z. \end{cases} \quad (5.93)$$

The only problem that remains is how to specify “large” and “small” r for a given value of z . In the cylindrically symmetric case, this was easily solved, as the length scales r_s and r_v determined the radii of the scalar and vector cores, respectively, at every point along the string. In the non-cylindrically symmetric case, therefore, we may expect the proposed substitutions (5.78)-(5.80) to imply the following (more specific) boundary conditions on the related functions F and A :

$$F(R_{|n|s}^{eff}(z)) = \begin{cases} 0 & \text{if } R_{|n|s}^{eff}(z) \rightarrow 0 \quad (r \ll r_{|n|s}^{eff}(z)) \\ 1 & \text{if } R_{|n|s}^{eff}(z) \rightarrow \infty \quad (r \gg r_{|n|s}^{eff}(z)) \end{cases} \quad (5.94)$$

and

$$A(R_{|n|v}^{eff}(z)) = \begin{cases} 0 & \text{if } R_{|n|v}^{eff}(z) \rightarrow 0 \quad (r \ll r_{|n|v}^{eff}(z)) \\ 1 & \text{if } R_{|n|v}^{eff}(z) \rightarrow \infty \quad (r \gg r_{|n|v}^{eff}(z)). \end{cases} \quad (5.95)$$

¹⁶Many thanks to V.M Red'kov for his insightful questions and comments regarding this point.

We then need only specify the forms of $r_{|n|s}^{eff}(z)$ and $r_{|n|v}^{eff}(z)$ precisely by introducing appropriate additional ansatzes and by verifying that these offer solutions to the EOM. To begin with we note that

$$\begin{aligned}\frac{\partial F_{|n|}}{\partial r} &= \frac{1}{r_{s|n|}^{eff}} \frac{dF}{dR_{s|n|}^{eff}}, \\ \frac{\partial^2 F_{|n|}}{\partial r^2} &= \frac{1}{(r_{s|n|}^{eff})^2} \frac{d^2 F}{d(R_{s|n|}^{eff})^2},\end{aligned}\tag{5.96}$$

$$\begin{aligned}\frac{\partial F_{|n|}}{\partial z} &= -\frac{1}{r_{s|n|}^{eff}} R_{s|n|}^{eff} \frac{dr_{s|n|}^{eff}}{dz} \frac{dF}{dR_{s|n|}^{eff}}, \\ \frac{\partial^2 F_{|n|}}{\partial z^2} &= \frac{1}{r_{s|n|}^{eff}} R_{s|n|}^{eff} \left[\frac{2}{r_{s|n|}^{eff}} \left(\frac{dr_{s|n|}^{eff}}{dz} \right)^2 - \frac{d^2 r_{|n|s}^{eff}}{dz^2} \right] \frac{dF}{R_{|n|s}^{eff}} \\ &\quad + \frac{1}{(r_{s|n|}^{eff})^2} (R_{s|n|}^{eff})^2 \left(\frac{dr_{s|n|}^{eff}}{dz} \right)^2 \frac{d^2 F}{d(R_{s|n|}^{eff})^2},\end{aligned}\tag{5.97}$$

with similar relations between $A_{|n|}(r, z)$ and $A(R_{s|n|}^{eff})$. The scalar EOM then becomes

$$\begin{aligned}0 &= \left[1 + (R_{s|n|}^{eff})^2 \left(\frac{dr_{s|n|}^{eff}}{dz} \right)^2 \right] \frac{d^2 F}{d(R_{s|n|}^{eff})^2} \\ &\quad + \left[1 + (R_{s|n|}^{eff})^2 \left\{ 2 \left(\frac{dr_{s|n|}^{eff}}{dz} \right)^2 - r_{s|n|}^{eff} \frac{d^2 r_{s|n|}^{eff}}{dz^2} \right\} \right] \frac{1}{R_{s|n|}^{eff}} \frac{dF}{dR_{s|n|}^{eff}} \\ &\quad + \frac{|n|^2 F}{(R_{s|n|}^{eff})^2} + \frac{1}{2} F(F^2 - 1) \left(\frac{r_{s|n|}^{eff}}{r_s} \right).\end{aligned}\tag{5.98}$$

By analogy with the cylindrically symmetric case, we may also write

$$\begin{aligned}0 &= \left[1 + (R_{v|n|}^{eff})^2 \left(\frac{dr_{v|n|}^{eff}}{dz} \right)^2 \right] \frac{d^2 F}{d(R_{v|n|}^{eff})^2} \\ &\quad + \left[1 + (R_{v|n|}^{eff})^2 \left\{ 2 \left(\frac{dr_{v|n|}^{eff}}{dz} \right)^2 - r_{v|n|}^{eff} \frac{d^2 r_{v|n|}^{eff}}{dz^2} \right\} \right] \frac{1}{R_{v|n|}^{eff}} \frac{dF}{dR_{v|n|}^{eff}} \\ &\quad + \frac{|n|^2 F}{(R_{v|n|}^{eff})^2} + \frac{1}{2} \beta_{|n|}^{eff} F(F^2 - 1)\end{aligned}\tag{5.99}$$

where we have defined

$$\beta_{|n|}^{eff}(z) = \left(\frac{r_{v|n|}^{eff}(z)}{r_{s|n|}^{eff}(z)} \right)^2. \quad (5.100)$$

Hence we see that, in the case of the pinched string, the assumptions $F = F(R_{s|n|}^{eff})$ and $F = F(R_{v|n|}^{eff})$ are equivalent, in correspondence with the cylindrically symmetric case.

The vector EOM becomes

$$\begin{aligned} 0 &= \left[1 + (R_{v|n|}^{eff})^2 \left(\frac{dr_{v|n|}^{eff}}{dz} \right)^2 \right] \frac{d^2 A}{d(R_{v|n|}^{eff})^2} \\ &+ \left[-1 + (R_{v|n|}^{eff})^2 \left\{ 2 \left(\frac{dr_{v|n|}^{eff}}{dz} \right)^2 - r_{v|n|}^{eff} \frac{d^2 r_{v|n|}^{eff}}{dz^2} \right\} \right] \frac{1}{R_{v|n|}^{eff}} \frac{dA}{dR_{v|n|}^{eff}} \\ &- F^2 (A - 1) \left(\frac{r_{v|n|}^{eff}}{r_v} \right)^2, \end{aligned} \quad (5.101)$$

so in the limit $r_{s|n|}^{eff}(z) \rightarrow r_s$, $r_{v|n|}^{eff}(z) \rightarrow r_v$ we recover the usual cylindrically symmetric equations (5.15)/(5.18) and (5.16).

We may proceed by specifying the conditions we wish $r_{s|n|}^{eff}(z)$ and $r_{v|n|}^{eff}(z)$ to satisfy. Let us assume that each function $r_{|n|i}^{eff}(z)$, $i \in \{s, v\}$, varies between two values $|n|l_p \leq r_{i|n|}^{eff}(z) \leq r_i$ (in accordance with conditions imposed along with the definitions (5.77) and (5.78)), such that

$$r_{i|n|}^{eff}(z = (m + 1/2)\Delta) = r_i \quad (5.102)$$

and

$$r_{i|n|}^{eff}(z) = |n|l_p \quad \forall z \in [m\Delta \pm |n|l_p]. \quad (5.103)$$

Additionally, we impose the following constraint on the derivatives in order to ensure continuity at the points $z = m\Delta \pm |n|l_p$,

$$\left| \frac{dr_{i|n|}^{eff}(z)}{dz} \right|_{z=m\Delta \pm |n|l_p} = 0, \quad (5.104)$$

which together with (5.103) also implies

$$\left| \frac{d^2 r_{i|n|}^{eff}(z)}{dz^2} \right|_{z=m\Delta \pm |n|l_p} = 0. \quad (5.105)$$

The most general form for the two functions $r_{i|n|}^{eff}(z)$ is

$$r_{i|n|}^{eff}(z) = A_{i|n|} G_i(B_{i|n|}(z + C_{i|n|})) + D_{i|n|} \quad (5.106)$$

where $\{G_i(z)\}$, $i \in \{s, v\}$, are periodic functions in z , valued between 0 and 1. The values of the constants $A_{i|n|}$, $B_{i|n|}$, $C_{i|n|}$ and $D_{i|n|}$ may be uniquely determined by requiring that $r_{i|n|}^{eff}(z)$ pass through the three points $(m\Delta + |n|l_p, |n|l_p)$, $((m + 1/2)\Delta, 1)$ and $((m + 1)\Delta - |n|l_p, |n|l_p) \forall m \in \mathbb{Z}$, together with the requirement that the first derivatives with respect to z are zero at the first and last points. Assuming that the functions $G_i(z)$ both have natural period π , this gives

$$r_{i|n|}^{eff}(z) = (r_i - |n|l_p) G_i\left(\frac{z - m\Delta - |n|l_p}{\pi^{-1}(\Delta - 2|n|l_p)}\right) + |n|l_p. \quad (5.107)$$

The variation of the scalar and vector core profiles (assuming non-critical coupling $r_v \neq r_s$) for a non-cylindrical ‘‘pinched’’ string are illustrated in figure 5.2 using $G_s(z) = G_v(z) = \sin^2(z)$ as an example ansatz.

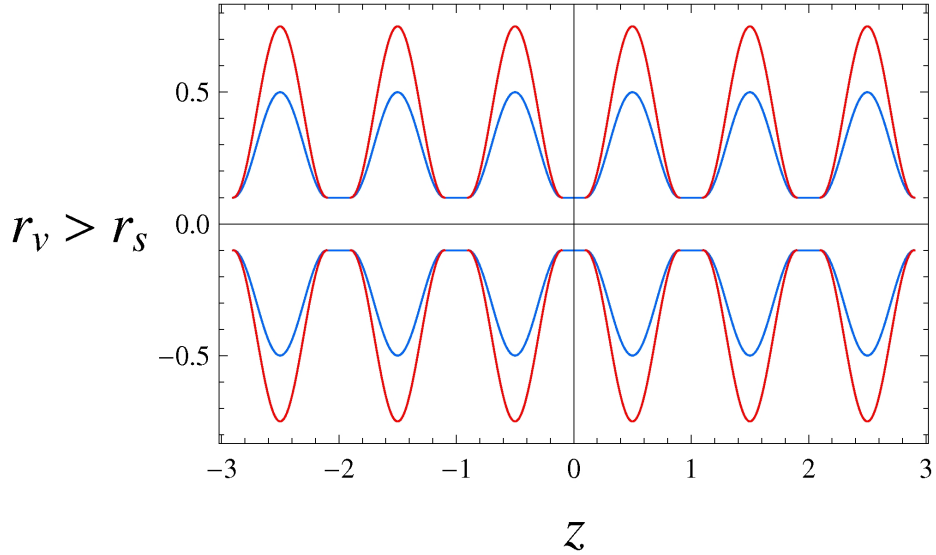


Figure 5.2: Profile of the pinched string solution in the range $-3\Delta \leq z \leq 3\Delta$, with $\Delta = 1$, $|n|l_p = 0.1$, $r_s = 0.5$ (blue curve) and $r_v = 0.75$ (red curve).

For later convenience, we note that for large r_i satisfying $r_i \gg |n|l_p$, we can make the

approximation

$$r_i^{eff}(z) \approx r_i G_i \left(\frac{\pi z}{\Delta} \right), \quad (5.108)$$

so that $r_{i|n|}^{eff}(z) \rightarrow r_i^{eff}(z)$ which becomes effectively *independent* of $|n|$. This also implies

$$\left| \frac{dG_i \left(\frac{\pi z}{\Delta} \right)}{dz} \right|_{z=m\Delta} = \left| \frac{dG_i \left(\frac{\pi z}{\Delta} \right)}{dz} \right|_{Z=(m+1/2)\Delta} = 0, \quad (5.109)$$

together with

$$\left| \frac{d^2 G_i \left(\frac{\pi z}{\Delta} \right)}{dz^2} \right|_{z=m\Delta} > 0, \quad \left| \frac{d^2 G_i \left(\frac{\pi z}{\Delta} \right)}{dz^2} \right|_{z=(m+1/2)\Delta} < 0. \quad (5.110)$$

In this limit, we may approximate the function $H_{|n|}(z)$ by the function $H(z)$, which is also independent of $|n|$ and defined via

$$H(z) = \begin{cases} 2\Theta(z - 2m\Delta) - 1, & (2m - 1)\Delta < z < (2m + 1)\Delta \\ -2\Theta(z - (2m + 1)\Delta) + 1, & 2m\Delta < z < (2m + 2)\Delta, \end{cases}$$

whose square is given by

$$H^2(z) = 1 \quad \forall z. \quad (5.111)$$

For future reference we note that

$$\frac{dH}{dz} = \sum_{m=-\infty}^{\infty} [\delta(z - 2m\Delta) - \delta(z - (2 + 1)m\Delta)], \quad (5.112)$$

$$\frac{d^2 H}{dz^2} = \sum_{m=-\infty}^{\infty} [\delta'(z - 2m\Delta) - \delta'(z - (2 + 1)m\Delta)], \quad (5.113)$$

$$\left(\frac{dH}{dz} \right)^2 = \sum_{m=-\infty}^{\infty} \delta^2(z - m\Delta). \quad (5.114)$$

In addition, in the limit $r_i \gg |n|l_p$, we also have $\beta_{|n|}^{eff}(z) \rightarrow \beta^{eff}(z)$ where

$$\beta^{eff}(z) = \left(\frac{r_v^{eff}(z)}{r_s^{eff}(z)} \right)^2 = \beta \left(\frac{G_v(z)}{G_s(z)} \right)^2. \quad (5.115)$$

If the z -dependence of r_s and r_v has the same functional form, i.e. if $G_s(z) = G_v(z) = G(z)$ so that

$$r_i^{eff}(z) \approx r_i G\left(\frac{\pi z}{\Delta}\right), \quad (5.116)$$

then the parameter $\beta^{eff}(z) \rightarrow \beta$ and becomes effectively independent of both $|n|$ and z . At critical coupling, therefore, it is also equal to unity.

Finally, defining the dimensionless variable Z by

$$Z \equiv \frac{\pi z}{\Delta}, \quad (5.117)$$

the functions $H(z)$, $r_i^{eff}(z) \approx r_i G_i(\pi z/\Delta)$ and $\beta^{eff}(z)$ may be rewritten as $H(Z)$, $r_i^{eff}(Z) \approx r_i G_i(Z)$ and $\beta^{eff}(Z)$ (this notation will be used later).

5.6 Solutions to the pinched string EOM

We are now at last able to turn our attention to the solutions of (5.98)/(5.99) and (5.101). If the terms in the square brackets in each equation satisfy

$$(R_{i|n|}^{eff})^2 \left(\frac{dr_{i|n|}^{eff}}{dz} \right)^2 \leq \mathcal{O}(1) \quad (5.118)$$

and

$$(R_{i|n|}^{eff})^2 \left\{ 2 \left(\frac{dr_{i|n|}^{eff}}{dz} \right)^2 - r_{i|n|}^{eff} \frac{d^2 r_{i|n|}^{eff}}{dz^2} \right\} \leq \mathcal{O}(1) \quad (5.119)$$

within the region of the effective string core (i.e. $R_{i|n|}^{eff} \leq 1$, or equivalently $r \leq r_{i|n|}^{eff}$), then the EOM take functional forms which are identical (to within an order of magnitude in the coefficients of the derivative terms) to those for the cylindrical symmetric ansatz, under the correspondences (5.78)-(5.80). They therefore admit functionally equivalent solutions under the same correspondences in both the small and large r limits, which may now be defined (for a given value of z) with respect to $r_{s|n|}^{eff}$ for the scalar EOM and $r_{v|n|}^{eff}$ for the vector EOM.

Let us consider first the constraint (5.118) which, using the definitions above, is approximately equivalent to

$$R_{i|n|}^{eff} \cdot \frac{r_i^2}{\Delta^2} (G'_i)^2 \leq 1 \quad (5.120)$$

where $R_i^{eff} = r/r_i^{eff}$ and a dash represents differentiation with respect to $Z = \pi z/\Delta$. Let us further assume that $G_i' \leq \mathcal{O}(1) \forall Z$,¹⁷ giving

$$\Delta \geq R_{i|n|}^{eff} r_i. \quad (5.121)$$

Since we are interested in the physics at scales $R_{i|n|}^{eff} \leq \mathcal{O}(1)$, this constraint is equivalent to the stronger condition

$$\Delta \geq r_i, \quad (5.122)$$

which appears reasonable on cosmic scales. As long as this condition is satisfied, we may be certain that the terms in the first set of square brackets in both the scalar and vector EOM are $\sim \mathcal{O}(1)$ for all r within the effective scalar and vector cores.

In fact, even for the limiting case $r_s \sim \Delta$, this still holds. Another way to think about this is to note that the former constraint (5.121) is equivalent to

$$r \leq \Delta \frac{r_{|n|i}^{eff}(z)}{r_i}. \quad (5.123)$$

Since $r_{|n|i}(z) \in [|n|l_p, r_i] \forall z$, this reduces to the minimum/maximum conditions,

$$r \leq \frac{\Delta |n| l_p}{r_i}, \quad z \in [m\Delta \pm |n|l_p] \quad (5.124)$$

or

$$r \leq \Delta, \quad z \rightarrow (m + 1/2)\Delta. \quad (5.125)$$

Hence the condition $\Delta \geq r_i$ implies that (5.121) is fulfilled for all $r \leq |n|l_p$ even at the boundaries of the region, i.e $z = m\Delta \pm |n|l_p$ (that is, for *all* r within the effective radius at *any* value of z).

It is also possible in this scenario to identify the distance between neighbouring pinches, Δ ,

¹⁷In the absence of a specific ansatz for $G_i(z)$, this assumption may be questioned. Realistically it is probably necessary to input an *initial*, smoothly varying, function $G_i(z)$ and to use that to calculate the initial forces acting on neighbouring string sections due to the interaction of the opposing magnetic fields. Ideally a dynamic theory will be developed, which describes the evolution of the string core ‘‘pinching’’ under the action of such forces. We may expect the pinching of the string to become increasingly localised in the central area of the neighbouring $\pm |n|$ regions, resulting in ever-increasing localisation of the string energy density. Ultimately, this would result in the formation of highly localised ‘‘beads’’, and of neighbouring bead-antibead pairs which repel each other. Furthermore, as we shall see later, each ‘‘pinch’’ in the physical radius of the string gives rise to *two* peaks in the effective tension (i.e. two beads or antibeads), associated with the points of maximum absolute gradient $(dr_i^{eff}/dz)^2$. Increasing localisation of the pinching therefore also corresponds to the coalescing of neighbouring $b - b$ and $\bar{b} - \bar{b}$ pairs, as well as the repulsion of neighbouring bs and $\bar{b}s$. It is therefore possible that this is the analogue of the creation of step-like windings in the formation of cosmic necklaces from *smoothly* wound strings, discussed in detail in chapter 3, which gives rise to similar phenomena. If so, we may hope that ultimately a future analysis of the interaction between neighbouring pinches may provide insights into the binding energy between neighbouring bead/antibead pairs in the wound-string picture (c.f. end of chapter 3 for a discussion of this point).

with *twice* the (average) distance between peaks in the periodic tension, i.e. between neighbouring beads or anti-beads (see later). In this case, by analogy with the wound-string necklaces discussed in chapter 3, it is possible to identify this with twice the correlation length of the string, ξ , so that the number of strings per Hubble volume is $\nu \propto \Delta^{-3} \propto \xi^{-3}$ and the average distance between neighbouring strings is of order Δ . It is likely therefore that condition (5.125) will always be fulfilled.¹⁸

A similar argument can be used to show that the terms in the second set of square brackets are also of order one (for the scalar EOM), or of order minus one (for the vector EOM), for all z . Imposing the bound (5.119) for *all* values of z requires

$$r^2 \{2(G'_i)^2 - G''_i\} \leq \Delta^2 G_i^2. \quad (5.126)$$

Now assuming that $G''_i(z) \sim G'_i(z) \sim \mathcal{O}(1) \forall z$, we have that

$$r \leq \Delta G_i(z) \quad (5.127)$$

which, accounting for the two limiting values of $r_{|n|i}^{eff}$, again gives rise to the minimum/maximum constraints (5.124) and (5.125) above.

These arguments imply that the rate of change of $F_{|n|}(r, z)$ (or $F(R_{s|n|}^{eff}(z))$) and $A_{|n|}(r, z)$ (or $A(R_{v|n|}^{eff}(z))$) with respect to z is sufficiently small at *any* value of r to make z -derivative terms in the Euler-Lagrange equations negligible, so long as we are restricted to the ranges $r \leq r_{s|n|}^{eff}$ and $r \leq r_{v|n|}^{eff}$, respectively, and so the long as the condition $r_s, r_v \leq \Delta$ holds. Though it is possible, in principle, that the physics of non-cylindrically symmetric strings in the asymptotic limit differs substantially from that of cylindrically symmetric strings beyond these ranges, it seems unlikely that this would cause significant problems, as the energy density of the field configuration tends rapidly to zero for $r \geq r_{v|n|}^{eff}(z)$ since $F \approx A \approx 1$. In addition, if we are able to identify Δ with the correlation length ξ , then $\Delta \gg r_s, r_v$ becomes a natural cut-off for r in accordance with (5.125).

It is reasonable to assume $r_i \leq \Delta$ if we regard the pinch as a “kink” or “twist” in the string (by analogy with our common sense ideas about ordinary lengths of string/rope). The condition is then equivalent to the statement that it is impossible to twist a length of rope through 360 degrees over a region less than the length of its diameter.

¹⁸However, in principle, $\Delta \sim r_s, r_v$, may occur, in which case it is doubtful whether the correspondence $\Delta \sim \xi$ may be maintained, except shortly after the epoch of the string network formation. Nonetheless, in a fully dynamical theory of pinched string formation/evolution an explicit model of $\Delta(t)$ could be obtained, which may also allow the correspondence $\Delta(t) \sim \xi(t)$ to hold for all t . This prospect is discussed briefly in section 5.8.

In the limit $r_s \leq \Delta$, therefore, the scalar EOM reduces to either

$$0 = \frac{d^2 F}{d(R_{s|n|}^{eff})^2} + \frac{1}{R_{s|n|}^{eff}} \frac{dF}{dR_{s|n|}^{eff}} + \frac{|n|^2 F}{(R_{s|n|}^{eff})^2} + \frac{1}{2} F(F^2 - 1) \quad (5.128)$$

or

$$0 = \frac{d^2 F}{d(R_{v|n|}^{eff})^2} + \frac{1}{R_{v|n|}^{eff}} \frac{dF}{dR_{v|n|}^{eff}} + \frac{|n|^2 F}{(R_{v|n|}^{eff})^2} + \frac{1}{2} \beta_{|n|}^{eff} F(F^2 - 1) \quad (5.129)$$

for all $r \leq r_{s|n|}^{eff}(z)$. In the limit $r_v \leq \Delta$ ($r_s \leq r_v$),¹⁹ the vector EOM reduces to

$$0 = \frac{d^2 A}{d(R_{v|n|}^{eff})^2} - \frac{1}{R_{v|n|}^{eff}} \frac{dA}{dR_{v|n|}^{eff}} - F^2(A - 1) \left(\frac{r_{v|n|}^{eff}}{r_v} \right)^2 \quad (5.130)$$

for all $r \leq r_{|n|v}^{eff}(z)$. In the uncoupled regime (i.e. setting $A = 0$), equation (5.128) has the small r solution

$$F(R_{s|n|}^{eff}) \approx (R_{s|n|}^{eff})^{|n|} \quad (5.131)$$

for $r \leq r_{s|n|}^{eff}(z)$, which is in accord with our physical intuition regarding the effective radius of the scalar core. Likewise, equation (5.129) has the small r solution

$$F(R_{|n|v}^{eff}) \approx (\sqrt{\beta_{|n|}^{eff}} R_{v|n|}^{eff})^{|n|}, \quad (5.132)$$

which is equivalent.

Similarly, in the uncoupled regime (i.e. setting $F = 0$), equation (5.130) admits the approximate solution

$$A(R_{v|n|}^{eff}) \approx (R_{v|n|}^{eff})^2 \quad (5.133)$$

for $r \leq r_{v|n|}^{eff}(z)$. Clearly, the correct asymptotic solutions in both the uncoupled and coupled regimes (together with the higher order corrections to the small r solutions in the latter) will be formally analogous to those given for the cylindrical string in the previous section, under the correspondences (5.78)-(5.80). However, we need not state them explicitly here. More important to our immediate task are the results (5.131) and (5.133), which we now use to calculate the periodic string tension $\mu_{|n|}(z)$ for the pinched string ansatz in the next section.

¹⁹This is automatically satisfied for a type II superconducting regime.

5.7 Calculation of the (periodic) string tension for non-cylindrically symmetric string $\mu_{|n|}(z)$

When calculating the approximate z -dependent tension $\mu_{|n|}(z)$ for the pinched string, we begin by considering the limit $r_i \gg |n|l_p$, $i \in \{s, v\}$.²⁰ There then exist exact analogues of all the terms which appear in the (constant) string tension $\mu_{|n|}$ of a cylindrically symmetric string, according to the correspondence

$$\begin{aligned} f &\longleftrightarrow F, \\ \alpha &\longleftrightarrow A, \\ r_i &\longleftrightarrow r_i^{eff}(z), \\ \beta &\longleftrightarrow \beta^{eff}(z) \end{aligned} \tag{5.134}$$

and $d \longleftrightarrow \partial$ where necessary.²¹ The D_r and D_θ terms of the gradient energy give contributions of the form

$$\begin{aligned} &\int_0^{2\pi} d\theta \int_0^{r_s^{eff}(z)} D_r \phi \bar{D}' \bar{\phi} r dr + \int_0^{2\pi} d\theta \int_0^{r_s^{eff}(z)} D_\theta \phi \bar{D}^\theta \bar{\phi} r dr \\ &= 2\pi\eta^2 \int_0^{r_s^{eff}(z)} \left(\frac{\partial F}{\partial r}\right)^2 r dr + 2\pi\eta^2 \int_0^{r_s^{eff}(z)} \frac{|n|^2 F^2}{r^2} (A-1)^2 r dr \\ &\approx 2 \times \frac{2\pi\eta^2 |n|^2}{(r_s^{eff}(z))^{2|n|}} \times \frac{1}{2|n|} (r_s^{eff}(z))^{2|n|} \approx 2\pi\eta^2 |n|, \end{aligned} \tag{5.135}$$

so exchanging $r_s \longleftrightarrow r_s^{eff}(z)$ makes no difference to the result of the calculation, as all factors of *either* r_s or $r_s^{eff}(z)$ cancel exactly in the final step. In the range $r_s^{eff}(z) \leq r \leq r_v^{eff}(z)$, the interchange of variables also makes no difference to the *form* of the contribution from the angular term, which is given by

$$\begin{aligned} \int_0^{2\pi} d\theta \int_{r_s^{eff}(z)}^{r_v^{eff}(z)} \eta^2 \frac{|n|^2 F^2}{r^2} (A^2 - 1)^2 r dr &\approx 2\pi\eta^2 |n|^2 \int_{r_s^{eff}(z)}^{r_v^{eff}(z)} \frac{dr}{r} \\ &= 2\pi\eta^2 |n|^2 \ln \left(\sqrt{\beta^{eff}(z)} \right). \end{aligned} \tag{5.136}$$

²⁰In all the calculations that follow, we use the approximations $\sqrt{\lambda_{|n|}^{eff}}(z) \rightarrow \sqrt{\lambda}^{eff}(z)$ and $e_{|n|}^{eff}(z) \rightarrow e^{eff}(z)$, so that the field couplings are effectively independent of $|n|$. This is equivalent to assuming $r_{v|n|}^{eff}(z) \rightarrow r_v^{eff}(z)$ and $r_{s|n|}^{eff}(z) \rightarrow r_s^{eff}(z)$ for $r_v, r_s \gg |n|l_p$.

²¹We have also used the fact that $H_{|n|}^2(z) \rightarrow H^2(z) = 1 \forall z$.

5.7. CALCULATION OF THE (PERIODIC) STRING TENSION FOR
NON-CYLINDRICALLY SYMMETRIC STRING $\mu_{|n|}(z)$

However, in addition there now exists a new D_z term in the derivative, which leads to

$$\begin{aligned} \int_0^{2\pi} d\theta \int_0^{r_s^{eff}(z)} D_z \phi \bar{D}^z \bar{\phi} r dr &= 2\pi \int_0^{r_s^{eff}(z)} \eta^2 \left(\frac{\partial F}{\partial z} \right)^2 r dr \\ &\approx 2\pi \eta^2 |n|^2 \frac{1}{|n|+1} \times \frac{1}{(r_s^{eff}(z))^{2|n|+2}} \left(\frac{dr_s^{eff}}{dz} \right)^2 \int_0^{r_s^{eff}(z)} r^{2|n|+1} dr \\ &\approx \pi \eta^2 |n|^2 \frac{1}{|n|+1} \left(\frac{dr_s^{eff}}{dz} \right)^2 \approx \pi \eta^2 |n| \times \frac{r_s^2}{\Delta^2} (G'_s)^2. \end{aligned} \quad (5.137)$$

Likewise, the contribution from the potential term is formally equivalent under the correspondence $r_s \longleftrightarrow r_s^{eff}(z)$, which gives

$$\begin{aligned} \int_0^{2\pi} d\theta \int_0^{r_s^{eff}(z)} V(|\phi|) r dr &= 2\pi \eta^2 \times \frac{1}{2(r_s^{eff})^2} \int_0^{r_s^{eff}(z)} F(F^2 - 1)^2 r dr \\ &\approx \frac{\pi \eta^2}{(r_s^{eff}(z))^2} \int_0^{r_s^{eff}(z)} F r dr \approx \frac{\pi \eta^2}{|n|+2}. \end{aligned} \quad (5.138)$$

Turning our attention to the gauge field term, we see that the contribution from the z -component of the magnetic flux B_z is analogous to that for the cylindrically symmetric case, so

$$\begin{aligned} \int_0^{2\pi} d\theta \int_0^{r_v^{eff}(z)} \frac{1}{2} B_z B^z r dr &= \pi \times \frac{|n|^2}{2(e^{eff}(z))^2} \int_0^{r_v^{eff}(z)} \frac{1}{r^2} \left(\frac{\partial A}{\partial r} \right)^2 r dr \\ &\approx \frac{2\pi |n|^2}{(e^{eff}(z))^2} \times \frac{1}{2} \frac{1}{(r_v^{eff}(z))^2} \approx 2\pi \eta^2 |n|^2. \end{aligned} \quad (5.139)$$

The only contribution left to calculate comes from the new radial \vec{B} -field component, $B_r = F_{z\theta}$. Recall that our new gauge field ansatz is

$$\begin{aligned} A_{|n|\theta} &= -\frac{|n|H(z)}{e^{eff}(z)} A(r, z) \\ &= -\sqrt{2}\eta |n| r_v^{eff}(z) H(z) A(r, z), \end{aligned} \quad (5.140)$$

so

$$\begin{aligned} B_r = F_{z\theta} &= \partial_z A_\theta \\ &= -\sqrt{2}\eta |n| \frac{\partial}{\partial z} (r_v^{eff}(z) H A) \\ &= -\sqrt{2}\eta |n| \left\{ r_v^{eff}(z) \frac{\partial A}{\partial z} H + r_v^{eff}(z) A \frac{dH}{dz} + \frac{dr_v^{eff}}{dz} A H \right\}. \end{aligned} \quad (5.141)$$

In the limit $r_v, r_s \gg |n|l_p$, we have that $\frac{dH}{dz} = 0$ for all z where $r_v^{eff}(z) \neq 0$ and $A \neq 0$ (i.e. for $z \neq m\Delta$). We also have $r_v^{eff}(z) = A = 0$ for all z where $\frac{dH}{dz} \neq 0$ (i.e. at $z = m\Delta$).

5.7. CALCULATION OF THE (PERIODIC) STRING TENSION FOR
NON-CYLINDRICALLY SYMMETRIC STRING $\mu_{|n|}(z)$

Together, these imply that the second term inside the brackets is zero for all z .²² The second term inside the curly brackets therefore vanishes, so that

$$B_r = -\sqrt{2}\eta|n| \left\{ r_v^{eff}(z) \frac{\partial A}{\partial z} H + \frac{dr_v^{eff}}{dz} AH \right\} \quad (5.142)$$

and

$$\frac{1}{2} F_{z\theta} F^{z\theta} = \frac{|n|^2}{r^2} \left\{ r_v^{eff}(z)^2 \left(\frac{\partial A}{\partial z} \right)^2 + 2r_v^{eff}(z) \frac{dr_v^{eff}(z)}{dz} A \frac{\partial A}{\partial z} + A^2 \left(\frac{dr_v^{eff}(z)}{dz} \right)^2 \right\} \quad (5.143)$$

The first term inside the brackets of (5.143) gives

$$\begin{aligned} 2\pi \int_0^{r_v^{eff}(z)} \frac{|n|^2}{r^2} (r_v^{eff})^2 \left(\frac{\partial A}{\partial z} \right)^2 r dr &\approx 8\pi\eta^2|n|^2 \frac{1}{(r_v^{eff}(z))^4} \left(\frac{dr_v^{eff}}{dz} \right)^2 \int_0^{r_v^{eff}} r^3 dr \\ &\approx 2\pi\eta^2|n|^2 \left(\frac{dr_v^{eff}}{dz} \right)^2 \\ &\approx 2\pi\eta^2|n|^2 \times \frac{r_v^2}{\Delta^2} (G'_v)^2 \end{aligned} \quad (5.144)$$

but this is cancelled by the contribution of the second term, which is

$$\begin{aligned} 2\pi \int_0^{r_v^{eff}(z)} \frac{|n|^2}{r^2} A \frac{\partial A}{\partial z} r dr &\approx 2\pi\eta^2|n|^2 \cdot 2r_v^{eff}(z) \frac{dr_v^{eff}}{dz} \times -\frac{2}{r_v^{eff}(z)^5} \frac{dr_v^{eff}}{dz} \int_0^{r_v^{eff}} r^3 dr \\ &\approx -2\pi\eta^2|n|^2 \times \frac{r_v^2}{\Delta^2} (G'_v)^2, \end{aligned} \quad (5.145)$$

so the only remaining contribution is the third term:

$$\begin{aligned} 2\pi \int_0^{r_v^{eff}(z)} \frac{|n|^2}{r^2} A^2 \left(\frac{dr_v^{eff}(z)}{dz} \right)^2 r dr &\approx 2\pi\eta^2|n|^2 \cdot \frac{1}{(r_v^{eff}(z))^4} \left(\frac{dr_v^{eff}}{dz} \right)^2 \int_0^{r_v^{eff}(z)} r^3 dr \\ &\approx \frac{\pi}{2} \eta^2 |n|^2 \times \frac{r_v^2}{\Delta^2} (G'_v)^2. \end{aligned} \quad (5.146)$$

The final approximate expression for the total string tension is then

$$\begin{aligned} \mu_{|n|}(z) &\approx 2\pi\eta^2|n| + 2\pi\eta^2|n|^2 \ln \left(\sqrt{\beta^{eff}(z)} \right)^2 + \pi\eta^2|n| \frac{1}{|n|+1} \times \frac{r_s^2}{\Delta^2} (G'_s)^2 \\ &+ \frac{\pi\eta^2}{|n|+2} + \frac{\pi}{2} \eta^2 |n|^2 \times \frac{r_v^2}{\Delta^2} (G'_v)^2. \end{aligned} \quad (5.147)$$

²²Similar considerations hold true even if we neglect to take the limit $r_i \gg |n|l_p$ and consider the Planck-sized regions explicitly.

Setting $G_s = G_v = G$ and $r_v = r_s = r_c$ (critical coupling) gives, to an order of magnitude, ²³

$$\mu_{|n|}(z) \approx 2\pi\eta^2|n|^2 + 2\pi\eta^2|n|^2 \times \frac{r_c^2}{\Delta^2}(G')^2. \quad (5.148)$$

As mentioned above, we have assumed that the function G has period π , so that $G(Z)$ has period Δ . This implies that $G'(Z)$ and $G'(Z)^2$ have period $\Delta/2$, so we may express the latter in form $(G')^2 = (G')^2(2\pi z/\Delta)$. If we also assume, as above, that $G' \sim (G')^2 \sim \mathcal{O}(1)$ for all z , a relatively simple and “natural” ansatz for $(G')^2$ is

$$(G')^2(z) = \frac{1}{2} \left[\sin^2 \left(\frac{2\pi z}{\Delta} \right) + \sin^4 \left(\frac{2\pi z}{\Delta} \right) \right], \quad (5.149)$$

though, in principle, there are an infinite number of possible ansatz choices. Our final expression for the approximate z -dependent tension of a pinched string is therefore

$$\mu_{|n|}(z) \approx 2\pi\eta^2|n|^2 + 2\pi\eta^2|n|^2 \times \frac{r_c^2}{\Delta^2} \times \frac{1}{2} \left[\sin^2 \left(\frac{2\pi z}{\Delta} \right) + \sin^4 \left(\frac{2\pi z}{\Delta} \right) \right]. \quad (5.150)$$

In the next section we look at F/D -strings wrapping cycles around the S^3 manifold at the tip of the KS throat. From the Lagrangian of the theory we then determine an approximate formula for the effective four-dimensional tension of the configuration. We find that, for an appropriate “natural” ansatz choice for the winding state, this is formally analogous to the result (5.150) and this allows us to draw a correspondence between the parameters which define the Abelian-Higgs model and those which define the tip geometry of KS background.

5.8 Relation of the pinched string to wound F/D -strings

Recall that the ansatz

$$X^\mu = (t, \rho \sin \sigma, \rho \cos \sigma, z_0, 0, 0, 0, \psi(\sigma) = 2n_\psi \sigma, \theta(\sigma) = 2n_\theta \sigma, \phi(\sigma) = 2n_\phi \sigma) \quad (5.151)$$

describes a *static* string loop of radius ρ with windings in all three angular directions in the S^3 at the tip of the warped deformed conifold. We have now chosen to label the loop radius ρ instead of r , as in chapter 3, in order to avoid confusion with the r -coordinate used in the previous section. For a string with no intrinsic worldsheet flux F_{ab} (i.e. $\Pi^2 = 0$), and

²³There is a discrepancy between the numerical factors multiplying the constant and periodic parts. Strictly speaking, these should be 2π and $\pi/2$ using the definitions we have adopted. As mentioned previously, changing the definition of r_v may alter the factor in front of the constant term to π , though there is still a factor of 2 “missing” in front of the $(G')^2$ term. We have also neglected the factor of π^2 which comes from the differentiation of G with respect to z . However, even if such numerical factors were included explicitly, we would still be free to choose the ansatz for $(G')^2$ (whose only physical restriction is that $(G(z)')^2 \in [0, \mathcal{O}(1)] \forall z$), so that $\mu_{|n|}(z) \approx 2\pi|n|^2 + 2\pi|n|^2 \times \frac{r_c^2}{\Delta^2} \times \tilde{G}(z)$ where $\tilde{G}(z)$ is some function which varies *exactly* between 0 and 1.

adopting canonical coordinates so that the ansatz above describes *non-geodesic* windings, the total energy is given by the Lagrangian

$$V = a_0 T_1 \int d\sigma \sqrt{a_0^2 \rho^2 + R^2 (4n_\psi^2 + \sin^2(n_\psi \sigma) (n_\theta^2 + \sin^2(n_\theta \sigma) n_\phi^2))} \quad (5.152)$$

where T_1 denotes the tension of either an F - or a D -string. In chapter 3 we employed the technique of “splitting up” the *total* string mass into a constant piece - corresponding to the mass of the string sections connecting the “beads” formed by extra-dimensional windings - and the mass of the beads themselves. In order to accomplish this, it was necessary to set $n_\psi = 0$ when calculating the mass of an *individual* bead, but to use $N_b = 2n_\psi > 0$ when calculating the *number* of beads in the loop. This was to avoid double counting the mass-contribution of the ψ -direction windings. We now perform the same procedure when calculating the effective four-dimensional tension.²⁴

We begin by setting $n_\psi \sim n_\theta \sim n_\phi \sim n_w$ in (5.152), except in the case of the constant piece ($\propto 4n_\psi^2$), in which we must set $n_\psi = 0$. Taking the limit $a_0^2 \rho^2 \gg n_w^2 R^2$, we then expand our expression for V (to first order) before dividing through by ρ to obtain

$$\mu(\sigma) \approx 2\pi a_0^2 T_1 + 2\pi a_0^2 T_1 \times \frac{1}{2} \frac{n_w^2 R^2}{a_0^2 \rho^2} [\sin^2(n_w \sigma) + \sin^4(n_w \sigma)]. \quad (5.153)$$

We may now make a change of variables

$$z = a_0 \rho \sigma \quad (5.154)$$

and define a new variable

$$d = \frac{2\pi a_0 \rho}{n_w} \quad (5.155)$$

which represents the interbead distance (or equivalently, the interwinding distance, i.e. the four-dimensional length over which a *single* full winding in the compact space is “spread”).

This gives

$$\mu(z) \approx 2\pi a_0^2 T_1 + 2\pi a_0^2 T_1 \times \frac{1}{2} \frac{R^2}{d^2} \left[\sin^2\left(\frac{2\pi z}{d}\right) + \sin^4\left(\frac{2\pi z}{d}\right) \right], \quad (5.156)$$

²⁴Although seemingly counter-intuitive, this is certainly necessary in the case of a true necklace configuration, when the bead mass is almost totally localised in space from a four-dimensional perspective. However, we also expect it to be necessary even if the beads are less highly localised than in the situation considered in the previous chapter. Although we *require* $n_\psi > 0$ in order for beads, or fluctuations in the effective four-dimensional mass-density to occur *at all*, we must still set $n_\psi \sim 0$ when calculating the approximate mass contained in localised areas.

which is formally equivalent to (5.150) under the correspondence

$$\begin{aligned} a_0^2 T_1 &\longleftrightarrow \eta^2 |n|^2, \\ R &\longleftrightarrow r_c, \\ d &\longleftrightarrow \Delta. \end{aligned} \tag{5.157}$$

Physically, what happens in the string picture is, when $z = d/2$ the string is instantaneously wrapping its *maximal* effective radius $R^{eff}(z) = R$ in the S^3 (i.e. a great circle), whereas at $z = d$ the string is instantaneously wrapping the “pole” of the S^3 (i.e. a point), so that the effective radius of the winding is $R^{eff}(z) = 0$.²⁵ At all values of z the string wraps some effective radius in the region $0 \leq R^{eff}(z) \leq R$ and the maximum increase in “winding rate” with respect to the z -coordinate, $\frac{dR^{eff}(z)}{dz} \sim \frac{dr_c^{eff}(z)}{dz}$, occurs at the points $z = d/4, 3d/4$. From the wound-string perspective, these are points at which the greatest length of string is “hidden” in the compact space (for a given interval dz), giving rise to maxima in the effective four-dimensional tension. Likewise, the periodic part of the tension in the pinched string picture is proportional to $\left(\frac{dr_c^{eff}(z)}{dz}\right)^2$ and we may draw the general correspondence²⁶

$$R^{eff}(z) \longleftrightarrow r_c^{eff}(z). \tag{5.158}$$

This also explains why we *must* set $r_v^{eff}(z) = r_s^{eff}(z)$ in the field theory picture in order to obtain the correspondence (5.157) - in this picture there is only one string, which cannot give rise to two separate radii. This allows us to interpret the (previously somewhat bizarre) z -dependence of the field couplings $\sqrt{\lambda}^{eff}(z)$ and $e^{eff}(z)$ via the relation

$$R^2 \sim b_0 g_s M \alpha', \quad b_0 \sim \mathcal{O}(1). \tag{5.159}$$

The parameter M is fixed and quantised, and α' is a fundamental unit, so that a string wrapping an effective radius in the S^3 , $R^{eff}(z) \leq R$, experiences an effective coupling of approximately

$$g_s^{eff}(z) = \frac{(R^{eff}(z))^2}{b_0 M \alpha'}. \tag{5.160}$$

This allows us to establish a relation between $g_s^{eff}(z)$, $\sqrt{\lambda}^{eff}(z)$ and $e^{eff}(z)$, which will be investigated shortly.

²⁵However, at *both* these points, $\frac{dR^{eff}(z)}{dz} = 0$, so the effective four-dimensional tension is $\mu(z) \approx 2\pi a_0^2 T_1$.

²⁶We may also interpret this result in the following manner: As shown in chapter 3, there exist *two* degenerate minima in the fundamental domain of the ψ -coordinate of the S^3 , giving rise to two beads *per winding*. If one full winding in the string picture corresponds to one full “pinch” in the field picture, we would therefore expect to find *two* peaks in the periodic part of the tension $\mu_{|n|}(z)$ for every one peak in the *physical* radius of the string core.

Importantly, we can also imagine a situation where the string completes one full winding in (say) the clockwise direction before reversing and wrapping the S^3 anticlockwise. The four-dimensional regions over which these windings take place may then correspond to regions of $\pm|n|$ string in the field picture. In addition, although we still have no effective description of the Planck-sized regions of the pinched string in the classical field theory, in the string picture we see that they admit a relatively natural interpretation, with $|r_c^{eff}|_{min} = |n|l_p \equiv |R^{eff}|_{min}$ corresponding to the minimum width of the string due to quantum effects.

In effect, when the string wraps a “point” at the pole of the S^3 at $z = d$, the approximation of the string as a one-dimensional object breaks down. It is therefore meaningless to consider the position of the string localised in the S^3 on scales smaller than the fundamental string width. Furthermore, the four-dimensional effective tension of the string in this region is clearly equal to the intrinsic warped tension $\tilde{T}_1 \sim a_0^2 T_1$, which under the correspondence in (5.157) is equivalent to the tension of a non-cylindrical defect string in the region of the “pinch”, $\mu_{|n|}(z \approx m\Delta) \sim \eta^2 |n|^2$. As stated in section 5.5, this goes some way towards justifying our original assumption that $\mu_{|n|}(z) \sim \eta^2 |n|^2$ within the regions $z \in [m\Delta \pm |n|l_p]$.

In addition, how tightly wound the string is from a four-dimensional perspective may affect the length-scale over which it is able to move from one winding orientation to the other, as well as to how localised $R^{eff}(z)$ may be. For example, if we identify the fundamental Planck length l_p with the fundamental string length $l_s \sim \sqrt{\alpha'}$, the fact that $|r_c^{eff}|_{min} \propto |n|$ (in addition to $l_p \equiv \sqrt{\alpha'}$) may be related to this effect, and we may use this to identify $|n|$ explicitly with a combination of string theory parameters based on physical arguments.

Intuitively, we expect a more tightly wound string to correspond a higher value of $|n|$ in the field picture, so the simple correspondence $n_w \longleftrightarrow |n|$ must be rejected. We may, however, arrive at a hypothetical correspondence between $|n|$ and the *dynamical* parameters which control winding formation in the string picture via the following argument: In the field theory picture we have assumed that the sections of “neutral” string which connect neighbouring regions of $\pm|n|$ string are of length $\sim 2|n|l_p$. We now justify this in the dual string picture by assuming that the four-dimensional length over which the string “sits” at the pole of the S^3 is proportional to (twice) the tangent of the angle of incidence (so that a more tightly wound string takes a greater distance to “unwind” in proportion to its angle of incidence), giving

$$\Delta z \sim 2|n|l_p \propto 2\frac{R}{d}\sqrt{\alpha'}. \quad (5.161)$$

Identifying $l_p \sim \sqrt{\alpha'}$, we then have

$$|n| \propto \frac{R}{d}. \quad (5.162)$$

However, clearly this cannot be our final expression, as for $d > R$ we have that $|n| < 1$. From the definition

$$\omega_l \sim \frac{n_w R}{\sqrt{a_0^2 \rho^2 + n_w^2 R^2}} \sim \frac{R}{d} \left(1 + \frac{R^2}{d^2}\right)^{-\frac{1}{2}} \quad (5.163)$$

we see that $\omega_l \rightarrow 0$ as $d \rightarrow \infty$. We therefore propose the correspondence

$$|n| \sim \frac{R}{\omega_l d} \sim \frac{n_w R}{a_0 \rho \omega_l} \sim \sqrt{1 + \frac{R^2}{d^2}} \sim \frac{1}{\sqrt{1 - \omega_l^2}} \quad (5.164)$$

which implies $|n| \rightarrow \infty$ as $\omega_l \rightarrow 1$ and $|n| \rightarrow 1$ as $\omega_l \rightarrow 0$, as expected. In other words, in the limit that we obtain and *unwound* F -string, the original duality proposed by Nielsen and Olesen [15] is recovered.²⁷ Topological winding numbers of opposite signs ($\pm n$) may be obtained by taking either physical winding numbers of opposite signs ($\pm n_w$) or opposite signs in front of the square root.

Recall that the tension of a general (p, q) -string at the tip of the warped throat is

$$T_{(p,q)} \approx \frac{1}{2\pi\alpha'} \sqrt{\left(\frac{q}{g_s}\right)^2 + \left(\frac{b_0 M}{\pi}\right)^2 \sin^2\left(\frac{p\pi}{M}\right)}, \quad (5.165)$$

so in the limit $M \gg 1$, the approximate tension of the F -string is

$$\begin{aligned} T_{(1,0)} &\approx \frac{1}{2\pi\alpha'} \left(\frac{b_0 M}{\pi}\right) \sin\left(\frac{p\pi}{M}\right) \approx \frac{1}{2\pi\alpha'} \times \frac{b_0 M}{\pi} \times \frac{\pi}{M}, \quad M \gg 1 \\ &\approx \alpha'^{-1}, \quad b_0 \sim \mathcal{O}(1). \end{aligned} \quad (5.166)$$

and that of the D -string is

$$T_{(0,1)} \approx \frac{1}{2\pi\alpha'} \frac{1}{g_s} \approx \alpha'^{-1} g_s^{-1}. \quad (5.167)$$

Dealing first with the F -string, we see that under the general correspondence given in (5.157), the only *consistent* correspondence between the individual elements η and $|n|$ in

²⁷However, in order for $|n|$ to be an integer greater than one (which corresponds to the limit $d \gg R$), we require $d < R$, which is equivalent to $\Delta < r_c$ in the pinched string picture. Hence, dealing with models in which $|n| > 1$ is potentially problematic, as the assumptions made in order to simplify the pinched string EOM break down. This suggests that further and more in depth analysis is needed in this limit, at least regarding the field-theoretic necklace model, though for the time being we will neglect such considerations.

the field theory picture and the parameters of the string theory is

$$\eta \sim a_0 \sqrt{\alpha'}^{-1}, \quad |n| \sim 1. \quad (5.168)$$

In chapter 3 it was necessary to identify the energy corresponding to the epoch of the (p, q) -string network formation (η_s) with the fundamental string energy scale (not the warped string energy scale), so that $\eta_s \sim \sqrt{\alpha'}^{-1}$ *not* $\eta_s \sim a_0 \sqrt{\alpha'}^{-1}$. Although this appears to contradict our identification (5.168), it is not immediately clear that this is so, since we have chosen to identify the fundamental string width $\delta \sim \eta_s^{-1}$ with the fundamental string scale (so that $\delta \sim \eta_s^{-1} \equiv l_s \sim \sqrt{\alpha'}$), which is in perfect agreement with our previous results. The identification of η with the warped string scale then tells us that it is inequivalent to η_s . In the string picture, the F/D -string network forms at $t_s \sim \eta_s^{-1} \sim \sqrt{\alpha'}$, but the windings begin to form some time later at $t_w > t_s$, where $t_w \sim a_0^{-1} \sqrt{\alpha'}$, at which point wound-strings are dual to defect strings with $|n| > 1$. The effective formation time is dependent on the warped string scale. What happens in the regime $l_s \leq t < t_w$ remains unclear within the field theory picture, though one possibility is suggested by combining the correspondences (5.169) and (5.170), which follow shortly, with (5.168).

Alternatively, it may *not* be possible to associate specific expressions involving string theory parameters with the individual elements η and $|n|$, but only to arrive at a composite expression of the form $\eta|n| \sim f(a_0, g_s, M)$ (e.g. $\eta|n| \sim a_0 \sqrt{\alpha'}^{-1}$, as suggested by the expression for the F -string tension above). However, we will arrive at three separate, but physically intuitive, expressions for both η and $|n|$, which seem to correspond to *two* separate dynamical models of winding formation in the string picture.

Consider now the expression for the the total energy of the wound-string loop, obtained in chapter 4, for geodesic windings formed via the velocity correlations regime, $E = 2\pi T_1 \rho$ (c.f. (4.26) and substitute $\rho(t_i) = (\alpha t_i)$). By the arguments given above, geodesic windings in the string picture correspond to cylindrically symmetric strings in the dual field theory model, whose total energy we expect to be $E = 2\pi \eta^2 |n|^2 \rho$ and whose (constant) tension is therefore $\mu = 2\pi \eta^2 |n|^2$ (where $|n| \sim 1/\sqrt{1 - \omega_l^2}$ as in (5.164)). Two self-consistent correspondences between the individual elements η and $|n|$ and the string theory parameters for the F -string then exist:

$$\eta \sim \sqrt{\alpha'}^{-1}, \quad |n| \sim 1 \quad (5.169)$$

and

$$\eta \sim a_0 \sqrt{\alpha'}^{-1}, \quad |n| \sim \frac{1}{a_0}. \quad (5.170)$$

Clearly, the second correspondence accounts for the possibility $|n| > 1$ through the condition $a_0 < 1$, though a strict correspondence would imply a *quantisation* of a_0 . In the first expression (5.169), the symmetry-breaking energy scale is the *fundamental string energy scale*, whereas in the second (5.170), it is the *warped string energy scale*.

It is unclear whether the string width should be set by the fundamental string length-scale or the warped string length-scale, as it is unclear whether the energy associated with F/D -string network production should be the fundamental string energy, or the warped string energy. Furthermore, it is unclear if the string width can be determined by the fundamental scale (i.e. $\sim \sqrt{\alpha'}$), while the energy associated with network formation (in the string picture) or symmetry-breaking (in the field theory picture) is determined by the warped string scale (i.e. $\sim a_0 \sqrt{\alpha'^{-1}}$) or vice-versa. Though the following comments are therefore highly conjectural and tentative, interesting interpretations will be put forward for the existence of *all* of the correspondences above, as well as for those suggested by the expression for the D -string tension (5.167).

We first consider the F -string correspondences. In the range $\sqrt{\alpha'} \leq t < a_0^{-1} \sqrt{\alpha'}$ there exists *no difference* between the random walk and velocity correlations regimes (as both create an equal number of windings over the period taken to move a single step length ϵ_l). We then propose that the correspondence (5.169) holds within this region, so that there exist simply unwound F -strings (in the string picture) which are dual to $|n| = 1$ defect strings (in field picture). For $t > a_0^{-1} \sqrt{\alpha'}$, we must adopt one of the correspondences (5.168) or (5.170), depending on our model of winding formation.

In the random walk regime of winding formation, $\omega_l(t_i) \rightarrow 0$ as $t_i \rightarrow \infty$ (see chapter 3), so $|n| \rightarrow 1$ according to the *general* proposed correspondence (5.164). These results are in complete agreement with (5.168). By contrast, in the velocity correlations regime, $\omega_l \sim \sqrt{1 - a_0^2}$, so $|n| \sim \frac{1}{\sqrt{1 - \omega_l^2}} \sim \frac{1}{a_0}$ in accordance with (5.170).²⁸

We are then left with two correspondences between the field theory parameters η and $|n|$ and the string theory parameters a_0 and $l_s \sim \sqrt{\alpha'}$ (valid for $t > t_w \sim a_0^{-1} \sqrt{\alpha'}$) which we interpret in terms of different winding formation mechanisms for the F -string. In addition, we have proposed a general correspondence between the dynamical parameters governing winding formation in the string picture and the topological winding number $|n|$ in the field

²⁸In the velocity correlations regime the string oscillates between states of maximal/minimal ω_l , determined by the value of a_0 , but here we deal only with its *initial* state at $t = t_i$. In the dual field picture, such expansion/contraction of the four-dimensional loop radius could correspond to expansion/contraction caused by quantised transitions between different topological winding states, e.g. the transition of a string of radius ρ and winding number $|n|$ to an identical energy state with radius $\rho/2$ and winding number $2|n|$ etc. This would be consistent with the idea, proposed in chapter 4, that the oscillations of a wound-string loop with $l > 0$ correspond to the “twisting” and “untwisting” of the string if we identify the field theory and string theory parameters $|n| \sim 1/\sqrt{1 - \omega_l^2}$ with a measure of *torsion*.

picture, which holds in both scenarios.

Turning our attention to the D -string tension and considering both winding formation mechanisms, we see that this also allows three possible identifications. These are

$$\eta \sim a_0 \sqrt{\alpha'}^{-1}, \quad |n| \sim \frac{1}{\sqrt{g_s}} \quad (5.171)$$

in the random walk regime, and

$$\eta \sim \sqrt{\alpha'}, \quad |n| \sim \frac{1}{\sqrt{g_s}} \quad (5.172)$$

or

$$\eta \sim a_0 \sqrt{\alpha'}, \quad |n| \sim \frac{1}{a_0 \sqrt{g_s}} \quad (5.173)$$

in the velocity correlations regime. Here the condition $|n| \geq 1$ may be realised by imposing either $g_s \leq 1$ or $g_s \leq a_0^{-1}$ (together with appropriate quantisation conditions for a_0 and g_s). Following the same arguments as before, we may now account for the existence of (5.171)-(5.173) by supposing that the D -string also follows either a random walk regime with step length $\epsilon_l \sim a_0^{-1} \sqrt{\alpha'}$ or velocity correlations regime with $c = \tilde{l}_s / \tilde{t}_s = 1$ as the additional factors of $\sqrt{g_s}^{-1}$ in these expressions (as opposed to the F -string case) are simply accounted for via the differing string tension.

Clearly, we may explore any of the proposed correspondences (5.168)-(5.170) or (5.171)-(5.173) in greater detail and in conjunction with (5.157), though we here restrict ourselves to considering (5.168) in order to illustrate the general procedure.

Combining the expression $R^2 \sim g_s M \alpha'$ with the general correspondence in (5.157), $R^2 \sim r_s^2 \sim (\sqrt{\lambda} \eta)^{-2} \sim r_v \sim (\epsilon \eta)^{-2}$, and the specific correspondence (5.168) gives

$$\lambda \sim e^2 \sim \frac{1}{a_0^2 M g_s} \sim \frac{\alpha'}{a_0^2 R^2} \quad (5.174)$$

and

$$\lambda^{eff}(z) \sim (e^{eff}(z))^2 \sim \frac{1}{a_0^2 M g_s^{eff}(z)} \sim \frac{\alpha'}{a_0^2 (R^{eff}(z))^2}. \quad (5.175)$$

Using the definition of the deformation parameter for the conifold (and adjusting the units so that $\tilde{\epsilon}^{-4/3} = \epsilon^{4/3} \alpha'$), we may then write

$$\lambda \sim e^2 \sim \frac{1}{a_0^2 M g_s} \sim \frac{\alpha'}{a_0^2 R^2} \sim \epsilon^{4/3}. \quad (5.176)$$

On the left-hand-side of (5.176) we have the Abelian-Higgs couplings which, together with the symmetry-breaking energy scale η , determine the effective masses of the particles present in the universe according to that model (i.e. the bosons associated with scalar and vector fields). On the right-hand-side we have string theory parameters which determine the large-scale geometry of the universe according to the KS model (including both the large and compact dimensions) and which control the fundamental mass-scales of the particles associated with that theory (i.e. the masses associated with the excitations of F/D -strings). Most importantly, if we also include the correspondence $\eta \sim a_0 \sqrt{\alpha'}^{-1}$, the field theory parameters which set the mass-scales for the particles at the current (post-symmetry-breaking) epoch may be equated with the parameters which control inflation and the cosmological expansion in the dual string picture.

At first sight, this may seem strange. However, according to the present cosmological paradigm, the presence of an inflaton field caused a period of rapid expansion in the very early universe. The inflaton then “decayed” and its energy was channelled into the production of defects and particles, whose remnants or “descendants” (following temperature changes and further symmetry-breaking phase transitions caused by the expansion and cooling of the universe) may be observed today. On reflection, therefore, the correspondences above appear quite natural as we may *expect* the parameters which control inflation to set the present day mass-scale of the universe.

We note that the Abelian-Higgs model is a “toy” symmetry-breaking model, in that there are only two fields (and two associated bosons). However, it is possible that a similar analysis may be performed for more realistic field theories (e.g. for standard model fields), allowing correspondences to be drawn between the parameters which control the mass-scales and couplings of observable particles and the dual string theory parameters which control the large scale evolution of the universe (though again, more refined models than the KS compactification may be needed, even in the string picture). If such duality correspondences are correct, we would expect *agreement* between the results of particle physics experiments and cosmological observations. This is an interesting prospect, since in principle, such dualities may be tested by comparing data from these related fields. Ultimately, we may even hope to search for constraints on the standard model Higgs mass in data from future CMB observations.

In this connection, it is worth considering two more important questions raised by the analysis above. The first regards the *nature* of the symmetry-breaking phase transition in the dual string picture. In the Abelian-Higgs model, the phase transition which gives rise to string formation is well-defined and it is the $U(1)$ symmetry of the vacuum which is broken. The transition is an example of a “static” symmetry-breaking process - the Higgs potential (i.e. the Mexican hat), may be interpreted as *really existing* and not as a phenomenological

device to describe the effects of a dynamical process, as in its condensed matter analogue (see [114]). However, from a philosophical point of view, such “static” symmetry-breaking processes are extremely unsatisfactory because the parameters which define the Higgs field must be put into the theory by hand (i.e. fine-tuned) and it is hard to imagine how they may be derived from some underlying theory (e.g. one governing a more fundamental dynamical process).

According to the analysis above, we may equate the parameters which determine the size and shape of the Mexican hat potential with their string analogues. But what is the “symmetry-breaking” process which takes place in the string model? Does it break a $U(1)$ symmetry? Is it static or somehow *dynamic*? Although the following argument is somewhat naive, in that we imagine a string “sitting” in space and evolving in time (as opposed to considering a relativistic string embedded in a spacetime geometry), a long, straight (i.e. unwound), F - or D -string should obey $U(1)$ symmetry with respect to rotation around its central axis. When windings form, this symmetry is broken and each point along the string adopts a “phase” factor, determined by its position in a $U(1) \equiv S^1$ submanifold of the full S^3 .²⁹ In the string picture the *dynamic* nature of the symmetry-breaking process is therefore manifest, and this helps us to understand why we may write *all* the parameters which define the field-theoretic strings (including $|n|$) in terms of the parameters which control the F/D -string dynamics, and in particular those which control the process of winding formation (regardless of the exact model of winding formation we adopt).

The second question relates to a point first raised in chapters 1 and 3. Cosmic necklaces formed from extra-dimensional windings were first proposed by Matsuda as possible DM candidates [6, 7]. The idea was that necklaces which had shrunk to their minimal size (determined by the fundamental string thickness) and which contained insufficient mass to undergo collapse would only be able to interact with other fields/matter gravitationally. However, the proposed correspondence between necklace configurations and “pinched” gauge strings suggests that this is unlikely as the presence of dual A_θ term (however this is defined) implies that necklaces may emit and absorb gauge field radiation as well as gravitons. Bearing this in mind, we suggest the following definitions for the effective scalar and vector fields in the wound-string model:

$$\begin{aligned} \phi(r, \theta, z) &= \phi(r, \theta, r_s^{eff}(z)) = \eta F \left(\frac{r}{r_s^{eff}(z)} \right) e^{\pm i|n|\theta} \\ &\equiv \frac{a_0}{\sqrt{\alpha'}} F \left(\frac{r}{R^{eff}(z)} \right) \exp \left(\pm i \left| \frac{n_w R}{\omega_l a_0 \rho} \right| \theta \right), \end{aligned} \quad (5.177)$$

²⁹Rotating the string around its fundamental axis will no longer leave the configuration invariant. It will instead be analogous to the turning of a screw, causing windings to change their position in the large dimensions, just as the threads of a screw move along its axis.

and

$$\begin{aligned}
 A_\theta(r, z) &= A_\theta(r, r_s^{eff}(z)) = \eta r_v^{eff}(z) |n| A \left(\frac{r}{r_v^{eff}(z)} \right) \\
 &\equiv \frac{a_0}{\sqrt{\alpha'}} R^{eff} \left| \frac{n_w R}{\omega_l a_0 \rho} \right| A \left(\frac{r}{R^{eff}(z)} \right), \tag{5.178}
 \end{aligned}$$

where F and A are subject to boundary conditions analogous to those imposed before. Here θ may also be interpreted as the angular coordinate of a point on the S^1 sub-manifold that defines the effective radius of the winding (for any value of z) and r as the distance from the ‘‘centre’’ of the S^1 to its circumference. Physically, a section of the wound string effectively ‘‘occupies’’ a volume $\sim 2\pi R^{eff}(z) dz$ in the large dimensions, so that r and θ also admit their usual interpretations for a string of finite width.

This gives rise to a flux at each point z which is quantised in terms of n_w in the string picture (for fixed values of the other parameters) and in terms of n in the field picture, so that

$$\Phi_{n_w}(z) = \frac{2\pi a_0}{\sqrt{\alpha'}} R^{eff}(z) \frac{n_w R}{\omega_l a_0 \rho} \equiv \Phi_n(z) = \frac{2\pi n}{e^{eff}(z)}. \tag{5.179}$$

5.8.1 Argument for a time-dependent bead mass

We now use physical arguments to construct explicit dynamical models of pinch formation which are the direct analogues of dynamical winding formation in the random walk and velocity correlations regimes. To construct the analogue of the former, consider a field configuration corresponding to an $|n_1|$ -vortex string undergoing random quantum fluctuations in both its phase θ and magnitude $f(r)\eta$ at *every point in the string*. In order for a section of string *within* the horizon to undergo a spontaneous transition to a new topological state $|n_2| \neq |n_1|$, the fluctuations in θ would need to be *perfectly correlated* at least over some distance $\Delta z \geq l_p$ (i.e. within a volume of approximately $\sim r_c^2 \Delta z$). For example, a transition from a $+|n|$ state to a $-|n|$ state at even a single point z would correspond to each degenerate vacuum state $\langle \phi \rangle = \eta f(r) e^{i|n|\theta}$ ($r \leq r_s, r_v$, $\theta \leq 2\pi$) tunnelling through the Mexican hat potential, so that $\theta \rightarrow \theta + \delta\theta = \theta + \pi$. Clearly, this is highly unlikely, regardless of the tunnelling amplitude for such a transition at any individual point.

It is also possible, in principle, for random fluctuations in the magnitude $\delta(f(r)\eta)$ at each point to result in a *total* reduction of the size of the vortex to a sub-Planck scale. However, if this were to occur *within* the horizon, it would again be necessary for such fluctuations to be correlated, at least over some length-scale $\Delta z \geq l_p$, in order for a finite section of string to ‘‘re-emerge’’ with a different topological winding number. Even if this constantly takes place over small regions (which would be the analogue of continuous Brownian motion at

every point along a wound string), it is clear that the net effect would be to leave the macroscopic structure of the string, and the total number of pinches, unchanged.

The situation is different, however, for the vortex slice which lies (instantaneously) on the horizon. In this case the vortex is “free” to re-emerge in a differing topological state, so that only fluctuations at the horizon may contribute to the *net* number of pinches. Let us assume that the radius of the vortex at the horizon moves with velocity v , but randomly increases or decreases within the range $[l_p, r_c]$, so that its net velocity may be estimated via

$$\langle v \rangle \sim \sqrt{\bar{v}} \sim \frac{n_p r_c}{\sqrt{\rho^2 + n_p^2 r_c^2}} \quad (5.180)$$

where n_p denotes the number of pinches and we have again assumed critical coupling. We note that $n_p \sim \frac{\rho}{\Delta} \sim \frac{\rho}{d}$, whereas, crucially, in the dual model $n_w \sim \frac{a_0 \rho}{d}$, so

$$n_p \sim \frac{n_w}{a_0}. \quad (5.181)$$

Clearly, using $R \sim r_c$, the expression for $\langle v \rangle$ is equivalent to that for ω_l :

$$\langle v \rangle \sim \sqrt{\bar{v}} \sim \frac{n_p r_c}{\sqrt{\rho^2 + n_p^2 r_c^2}} = \omega_l \sim \frac{n_w R}{\sqrt{a_0^2 \rho^2 + n_w^2 R^2}}. \quad (5.182)$$

The number of pinches per loop for loops formed at $t = t_i$ is then

$$n_p(t_i) \sim \frac{\sqrt{\langle v \rangle \epsilon_l \alpha t_i}}{r_c} \quad (5.183)$$

where ϵ_l is again the step length. Setting $\epsilon_l \sim \alpha \eta^{-1} \sim \alpha a_0^{-1} \sqrt{\alpha'}$ then results in expressions for $n_p(t_i)$, $\langle v \rangle(t_i)$ and $\Delta(t_i)$ in the field picture which are the analogues of those for $n_w(t_i)$, $\omega_l(t_i)$ and $d(t_i)$ in the string picture:

$$\begin{aligned} n_p &\approx \frac{1}{\sqrt{2}} \frac{(\alpha t_i)}{r_c} \left(-1 + \sqrt{1 + \frac{4m_p^2}{\eta^4 t_i^2}} \right)^{\frac{1}{2}} \\ &= \frac{n_w}{a_0} \approx \frac{1}{\sqrt{2}} \frac{(\alpha t_i)}{R} \left(-1 + \sqrt{1 + \frac{4\alpha'}{a_0^4 t_i^2}} \right)^{\frac{1}{2}} \end{aligned} \quad (5.184)$$

$$\begin{aligned} \langle v \rangle(t_i) &\approx \frac{1}{2} \left(\frac{\eta}{m_p} \right)^2 (\alpha t_i) \left(-1 + \sqrt{1 + \frac{4m_p^2}{\eta^4 t_i^2}} \right) \\ &= \omega_l \approx \frac{1}{2} a_0^2 (\alpha t_i) \left(-1 + \sqrt{1 + \frac{4\alpha'}{a_0^4 t_i^2}} \right) \end{aligned} \quad (5.185)$$

$$\begin{aligned}
 \Delta(t_i) &\approx \sqrt{2}r_c \left(-1 + \sqrt{1 + \frac{4m_p^2}{\eta^4 t_i^2}} \right)^{-\frac{1}{2}} \\
 &= d(t_i) \approx \sqrt{2}R \left(-1 + \sqrt{1 + \frac{4\alpha'}{a_0^4 t_i^2}} \right)^{-\frac{1}{2}}
 \end{aligned} \tag{5.186}$$

where we have also identified $l_p \sim t_p \sim \sqrt{\alpha'}$ and $m_p \sim \sqrt{\alpha'}^{-1}$. One may check that these correspondences imply

$$|n|(t_i) \sim \frac{R}{\omega_l(t_i)d(t_i)} \sim \frac{\sqrt{\alpha'}}{a_0 R} |n_w(t_i)|^{-1} \sim \left(\frac{m_c}{\eta} \right) |n_p(t_i)|^{-1}, \tag{5.187}$$

(where $m_c = r + c^{-1}$), so as $n_w(t_i) \rightarrow \frac{\sqrt{\alpha'}}{a_0 R}$ for $t_i \rightarrow \infty$, we have that $|n|(t_i) \rightarrow |n| \sim 1$, as required. Importantly, we can now *predict* the vorticity of the field theoretic strings, at least in terms of the velocity associated with the fluctuations at the horizon (or equivalently, the observed number of pinches).

This opens up the possibility that, if a suitable quantum theory of the vortice configuration is developed, it may be possible to predict both $|n|$ and Δ (or n_p) in terms of some more fundamental underlying dynamics. As a first step towards this, we note that in the scaling regime

$$d(t_i) \sim \frac{1}{2} \frac{a_0^2 R}{\sqrt{\alpha'}} t_i. \tag{5.188}$$

In chapter 3 we used the standard field theory scaling model *in an explicitly warped space* (so that $\xi(t_i) \sim a_0 \gamma t_i$) to infer $d(t_i) \sim \xi(t_i)$, yielding $\gamma \sim \frac{1}{2} \frac{a_0 R}{\sqrt{\alpha'}}$. However, we have now constructed an explicit duality between a wound-string model in warped space and a defect string in *unwarped* space (where we expect $\xi(t_i) \sim \gamma t_i$). Identifying $\Delta(t_i) \sim d(t_i) \sim \xi(t_i) \sim \gamma t_i$ then yields

$$\gamma \sim \frac{1}{2} \frac{a_0^2 R}{\sqrt{\alpha'}} \sim \frac{1}{2} \frac{a_0 \alpha}{|n_w(t_i \rightarrow \infty)|} \sim \frac{1}{2} \frac{1}{\sqrt{\lambda}} \left(\frac{\eta}{m_p} \right) \sim \frac{1}{2} \frac{\alpha}{|n_p(t_i \rightarrow \infty)|}. \tag{5.189}$$

The physical constraints $|n_w(t_i \rightarrow \infty)| \geq 1$ and $\alpha, \gamma \leq 1$ then imply

$$\lambda \sim e^2 \geq 1, \tag{5.190}$$

which in conjunction with (5.174) yield $Mg_s \leq a_0^{-2}$, though this is perfectly consistent with the SUGRA approximation $Mg_s \gg 1$ for $a_0^2 \ll 1$.

Recall now that the total mass of the pinched string loop is

$$M_T \sim 2\pi\eta^2|n|^2\rho + 2\pi\eta^2|n|^2 \times \frac{1}{2} \frac{r_c^2}{\Delta^2} \int_{z=0}^{z=n_p\Delta} |G'|^2 dz \quad (5.191)$$

which may be approximated by

$$M_T \sim 2\pi\eta^2|n|^2\rho + 2\pi\eta^2|n|^2 \times \frac{1}{2} \frac{r_c^2}{\Delta^2} \times n_p\Delta |G'|_{max}^2. \quad (5.192)$$

As well as controlling the exact mass of the bead itself, the value of $|G'|_{max}^2$ indicates the “spread” of the density fluctuation, with a higher maximum gradient indicating a higher degree of localisation.

Until now we have assumed that $|G'|_{max}^2 \sim \mathcal{O}(1)$. However, in order for our expression for the pinched string bead mass to “match up” with our expression for the wound-string bead mass (3.23), using the correspondences already established, we must now make the additional assumption $|G'|_{max}^2 \sim n_p$. While this seems physically reasonable, as a greater number of pinches (for a given value of Δ) should result in proportionately greater concentration of the bead mass, at present we have no way of testing the validity of this assumption and it is likely that a full dynamical theory of pinch *evolution* would be required for this. In addition, for $n_p > \mathcal{O}(1)$, this directly contradicts the assumptions made in order to obtain the simplified forms of the pinched string EOM, whose solutions we used to calculate $\mu_{|n|}(z)$ and on which the expressions for M_T above are based.

Although more work is needed, we content ourselves here demonstrating an order of magnitude equivalence between the pinched string bead mass and the wound-string bead mass, based on the assumption that $|G'|_{max}^2 \sim n_p$ in the latter (which roughly corresponds to multiplying the ansatz (5.150) in section 5.7 by n_p), and using the correspondences already established). This gives

$$M_b \sim \frac{\pi}{2}\eta^2|n|^2 \times \frac{r_c^2}{\Delta} |G'|_{max}^2 \sim \frac{\pi}{2}\eta^2|n|^2 \times \frac{r_c^2 n_p}{\Delta}, \quad (5.193)$$

where we have assumed the mass of an individual bead is *half* that associated with the a single pinch. We then make use of the previously established correspondences $\eta \sim a_0\sqrt{\alpha'}^{-1}$, $T_1 \sim T_{(1,0)} \sim \alpha'^{-1}$, $r_c \sim R$, $n_p \sim \frac{n_w}{a_0}$ and $d \sim \Delta$ to obtain

$$M_b \sim \frac{\pi}{2}T_1 \frac{n_w R^2}{d} |n|^2. \quad (5.194)$$

The correspondence $d \sim \frac{a_0\rho}{n_w}$ then yields

$$M_b \sim \frac{\pi}{2}T_1 \frac{n_w^2 R^2}{\rho} |n|^2 \sim \frac{\pi}{2}T_1 \frac{n_w^2 R^2}{\rho} \quad (5.195)$$

if $|n| \sim \mathcal{O}(1)$. As shown above, for pinches formed from random fluctuations in the string radius, $|n|^2 \sim 1$. Ignoring an arbitrary factor of $1/2$, the expression (5.195) is then *exactly* equivalent to the expression for the bead mass (3.23), obtained from the wound-string lifting potential (setting $\Pi = 0$). Clearly, in this case, the late-time fall-off of $M_b(t_i)$ is proportional to t_i^{-1} and the behaviour of pinched string networks matches that of necklaces formed from wound strings.

We may now hope to use the dual pinched string model to help answer the question first posed at the end of chapter 3: does the bead mass remain fixed after the time of loop formation t_i ? Unfortunately, in the absence of a full dynamical model of pinch evolution, we are still unable to answer this question with any certainty. As the bead mass in this model depends on the quantity $\left(\frac{dr_c^{eff}}{dz}\right)^2 \sim \frac{r_c^2}{\Delta^2}|G'|^2$, two competing factors come into play - the time evolution of Δ (i.e. $\Delta(t_i, t)$ in an explicitly dynamic model) and that of $|G'|^2$. In principle it is possible for either factor to outweigh the other, so that the bead mass may even increase. This too may have an analogue in the string picture, since the contraction of the string causes neighbouring windings to move closer together, thereby increasing their effective radii. Clearly, much more work is needed in both the string and field theory models in order to develop a full dynamical theory. ³⁰

Finally, we note that a model of pinch “formation” which is the analogue of winding production in the velocity correlations regime may also be constructed. In this case, we must assume that the radius of the vortex at the horizon has a *classical* velocity which causes the string core to shrink to the Planck scale before regrowing to its maximum radius and again reversing its direction to repeat the cycle. It is unclear *dynamically* why this should be so, but an alternative view of this scenario is simply that the defect string formed “ready pinched” at the symmetry-breaking phase transition, so that successive pinches (separated by a characteristic length-scale Δ) are then uncovered by the advancing horizon at a rate

³⁰It is also possible that our expression for the bead mass (3.23) is incorrect. That $M_b \propto n_w^2$ results directly from the identification of $d\psi \sim d\sigma$ in the region of a bead. However, traversing the four-dimensional circumference of the loop *once*, we traverse the ψ -direction n_ψ times. This suggests we should integrate over a region $d\sigma \sim d\psi/n_\psi$ instead and gives $M_b \sim \frac{\pi}{4}T_1 \frac{R^2 n_w}{\rho}$ (where we have identified $n_w \sim n_\psi$ and set $\Pi = 0$). We may obtain agreement between this expression and (5.193) by continuing to assume $|G'|_{max}^2 \sim \mathcal{O}(1)$ and $|n| \sim \mathcal{O}(1)$ and by modifying our estimate of the distance between neighbouring windings so that $d \sim a_0^2 \rho / n_w$. Our original identification, $d \sim a_0 \rho / n_w$, is motivated by the Minkowski part of the conifold metric, $ds^2 \sim a_0^2 \eta_{\mu\nu} dx^\mu dx^\nu + \dots$, which suggests $dx^\mu \rightarrow a_0 dx^\mu$ in the transition from unwarped to warped space. However, the expression for the four-dimensional rest mass of an *unwound* string, $M_T \sim 2\pi a_0^2 T_1 \rho$ (c.f. (3.19)), suggests instead the modified form above and is equivalent to assuming $n_p \sim n_w / a_0^2$. By identifying $n_w \sim 2n_\psi$ (c.f. chapter 4), we may also account for the discrepancy in the numerical factor, so that $\pi/4 \rightarrow \pi/2$ in the expression for the wound-string bead mass. Using the assumptions above, this is then in complete agreement with (5.193). If correct, these remarks imply that the results presented in chapter 3 must be modified and the bounds on PBH production recalculated, which may also require an erratum for [1] to be issued. These subtleties are yet another example of the difficulty in transferring intuitively obvious ideas from unwarped to warped-space models.

proportional to t .³¹

5.9 Additional Notes

In this section we briefly address a number of issues raised in this chapter, some of which relate to questions raised earlier in this thesis. We aim to tie up loose ends and to identify open questions.

5.9.1 Effective actions

In our chosen gauge the pinched string tension is a function of the position along the string, $z = \rho\sigma$. However, covariantly - even in a static gauge - it must be expressed as function of *all* the spatial coordinates. In addition, intuitively we may expect the dynamics of the pinched string to differ profoundly from those of its cylindrical counterpart. Even ignoring the prospect of pinch evolution/bead localisation along the string itself, perturbations along the length of the string ought to lead to genuine density fluctuations, equivalent to longitudinal waves. Furthermore, for a pinched string, a drift velocity $v < c$ may be uniquely defined *along its length*. Because the pinched string has internal structure along its central axis, it becomes meaningful to talk about “part” of the string moving.

We therefore propose a generalisation of the standard Nambu-Goto action to describe the pinched string dynamics. Assuming that $r_v \ll \mathcal{R}$ ($r_s \leq r_v$), where \mathcal{R} is the curvature radius of the string, and parameterising the effective two-dimensional worldsheet in terms of the space and time-like variables σ and τ , we have

$$S = - \int d\sigma d\tau \mu(\sigma, \tau) \sqrt{-\gamma(\sigma, \tau)} \quad (5.196)$$

where $\gamma = \det\gamma_{ab}$, $a, b \in \{\tau, \sigma\}$ and the induced metric is now

$$\gamma_{ab} = G_{\mu\nu}(X(\sigma, \tau)) \partial_a X^\mu(\sigma, \tau) \partial_b X^\mu(\sigma, \tau) \quad (5.197)$$

where $X^\mu(\sigma, \tau)$ represents the embedding of the string *in four dimensions*.

We may make contact with the wound-string theory by defining an effective four-dimensional

³¹In the pinched string model in unwarped space, the number of pinches uncovered, per unit time, by the advancing horizon is $N_p(t) \sim t/\Delta \sim n_p t/\rho$ (in either model of pinch formation). In the wound-string model in warped space, the number of windings uncovered is $N_w(t) \sim a_0 t/d \sim n_w t/\rho$. Thus, the four-dimensional appearance and phenomenology of wound-string and pinched string necklaces are indistinguishable. In other words, direct observations of necklaces cannot be used to determine if the space we live in is warped.

tension

$$\mu_{(4)}(\sigma, \tau) \sim T_1 \sqrt{-\gamma_{(10)}(\sigma, \tau)} \quad (5.198)$$

where $\gamma_{(10)}(\sigma, \tau)$ is the determinant of the induced metric on the wound-string embedded in the full *ten-dimensional* spacetime, i.e.

$$\gamma_{(10)ab}(\sigma, \tau) = G_{MN}(X(\sigma, \tau)) \partial_a X^M(\sigma, \tau) \partial_b X^N(\sigma, \tau) \quad (5.199)$$

where $M, N \in \{0, 1, \dots, 9\}$. We then use the four-dimensional (e.g. Minkowski) part of the string embedding to define an induced metric for the effective worldsheet in the large dimensions $\gamma_{(4)}(\sigma, \tau)$ and define an effective four-dimensional action as

$$S = - \int d\sigma d\tau \mu_{(4)}(\sigma, \tau) \sqrt{-\gamma_{(4)}(\sigma, \tau)}. \quad (5.200)$$

Ultimately, if the correspondence between static defect strings and static wound F/D -strings is to hold with regard to the string dynamics, the EOM derived from (5.196) and (5.200) should take the same form for pinched/wound-string ansatz choices intuitively expected to correspond to equivalent configurations from a four-dimensional perspective. As well as providing an important confirmation of the (less general) static gauge work given above, such dynamics would be well worth studying in their own right and a possible program of extension of the current work in this direction is outlined in section 5.10.

5.9.2 Model mixing

As promised in chapters 1 and 3, we now add a brief note on “model mixing”, that is, we ask what happens if we embed a defect string with topological winding number $|n|$ in a geometry with compact extra-dimensions and require it to wrap windings in the internal space? This question may be answered along the following lines: Let us first consider an unwound $|n| = 1$ string, which is dual to an *unwound* F -string in the higher-dimensional geometry. Suppose that this string wraps windings and acquires an *apparent* topological winding number $|m| \sim 1/\sqrt{1 - \omega_l^2} > 1$. Beginning instead with an unwound string of topological charge $|n| > 1$, the *net* apparent winding from a four-dimensional perspective should then be

$$|m| \sim \frac{1}{\sqrt{1 - \omega_l^2}} + |n| - 1. \quad (5.201)$$

However, we may also construct a purely string-theoretic model of this scenario. Instead of a background geometry in which the string may wrap windings with a *single* effective radius at any point (t, r, θ, z) in the four-dimensional manifold, consider a compact space with a *hierachical* structure. For example, instead of a single S^3 , suppose that we have an internal

manifold of the form $S^3 \times S^3$. At any point in the Minkowski directions (t, r, θ, z) , the string may wind in *two* separate $S^1 \equiv U(1)$ sub-manifolds. This would give rise to two winding parameters, $\omega_i^{(1)}$, which measures the proportion of the total string length contained in the windings around the first S^3 , and $\omega_i^{(2)}$, which measures the proportion contained in windings around the second S^3 . Hence the total apparent winding number would become

$$|m| \sim \frac{1}{\sqrt{1 - (\omega_i^{(1)})^2}} + \frac{1}{\sqrt{1 - (\omega_i^{(2)})^2}} - 1, \quad (5.202)$$

so we have

$$|n| \sim \frac{1}{\sqrt{1 - (\omega_i^{(2)})^2}}. \quad (5.203)$$

In addition, as the windings may wrap S^1 sub-manifolds (in either S^3) with continually changing effective radii, we may even mimic the effect of a pinched string wrapping an internal manifold.

5.9.3 A note on the magnetic fields generated by pinched string beads

From the work presented in chapter 3 it is clear that, though superficially similar, necklaces formed from wound strings behave very differently to true string-monopole networks. The main difference between beads formed from pinches/windings and monopoles formed in discrete phase transitions is the existence of a time-dependent bead mass for the former. However, there exists yet another, perhaps even more fundamental reason why necklace “beads” are not true monopoles.

To see this directly, we consider the pinched string dual, and then extrapolate our findings to the wound-string model. The magnetic field around a pinched string with neighbouring $\pm|n|$ sections is illustrated schematically in figure 5.3. In the model presented above, which contains only a single non-zero gauge field component A_θ , the key point is that $B_r = 0$ at the points $z \approx m\Delta$ and $z = m\Delta/2$ (taking the limit $\Delta \gg r_c \gg |n|l_p$), whereas $B_z = 0$ only at $z \approx m\Delta$ and $B_\theta = 0$ for all z . In this case, field lines emanating from the core do a “U-turn” and meet at $r = \infty$, though one can easily imagine adapting the model to include an A_r term in the gauge field ansatz, which allows the \vec{B} -field lines to meet at some finite value of r , perhaps corresponding to the average interstring distance. Alternatively, we may even imagine placing strings with neighbouring $\pm|n|$ regions side by side, but “out of phase” by a length scale $\sim m\Delta$, so that field lines flow from one string into the next.

However, despite these technicalities, *whatever* the precise form of the magnetic field lines generated by the pinches, they may *not* flow from $+|n|$ to $-|n|$ vortex pinches (and vica-

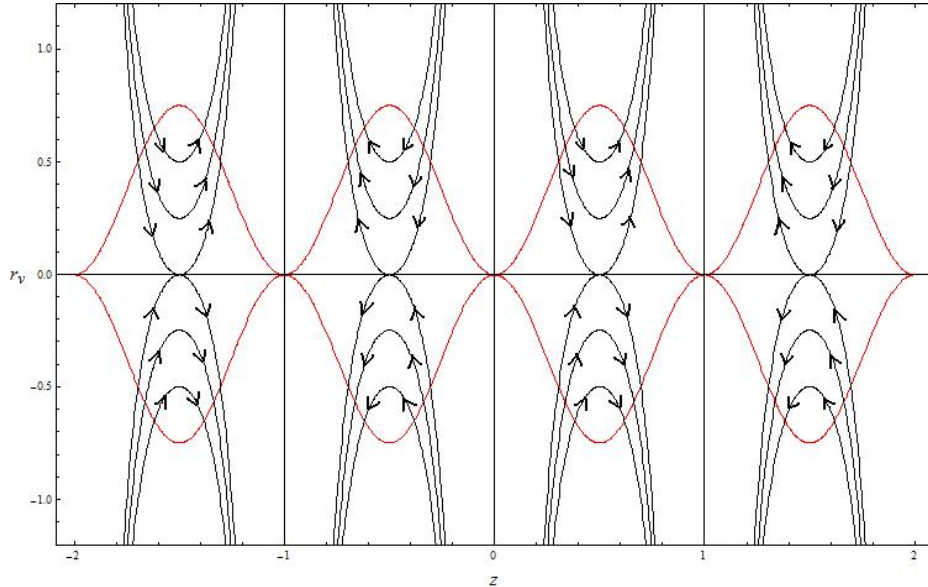


Figure 5.3: This figure illustrates the magnetic field around a pinched string with neighbouring $\pm|n|$ regions. Here we have assumed critical coupling and taken the limit $|n|l_p \ll r_c$. The key point is that the magnetic flux is zero in the region of the pinch, so that flux lines cannot flow between neighbouring “beads”.

versa) along the same string. This is in stark contrast to the field lines emanating from true magnetic monopoles, which by definition can begin on one monopole and end on *any* other monopole of opposite topological charge with which the former is in causal contact.

The term “monopole” should therefore be used with great caution when referring to localised masses associated with extra-dimensional windings, and the term beads, which has largely been adopted in the literature, is far more appropriate.³²

5.9.4 On the instability of non-integer windings

As mentioned in chapter 3, the question of the stability of non-integer windings in the string picture may now be addressed in the dual field theory. The transition from a positive to a negative winding state (i.e. from $|n_w| \rightarrow -|n_w|$), corresponds to a transition from positive to negative topological winding ($|n| \rightarrow -|n|$), in the dual defect string. Although this occurs explicitly in the pinched string ansatz developed above, it may *only* occur in the region of the pinch, where the string core is localised in a Planck scale region $\Delta r \sim |n|l_p$.

In the string theory picture this corresponds to the point at which the string crosses the “pole” of the S^3 *after* completing a full winding. A string which changed direction in the

³²Many thanks are due to Yuri Sitenko for his insightful questions, which helped to clarify these points.

internal space *mid-winding* would therefore correspond to a defect string with neighbouring vortex/anti-vortex regions of radius $\Delta r > |n|l_p$. At these radii vorticity *can* be consistently defined and we would expect such regions to immediately annihilate.

This instability can also be demonstrated explicitly (though only qualitatively within the limits of the present, non-dynamical analysis) in the string picture with the help of diagrams: Figure 5.4 represents a winding configuration in which the string wraps a half-winding in the positive ψ -direction of the S^3 , before changing direction and wrapping a half-winding in the negative ψ -direction. From figures 3.2a and 3.2b, we see that the necklace configuration is formed by successive half-integer windings “falling off” the potential hump in the “same direction” with respect to the θ -coordinate of the diagram (i.e, both string sections fall either to the left or to the right), leading to the production of two beads at separate values of θ . Similarly, if successive half-integer windings were to fall off the potential hump in opposite directions, this would simply lead to the creation of two beads at the *same* value of θ and the necklace structure would be preserved.

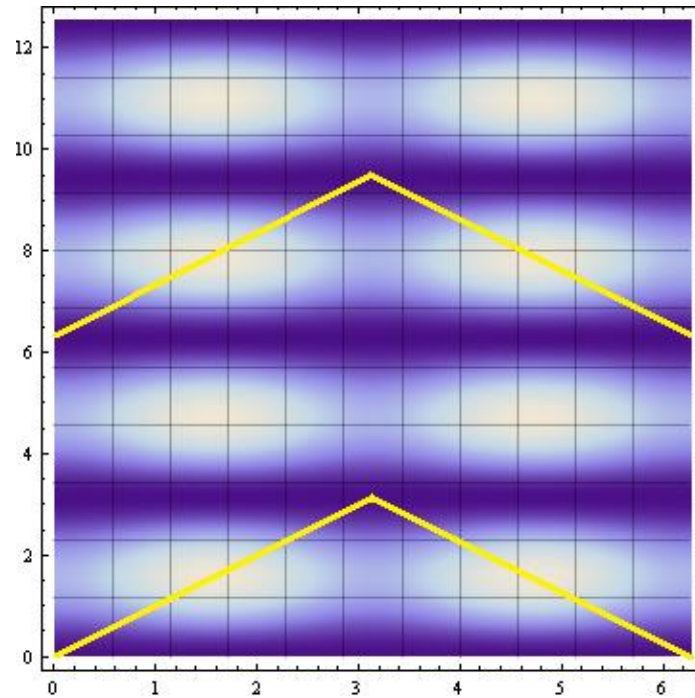


Figure 5.4: Successive half-integer windings of a string in the ψ -direction of the three-sphere. Such a configuration is clearly unstable and its collapse results in the annihilation string section involved in the wrapping.

In the case of successive half-integer windings in *opposite* directions, however, we see that it is not possible for these to fall off the potential hump in this way, as it would imply a discontinuity in the string. The only possibility that remains is for both string sections to

fall off the hump in the same direction, but this leads to the annihilation of the winding.

Dynamically, we may interpret this as resulting from the action of the string tension (viewed as a vector quantity in the compact space), which causes the point at which the string undergoes an inflection to feel a force “pulling” it back to the $\psi = \theta = \phi = 0$ configuration and into line with the four-dimensional string axis. At the point at which a whole winding has been completed, this force is not present - even if the string undergoes an inflection - as the string already “sits” on the four-dimensional axis of the loop (i.e. at the pole of the S^3).

On a related note regarding string transistions, we also see that requiring each point in a finite section of F/D -string to have enough energy to “jump” the potential barrier is equivalent to each point in a finite section of a vortex string acquiring enough energy to “jump” the central region of the Mexican hat potential. In the field picture, the topological defect must “melt away” and then “reform” in a new but energetically equivalent winding state, i.e. with $+|n| \rightarrow -|n|$. This in turn implies that $b - \bar{b}$ annihilation in the wound-string picture, which corresponds to a collision arising through the transition of the connecting string section to a degenerate vacuum state, is likely to be a fairly rare occurrence, which is perhaps far less trivial and less easily realised than previously envisaged (see [6]-[9]). However, there also exists an alternative form of $b - \bar{b}$ collision in the string picture, arising through the outright *annihilation* of neighbouring string sections in degenerate vacuum states. This too has an analogue in the field theory model, as neighbouring sections of $\pm|n|$ string may annihilate if they collide.

5.9.5 Alternative pinched/wound-string configurations

The pinched string ansatz which interpolates between degenerate $+|n|$ and $-|n|$ vortex regions is not the only model we may develop. We may imagine, for example, making the transistion $H_{|n|}(z) \rightarrow \pm(H_{|n|}(z))^2$ in (5.82) so that our string interpolates between identical $+|n|$ and $+|n|$ or $-|n|$ and $-|n|$ regions. Such a model would correspond to wound strings with net windings in only a single direction, which may in fact be the most realistic possibility, given the dynamical models of winding formation we have considered.

Alternatively, we could imagine defining a function $H_{|n_i|}(z)$ where $i \in \{1, 2, 3, \dots\}$ in which neighbouring pinch regions contain vortices of arbitrary topological charge. In addition, these regions may or may not be of equal length. Clearly there are an infinite number of specific pinched string models, even if we restrict ourselves to varying the form of the H -function in the ansatz and do not worry about the functions G_s and G_v , each of which should correspond in some way to a different model of winding formation in the dual string picture.

What is important is that we have shown the generic possibility of a pinched string which may interpolate between regions of $|n_1|$ and $|n_2|$ vortex slices (for $|n_1| \neq |n_2|$) via Planck-sized segments in which vorticity becomes undefined. The only remaining question is, how to link segments with different minimal widths, i.e. $\Delta r = |n_1|l_p$ and $\Delta r = |n_2|l_p$? Clearly, an effective model could be constructed by creating $|n_2 - n_1|$ string sections of length $\Delta z = l_p$ and radii $\Delta r = |n_2 - 1|, |n_2 - 2|, \dots, |n_1 + 1|, |n_1|$ (assuming $|n_2| > |n_1|$), though again, a full field-theoretic description would require a theory of sub-Planck-scale physics.

5.10 Conclusions and discussion of prospects for future work

We have shown that, by introducing spatially-dependent field couplings into the standard Abelian-Higgs model, we may obtain static vortex solutions to the resulting EOM which describe non-cylindrical strings. By hypothesising the existence of Planck-sized regions in which vorticity itself becomes undefined, it has also been possible to construct a model in which neighbouring sections of string carry different topological charges.

Assuming a periodic variation in the pinched string profile, a formal correspondence between the resulting periodic tension and the effective four-dimensional tension of a wound F/D -string in the KS geometry was then obtained. Using a specific but natural ansatz for the string embedding, which describes non-geodesic windings, we were able to obtain specific correspondences between the string theory parameters which define the KS geometry and the field theory parameters which define the Abelian-Higgs model. In the dual string picture, the spatial-dependence of the field couplings was found to be related to the effective radius of the windings.

Though there are many possible ways in which to improve and build upon the research presented in this thesis, perhaps the most valuable would be to extend the present analysis from the purely static case to the more general dynamical one. Ideally, complete dynamical models of pinched string formation and evolution would be developed, which allow the cosmological consequences of pinched string networks to be determined with greater accuracy. It would also be instructive to compare these with general dynamical models of wound (p, q) -strings in order to determine if correspondences exist for all string species. To these ends, we therefore propose the following research plan:

Project 1 - String theory/field theory dualities; Dualities between the dynamics of pinched field-theoretic strings in four-dimensional space and F/D -strings with windings in the extra dimensions may be established by perturbing our existing static solutions and studying the resultant time-dependent behaviour. We may then conjecture effective actions for each configuration (in four-dimensional space) and determine the resulting EOM. If these equations admit solutions which match the expansion obtained previously, equivalence will have been

demonstrated. Specifically, if the two descriptions are equivalent, the motion of the wound-string states should give rise to a time-dependent variation in the four-dimensional effective tension. We therefore expect the four-dimensional effective action for each string to be a variant of the standard Nambu action for F/D-strings and cylindrical field-theoretic strings, but with a modified tension term whose value is a function of the worldsheet coordinates (as proposed in section 5.8.1). Dynamically we expect these perturbations to represent longitudinal waves in four dimensions, in contrast to the behaviour of standard relativistic strings. In the string picture, such longitudinal waves would correspond to genuine compressions and rarefactions in the winding density, analogous to motion of waves on a “slinky”.

Project 2 - Gravitational wave spectrum of an oscillating string loop; This may be calculated by determining the time-dependent energy-momentum tensor for the loop and searching for approximate or exact solutions to the Einstein equations using this as a source. If determining the full, exact, solution proves to be intractable analytically, we may instead search for a solution to the linearised field equations or solve the full non-linear equations numerically. In either case we expect the resulting gravitons to carry momentum in the compact directions. This implies that their wavelengths must be quantized in terms of integer multiples of the length-scale of the compact dimensions. It is this crucial fact that allows us to distinguish between “extra-dimensional” and “four-dimensional” GW spectra and which may enable us to extract information about compact dimensions in future observations.

Project 3 - Macroscopic behaviour of (p, q) -string networks; Using the Compton wavelength associated with the mass-scale of the string tension as an estimate of the string width, and combining this with the length-scale and dimensionality of the compact space (as free parameters of the theory), we may estimate the probability P of a string intersection resulting in the formation of a loop which chops off from the network. This will allow us to calculate the loop production efficiency parameter \tilde{c} and to determine the macroscopic behaviour of the network. In particular, Jun’ichi Yokoyama has suggested³³ that the presence of extra dimensions, combined with randomly distributed motion in the compact space, may greatly decrease the probability of either static or dynamically stabilized loops chopping off from the string network. This may result in the failure of the network to reach a scaling solution, which is the usual assumption applied to all models of field-theoretic networks in the existing literature. It is therefore possible that the effects of microscopic, perhaps even Planck-sized, extra dimensions may be manifested in the large-scale structure of the early universe, greatly influencing its subsequent evolution. However, detailed calculations are needed to confirm this and to determine exactly what influence this may have on cosmologically observable parameters.

³³Private correspondence.

Project 4 - Gravitational field around a pinched/wound string; It is worth calculating the gravitational field surrounding both a static, long, straight string-necklace and a static necklace loop. As in project 3, we may begin by determining the energy-momentum tensor of the string configuration before solving the Einstein equations with this as a source, or we may adopt an inverse method (c.f. [4]) by selecting an ansatz for the metric of the spacetime surrounding the necklace and determining the resulting energy-momentum tensor by substituting this into the field equations. It is well known that the spacetime surrounding a long, straight, uniform string is conical, with an angular deficit proportional to the string tension. We may therefore conjecture that, as the tension of a necklace varies periodically along the length of the string, the surrounding spacetime resembles a “fluctuating” cone, with the angle deficit varying as we move parallel to the string. Again, detailed calculations are needed to confirm this. It would also be interesting, ultimately, to extend this analysis to the full dynamical case.

Project 5 - Fitting models of pinched/wound string networks to CMB anisotropy data; As mentioned in chapter 2, the best fit to existing CMB anisotropy data uses a Λ CDM model incorporating Abelian-Higgs strings which contribute to the temperature fluctuations at the surface of last scattering to the level of approximately ten percent (at multipole $l = 10$) [126, 127]. This exciting result also suggests that still better fits may be obtained using models containing more exotic string species. The work presented here implies that, at least in extra-dimensional models, wound-strings/necklaces are likely to be the most generic string-like objects present in the early universe. The dual pinched string model also suggests that this may be the case, even in the absence of extra dimensions. Unfortunately, no necklace/pinched string fit to the CMB data has been attempted and it would be interesting to extend our present analysis along these lines.

CHAPTER 6

FINAL CONCLUSIONS

In this thesis we have considered a model of static cosmic string loops in the KS background of type IIB string theory where the strings wrap cycles in the internal space. As the compact manifold of this geometry is simply connected, these cycles are not topologically stabilised. However, it was shown that the presence of a lifting potential (resulting from the string embedding) traps sections of string in the compact space, giving rise to strings with step-like winding configurations. From a four-dimensional perspective these configurations then appear as a series of beads connected by strings, which are referred to in the literature as cosmic necklaces.

Before chopping off the network to form a loop, the end point of the string was assumed to undergo random motion in the internal directions. This allowed us to develop an explicit model of non-geodesic winding formation which was found to give rise to a time-dependent lifting potential, in direct contrast to existing models of necklace formation, which assumed the presence a constant bead mass. In this model the bead mass was not a monotonic function of time, but increased from zero initially before peaking and monotonically decreasing at late times. However, the bead number density quickly reached a constant value, so the interbead distance scaled with the horizon. Identifying this with the correlation length of the string network therefore allowed us to propose the existence of a scaling regime, equivalent to that assumed in field-theoretic models of cosmic strings.

As the late-time increase in the number of beads per loop was insufficient to compensate for the fall in individual bead mass, we found that only necklaces formed within a certain window were able to undergo gravitational collapse to form PBHs. Necklaces formed at later times in the scaling regime formed stable relics, with a minimum radius corresponding to the fundamental string width. By considering the contribution to the extragalactic gamma-ray flux from PBHs expiring at the current epoch, we were able to use experimental data from the EGRET experiment to impose bounds on the bead mass, and hence on the underlying string theory parameters which determine it. These bounds were found to directly constrain the background geometry via the deformation parameter, which determines both the size of the S^3 which regularises the conifold and the warping of the Minkowski directions caused by the back-reaction of the fluxes which stabilise its radius.

Throughout this analysis, we have followed previous models in assuming that the bead

mass remains constant after the epoch of loop formation. However, the reparameterisation invariance of the Nambu-Goto action suggests that this approximation may not be valid and further work may be required to determine the full time-dependent behaviour of wound-string networks.

Extending our initial static model, we then proposed a mechanism for the creation of cosmic string loops with dynamically stabilised windings in the internal space. Assuming a velocity correlations regime in the post-inflationary epoch, such windings were seen to arise naturally in string networks prior to loop formation. Considering strings with geodesic windings, the angular momentum of the string in the compact space was found to be sufficient to ensure that the windings remained stable after the loop chops off from the network, even though the internal manifold is simply connected. In addition, we found that the interaction of angular momentum with the string tension may cause the loop to oscillate between alternate phases of expansion and contraction, though a critical solution exists in which the two forces are exactly balanced. This raises the possibility that an oscillating wound-string loop could produce a distinct GW signature, the future detection of which could provide evidence for the existence of extra dimensions.

In the final part of our work we proposed a modification of the standard Abelian-Higgs model, introducing spatially-dependent couplings for the scalar and vector fields. We investigated static, non-cylindrically-symmetric solutions of the resulting field equations and proposed a pinch solution which interpolates between degenerate vacuum states along the string, labelled by $\pm |n|$. This configuration corresponds to a vortex which shrinks until it reaches the Planck scale, before re-emerging as an anti-vortex, and which results in the formation of a bead pair with one bead either side of the intersection. The string is then topologically stable and was shown to be a valid solution to the EOM, except in the Planck-scale regions where no solution could be obtained.

The key assumption governing our treatment of these regions was that quantities like phase and winding number, along with others which depend on them, such as the magnetic flux of the gauge field, become undefined at the Planck scale, so that string sections with opposite winding may be joined via a Planck-sized segment of neutral string. The pinched string ansatz was found to give rise to a periodic tension, which required us to assume a value in the pinch regions equal to the tension of a cylindrically symmetric string, in order to ensure continuity.

Similarities between this solution and the wound-string states considered previously were then explored. Using natural ansatz choices for the pinched string profile and wound-string embedding, a formal correspondence between the pinched string tension and the effective four-dimensional tension of the wound string was established. This allowed a formal cor-

response between the field-theoretic parameters which define the Abelian-Higgs model and the string theory parameters which define the KS geometry to be inferred. The spatial-dependence of the field couplings was then interpreted as resulting from the spatial variation in the effective radius of the windings which leads to a varying string coupling.

One especially interesting result was an estimate of the Higgs mass at critical coupling, which was found to be equal to the energy scale associated with the three-sphere radius. This may also be written in terms of a product involving the deformation parameter and warp factor which distorts the Minkowski directions and which, as demonstrated by the work presented here, may be constrained by cosmological observations.

Appendices

Appendix A: Eulerian substitution of the third kind

The quadratic equation in the integral defined by (4.47) and (4.48) has a discriminant $\Delta = b^2 - 4ac$ which is everywhere non-negative for values of a_0^2 in the range $0 < a_0^2 < 1$. We may therefore evaluate the integral using a Eulerian transformation of the third kind, which takes advantage of the fact that there exist two *real* roots in y . Let A and B be the two real roots of the quadratic equation $-ay^2 + by - c = 0$. We then define a dummy variable u by

$$\sqrt{-ay^2 + by - c} = (y - A)u. \quad (\text{A-1})$$

In general, we have

$$-ay^2 + by - c = a(y - A)(B - y), \quad (\text{A-2})$$

so combining (A-1) and (A-2) implies

$$a(B - y) = (y - A)u^2 \quad (\text{A-3})$$

or equivalently

$$y = \frac{aB + Au^2}{a + u^2} \quad (\text{A-4})$$

and

$$\frac{y}{\sqrt{a}} = \pm \sqrt{\frac{B - y}{y - A}}. \quad (\text{A-5})$$

Using the second solution for y as function of u and differentiating the expression above, then gives

$$dy = \frac{2du}{a + u^2} \left\{ - \left(\frac{aB + Au^2}{a + u^2} \right) + A \right\} u. \quad (\text{A-6})$$

Finally, substituting (A-1), (A-4) and (A-6) into the right-hand-side of (4.47) gives

$$\begin{aligned} \int dt &= \pm \frac{1}{2} \int \frac{dy}{\sqrt{-ay^2 + by - c}} = \pm \frac{1}{2} \int \frac{dy}{(y - A)u} \\ &= \pm \frac{1}{2} \int \frac{\frac{2du}{a+u^2} \left\{ - \left(\frac{aB+Au^2}{a+u^2} \right) + A \right\} u}{\left\{ \left(\frac{aB+Au^2}{a+u^2} \right) - A \right\} u} = \mp \int \frac{du}{a + u^2}. \end{aligned} \quad (\text{A-7})$$

Using the standard integral $\int \frac{dx}{\kappa^2 + x^2} = \tan^{-1} \left(\frac{x}{\kappa} \right)$ and (A-5) then gives (4.50).

Appendix B: The Hopf fibration of the three-sphere

As stated in the introduction, we chose to use the Hopf fibration of the S^3 when considering geodesic windings, as this allows the metric and Killing vectors to be written in a particularly simple form, viz, (4.4) and (4.17). Choosing windings which wrap only Killing directions in the S^3 then leads to *manifest* σ -independence in the constants of motion (4.21).

The ansatz corresponding specifically to *geodesic* windings is the linear ansatz (4.17) and this choice of coordinates naturally reflects the $SO(3)$ symmetry of the internal space.

We will now discuss the origin of the Hopf fibration from a geometric point of view. However, it will also be useful to discuss the origin of the canonical coordinate system from a similar perspective. By comparing the two (equivalent) descriptions, we hope to clarify the advantage of using the former coordinate system in the present work and to demonstrate explicitly the coordinate-independence of our results.

One very natural choice of coordinates on the S^3 is the so-called “canonical parameterisation”. In this case, the group element of the S^3 manifold is

$$g = e^{(i/2)[x\sigma_1 + y\sigma_2 + z\sigma_3]}, \quad (\text{B-1})$$

where σ_i , $i \in \{1, 2, 3\}$ are the usual Pauli matrices. Writing the usual Cartesian coordinates x, y and z in terms of polars r, θ, ϕ , the line element becomes

$$ds^2 = -\frac{1}{2}Tr([dgg^{-1}]^2) = dr^2 + \sin^2 r(d\theta^2 + \sin^2 \theta d\phi^2) \quad (\text{B-2})$$

which is exactly that given in (4.1) if we identify $\psi = r$ and multiply the whole metric by R^2 .

By contrast, following Iglesias and Blanco-Pillado [276], we chose to parameterise the S^3 using Eulerian variables. We regard the S^3 as an $SU(2)$ group manifold with element g given by [288]

$$g(\psi, \theta, \phi) = e^{i(\psi/2)\sigma_1} e^{i(\theta/2)\sigma_2} e^{i(\phi/2)\sigma_3}, \quad (\text{B-3})$$

where σ_i are the Pauli matrices as before. The group-invariant metric (i.e. the metric on S^3 in these coordinates) can then be written in the form

$$ds^2 = -\frac{1}{2}Tr([dgg^{-1}]^2) = \frac{1}{4}(d\theta^2 + (d\psi + \cos \theta d\phi)^2). \quad (\text{B-4})$$

It may be seen that, in these coordinates, the submanifolds where $\theta = \theta_0$ is constant correspond to flat two-tori with metrics

$$ds^2 = \frac{1}{4}(d\psi + \cos \theta_0 d\phi)^2. \quad (\text{B-5})$$

This shows that the Hopf fibration corresponds to describing the three-sphere as a one-parameter family of flat two-tori (to which it is topologically equivalent). Again we follow Iglesias [276] in choosing $\theta_0 = 0$ in order to simplify the metric as much as possible. It is also necessary to rescale the metric so that $1/4 \rightarrow R^2$, as we are dealing with a physical S^3 of radius R .

Let us now consider an arbitrary string embedding which is a function of both space and time, $X^i(\sigma, t)$ where $i \in \{0, 1, \dots, 9\}$. The general - coordinate-independent - expression for the string Lagrangian is

$$L = -T_1 a_0^2 \int d\sigma \sqrt{(1 - \dot{r}^2)(r^2 + a_0^{-2} R^2 W) - a_0^{-2} R^2 r^2 P + a_0^{-4} R^4 Q} \quad (\text{B-6})$$

where

$$\begin{aligned} W &= X'^i(\sigma, t) g_{ij}(X(\sigma, t)) X'^j(\sigma, t) \\ P &= \dot{X}^i(\sigma, t) g_{ij}(X(\sigma, t)) \dot{X}^j(\sigma, t) \\ Q &= (\dot{X}^i(\sigma, t) g_{ij}(X(\sigma, t)) X'^j(\sigma, t))^2 \\ &\quad - (\dot{X}^i(\sigma, t) g_{ij}(X(\sigma, t)) \dot{X}^j(\sigma, t)) (X'^i(\sigma, t) g_{ij}(X(\sigma, t)) X'^j(\sigma, t)) \end{aligned} \quad (\text{B-7})$$

and a dash/dot indicates differentiation with respect to σ/t , respectively. In the static case, the term $W(\sigma) = X'^i(\sigma) g_{ij}(X(\sigma)) X'^j(\sigma)$ corresponds to the length of the wrapped string on the S^3 . Demanding $\frac{dW}{d\sigma} = 0$, one obtains the geodesic equation

$$X''^i(\sigma) + \Gamma_{jk}^i X'^j(\sigma) X'^k(\sigma) = 0 \quad (\text{B-8})$$

where Γ_{jk}^i are the usual Christoffel symbols. Thus minimal (i.e. geodesic) windings on a general manifold (in our case, S^3) with metric g_{ij} is enough to guarantee σ -independence of the winding terms.

This statement still holds if we allow time-dependence into the string ansatz, $X^i(\sigma, t)$, as long as for each instant in time the latter still satisfies the geodesic equation. Physically this means that the wrapped loop only ever evolves along geodesic curves. A simple example on the S^2 would be a great circle passing through the north and south poles and rotating about an axis through the poles. Thus we require our embedding function to satisfy

$$X''^i(\sigma, t) + \Gamma_{jk}^i X'^j(\sigma, t) X'^k(\sigma, t) = 0. \quad (\text{B-9})$$

With time-dependence we also have a non-zero kinetic energy term of the wrapped string inside the square root factor in our Lagrangian

$$P(\sigma, t) = \dot{X}^i(\sigma, t) g_{ij}(X(\sigma, t)) \dot{X}^j(\sigma, t). \quad (\text{B-10})$$

Demanding that $\frac{dP}{d\sigma} = 0$, we find

$$\dot{X}''^i(\sigma, t) + \Gamma_{jk}^i \dot{X}^j(\sigma, t) \dot{X}^k(\sigma, t) = 0. \quad (\text{B-11})$$

Geometrically this states that the velocity vector, \dot{X}^i , is preserved under parallel transport along a geodesic curve that is wrapped by the string. One can equally interpret this equa-

tion as saying that under parallel transport of the tangent vector to the geodesic curve, X'^i , along a curve whose tangent vector is \dot{X}^i , the former is preserved. Mathematically, this is simply the statement that $\nabla_{\dot{\gamma}}\gamma' \equiv \nabla_{\gamma'}\dot{\gamma} = 0$.

The nice consequence of demanding the above is that the winding term is not only σ -independent (if we take geodesic wrapping) but also time-independent, i.e. $\frac{dW}{dt} = 0$. Thus σ -independence of the kinetic function P guarantees time-independence of W . This is an important statement.

Let us now consider what the situation above implies for the case where the wrapping is over flat submanifolds, as in the case of Iglesias, where the Γ_{jk}^i all vanish. The geodesic equation (B-9) and (B-11) trivially imply $X''^i = 0$, $\dot{X}^i = 0$ and the solution of these equations is

$$X^i(\sigma, t) = X_0^i + n^i\sigma + u^i(t). \quad (\text{B-12})$$

This provides the origin of the linear σ ansatz of Iglesias. Apart from the winding and kinetic terms mentioned above, there are additionally the two R^4 terms appearing inside the square root in the Lagrangian in $Q(\sigma, t)$. The σ -independence of the second term follows from our previous results, because this term is simply WP . The σ -independence of the first term above follows after a simple calculation making use of (B-9) and (B-11). In the case of wrapping along a flat submanifold, one sees that Q vanishes identically.

However, what is important is that σ -independence of all the relevant terms in the Lagrangian is guaranteed by requiring the strings to wrap geodesics and that the velocity vector is preserved under parallel transport along this geodesic. Thus $L = \int d\sigma \mathcal{L} = 2\pi\mathcal{L}$, as stated in the introduction.

We now have the possibility of working in *any* coordinate system, though the choice of explicit string wrapping ansatz is constrained by the requirement of solving (B-9), (B-11) *if* we require geodesic windings. In general, explicit solutions to the geodesic equations are hard to come by but for very symmetric spaces - like spheres - they are known. ¹

Let us now compare the form of these explicit solutions in canonical coordinates to the simple linear ansatz in (B-12). In order to determine the appropriate ansatz for geodesic windings in canonical coordinates, we must first calculate the Killing vectors in this coordinate system. We know that the Killing fields corresponding to the $SU(2)$ rotations of the S^3 generate isometries of the above metric. Therefore, if we think of the S^3 as being

¹For general wrappings of the string around the full S^3 , however, the ansatz will certainly never be linear in σ and nor will the σ - and time-dependence factorize in an additive way, as it did in the flat space case, no matter what the choice of coordinates.

embedded in R^4 where X, Y, Z, U represent the four Cartesian coordinates,

$$X^2 + Y^2 + U^2 + Z^2 = 1, \quad (\text{B-13})$$

the three independent isometries are generated by

$$J_1 = J_{XU} + J_{YZ}, \quad J_2 = J_{XZ} + J_{YU}, \quad J_3 = J_{XY} + J_{ZU}, \quad (\text{B-14})$$

where $J_{ZU} = Z\partial_U - U\partial_Z$ is the generator of rotations in the $Z - U$ plane etc. The above J_i clearly generate an $SU(2)$ algebra. Then the three Killing vectors are

$$k_1^i = (-U, -Z, X, Y); \quad k_2^i = (-Z, U, -Y, X); \quad k_3^i = (-Y, X, Z, -U) \quad (\text{B-15})$$

which define an orthonormal basis for the $SU(2)$ Lie algebra. However, *unlike* the Killing vector fields of the two-torus, those of the whole S^3 are in general coordinate-dependent.

Since we work with coordinates $\{\psi, \theta, \phi\}$ rather than the embedding coordinates $\{X, Y, U, Z\}$ one can re-express the above Killing vectors in terms of $k_a^i(\psi, \theta, \phi)$ with $i = 1 \dots 3$ of the S^3 . To obtain these, consider the left-action of rigid group elements

$$g_a = e^{i\epsilon\sigma_a} \quad (\text{B-16})$$

on the group element g of $SU(2)$ written in terms of canonical coordinates described above. Explicitly we have that

$$\begin{aligned} g_{11} &= \cos(\psi) + i \sin(\psi) \cos(\theta), \\ g_{12} &= i \sin(\psi) \sin(\theta) e^{-i\phi}, \\ g_{21} &= i \sin(\psi) \sin(\theta) e^{i\phi}, \\ g_{22} &= \cos(\psi) - i \sin(\psi) \cos(\theta). \end{aligned} \quad (\text{B-17})$$

Expanding to linear order in ϵ in the g_i , reading off the infinitesimal variations $\delta\psi, \delta\theta, \delta\phi$ and equating

$$\delta X^i = \epsilon k_a^j \partial_j X^i, \quad (\text{B-18})$$

we can then read off the components of the Killing vector k_a^i for each of the isometries induced by left-action with group element $g_a, a = 1, 2, 3$ of $SU(2)$. This gives

$$\begin{aligned} k_1 &= [\sin(\theta) \cos(\phi), \sin(\phi) - \cot(\psi) \cos(\theta) \cos(\phi), -\cot(\theta) \cos(\phi) - \cot(\psi) \frac{\sin(\phi)}{\sin(\theta)}] \\ k_2 &= [-\sin(\theta) \sin(\phi), \cos(\phi) - \cot(\psi) \cos(\theta) \sin(\phi), -\cot(\theta) \sin(\phi) - \cot(\psi) \frac{\cos(\phi)}{\sin(\theta)}], \\ k_3 &= [\cos(\theta), -\cot(\psi) \sin(\theta), -1]. \end{aligned} \quad (\text{B-19})$$

One can check that the above Killing vectors are orthonormal with respect to the canonical metric on S^3 ,

$$k_a^i g_{ij} k_b^j = \delta_{ab}. \quad (\text{B-20})$$

Using the above results, it is *possible* to show the σ -independence of the Lagrangian for geodesic windings, but even when working in canonical coordinates, the resulting expressions are complicated. If we now return to our coordinate-independent description, armed with the knowledge that the Lagrangian density *must* be σ -independent for geodesic windings, we find that we can reproduce most of our results without reference to a specific coordinate system.

Looking at the effective potential (setting all time derivatives to zero), we find

$$V = a_0^2 T_1 \sqrt{r^2 + a_0^{-2} R^2 W} \quad (\text{B-21})$$

and we now know that the second term is just the warped length squared of the wrapped string on the S^3 . The tangent vector to a geodesic x^i (where a dash here refers to differentiation with respect to the affine parameter along the curve) can always be defined to have unit length ie $x^i g_{ij} x^j = 1$. In our case, the string wraps closed curve geodesics with different winding numbers in general. A nice example of closed curve geodesics on the S^3 are the integral curves whose tangent vectors are the three Killing vectors k_a^i , $a = 1, 2, 3$ that generate the $SU(2)$ isometry group of S^3 (see above). Thus it is natural to take the following ansatz for our static wrapped string:

$$X_G^i(\sigma) = \sum_a n_a x_a^i = \sum_a n_a k_a^i(X(\sigma)) \quad (\text{B-22})$$

where we have used the fact that the tangent vectors to the $SU(2)$ generated geodesics are the Killing vectors k_a^i (and where the subscript G implies that the embedding ansatz satisfies (B-9) and (B-11)). The Killing vectors not only have unit length with respect to the canonical metric on the S^3 but they are orthonormal. Using this, it is easy to see that $W = \sum_a n_a n_a$, which is a constant and so consistent with our previous analysis.

The above makes sense because it is known that flows of the Killing vector fields on S^3 induced by rigid $SU(2)$ rotations are geodesics. Our wrapping ansatz is guaranteed to be “minimal” - in the same sense as the linear ansatz of Iglesias for winding around the torus - because the flows of the Killing vectors in that case are geodesic circles around the torus.

In equation (B-22) we have written the expression for $X^i(\sigma)$ and not $X^i(\sigma)$. The latter can be obtained in principle by integration. In the simple case where the Killing vectors are coordinate-independent (e.g. Abelian isometries, shift isometries), integration directly gives us $X_G^i = X_0^i + \sigma n_a k_a^i$, as found in the case of flat submanifolds discussed earlier. The

$SU(2)$ Killing vectors, however, are not constant, so integration is non-trivial and will lead to non-linear dependence on σ in general.

It is a general result that if a Killing vector field has constant length, then it will generate geodesics along the manifold. In our case, we know that the $k_a^i(X)$ have unit length with respect to the canonical metric on the S^3 . Therefore we can be sure that equation (B-9) will be solved by $X^i(\sigma) \sim k_a^i(X)$ on the three-sphere according to the ansatz in (B-22). One can see this more clearly by taking the normalisation constraint $g_{ij}k_a^ik_b^j = \delta_{ab}$ and differentiating this with respect to some arbitrary vector field Y . The resultant Killing equation gives us $\nabla_{k_a}k_b = 0$, which more generally implies

$$\nabla_{n_a k_a} n_b k_b = 0. \quad (\text{B-23})$$

This is just a restatement of the fact that $n_a k_a^i$ is a geodesic.

Since we are interested in the dynamics of such an embedding, we now need to extend our solution to incorporate time-dependence. This means that we need to preserve the geodesics under time evolution. To ensure this, let us use the $SU(2)$ transformations, since these are isometries which preserve the canonical metric and map geodesics to geodesics. The modified ansatz for the embedding functions reads

$$\begin{aligned} X^i(\sigma, t) &= \sum_a n_a k_a^i(X(\sigma, t)), \\ \dot{X}^i(\sigma, t) &= \sum_a \lambda_a k_a^i(X(\sigma, t)), \end{aligned} \quad (\text{B-24})$$

where we have introduced new variables $\lambda_a \in \mathbb{R}$. The string modes will therefore be wrapped along any curve defined by $n_a k_a^i$, and this curve will evolve via the second geodesic equation (with tangent vector $\lambda_a k_a^i$). This means that the functions in the action will take a simplified form,

$$W \rightarrow \sum_a n_a n_a, \quad P \rightarrow \sum_a \lambda_a \lambda_a, \quad (\text{B-25})$$

which are both constant, and λ_a is related to the average speed of the string along the S^3 .

If n_a and λ_a are such that the X^i and \dot{X}^i are parallel, then the R^4 terms will vanish from the action. If these vectors are not parallel, there is no cancellation, which means that the wrapped geodesic must have a perpendicular component along the winding direction satisfying $\dot{X}^i X'^j g_{ij} = 0$.

How does this affect the resultant action constructed in equation (B-6)? We can define a unit vector pointing parallel to the winding direction in the usual manner. This allows

us to split the velocity into components $\dot{X}^i = \dot{X}_{\parallel}^i + \dot{X}_{\perp}^i$. After some manipulation we find that the Lagrangian simplifies to

$$L = -\mathcal{T}a^2 \sqrt{(1 - \dot{r}^2 - a^{-2}R^2 \dot{X}_{\perp}^i g_{ij} \dot{X}_{\perp}^j)(r^2 + a^{-2}R^2 W) - a^{-2}R^2 r^2 \dot{X}_{\parallel}^i g_{ij} \dot{X}_{\parallel}^j} \quad (\text{B-26})$$

where the R^4 terms have cancelled, as already stated. Physically this makes sense, since the perpendicular modes lie in the normal bundle and therefore contribute to the transverse boost of the string, much like the velocity in the Minkowski directions. The net effect is an enhancement of the relativistic “gamma” factor.

In the simplest case, where we neglect the transverse modes, the resultant energy and momentum are

$$\begin{aligned} E &= 2\pi T_1 \frac{a_0^2(r^2 + a_0^{-2}R^2 W)}{\sqrt{(1 - \dot{r}^2)(r^2 + a_0^{-2}R^2 W) - a_0^{-2}R^2 r^2 P}}, \\ l &= 2\pi T_1 \frac{R^2 r^2 \lambda_a n_a}{\sqrt{(1 - \dot{r}^2)(r^2 + a_0^{-2}R^2 W) - a_0^{-2}R^2 r^2 P}}, \end{aligned} \quad (\text{B-27})$$

where we have defined l in the same manner as [276]:

$$l = \frac{\delta L}{\delta \dot{X}^i} X^i. \quad (\text{B-28})$$

For the case where there is no velocity in the Minkowski direction, we can write the energy as a function of l and minimise it to obtain

$$r_*^4 = \frac{l^2}{a_0^4(2\pi)^2 T_1^2}, \quad (\text{B-29})$$

which is the generalisation of the $r \sim \sqrt{l}$ dependence obtained in Iglesias. Moreover, the velocity at the minimal radius is

$$\dot{X}_{\parallel}^2 = \lambda_a \lambda_a = \frac{a_0^2}{R^2}. \quad (\text{B-30})$$

Considering the general case, where there is non-zero \dot{X}_{\perp}^i , we see that solutions which minimise the energy with non-zero l require us to set $\dot{r} = \dot{X}_{\perp}^i = 0$. This is easily understood since non-zero velocity in these directions only ever increases the energy through enhancement of the “gamma” factor.

In the general case we see that the above expressions can be written in the modified form

$$\begin{aligned}
E &= 2\pi T_1 \frac{(r^2 + a_0^{-2} R^2 n_a n_a)}{\sqrt{(1 - \dot{r}^2 - a_0^{-2} R^2 \dot{X}_\perp^i g_{ij} \dot{X}_\perp^j)(r^2 + a_0^{-2} R^2 n_b n_b) - a_0^{-2} R^2 r^2 \lambda_b \lambda_b}}, \\
l &= 2\pi T_1 \frac{R^2 r^2 \lambda_a n_a}{\sqrt{(1 - \dot{r}^2 - a_0^{-2} R^2 \dot{X}_\perp^i g_{ij} \dot{X}_\perp^j)(r^2 + a_0^{-2} R^2 n_b n_b) - a_0^{-2} R^2 r^2 \lambda_b \lambda_b}}. \quad (\text{B-31})
\end{aligned}$$

References

- [1] M. Lake, S. Thomas and J. Ward, *String necklaces and primordial black holes from type IIB strings* JHEP **12**, 033 (2009) [arXiv:0906.3695v2] (hep-ph).
- [2] M. Lake, S. Thomas and J. Ward, *Non-topological cycloops* JCAP **01**, 026 (2010) [arXiv:0911.3118v2] (hep-th).
- [3] M. Lake and J. Ward, *A generalisation of the Nielsen-Olesen vortex: Non-cylindrical strings in a modified Abelian-Higgs model* (submitted to JHEP) [arXiv:1009.2104] (hep-ph).
- [4] M. Lake and T. Harko, *Null fluid collapse in Randall-Sundrum type II brane-worlds* (in preparation).
- [5] I. R. Klebanov and M. J. Strassler, *Supergravity and a confining gauge theory: Duality cascades and χ SB-resolution of naked singularities* JHEP **0008**, 052 (2000) [arXiv:hep-th/0007191].
- [6] T. Matsuda, *PBH and DM from cosmic necklaces* [arXiv:hep-ph/0601014] (2006).
- [7] T. Matsuda, *Dark matter production from cosmic necklaces* JCAP **0604**, 005 (2006) [arXiv:hep-ph/0509064].
- [8] T. Matsuda, *Primordial black holes from cosmic necklaces* JHEP **0604**, 017 (2006) [arXiv:hep-ph/0509062].
- [9] T. Matsuda, *Brane necklaces and brane coils* JHEP **0505**, 015 (2005) [arXiv:hep-ph/0412290].
- [10] M.B. Green, J.H. Schwarz and E. Witten *Superstring Theory: Introduction v1* (1988), CUP, ISBN-13: 978-0521357524 (hardback).
- [11] J. Polchinski *String Theory: Introduction to the Bosonic String v1* (2005), CUP, ISBN-13: 978-0521672276 (paperback).
- [12] P. Sreekumar *et al* (EGRET collaboration) *EGRET Observations of the Extragalactic Gamma Ray Emission* [arXiv:astro-ph/9709257v1].

-
- [13] R. C. Hartman *et al.* (EGRET Collaboration), *The Third EGRET catalog of high-energy gamma-ray sources* *Astrophys. J. Suppl.* **123**, 79 (1999).
- [14] C. von Montigny *et al.* (EGRET Collaboration), *High-energy gamma-ray emission from active galaxies: EGRET observations and their implications* *Astrophys. J.* **440**, 525 (1995).
- [15] H. B. Nielsen and P. Olesen, *Vortex-line Models for Dual Strings* *Nucl. Phys.* **B61**, 45-61 (1973).
- [16] A. Avgoustidis and E. P. S. Shellard, *Cycloops: Dark matter or a monopole problem for brane inflation?* *JHEP* **0508**, 092 (2005) [arXiv:hep-ph/0504049].
- [17] M. Sasaki, T. Shiromizu and K. Maeda, *Gravity, Stability and Energy Conservation on the Randall-Sundrum Brane-World* *Phys. Rev.* **D62**, 024008 (2000) [arXiv:hep-th/9912233v3].
- [18] T. Shiromizu, K. Maeda and M. Sasaki, *The Einstein Equations on the 3-Brane World* *Phys. Rev.* **D62**, 024012 (2000) [arXiv:gr-qc/9910076v3].
- [19] L. Randall and R. Sundrum, *A Large Mass Hierarchy from a Small Extra Dimension* *Phys. Rev. Lett* **83**, 3370 (1999) [arXiv:hep-ph/9905221v1].
- [20] L. Randall and R. Sundrum, *An alternative to compactification* *Phys. Rev. Lett* **83**, 4690 (1999) [arXiv:hep-th/9906064].
- [21] N. Dadhich and S.G. Ghosh, *Gravitational collapse of null fluid on the brane* *Phys. Lett.* **B518**, 1-7, (2001) [arXiv:hep-th/0101019v1].
- [22] R. Hagedorn, *Suppl. Nuovo Cimento* **3**, 147, (1965)
- [23] T. Harko, *Gravitational collapse of a Hagedorn fluid in Vaidya geometry* *Phys. Rev.* **D68**, 064005 (2003) [arXiv:gr-qc/0307064v1].
- [24] T. Harko and K. S. Cheng, *Collapsing strange quark matter in Vaidya geometry* *Phys. Lett.* **A266**, 249 (2000) [arXiv:gr-qc/0104087v1].
- [25] V. Hussain, *Exact solutions for null fluid collapse* *Phys. Rev.* **D53**, R1759 (1996)
- [26] D. Brown and V. Hussain, *Black holes with short hair* *Int. J. Mod. Phys.* **D6**, 563-573 (1997) [arXiv:gr-qc/9707027v2].
- [27] A. Wang and Y. Wu, *Generalized Vaidya Solutions* *Gen. Rel. Grav.* **31**, 107, (1999) [arXiv:gr-qc/9803038].
- [28] P.T. Crusciel, *“No Hair” Theorems - Folklore, Conjectures, Results* *Contemp. Math.* **170**, 23-49, (1994) [arXiv:gr-qc/9402032].

-
- [29] M. Huesler, *No Hair Theorems and Black Holes with Hair* *Helv. Phys. Acta.* **69**, 501-528, (1996) [arXiv:gr-qc/9610019v1].
- [30] S. Mukohyama, T. Shiromuzu and K. Maeda, *Global structure of exact cosmological solutions in the brane world* *Phys. Rev.* **D62**, 024028, (2000); Erratum-ibid. **D63**, 029901, (2001) [arXiv:hep-th/9912287v2].
- [31] T. Shiromuzu and D. Ida, *Anti-de Sitter no-hair, AdS/CFT and the brane-world* *Phys. Rev.* **D64**, 044015, (2001) *Phys. Rev.* **D64**, 044015 (2001) [arXiv:hep-th/0102035v3].
- [32] R. Penrose, *Naked Singularities* *Annals of the New York Academy of Sciences*, Sixth Texas Symposium on Relativistic Astrophysics, **224**, 125134, (Dec. 1973)
- [33] V. Moncrief and D.M. Eardley, *The global existence problem and cosmic censorship in general relativity* *Gen. Rel. and Grav.* **13**, 9, 887-892, (1980)
- [34] R.M. Wald, *Gravitational Collapse and Cosmic Censorship* [arXiv:arXiv:gr-qc/9710068v3] (1997).
- [35] P.R. Brady, I.G. Moss and R.C. Myers, *Cosmic Censorship: As Strong As Ever* *Phys. Rev. Lett.* **80**, 34323435, (1998).
- [36] S.L. Shapiro and S.A. Teukolsky, *Formation of naked singularities: The violation of cosmic censorship* *Phys. Rev. Lett.* **66**, 994997, (1991).
- [37] S.L. Shapiro and S.A. Teukolsky, *The Hoop Conjecture and Cosmic Censorship in the Brane-World* *Phys. Lett.* **B564**, 143-148, (2003) [arXiv:gr-qc/0112067v2].
- [38] J. Preskill, *Do Black Holes Destroy Information?* [arXiv:hep-th/9209058v1] (1992).
- [39] S.B. Giddings, *The Black Hole Information Paradox* [arXiv:hep-th/9508151v1] (1995).
- [40] S.B. Giddings and M. Lippert, *The information paradox and the locality bound* *Phys. Rev.* **D69**, 124019, (2004) [arXiv:hep-th/0402073v3].
- [41] S.W. Hawking, *Information Loss in Black Holes* *Phys. Rev.* **D72**, 084013, (2005) [arXiv:hep-th/0507171v2].
- [42] L. Susskind and J. Lindesay, *An Introduction to Black Holes, Information and the String Theory Revolution: The Holographic Universe* (2005), World Scientific, ISBN:981-256-131-5 (paperback).
- [43] S.W. Hawking, *MNRAS* **152**, 75 (1971).
- [44] Y.B. Zel'dovich and I.D. Novikov, *Sov. Astron.* **10**, 602 (1967).

- [45] B.J. Carr and S.W. Hawking, *Gamma rays from primordial black holes* MNRAS **168**, 399 (1974).
- [46] B.J. Carr, *The primordial black hole mass spectrum* Astrophys. J. **201**, 1 (1975).
- [47] D.K. Nadezhin, I.D. Novikov and A.G. Polnarev, *The hydrodynamics of primordial black hole formation* Sov. Astron. **22**, 129 (1978).
- [48] G.V. Bicknell and R.N. Henrikson, *Formation of primordial black holes* Astrophys. J. **232**, 670 (1979).
- [49] B.J. Carr, *Primordial black holes: Do they exist and are they useful?* [arXiv:astro-ph/0511743v1] (2005).
- [50] J. Kormendy and D. Richstone *Inward bound - the search for supermassive black holes in galactic nuclei* Annual Review of Astronomy and Astrophysics **33**, 581-624 (1995).
- [51] S. Hawking *Black hole explosions* Nature **248**, 30 (1974).
- [52] S. Hawking *Particle Creation by Black Holes* Commun. Math. Phys. **43**, 199-220 (1975).
- [53] J.D. Bekenstein *Black holes and entropy* Phys. Rev. **D7**, 2333 (1973).
- [54] J.M. Bardeen, B. Carter and S.W. Hawking *The four laws of black holes mechanics* Commun. Math. Phys. **31**, 161 (1973).
- [55] W.G. Unruh, *Notes on black hole evaporation* Phys. Rev. **D14**, 870 (1976).
- [56] T. Kanazawa, M. Kawasaki, and T. Yanagida, *Double inflation in supergravity and the primordial black hole formation* Phys. Rev. Lett. **B482**, 174 (2000) [arXiv:hep-ph/0002236].
- [57] D. Blais, C. Kiefer, and D. Polarski, *Can Primordial Black Holes be a Significant Part of Dark Matter?* Phys. Rev. Lett. **B535**, 11 (2002) [arXiv:astro-ph/0203520].
- [58] D. Blais, T. Bingham, C. Kiefer and D. Polarski, *Accurate results for primordial black holes from spectra with a distinguished scale* Phys. Rev. **D67**, 024024 (2003) [arXiv:astro-ph/0206262].
- [59] R. Saito, J. Yokoyama and R. Nagata, *Single-field inflation, anomalous enhancement of superhorizon fluctuations, and non-Gaussianity in primordial black hole formation* J. Cosmol. Astropart. Phys. (JCAP) **0806**, 024 (2006) [arXiv:0804.3470] (astro-ph).
- [60] K.J. Mack, J.P. Ostriker and M. Ricotti, *Growth of structure seeded by primordial black holes* Astrophys. J. **665**, 1277 (2007) [arXiv:astro-ph/0608642].

-
- [61] D.N. Page *Particle emission rates from a black hole II. Massless particles from a rotating hole* Phys. Rev. **D14**, 12, 3260-3273 (1976).
- [62] D.N. Page and S.W. Hawking *Gamma rays from primordial black holes* Astrophys. J. **206**, 1-7 (1976).
- [63] B.J. Carr, K. Kohri, Y. Sentouza and J. Yokoyama, *New cosmological constraints on primordial black holes* Phys. Rev. **D81**, 104019 (2010) [arXiv:0912.5297v1] (astro-ph.CO).
- [64] M.Y. Khlopov, *Primordial Black Holes* Res. Astron. Astrophys. **10**, 495, (2010) [arXiv:0801.0116v1] (astro-ph).
- [65] A.H. Guth, *Inflationary universe: A possible solution to the horizon and flatness problems* Phys. Rev. **D23**, 347356 (1981).
- [66] J.D. Guth and M.S. Turner, *Inflation in the Universe* Nature **292**, 35-38 (1981).
- [67] B.J. Carr and J.E. Lidsey, *Primordial black holes and generalized constraints on chaotic inflation* Phys. Rev. **D48**, 543-553 (1993).
- [68] B.J. Carr, J.H. Gilbert and J.E. Lidsey, *Black Hole Relics and Inflation: Limits on Blue Perturbation Spectra* Phys. Rev. **D50**, 4853 (1994) [arXiv:astro-ph/9405027].
- [69] I. Zaballa, A.M. Green, K.A. Malik, M. Sasaki, *New calculation of the mass fraction of primordial black holes* J. Cosmol. Astropart. Phys. (JCAP) **0703**, 010 (2007) [arXiv:astro-ph/06123979].
- [70] K. Kohri, C.-M. Lin and D.H. Lyth *More hilltop inflation models* J. Cosmol. Astropart. Phys. (JCAP) **0712**, 004 (2007) [arXiv:0707.3826] (hep-ph).
- [71] M. Kawasaki, T. Takayama, M. Yamaguchi and J. Yokoyama, *Formation of intermediate-mass black holes as primordial black holes in the inflationary cosmology with running spectral index* Mod. Phys. Lett. **A22**, 1911 (2008) [arXiv:0711.3886] (astro-ph).
- [72] B.J. Carr, *The statistical clustering of primordial black holes* Astron. Astrophys. **56**, 377 (1977).
- [73] B.J. Carr and J. Silk, *Can graininess in the early universe make galaxies?* Astrophys. J. **268**, 1 (1983).
- [74] N. Afshordi, P. McDonald and D.N. Spergel, *Primordial Black Holes as Dark Matter: The Power Spectrum and Evaporation of Early Structures* Astrophys. J. **594**, L71 (2003) [arXiv:astro-ph/0302035].

- [75] B.J. Carr and M.J. Rees, *How large were the first pregalactic objects?* MNRAS **206**, 801 (Feb. 1984)
- [76] M.Y. Khlopov, S.G. Rubin and A.G. Sakharov, *Primordial Structure of Massive Black Hole Clusters* J. Astropart. Phys. **23**, 265 (2005) [arXiv:astro-ph/0401532].
- [77] B.J. Carr, *Cosmological gravitational waves - Their origin and consequences* Astron. Astrophys. **89**, 6 (1980).
- [78] T. Nakamura, M. Sasaki, T. Tanaka and K.S. Thorne, *Gravitational Waves from Coalescing Black Hole MACHO Binaries* Astrophys. J. Lett. **487**, L139 (1997) [arXiv:astro-ph/9708060].
- [79] K. Hayasaki, K. Takahashi, Y. Sendouda and S. Nagataki, *Rapid Merger of Binary Primordial Black Holes* Astrophys. J. Lett. **487**, L139 (2009) [arXiv:0909.1738] (astro-ph.CO).
- [80] D.B. Cline, *Primordial black holes and short gamma-ray bursts* Phys. Rep. **307**, 1-4, 173-180 (1998).
- [81] A.M. Green, *Viability of primordial black holes as short period gamma-ray bursts* Phys. Rev. **D65**, 027301 (2002) [arXiv:astro-ph/0105253v2].
- [82] M.J. Rees, *A better way of searching for black-hole explosions?* Nature **266**, 333 (Mar. 1977).
- [83] P.N. Okele and M.J. Rees, *Observational consequences of positron production by evaporating black holes* Astrophys. **81**, 263 (Jan. 1980).
- [84] E. Bugaev and P. Klimai, *Constraints on amplitudes of curvature perturbations from primordial black holes* Phys. Rev. **D79**, 103511 (2009) [arXiv:0812.4247] (astro-ph).
- [85] Y.B. Zel'dovich and A.A. Starobinskii, *Sov. J. Exp. Theor. Phys. Lett.* **24**, 571 (Dec. 1976).
- [86] M.S. Turner, *Baryon production by primordial black holes* Phys. Lett. **B89**, 155 (1979).
- [87] J.D. Barrow, E.J. Copeland, E.W. Kilb and A.R. Liddle, *Baryogenesis in extended inflation. II. Baryogenesis via primordial black holes* Phys. Rev. **D43**, 984 (1991).
- [88] A.D. Dolgov, P.D. Naselsky and I.D. Novikov, *Gravitational waves, baryogenesis, and dark matter from primordial black holes* [arXiv:astro-ph/0009407] (2000).
- [89] E. Bugaev, M.G. Elbakidze and K.V. Konishchev, *Baryon asymmetry of the Universe from evaporation of primordial black holes* Phys. Atom. Nucl. **66**, 476 (2003) [arXiv:astro-ph/0110660].

-
- [90] E. Bugaev and K.V. Konishchev, *Cosmological constraints from evaporations of primordial black holes* Phys. Rev. **D66**, 084004 (2002) [arXiv:astro-ph/0206082].
- [91] P. He and L.-Z. Fang, *Constraints on primordial black holes and primeval density perturbations from the epoch of reionization* Astrophys. J. **568**, L1 (2002) [arXiv:astro-ph/0202218].
- [92] K.J. Mack and D.H. Wesley, *Primordial black holes in the Dark Ages: Observational prospects for future 21cm surveys* Astrophys. J. **568**, L1 (2008) [arXiv:0805.1531v2] (astro-ph).
- [93] M. Izawa and K. Sato, *Can Primordial Black Holes Solve the Overproduction Problem of Monopoles?* Prog. Theor. Phys. **72**, 768 (1984).
- [94] D. Stokojkovic and K. Freese, *A black hole solution to the cosmological monopole problem* Phys. Lett. **B606**, 251 (2005) [arXiv:hep-ph/0403248].
- [95] D. Stokojkovic and K. Freese, *Holes in the walls: primordial black holes as a solution to the cosmological domain wall problem* Phys. Rev. **D72**, 045012 (2005) [arXiv:hep-ph/0505026].
- [96] J.H. MacGibbon, *Can Planck-mass relics of evaporating black holes close the Universe?* Nature **329**, 308 (1987).
- [97] J.D. Barrow, E.J. Copeland and A.R. Liddle, *The Cosmology of black hole relics* Phys. Rev. **D46**, 645 (1992).
- [98] K. Nozari and S.H. Mehdipour, *Gravitational Uncertainty and Black Hole Remnants* Mod. Phys. Lett. **A20**, 2937 (2005) [arXiv:0809.3144] (gr-qc).
- [99] S. Alexander and P. Meszaros, *Reheating, Dark Matter and Baryon Asymmetry: a Triple Coincidence in Inflationary Models* [arXiv:hep-th/0703070] (2007).
- [100] M.Y. Khlopov and A.G. Polnarev, *Primordial black holes as a cosmological test of grand unification* Phys. Lett. **B97**, 383 (1980).
- [101] A.G. Polnarev and M.Y. Khlopov, *Primordial Black Holes and the ERA of Superheavy Particle Dominance in the Early Universe* Sov. Astron. **25**, 406 (Aug. 1981).
- [102] A.G. Polnarev and M.Y. Khlopov, *Cosmology, primordial black holes, and supermassive particles* Sov. Phys. Uspekhi. **28 (3)**, 213232 (1985).
- [103] K. Jedamzik, *Primordial Black Hole Formation during the QCD Epoch* Phys. Rev. **D55**, 5871 (1997) [arXiv:astro-ph/9605152].

-
- [104] K. Jedamzik and J.C. Niemeyer, *Primordial Black Hole Formation during First-Order Phase Transitions* Phys. Rev. **D59**, 124014 (1999) [arXiv:astro-ph/9901293].
- [105] V.A. Berezin, V.A. Kuzmin and I.I. Tkachev, *Thin-wall vacuum domain evolution* Phys. Lett. **B120**, 91 (1983).
- [106] S.G. Rubin, M.Y. Khlopov and A.S. Sakharov, *Primordial black holes from non-equilibrium second order phase transition* Grav. Cosmol. **S6**, 51 (2000) [arXiv:hep-ph/0005271].
- [107] V. Dokuchaev, Y. Eroshenko and S.G. Rubin *Quasars formation around clusters of primordial black holes* Grav. Cosmol. **1**, 99 (2005) [arXiv:astro-ph/0412418v2].
- [108] S.G. Rubin, A.S. Sakharov and M.Y. Khlopov, *The formation of primary galactic nuclei during phase transitions in the early universe* J. Exp. Theor. Phys. **91**, 921 (2001) [arXiv:hep-ph/0106187v1].
- [109] M.Y. Khlopov, S.G. Rubin and A.S. Sakharov, *Primordial Structure of Massive Black Hole Clusters* CERN-ph-th, 004, (2004) [arXiv:astro-ph/0401532].
- [110] S.W. Hawking, I.G. Moss and J.M. Stewart, *Bubble collisions in the very early universe* Phys. Rev. **D26**, 2681, (1982).
- [111] I.G. Moss, *Singularity formation from colliding bubbles* Phys. Rev. **D50**, 676, (1994).
- [112] M.Y. Khlopov, R.V. Konoplich, S.G. Rubin and A.S. Sakharov, *First Order Phase Transitions as a Source of Black Holes in the Early Universe* Grav. Cos. 2, **S1**, (1999) [arXiv:hep-ph/9912422v1].
- [113] R.V. Konoplich, S.G. Rubin, A.S. Sakharov and M.Y. Khlopov, *Formation of black holes in first-order phase transitions as a cosmological test of symmetry-breaking mechanisms* Phys. Atom. Nucl. **62**, 1593 (1999).
- [114] A. Vilenkin and E.P.S. Shellard, *Cosmic strings and other topological defects* (2000), CUP, ISBN: 0-521-65476-9 (paperback).
- [115] S.W. Hawking *Black holes from cosmic strings* Phys. Lett. B **231**, 3, 237-239 (1989).
- [116] A. Polnarev and R. Zembowicz *Formation of primordial black holes from cosmic strings* Phys. Rev. **D36**, 4, 1106-1109 (1991).
- [117] R.R. Caldwell and P. Casper *Formation of black holes from collapsed cosmic string loops* Phys. Rev. **D53**, 6, 3002-3010 (1996) [arXiv:gr-qc/9509012].
- [118] U. F. Wichoski, J. H. MacGibbon and R. H. Brandenberger, *Astrophysical constraints on primordial black hole formation from collapsing cosmic strings* Phys. Rept. **307**, 191 (1998) [arXiv:astro-ph/9804341].

-
- [119] J. Garriga and M. Sakellariadou, *Effects of friction on cosmic strings* Phys. Rev. **D48**, 2502 (1993) [arXiv:hep-th/9303024].
- [120] H.-B. Cheng, X.-Z Li and , *Primordial black holes and cosmic string loop* Chin. Phys. Lett. **13**, 317 (1996).
- [121] R.N. Hansen, M. Christensen and A.L. Larsen, *Cosmic String Loops Collapsing to Black Holes* Int. J. Mod. Phys. **A15**, 4433 (2000) [arXiv:gr-qc/9902048].
- [122] M. Nagasawa, *Primordial black hole formation by stabilized embedded strings in the early universe* Gen. Rel. Grav. **37**, 1635 (2005).
- [123] T. W. B. Kibble, *Topology of cosmic domains and strings* J. Phys. **A9**, 1387 (1976).
- [124] M. B. Hindmarsh and T. W. B. Kibble, *Cosmic strings* Rept. Prog. Phys. **58**, 477 (1995) [arXiv:hep-ph/9411342].
- [125] A. Vilenkin, *Cosmic Strings: Progress and Problems* Frontiers in Science Series (2006) [arXiv:hep-th/0508135v2].
- [126] N. Bevis, M. Hindmarsh, M. Kunz and J. Urrestilla, *CMB power spectrum contribution from cosmic strings using field-evolution simulations of the Abelian Higgs model* Phys. Rev. **D75**, 065015 (2007) [arXiv:astro-ph/0605018].
- [127] N. Bevis, M. Hindmarsh, M. Kunz and J. Urrestilla *Fitting CMB data with cosmic strings and inflation* Phys. Rev. Lett. **100**, 021301 (2008) [arXiv:astro-ph/0702223v3].
- [128] N. Bevis, M. Hindmarsh, M. Kunz and J. Urrestilla, *CMB power spectra from cosmic strings: predictions for the Planck satellite and beyond* [arXiv:1005.2663v1] (astro-ph.CO), (2010).
- [129] N. Bevis, M. Hindmarsh, M. Kunz and J. Urrestilla, *CMB polarization power spectrum contributions from a network of cosmic strings* Phys. Rev. **D76**, 043005 (2007) [arXiv:0704.3800v3] (astro-ph).
- [130] J. Urrestilla, P. Mukherjee, A.R. Liddle, N. Bevis, M. Hindmarsh and M. Kunz, *On the degeneracy between primordial tensor modes and cosmic strings in future CMB data from Planck* Phys. Rev. **D77**, 123005 (2008) [arXiv:0803.2059v2] (astro-ph).
- [131] J. Garcia-Bellido, R. Durrer, E. Fenu, D.G. Figueroa and M. Kunz, *The local B-polarization of the CMB: a very sensitive probe of cosmic defects* [arXiv:1003.0299v2] (astro-ph.CO), (2010).
- [132] S. Weinberg, *The Quantum Theory of Fields, Volume 1, Foundations* (2005), CUP, ISBN: 978-0521670531.

-
- [133] S. Weinberg, *The Quantum Theory of Fields, Volume 2, Modern Applications* (2005), CUP, ISBN: 978-0521670548.
- [134] S. Weinberg, *The Quantum Theory of Fields, Volume 3, Supersymmetry* (2005), CUP, ISBN: 978-0521670551.
- [135] K.S. Cheng, Yun-Wei Yu and T. Harko, *High Redshift Gamma-ray Bursts: Observational Signatures of Superconducting Cosmic Strings?* Phys. Rev. Lett. **104**, 241102 (2010) [arXiv:1005.3427v2] (astro-ph.HE).
- [136] P. Meszaros, *Gamma-ray Bursts* Rept. Prog. Phys. **69**, 2259 (2006).
- [137] J. Grenier *et al*, *GRB 080913 at $z=6.7$* Astrophys. J. **693**, 1610 (2009).
- [138] N.R. Tanvir *et al*, *A Gamma-Ray Burst at $z=8.2$* Nature **461**, 1254 (2009).
- [139] A.M. Hopkins and J.F. Beacom, *On the normalisation of cosmic star formation history* Astrophys. J. **651**, 142 (2006) [arXiv:astro-ph/0601463v3].
- [140] E. Witten, *Superconducting Strings* Nucl. Phys. **B249**, 557 (1985)
- [141] J.J. Blanco-Pillado, K.D. Olum and A. Vilenkin, *Dynamics of superconducting strings with chiral currents* Phys. Rev. **D63**, 103513 (2001) [arXiv:astro-ph/0004410v3].
- [142] M.D. Kistler, *The Star Formation Rate in the Reionization Era as Indicated by Gamma-ray Bursts* Astrophys. J. **705**, L104 (2009) [arXiv:0906.0590] (astro-ph.CO).
- [143] S. Weinberg *Gauge and global symmetries at high temperature* Phys. Rev. **D9**, 3357-3378 (1974).
- [144] T.W.B. Kibble, *Evolution of a system of cosmic strings* Nucl. Phys. **B252**, 227 (1985), Erratum: Nucl. Phys. B **261**, 750.
- [145] D.P. Bennett, *The evolution of cosmic strings* Phys. Rev. **D34**, 3932 (1986).
- [146] D.P. Bennett, *The evolution of cosmic strings: 2* Phys. Rev. **D34**, 3592 (1986).
- [147] A.G. Smith and A. Vilenkin *Fragmentation of cosmic string loops* Phys. Rev. **D36**, 987 (1987).
- [148] A.G. Smith and A. Vilenkin *Numerical simulation of string evolution in flat space-time* Phys. Rev. **D36**, 990 (1987).
- [149] M. Sakellariadou and A. Vilenkin *Numerical experiments with cosmic string evolution in flat space-time* Phys. Rev. **D37**, 885 (1988).

- [150] M. Sakellariadou and A. Vilenkin *Cosmic string evolution in flat space-time* Phys. Rev. **D42**, 439 (1990).
- [151] J. Dai, R. G. Leigh and J. Polchinski, *New Connections Between String Theories* Mod. Phys. Lett. A **4**, 21, 2073-2083 (1989) [arXiv:astro-ph/9804341].
- [152] J. Polchinski *Dirichlet Branes and Ramond-Ramond Charges* Phys. Rev. Lett. **75**, 4724-4727 (1995) [arXiv:hep-th/950017v3].
- [153] J. Polchinski *TASI Lectures on D-Branes* [arXiv:hep-th/9611050v2] (1997).
- [154] A. Avgoustidis and E. P. S. Shellard, *Cosmic string evolution in higher dimensions* Phys. Rev. D **71**, 123513 (2005) [arXiv:hep-ph/0410349].
- [155] B. Zwiebach *A First Course in String Theory 2nd Ed.* (2009), CUP, ISBN-13: 978-0521880329 (hardback).
- [156] R. Maartens *Brane-world gravity* Living Reviews in Relativity (2004) [arXiv:gr-qc/0312059v2].
- [157] M.B. Green, J.H. Schwarz and E. Witten *Superstring Theory: Loop Amplitudes, Anomalies and Phenomenology v2* (2009), CUP, ISBN-13: 978-0521357531 (hardback)
- [158] J. Polchinski *String Theory: Superstring Theory and Beyond v2* (2005), CUP, ISBN-13: 978-0521672287 (paperback).
- [159] K. Becker, M. Becker and J.H. Schwarz *String Theory and M-theory: A Modern Introduction* (2006), CUP, ISBN-13: 978-0521672287 (hardback).
- [160] M. Nakahara *Geometry, Topology and Physics 2nd Ed.* (2006), Taylor and Francis, ISBN-13: 978-0750306065 (paperback).
- [161] F. Denef, M.R. Douglas and S. Kachru *Physics of String Flux Compactifications* Annual Review of Nuclear and Particle Science **57**, 119-144 (2007) [arXiv:hep-th/0701050v1].
- [162] V. Balasubramanian, P. Berglund, J.P. Conlon and F. Quevedo *Systematics of moduli stabilisation in Calabi-Yau flux compactifications* JHEP **03**, 007 (2005) [arXiv:hep-th/0502058].
- [163] R. Blumenhagen, B. Kors, D. Lust and S. Stieberger *Four-dimensional string compactifications with D-branes, orientifolds and fluxes* Physics Reports **445**, 1-6, 1-193 (2007) [arXiv:hep-th/0610327].
- [164] M. Grana, *Flux compactifications in string theory: A comprehensive review* Phys. Rept. **423**, 91 (2006) [arXiv:hep-th/0509003].

-
- [165] A. Quevedo, *Lectures on string/brane cosmology* Class. Quantum Grav. **19**, 5721-5779 (2002) [arXiv:hep-th/0210292].
- [166] S. Kecskemeti, J. Maiden, G. Shiu and B. Underwood *DBI Inflation in the Tip Region of a Warped Throat* JHEP **09**, 076 (2006) [arXiv:hep-th/00605189v3].
- [167] P. Candelas and X.C. de la Ossa *Comments on conifolds* Nucl. Phys. **B342**, 1, 242-268 (1990).
- [168] F. Gliozzi, J. Scherk and D. Olive, *Supersymmetry, supergravity theories and the dual spinor model* Nucl. Phys. **B122**, 253 (1977).
- [169] C. P. Herzog, I. R. Klebanov and P. Ouyang, *Remarks on the warped deformed conifold* [arXiv:hep-th/0108101] (2003).
- [170] R. Minasian and D. Tsimpis *On the Geometry of Non-Trivially Embedded Branes* [arXiv:hep-th/9911042] (2000).
- [171] E. Silverstein and D. Tong *Scalar Speed Limits and Cosmology: Acceleration from D-acceleration* Phys. Rev. **D70**, 103505 (2004) [arXiv:hep-th/0310221].
- [172] M. Alishahiha, E. Silverstein and D. Tong *DBI in the sky* Phys. Rev. **D70**, 123505 (2004) [arXiv:hep-th/0404084].
- [173] D. Langlois, S. Renaux-Petel and D.A. Steer *Multi-field DBI inflation: introducing bulk forms and revisiting the gravitational wave constraints* JCAP **04**, 021 (2009) [arXiv:0902.2941] (hep-th).
- [174] D. Langlois, S. Renaux-Petel, D.A. Steer and T. Tanaka *Primordial perturbations and non-Gaussianities in DBI and general multi-field inflation* Phys. Rev. **D78**, 063523 (2008) [arXiv:0806.0336] (hep-th).
- [175] D. Langlois, S. Renaux-Petel, D.A. Steer and T. Tanaka *Primordial fluctuations and non-Gaussianities in multi-field DBI inflation* Phys. Rev. Lett. **101**, 061301 (2008) [arXiv:0804.3139] (hep-th).
- [176] H.Y. Chen, J.O. Gong and G. Shiu *Systematics of multi-field effects at the end of warped brane inflation* JHEP **09**, 011 (2008) [arXiv:0807.1921v3] (hep-th).
- [177] D. Easson, R. Gregory, I. Zavala and G. Tasinato *Cycling in the throat* JHEP **04**, 026 (2007) [arXiv:hep-th/0701252v2].
- [178] J. Ward *DBI N-flation* JHEP **12**, 045 (2007) [arXiv:0711.0706v3] (hep-th).
- [179] Y.-F. Cai and W. Xue *N-flation from multiple DBI type actions* Phys. Lett. **B680**, 395-398 (2009) [arXiv:0809.4134v1] (hep-th).

-
- [180] S. Dimopolous, S. Kachru, J. McGreevy and J.G. Wacker *N-flation* [arXiv:hep-th/0507205] (2005).
- [181] S.A. Kim and A.R. Liddle *DBI N-flation* Phys. Rev. **D74**, 023513 (2006) [arXiv:hep-th/0605604v2].
- [182] X. Chen *Multi-Throat Brane Inflation* Phys. Rev. **D71**, 063506 (2005) [arXiv:hep-th/0408084].
- [183] X. Chen *Inflation from Warped Space* JHEP, **0509**, 004 (2005) [arXiv:hep-th/0501184].
- [184] A.R. Liddle, A. Mazumdar and F.E. Schunk *Assisted Inflation* Phys. Rev. **D58**, 061301 (1998) [arXiv:astro-ph/9804177v2].
- [185] E.J. Copeland and A. Mazumdar *Generalised Assisted Inflation* Phys. Rev. **D60**, 083506 (1999) [arXiv:astro-ph/9904309v1].
- [186] P. Kanti and K.A. Olive *Generalised Assisted Inflation in Higher Dimensional Theories* Phys. Lett. **B464**, 192-198 (1999) [arXiv:hep-ph/9906331v1].
- [187] P. Kanti and K.A. Olive *On the Realisation of Assisted Inflation* Phys. Rev. **D60**, 043502 (1999) [arXiv:hep-ph/9812204].
- [188] K.A. Malik and D. Wands *Dynamics of Assisted Inflation* Phys. Rev. **D59**, 123501 (1999) [arXiv:astro-ph/9812204v1].
- [189] J. Ward *Instantons, Assisted Inflation and Heterotic M-Theory* Phys. Rev. **D73**, 026004 (2006) [arXiv:hep-th/0511079v4].
- [190] J. Ward and S. Thomas *IR Inflation from Multiple Branes* Phys. Rev. **D76**, 023509 (2007) [arXiv:hep-th/0702229v4].
- [191] M. Majumdar, *A tutorial on links between cosmic string theory and superstring theory* [arXiv:hep-th/0512062] (2005).
- [192] S.-H.H. Tye *Brane Inflation: String Theory Viewed from the Cosmos* (2008), Springer, ISBN-13: 978-3-540-74232-6 [arXiv:hep-th/0619221v2] (2006).
- [193] E. J. Copeland, R. C. Myers and J. Polchinski, *Cosmic F and D-strings* JHEP **0406**, 013 (2004) [arXiv:hep-th/0312067].
- [194] J.L. Petersen *Introduction to the Maldacena Conjecture on AdS/CFT* [arXiv:hep-th/9902131v2] (1999).
- [195] J. Maldacena *TASI 2003 lectures on AdS/CFT* [arXiv:hep-th/0309246v5] (2004).
- [196] E. Witten, *Cosmic Superstrings* Phys. Lett. **B153**, 243 (1985).

-
- [197] D.H. Lyth and A. Riotto *Particle Physics Models of Inflation and the Cosmological Density Perturbation* Phys. Rept. **341**, 1 (1999) [arXiv:hep-ph/9807278].
- [198] A.R. Liddle and D.H. Lyth *Cosmological Inflation and Large-Scale Structure* (2000), (CUP), ISBN-13: 978-0521660228.
- [199] M. Wyman, L. Pogosian and I. Wasserman, *Bounds on Cosmic Strings from WMAP and SDSS* Phys. Rev. **D72**, 023513, (2005); Erratum-ibid. **D73**, 089905, (2006) [arXiv:astro-ph/0503364v2].
- [200] A. Fraisse, *Constraints on Topological Defects Energy Density from First-Year WMAP Results* [arXiv:astro-ph/0503402] (2005).
- [201] J. Polchinski, *Introduction to Cosmic F- and D-strings* [arXiv:hep-th/0412244] (2006).
- [202] N.T. Jones, H. Stoica and S.H. Tye, *The Production, Spectrum and Evolution of Cosmic Strings in Brane Inflation* Phys. Lett. **B563**, 6 (2003) [arXiv:hep-th/0303269v1].
- [203] L. Pogosian, S.-H. Tye, I. Wasserman and M. Wyman, *Observational Constraints on Cosmic String Production During Brane Inflation* Phys. Rev. **D68**, 023506, (2003); Erratum-ibid. **D73**, 089904, (2006) [arXiv:hep-th/0304188v3].
- [204] S.M. Carroll *TASI Lectures: Cosmology for String Theorists* [arXiv:hep-th/0011110v2] (2000).
- [205] F. Quevedo *Lectures on string/brane cosmology* Class. Quant. Grav. **19**, 5721-5779 (2002) [arXiv:hep-th/0210292v1].
- [206] U.H. Danielsson *Lectures on string theory and cosmology* Class. Quant. Grav. **22**, S1-S40 (2005) [arXiv:hep-th/0409274].
- [207] A. Linde *Inflation and String Cosmology* J. Phys. Conf. Ser. **22**, 151-160 (2005) [arXiv:hep-th/0503195].
- [208] M. Sakkellariadou *Cosmic Strings* Lec. Notes. Phys. **178**, 247-288 (2007) [arXiv:hep-th/0602276].
- [209] D.H. Lyth and A.R. Liddle *The Primordial Density Perturbation: Cosmology, Inflation and the Origin of Structure* (2009), (CUP), ISBN-13: 978-0521828499.
- [210] G.F. Smoot, C.L. Bennett, A. Kogut and E.L Wright *et al Structure in the COBE DMR first year maps* Ap. J. **396**, L1 (1992).
- [211] D.P. Bennet, A. Stebbins and F.R. Bouchet *The implications of COBE DMR results for cosmic strings* Ap. J. **399**, 5 (1992).

- [212] N. Turok and R.H. Brandenberger *Cosmic strings and the formation of galaxies and clusters of galaxies* Phys. Rev. **D33** (1986).
- [213] V.M. Kaspi, J.H. Taylor and M.F. Ryba, *High-precision timing of millisecond pulsars. 3: Long-term monitoring of PSRs B1855+ 09 and B1937+ 21* Astrophys. J. **428**, 713 (1994).
- [214] T. Damour and A. Vilenkin, *Gravitational radiation from cosmic (super)strings: bursts, stochastic background, and observational windows* Phys. Rev. **D71**, 063510 (2005) [arXiv:hep-th/0410222v2].
- [215] A.G. Riess *et al* *Observational Evidence from Supernovae for an Accelerating Universe and a Cosmological Constant* Astron. J. **116**, 1009-1038 (1998) [arXiv:astro-ph/9805201].
- [216] A.G. Riess *et al* *BVRI Light Curves for 22 Type Ia Supernovae* Astron. J. **117**, 707-724 (1999) [arXiv:astro-ph/9810291].
- [217] S. Perlmutter *et al* *Measurements of Omega and Lambda from 42 High-Redshift Supernovae* Astrophys. J. **517**, 565-586 (1999) [arXiv:astro-ph/9812133].
- [218] W.J. Percival *et al* *The 2dF Galaxy Redshift Survey: The power spectrum and the matter content of the universe* Not. Roy. Astron. Soc. **327**, 1297 (2001) [arXiv:astro-ph/0105252].
- [219] S. Cole *et al* *The 2dF Galaxy Redshift Survey: Power-spectrum analysis of the final dataset and cosmological implications* Not. Roy. Astron. Soc. **362**, 505-534 (2005) [arXiv:astro-ph/0501174].
- [220] M. Tegmark *et al* (SDSS collaboration) *Cosmological parameters from SDSS and WMAP* Phys. Rev. D, **69**, 103501 (2004) [arXiv:astro-ph/0310723].
- [221] K. Abazajian *et al* (SDSS collaboration) *The Second Data Release of the Sloan Digital Sky Survey* Astron. J. **128**, 502-515 (2004) [arXiv:astro-ph/0403325].
- [222] C.L. Bennett *et al* (WMAP collaboration) *First Year Wilkinson Microwave Anisotropy Probe (WMAP) Observations: Preliminary Maps and Basic Results* Astron. J. Suppl. **148**, 1 (2003) [arXiv:astro-ph/0302207v3].
- [223] D.N. Spergel *et al* (WMAP collaboration) *Wilkinson Microwave Anisotropy Probe (WMAP) Three Year Results: Implications for Cosmology* Astron. J. Suppl. **170**, 377 (2007) [arXiv:astro-ph/0603449v2].
- [224] *Final results from the Hubble space telescope key project to measure the Hubble constant* W.L. Freedman *et al.* (Hubble Key Project collaboration) Astrophys. J. **553**, 47 (2001).

- [225] *The cosmological baryon density from the deuterium-to-hydrogen ratio in QSO absorption systems: D/H toward Q1243+ 3047* D. Kirkman, D. Tytler, N. Suzuki, J.M. O'Meara and D. Lubin, *Astrophys. J. Suppl.* **149**, 1 (2003) [arXiv:astro-ph/0302006v1].
- [226] Planck satellite, ESA, URL <http://www.rssd.esa.int/index.php?project=Planck>.
- [227] CMB polarization satellite, URL <http://cmbpol.uchicago.edu/>.
- [228] *Clover - A B-mode polarization experiment* A.C. Taylor (Clover collaboration) *New Astron. Rev.* **50**, 993 (2006) [arXiv:astro-ph/0610716].
- [229] Y. Nambu *String-like configurations in Weinberg-Salam theory* *Nucl. Phys.* **B130**, 505 (1977).
- [230] T. Goto *Relativistic quantum mechanics of a one-dimensional mechanical continuum and subsidiary condition of dual resonance model* *Prog. Theor. Phys.* **46**, 1560 (1971).
- [231] M. Born and L. Infeld *Foundations of the new field theory* *Proc. Roy. Soc.* **1** 144 (1934).
- [232] S. Chern and J. Simons *Characteristic forms and geometric invariants* *Ann. Math.* **99** 48 (1974).
- [233] J. Polchinski *Cosmic Superstrings Revisited* [arXiv:hep-th/0410082v2] (2004).
- [234] J.H. Schwarz *An $SL(2, z)$ multiplet of Type IIB strings* *Phys. Lett.* **B360**, 13-18 (1995) [arXiv:hep-th/9508143].
- [235] A. Sen, *A Note on Enhanced Gauge Symmetries in M- and String Theory* *JHEP* **09** 001 (2007) [arXiv:hep-th/9707123v2].
- [236] E. Witten, *Bound States of Strings and p-branes* *Nucl. Phys.* **B460** 335 (1996) [arXiv:hep-th/9510135].
- [237] I. Antoniadis, E. Kiritsis, J. Rizos and T.N. Tomaras *D-Branes and the Standard Model* *Nucl. Phys.* **B660** 1-2 (2003) [arXiv:hep-th/0210263v2].
- [238] S.A. Abel and A.W. Owen *Interactions in Intersecting Brane Models* *Nucl. Phys.* **B663** 1-2 (2003) [arXiv:hep-th/0303124v4].
- [239] D. Lust *Intersecting Brane Worlds - A Path to the Standard Model?* *Clas. Q. Grav.* **21** 10 (2004) [arXiv:hep-th/041156v2].
- [240] A.A. Tseytlin, *Born-Infled action, supersymmetry and string theory* Yuri Goldfand memorial volume, World Scientific (2000) [arXiv:hep-th/9908105].

-
- [241] R.C. Myers *Dielectric Branes* JHEP, **022**, 9912 (1999) [arXiv:hep-th/9910053].
- [242] R.C. Myers *Nonabelian Phenomena on D-branes* Class. Quant. Grav., **20**, S347-S372 (2003) [arXiv:hep-th/0303072].
- [243] C.V. Johnson, *D-branes* (2006), CUP, ISBN: 978-0521030052 (paperback).
- [244] L. LeBlond and S.-H. Tye *Stability of D1-Strings Inside a D3-Brane* JHEP **0403** 10 (2004) [arXiv:hep-th/0402072v1].
- [245] H. Firouzjahi, L. Leblond and S. H. Henry Tye, *The (p,q) string tension in a warped deformed conifold* JHEP **0605**, 047 (2006) [arXiv:hep-th/0603161].
- [246] M. Ali-Akbari and M.A. Ganjali *Multiple D_p -branes as a D_{p+2} -brane* [arXiv:1002.0486v1] (hep-th),(2010).
- [247] S. Sarangi and S.-H. Tye *Cosmic String Production Towards the End of Brane Inflation* Phys. Lett. **B536** 185-192 (2002) [arXiv:hep-th/0204074v1].
- [248] J. Ward and S. Thomas *Non-Abelian (p,q) Strings in the Warped Deformed Conifold* JHEP, **12** 057 (2006) [arXiv:hep-th/0605099v2].
- [249] C.P. Herzog and I.R. Klebanov *On String Tensions in Supersymmetric $SU(M)$ Gauge Theory* Phys. Lett. **B526**, 388-392 (2002) [arXiv:hep-th/0111078v4].
- [250] S. Gubser, C.P. Herzog and I.R. Klebanov *Symmetry Breaking and Axionic Strings in the Warped Deformed Conifold* JHEP, **09**, 036 (2002) [arXiv:hep-th/0405282].
- [251] E. Witten *Bound States Of Strings and p-Branes* Nucl. Phys. **B460**, 335-350 (1996) [arXiv:hep-th/9510135].
- [252] N. Seiberg and E. Witten *String Theory and Noncommutative Geometry* JHEP, **09**, 032 (1999) [arXiv:hep-th/9908142].
- [253] J. Ward and S. Thomas *Electrified Fuzzy Spheres and Funnel in Curved Backgrounds* JHEP, **0602** 019 (2006) [arXiv:hep-th/0602071v2].
- [254] J. Ward and S. Thomas *Fuzzy Sphere Dynamics and Non-Abelian DBI in Curved Backgrounds* JHEP, **0610** 039 (2006) [arXiv:hep-th/0508085v3].
- [255] J. Ward *Aspects of Brane Dynamics in String Theory* PhD Thesis, Queen Mary, University of London (2006)
- [256] H. Firouzjahi *Dialectric (p,q) Strings in a Throat* JHEP, **0612** 031 (2006) [arXiv:hep-th/0610130].
- [257] S. McNamara, C. Papageorgakis, S. Ramgoolam and B. Spence *Finite N effects on the collapse of fuzzy spheres* JHEP, **0605** 060 (2006) [arXiv:hep-th/0512145v1].

- [258] E. Komatsu *et al.* (WMAP Collaboration), *Five-Year Wilkinson Microwave Anisotropy Probe (WMAP) Observations: Cosmological Interpretation* *Astrophys. J. Suppl.* **180** 330 (2009) [arXiv:0803.0547] (astro-ph).
- [259] E. Komatsu *et al.* (WMAP Collaboration), *Seven-Year Wilkinson Microwave Anisotropy Probe (WMAP) Observations: Cosmological Interpretation* [arXiv:1001.4538v2] (astro-ph.CO), (2010).
- [260] K. Abazajian *et al.* (SDSS Collaboration), *The Third Data Release of the Sloan Digital Sky Survey* *Astron. J.* **129**, 1755-1759 (2005) [arXiv:astro-ph/0410239].
- [261] J. K. Adelman-McCarthy *et al.* (SDSS Collaboration), *The Fourth Data Release of the Sloan Digital Sky Survey* *Astrophys. J. Suppl.* **162**, 38 (2006) [arXiv:astro-ph/0507711].
- [262] S. B. Giddings, S. Kachru and J. Polchinski, *Hierarchies from fluxes in string compactifications* *Phys. Rev.* **D66**, 106006 (2002) [arXiv:hep-th/0105097].
- [263] V. Berezhinsky and A. Vilenkin, *Cosmic necklaces and ultrahigh energy cosmic rays* *Phys. Rev. Lett.* **79**, 5202 (1997) [arXiv:astro-ph/9704257].
- [264] E. J. Copeland and P. M. Saffin, *On the evolution of cosmic-superstring networks* *JHEP* **0511**, 023 (2005) [arXiv:hep-th/0505110].
- [265] J. Polchinski, *Cosmic String Loops and Gravitational Radiation* [arXiv:0707.0888] (astro-ph), (2007).
- [266] M. Sakellariadou, *Cosmic Strings and Cosmic Superstrings* [arXiv:0902.0569] (hep-th), (2009).
- [267] A. Rajantie, M. Sakellariadou and H. Stoica, *Numerical experiments with p F - and q D -strings: the formation of (p, q) bound states* *JCAP* **0711**, 021 (2007) [arXiv:0706.3662] (hep-th).
- [268] L. Leblond and M. Wyman, *Cosmic Necklaces from String Theory* *Phys. Rev.* **D75**, 123522 (2007) [arXiv:astro-ph/0701427].
- [269] J. V. Rocha, *Analytic Approaches to the Study of Small Scale Structure on Cosmic String Networks* [arXiv:0812.4020] (gr-qc), (2008).
- [270] L. Leblond, B. Shlaer and X. Siemens, *Gravitational Waves from Broken Cosmic Strings: The Bursts and the Beads* *Phys. Rev.* **D79**, 123519 (2009) [arXiv:0903.4686] (astro-ph.CO).
- [271] N. Bevis, E. J. Copeland, P. Y. Martin, G. Niz, A. Pourtsidou, P. M. Saffin and D. A. Steer, *On the stability of Cosmic String Y-junctions* *Phys. Rev.* **D80**, 125030 (2009) [arXiv:0904.2127] (hep-th).

- [272] B. Abbott [LIGO Scientific Collaboration], *First LIGO search for gravitational wave bursts from cosmic (super)strings* Phys. Rev. **D80**, 062002 (2009) [arXiv:0904.4718] (astro-ph.CO).
- [273] I. R. Klebanov and A. Murugan, *Gauge/Gravity Duality and Warped Resolved Conifold* JHEP **0703**, 042 (2007) [arXiv:hep-th/0701064].
- [274] I. R. Klebanov, A. Murugan, D. Rodriguez-Gomez and J. Ward, *Goldstone Bosons and Global Strings in a Warped Resolved Conifold* JHEP **0805**, 090 (2008) [arXiv:0712.2224] (hep-th).
- [275] A. Avgoustidis, *Cosmic String Dynamics and Evolution in Warped Spacetime* Phys. Rev. **D78**, 023501 (2008) [arXiv:0712.3224] (hep-th).
- [276] J. J. Blanco-Pillado and A. Iglesias, *Strings at the bottom of the deformed conifold* JHEP **0508**, 040 (2005) [arXiv:hep-th/0504068].
- [277] <http://mathworld.wolfram.com/EllipticIntegraloftheSecondKind.html>
- [278] J. H. MacGibbon, B. J. Carr, *Cosmic rays from primordial black holes* Astrophys. J. **371**, 447 (1991).
- [279] W.L. Freedman et al. (HST collaboration) *Final Results from the Hubble Space Telescope Key Project to Measure the Hubble Constant* Astrophys. J. **553**, 47 (2001) [arXiv:astro-ph/0012376]
- [280] R. Lehoucq, M. Casse, J. M. Casandjian and I. Grenier, *New constraints on the primordial black hole number density from Galactic gamma ray astronomy* [arXiv:0906.1648] (astro-ph.HE), (2009).
- [281] K. Becker, M. Becker and A. Krause, *Heterotic cosmic strings* Phys. Rev. **D74**, 045023 (2006) [arXiv:hep-th/0510066].
- [282] E. I. Buchbinder, *Stable and metastable cosmic strings in heterotic M-theory* Nucl. Phys. **B749**, 225 (2006) [arXiv:hep-th/0602070].
- [283] R. Gwyn, S. Alexander, R. H. Brandenberger and K. Dasgupta, *Magnetic Fields from Heterotic Cosmic Strings* Phys. Rev. **D79**, 083502 (2009) [arXiv:0811.1993] (hep-th).
- [284] V. Niarchos and N. Prezas, *Boundary Superstring Field Theory* Nucl. Phys. **B619**, 51-74 (2001) [arXiv:hep-th/0103102].
- [285] M. Boezio et al. (PAMELA Collaboration), *The PAMELA space experiment: First year of operation* J. Phys. Conf. Ser. **110**, 062002 (2008).

-
- [286] O. Adriani *et al.* (PAMELA Collaboration), *Observation of an anomalous positron abundance in the cosmic radiation* Nature **458**, 607-609 (2009) [arXiv:0810.4995] (astro-ph).
- [287] R. Brandenberger, Y. F. Cai, W. Xue and X. Zhang, *Cosmic Ray Positrons from Cosmic Strings* [arXiv:0901.3474] (hep-ph), (2009).
- [288] I. Bengtsson and K. Zyczkowski, *Geometry of Quantum States* (2006), CUP, ISBN: 978-0-521-81451-5 (hardback).
- [289] T. Vaschpati, and A. Vilenkin, *Gravitational radiation from cosmic strings* Phys. Rev. **D30**, 2036 (1985).
- [290] C.J. Burden, *Gravitational radiation from a particular class of cosmic strings* Phys. Lett. **164B**, 277 (1985).
- [291] D. Garfinkle and T. Vaschpati, *Radiation from kinky, cusplless, cosmic loops* Phys. Rev. **D36**, 2229 (1987).
- [292] B. Allen and E.P.S. Shellard, *Gravitational radiation from a cosmic string network* Phys. Rev. **D45**, 1898 (1992).
- [293] W. Weinberg *Gravitation and Cosmology* (1972), Wiley, New York, ISBN: 978-81-265-1755-8.
- [294] R. Durrer, *Gravitational angular momentum radiation of cosmic strings* Nucl. Phys. **B328**, 238 (1989).
- [295] K. Danzmann *et al.* (LISA Science Team), *LISA Mission Overview* Advances in Space Research **25**, 6, 1129-1136 (2000).
- [296] K. Danzmann *et al.* (LISA Science Team), *LISA An ESA cornerstone mission for the detection and observation of gravitational waves* Advances in Space Research **32**, 7, 1233-1242 (2003).
- [297] K. Danzmann and A. Rdiger, *LISA technologyconcept, status, prospects* Class. Quantum Grav. **20**, S1 (2003).
- [298] F. Hechlera and W. M. Folknerb, *Mission analysis for the Laser Interferometer Space Antenna (LISA) mission* Advances in Space Research **32**, 7, 1277-1282 (2003).
- [299] P. McNamara, S. Vitale and K. Danzmann *et al.* (LISA Science Team), *LISA Pathfinder* Class. Quantum Grav. **25**, 11, 4034 (2008).
- [300] A. Abramovici *et al.*, *LIGO: The Laser Interferometer Gravitational-Wave Observatory* Science **17** **256**, 5055, 325-333 (1992).

-
- [301] B.P. Abbott *et al.* (LIGO Scientific Collaboration), *LIGO: The Laser Interferometer Gravitational-Wave Observatory* Rep. Prog. Phys. **72**, 076901 (2009). [arXiv:0711.3041v2] (gr-qc).
- [302] P.R. Brady, T. Creighton, C. Cutler and B.F. Schutz, *Searching for periodic sources with LIGO* Phys. Rev. **D57**, 21012116 (1997) [arXiv:gr-qc/9702050v1].
- [303] P.R. Brady, T. Creighton, *Searching for periodic sources with LIGO. II. Hierarchical searches* Phys. Rev. **D61**, 082001 (2000) [arXiv:gr-qc/9812014v1].
- [304] B.P. Abbott *et al.* (LIGO Scientific Collaboration), *First all-sky upper limits from LIGO on the strength of periodic gravitational waves using the Hough transform* Phys. Rev. **D72**, 102004 (2005).
- [305] B.P. Abbott *et al.* (LIGO Scientific Collaboration), *Searches for periodic gravitational waves from unknown isolated sources and Scorpius X-1: Results from the second LIGO science run* Phys. Rev. **D76**, 082001 (2007).
- [306] B.P. Abbott *et al.* (LIGO Scientific Collaboration), *All-sky search for periodic gravitational waves in LIGO S4 data* Phys. Rev. **D77**, 022001 (2008).
- [307] B. Allen and R. Brustein, *Detecting relic gravitational radiation from string cosmology with LIGO* Phys. Rev. **D55**, 32603264 (1997) [arXiv:gr-qc/9609013v1].
- [308] R. Brustein, M. Gasperini, M. Giovannini and G. Veneziano, *Gravitational Radiation from String Cosmology* [arXiv:hep-th/9510081v1] (1995).
- [309] A. Buonanno, M. Maggiore and C. Ungarelli, *Spectrum of relic gravitational waves in string cosmology* Phys. Rev. **D55**, 33303336 (1997) [arXiv:gr-qc/9605072].
- [310] R. Brustein, M. Gasperini and G. Veneziano, *Peak and end point of the relic graviton background in string cosmology* Phys. Rev. **D55**, 38823885 (1997) [arXiv:hep-th/9604084v1].
- [311] M. Massimo Galluccio¹, M. Litterio and F. Occhionero¹, *Graviton Spectra in String Cosmology* Phys. Rev. Lett. **79**, 970973 (1997) [arXiv:gr-qc/9608007v1].
- [312] M. Maggiore, *Graviton background at early times in string cosmology* Phys. Rev. **D56**, 13201323 (1997) [arXiv:gr-qc/9701030v1].
- [313] R. Brustein, *Cosmic Gravitational Wave Background in String Cosmology* [arXiv:gr-qc/9804078] (1998).
- [314] R. Brustein, *Production and detection of cosmic gravitational wave background in string cosmology* Chaos, Solitons and Fractals **10**, 2-3, 283-294 (2003)

-
- [315] C. Cartier, E. J. Copeland and M. Gasperini, *Gravitational waves in non-singular string cosmologies* Nucl. Phys. **B607**, 1-2, 406-428 (2001).
- [316] M. Gasperini and M. Giovannini, *Dilaton contributions to the cosmic gravitational wave background* Phys. Rev. **D47**, 15191528 (1993).
- [317] M. Gasperini, *Elements of String Cosmology* (2006), CUP, ISBN-13:978-0521868754 (hardback).
- [318] J.M. Cline, *String Cosmology* [arXiv:hep-th/0612129] (2006).
- [319] C.J. Isham, *Lectures on Quantum Theory: Mathematical and Structural Foundations* (2001), Imperial College Press, ISBN: 1860940013 (paperback).
- [320] L. Perivalopolous *Asymptotics of Nielsen-Olesen Vortices* Phys. Rev. **D48**, 12, 5961-5962 (1993) [arXiv:hep-th/9310264v1].
- [321] J. Preskill *Vortices and Monopoles* Lectures presented at the 1985 Les Houches Summer School US D.O.E. Research and Development Report, CALT-66-1287 (1986).
- [322] E.B. Bogomol'nyi and A.I. Vainstein *Stability of strings in gauge abelian theory* Sov. J. Nucl. Phys. **23**, 588 (1976)
- [323] E.B. Bogomol'nyi *Stability of classical solutions* Sov. J. Nucl. Phys. **24**, 449 (1976)
- [324] H.J. de Vega and F.A. Schaposnik *A classical vortex solution of the Abelian Higgs model* Phys. Rev. **D14**, 1100 (1976)
- [325] W.H. Zurek, *Cosmological experiments in superfluid helium?* Nature *317*, 505-508 (1985).
- [326] W.H. Zurek, *Cosmological Experiments in Condensed Matter Systems* Phys. Rept. **276**, 177-221 (1996) [arXiv:cond-mat/9607135v1].
- [327] W.H. Zurek, *Cosmological Experiments in Superfluids and Superconductors* [arXiv:hep-ph/9501207v1] (1995).
- [328] M.J. Bowick, L. Chandar, E.A. Schiff, A.M. Srivastava, *The Cosmological Kibble Mechanism in the Laboratory: String Formation in Liquid Crystals* Science **263**, 943-945 (1994) [arXiv:hep-ph/9208233v1].
- [329] G.A. Williams, *Vortex-Loop Phase Transitions in Liquid Helium, Cosmic Strings, and High- T_c Superconductors* Phys. Rev. Lett. **82**, 12011204 (1999) [arXiv:cond-mat/9807338v3].

- [330] P.C. Hendry, N.S. Lawson, R.A.M. Lee, P.V.E. McClintock and C.D.H. Williams, *Creation of quantized vortices at the lambda transition in liquid helium-4* J. Low Temp. Phys. **93**, 5-6, 1059-1067 (1995) [arXiv:cond-mat/9502119].
- [331] I. Chuang, R. Durrer, N. Turok, B. Yurke, *Cosmology in the laboratory: Defect dynamics in liquid crystals* Science **251**, 1336-1342 (1991).
- [332] J.R. Hook and H.E. Hall, *Solid State Physics (2nd Ed.)* (2001), John Wiley and Sons, ISBN: 0-471-92805-4 (paperback).
- [333] J.F. Annett, *Superconductivity, Superfluids and Condensates* (2004), OUP, ISBN-13: 978-0198507567 (paperback).